**Contract No:**

This document was prepared in conjunction with work accomplished under Contract No. DE-AC09-08SR22470 with the U.S. Department of Energy (DOE) Office of Environmental Management (EM).

**Disclaimer:**

We put science to work.™

Savannah River National Laboratory®

OPERATED BY SAVANNAH RIVER NUCLEAR SOLUTIONS

A U.S. DEPARTMENT OF ENERGY NATIONAL LABORATORY • SAVANNAH RIVER SITE • AIKEN, SC

# Hanford Double Shell Waste Tank Corrosion Studies- Final Report FY2019

**Authors:**

**R. E. Fuentes**

**P. K. Shukla**

**Contributors:**

**S. Crossland**

**B. Peters**

**D. Hitchcock**

July 2020

SRNL-STI-2020-00109, Revision 0

SRNL.DOE.GOV

**DISCLAIMER**



**Printed in the United States of America**

**Prepared for**
**U.S. Department of Energy**

SRNL-STI-2020-00109
Revision 0

**Keywords:** *vapor space corrosion, pitting factor, Hanford, waste tanks*

**Retention:** *Permanent*

# Hanford Double Shell Waste Tank Corrosion Studies- Final Report FY2019

Authors:
R. E. Fuentes
P. K. Shukla

Contributors:
S. Crossland
B. Peters
D. Hitchcock

July 2020

Prepared for the U.S. Department of Energy under contract number DE-AC09-08SR22470.

Savannah River National Laboratory®
OPERATED BY SAVANNAH RIVER NUCLEAR SOLUTIONS

# REVIEWS AND APPROVALS

AUTHORS:

R. E. Fuentes, Materials Science and Engineering Date

P. K. Shukla, Materials Science and Engineering Date

TECHNICAL REVIEW:

J. T. Boerstler, Materials Science and Engineering, Reviewed per E7 2.60 Date

APPROVAL:

B. J. Wiersma, Group Leader, Corrosion Science and Engineering, Materials Science and Engineering
Date

J. Manna, Director Date
Materials Science and Engineering

J. S. Page, Washington River Protection Solutions Date

J. Castleberry, Project Manager Date
Washington River Protection Solutions

# ACKNOWLEDGEMENTS

The authors want to acknowledge the technical support of T. Murphy in performing experiments and characterizations and the assistance of S. Harris for developing statistical design of experiments and collaboration to validate the pitting factor for the New Limits Pitting Corrosion Task. Guidance from L. Stock and the Corrosion sub-group were appreciated for the achievement of tasks. Additional contributions to the report by S. Crossland for reporting the water analysis on microbiologically induced corrosion using commercially available kits and, B. Peters and D. Hitchcock for reporting summary of the work related to the quartz enhanced photoacoustic spectroscopy system are greatly appreciated.

# EXECUTIVE SUMMARY

During fiscal year (FY) 2019, the Savannah River National Laboratory (SRNL) focused on four primary tasks for Hanford Double Shell Tanks (DSTs) corrosion studies. The first task, New Limits, was a continuation from the electrochemical work started in FY16, to expand electrochemical testing to elevated temperatures and elevated hydroxide concentrations and evaluate how these factors will influence pitting corrosion. Using the pitting factor (PF) equation, these new conditions were validated to provide a conservative estimate for the susceptibility of pitting corrosion on legacy carbon steel. The second task, Secondary Liner Corrosion, focused on Vapor Space Corrosion (VSC) and immersion testing studies using two commercially available vapor corrosion inhibitors (VCIs). For this FY, the VCI strategy was applied mid-experiment to determine performance on weathered coupons. The third task, Long-Term Open Circuit Potential (OCP) Drift, was performed using simplified simulated chemistries to evaluate change in pitting corrosion risk due to evolution of corrosion potential for mill-scale and freshly polished 600-grit surfaces. Finally, the fourth task, Microbiologically-Influenced Corrosion (MIC) studies, was focused on the study of leak detection pit (LDP) water sent from the Hanford tank farm for determination of bacteria that can be conducive to corrosion using commercially available kits: BART™ and MICkit® 5. In addition, this FY, a secondary task was added which was a continuation of the study of the Quartz-enhanced Photoacoustic Spectroscopy (QEPAS) system. Work was started but was ultimately not pursued. A summary of each task performed is presented below.

## 1. New Limits Pitting Corrosion Tests

New Limits Pitting Corrosion Testing has been focusing on establishing the PF as an acceptable criterion for the development of a new waste chemistry envelope. For FY19, electrochemical testing was performed to expand the temperature limit for the PF equation from 50 to 75 ºC. Tests were performed at temperatures up to 75 ºC selected from a statistical design analysis to determine the impact of elevated temperatures on pitting susceptibility. Tests at temperatures up to 75 ºC with hydroxide concentration up to 6 M were also performed (previous maximum hydroxide concentration was 1.2 M). The elevated hydroxide concentration was used to cover cases that have an excess amount of hydroxide (up to 6 M) The elevated hydroxide concentration was used to address anticipated maximum hydroxide concentrations for the waste tank contents. Supplemental testing to address gaps in historical data was performed for hydroxide concentrations of 0.01 to 0.1 M at low and elevated temperatures (i.e., 35 and 75 ºC) to verify the PF equation at these conditions. The results showed that for most tests, the PF equation for temperatures less than 50 °C, was able to accurately predict the results for tests performed at 75 ºC. It was shown that PFs greater than 1.2 predicted no pitting susceptibility, while PFs less than 1.2 were more likely to predict pitting susceptibility. However, in some cases “pass” conditions were observed for PF values less than 1.2. Generally, the model conservatively predicts whether carbon steel is vulnerable to pitting corrosion. Thus, at elevated temperatures the PF equation is still valid and can be used efficiently to predict vulnerability towards localized corrosion of carbon steel for liquid radioactive waste environments.

## 2. Secondary Liner Corrosion Tests

VSC and immersion tests with commercially available VCIs were performed on rail-road car carbon steel samples at specific concentrations mixed with the groundwater (GW) simulant. The VCIs recommended dosages used for the study are:

- VCI-A: VpCI-337 – 10% v/v solution in GW simulant, i.e., 100 mL in VpCI-337 plus 900 mL of GW for 1 L VCI formulation.
- VCI-B: 10% wt.VpCI-609 in GW simulant (100 g VpCI-609 in 1 liter) and 0.75% v/v VpCI-649MF (7.5 mL/L)

VCIs formulations were added during mid-course of experiments, i.e., after coupons have experienced corrosion in the untreated GW simulant. Three tests were conducted using VCI-A and VCI-B. The first two tests were conducted using 100% recommended dosages of VCI-A and VCI-B. The third test was conducted at 10% of the recommended dosage of VCI-B. Following conclusions are made from the experimental data and results:

- The corrosion rate data indicated that 10% of the recommended dosage is insufficient in mitigating corrosion. This observation is consistent with a prior study which also concluded that VCIs' effectiveness vanishes at 10% of the recommended dosages for the aboveground tank bottom underside application.

- The data also showed that 100% recommended dosages of VCI-A and VCI-B mitigated pitting corrosion of weathered coupons. Specifically, VCI-A mitigated pitting corrosion in immersed, Level 2, and Level 3 coupons, whereas VCI-B mitigated pitting corrosion in immersed, Level 1, and Level 3 coupons. Statistical significance of corrosion rate decrease in Level 1 coupons for 100% recommended dosage of VCI-A and Level 2 coupons for 100% recommended dosage of VCI-B could not be established; this may be due to choice of coupons' surface orientation being vertical during the tests, leading to limited and uneven weathering during groundwater only and groundwater plus VCI exposures.

### 3. Long term OCP Drift Tests

OCPs of carbon steel were measured in three simulants from the new limits testing. Two sets of coupons, with three coupons in each set, were fabricated with differing surface conditions. The coupons' surface conditions included a 600-grit polished surface, and a surface with mill-scale plus corrosion products from legacy carbon steel (rail car steel AAR TC-128). Two coupons, one coupon from each set, were placed in each chemistry, and OCPs of the coupons were monitored for five months. OCPs of the coupons with polished surfaces evolved in the anodic direction with respect to the initial values, whereas OCPs of two of the three coupons with mill-scale plus corrosion products evolved in cathodic direction with respect to the initial values. Terminal OCP of one mill-scale plus corrosion products coupon was about 100 mV anodic with respect to the initial value. CPP data of the polished coupons before OCP evolutions showed mixed responses, i.e., a clear delineation between pitting and no-pitting cannot be made, and CPP data after OCP evolutions remained mixed (category 3), indicating that change in OCP values did not affect the CPP responses. Following exposures of the coupons during OCP evolutions, CPP data for the mill-scale plus corrosion products coupons in the three simulants showed negative hysteresis (category 1), which is a sign of no-pitting. The OCP and CPP data indicate that simulant chemistry and surface condition affect extent and direction of OCP evolution, however, OCP evolution does not affect the pitting susceptibility. Electrochemical Impedance Spectroscopy (EIS) spectra of the polished coupons differed compared to mill-scale plus corrosion product coupons in the three simulants. A qualitative analysis indicated that low-frequency asymptotic impedance values for the mill-scale plus corrosion products coupons are expected to be higher than the polished coupons. The EIS data suggest slower kinetics of the corrosion reactions at the mill-scale coupons compared the polished coupons.

### 4. MIC Tests

The Hanford tank farm facility is seeking to understand the observations of accelerated corrosion on the exterior side of the secondary liner of several of the DSTs. One possibility is that the liner is in contact with stagnant water with high biological activity that induces microbiological corrosion. Two, 250 ml bottles of water from an LDP were sent to SRNL to determine the bacterial activity levels. MICkit® 5 and BART™ commercial kits were used to determine the range of bacteria in the water samples. The two testers showed

similar negative results for sulfate reducing bacteria and acid producing bacteria which are commonly associated with MIC.

## 5. QEPAS Studies

QEPAS is a pass-through type method for measuring trace impurities in gas streams. The QEPAS system at SRNL was designed to monitor both ammonia ($NH_3$) and methane ($CH_4$) in gas streams at varying pressures with detection limits as low as 2 ppm $NH_3$ and 10ppm $CH_4$. To date, the two gas QEPAS detectors have been assembled and tested. The current control electronics unit (CEU) and laser were designed to be modular, which limited their efficacy in studying gasses other than $NH_3$ and $CH_4$. In FY19 a benchtop QEPAS setup was assembled that allowed for QEPAS measurement of other analytes. Specific efforts were directed toward QEPAS detection of other vapor space corrosion inhibitors being studied by SRNL. However, before efforts were initiated, WRPS communicated that they would not be pursuing the QEPAS technology in the near future. Recommendations for future development of QEPAS were requested. SRNL recommends the following:

1. Design a mounted unit that can be placed in the field (e.g., the ventilation exhaust). The system can be miniaturized to adapt to various configurations.
2. The present system that is being tested was developed in 2011. Upgrades to the system design should be pursued.

A summary of the QEPAS system work that was undertaken by SRNL from FY16 up to this FY is presented in this report.

# TABLE OF CONTENTS

# LIST OF TABLES

# LIST OF FIGURES

# LIST OF ABBREVIATIONS

| | |
|---|---|
| APB | Acid Producing Bacteria |
| ADM | Acoustic Detection Module |
| ADS | Acoustic Detection Module |
| ASTM | American Society for Testing and Materials |
| ANA | Anaerobic |
| cfu | colony forming unit |
| CEU | Control Electronics Unit |
| CPP | Cyclic Potentiodynamic Polarization |
| DNV-GL | Det Norske Veritas-Germanischer Lloyd |
| DST | Double-Shell tank |
| EDM | Electrical Discharge Machine |
| ER | Electrical Resistance |
| FY | Fiscal Year |
| GW | Ground Water |
| HAB | Heterotrophic Aerobic Bacteria |
| IRB | Iron-related Bacteria |
| LDP | Leak Detection Pit |
| LOD | Limit of Detection |
| LAI | Liquid-Air Interface |
| LNB | Low Nutrient Bacteria |
| MIC | Microbiologically Influenced Corrosion |
| mpy | mils per year |
| OCP | Open Circuit Potential |
| PF | Pitting Factor |
| PTFE | Polytetrafluoroethylene |
| QTF | Quartz Tuning Fork |
| QEPAS | Quartz-enhanced Photoacoustic Spectroscopy |
| SCE | Saturated Calomel Electrode |
| SRNL | Savannah River National Laboratory |
| SRS | Savannah River Site |
| SST | Single-Shell Tank |
| sccm | standard cubic centimeter per minute |
| SCC | Stress Corrosion Cracking |
| SRB | Sulfate Reducing Bacteria |

| | |
|---|---|
| TAPI | Tank and Pipeline Integrity |
| TIEP-CSG | Tank Integrity Expert Panel-Corrosion Sub-Group |
| TIC | Total Inorganic Carbon |
| VCI | Vapor Corrosion Inhibitor |
| VSC | Vapor Space Corrosion |
| WRPS | Washington River Protection Solutions |

## 1.0 Introduction

Millions of gallons of liquid radioactive waste at Hanford site are stored in single-shell tanks (SSTs) built during the 1940s to 60s, and double-shell tanks (DSTs) built during the 1960s to 80s. The newer DSTs have been used to store waste from SSTs with suspected leaks and those being monitored pending the processing to immobilize the waste by vitrification or grout formulation. The tanks were fabricated from carbon steel, and a comprehensive chemical control program is in place to maintain tank integrity and corrosion minimization until a disposition path for the liquid waste is in place. The program is overseen by the Tank and Pipeline Integrity (TAPI) group from Washington River Protection Solutions (WRPS).

The liquid waste is currently being inhibited by sodium hydroxide additions to maintain alkaline conditions and by sodium nitrite additions into the tank. However, certain species in the waste such as nitrate, chloride and fluoride can be aggressive within the waste at elevated concentrations and could cause localized corrosion. To continue to prevent localized corrosion due to waste chemistry changes, the chemical control program is being updated. Waste chemistry changes can occur due to waste transference into DSTs from SSTs and returned processing streams from waste immobilization operations.

Corrosion testing for DSTs has been guided by the Tank Integrity Expert Panel-Corrosion Sub-Group (TIEP-CSG) to provide the technical guidelines for the corrosion control program. Corrosion testing has been performed at three independent laboratories: Det Norske Veritas-Germanischer Lloyd (DNV-GL), Savannah River National Laboratory (SRNL), and the 222-S facility at Hanford operated by WRPS. SRNL has focused its corrosion studies on vapor space corrosion (VSC), development of corrosion chemistry limits to mitigate pitting corrosion, and corrosion protection for the tank secondary liner in DSTs.

For this fiscal year (FY), SRNL focused on four primary tasks. Task one was a continuation from the new limits work to expand electrochemical testing to elevated temperatures and elevated hydroxide concentrations and evaluate the influence of these expanded condition ranges on pitting corrosion. The PF equation was validated against these conditions to provide a conservative estimate for susceptibility of pitting corrosion. Task two focused on VSC studies for the secondary liner using two commercially available vapor corrosion inhibitors (VCIs) at manufacturer recommended dosages. The VCI formulation was applied mid-experiment to determine performance on weathered coupons. Task three was dedicated to the study of long-term open circuit potential (OCP) drift using simplified chemistries to evaluate change in pitting corrosion risk due to evolution of corrosion potential for mill-scale and freshly polished surfaces. Finally, task four focused on the study of leak detection pit (LDP) water sent from the Hanford tank farm to determine if bacteria are present in sufficient concentrations to create a risk for microbiologically influenced corrosion (MIC) using kits commercially available: BART™ and MICkit® 5. In addition, this FY, the study of the Quartz-enhanced Photoacoustic Spectroscopy (QEPAS) system was a secondary task and work was started for performing a test with $SF_6$ gas but was not pursued. A summary of the work performed using QEPAS from the inception of the program is presented.

## 2.0 Background

DSTs corrosion testing for FY19 consisted of seven experimental tasks [1]. From these tasks, four were performed during the FY, while the rest were mostly put on hold. New Limits Pitting Corrosion work was prioritized again this year to involve additional electrochemical testing to develop a more robust pitting corrosion evaluation due to significant species in the waste (i.e., hydroxide, nitrite, nitrate, chloride and fluoride). Long-term testing for VSC using VCIs and OCP drift studies were also performed. In addition, MIC studies were carried out using water collected from an LDP near a DST to be representative of water

chemistry near the secondary liner. The tasks performed are numbered below and a background is provided with objectives.

2.1 New Limits Pitting Corrosion

The chemistry control limits used in FY19 at Hanford is shown in
Table 2-1, The chemistry control program mostly depends on nitrite and hydroxide concentrations for carbon steel inhibition maintaining the waste at alkaline conditions. Nitrite and hydroxide can be added into the waste, however nitrite can also be produced from nitrate by radiolysis [2] In the table it is listed the hydroxide and nitrite range needed depending on nitrate and temperature limits. Currently all DST supernates are above 0.01 M hydroxide.

**Table 2-1 Double-Shell Tank Waste Chemistry Limits for Corrosion Control**

| **$[NO_3^-]$ Range** | **Variable** | **Waste Temperature (T) Range** | | |
|---|---|---|---|---|
| | | **T < 167 °F (75 °C)** | **167 °F (75 °C) ≤ T ≤ 212 °F (100 °C)** | **T > 212 °F (100 °C)** |
| $[NO_3^-] \leq 1.0$ M | $[OH^-]$ | 0.010 M ≤ $[OH^-]$ ≤ 8. 0 M | 0.010 M ≤ $[OH^-]$ ≤ 5.0 M | 0.010 M ≤ $[OH^-]$ ≤ 4.0 M |
| | $[NO_2^-]$ | 0.011 M ≤ $[NO_2^-]$ ≤ 5.5 M | 0.011 M ≤ $[NO_2^-]$ ≤ 5.5 M | 0.011 M ≤ $[NO_2^-]$ ≤ 5.5 M |
| | $[NO_3^-]$/ ($[OH^-]$ + $[NO_2^-]$) | < 2.5 | < 2.5 | < 2.5 |
| 1.0M<$[NO_3^-]$ ≤ 3.0 M | $[OH^-]$ | 0.1 ($[NO_3^-]$) ≤ $[OH^-]$ < 10 M | 0.1 ($[NO_3^-]$) ≤ $[OH^-]$ < 10 M | 0.1 ($[NO_3^-]$) ≤ $[OH^-]$ < 4.0 M |
| | $[OH^-]$ + $[NO_2^-]$ | ≥ 0.4 ($[NO_3^-]$) | ≥ 0.4 ($[NO_3^-]$) | ≥ 0.4 ($[NO_3^-]$) |
| $[NO_3^-] > 3.0$ M | $[OH^-]$ | 0.3 M ≤ $[OH^-]$ < 10 M | 0.3 M ≤ $[OH^-]$ < 10 M | 0.3 M ≤ $[OH^-]$ < 4.0 M |
| | $[OH^-]$ + $[NO_2^-]$ | ≥ 1.2 M | ≥ 1.2 M | ≥ 1.2 M |
| | $[NO_3^-]$ | ≤ 5.5 M | ≤ 5.5 M | ≤ 5.5 M |

As waste is being transferred to and from DSTs, the chemistry may become more dilute or aggressive species can become more concentrated (e.g., chloride, fluoride, sulfate, etc.). Additional inhibitor may be necessary to ensure that the risk of pitting corrosion is minimized. Therefore, the corrosion control program is being evaluated to adapt to anticipated changes in chemistry and provide a conservative approach to prevent localized corrosion, in particular pitting corrosion.

SRNL initiated the New Limits testing in FY16 using statistical analysis to design matrices for a wide range of chemistries and to determine significant species that contribute and inhibit pitting corrosion [4]. The testing was performed using the standardized Cyclic Potentiodynamic Polarization (CPP) test developed by TIEP-CSG [3] and presented in Table 2-2.

**Table 2-2 Standardized CPP protocol with the parameters utilized for testing**

| **Parameters** | **Results** |
|---|---|
| Potential Stabilization (hrs.) | 2 |
| Start Potential (V vs. OCP) | -0.05 |
| Scan Rate (mV/s) | 0.167 |
| Vertex Threshold ($mA/cm^2$) | 1 |
| Finish Potential (V vs. OCP) | 0 |

| Sample geometry | bullet |
|---|---|
| Surface Preparation | 600 grit |

The results of the CPP tests were analyzed by logistic regression. The initial 53 tests performed in FY16 (i.e., Plackett-Burman and Box-Behnken experimental designs) indicated that the significant aggressive species were nitrate and chloride, while significant inhibitor species were hydroxide and nitrite. Over the temperature range studied, from 25 to 50 ºC, temperature was not identified as a statistically significant variable influencing pitting corrosion. In FY17, the pitting corrosion study was expanded to include hydroxide concentrations up to 1.2 M (from previous 0.6 M) and additional interior points within the experimental design matrix. At the conclusion of this testing, the combined results were about 95 tests and the initial PF was developed [5]. The PF was defined as the ratio of inhibitor to aggressive species using coefficients obtained from a logistic regression analysis. PFs less than 1 were indicative of pitting susceptibility, which was utilized as an initial criterion. PFs between 1 and 2 occasionally resulted in pitting, particularly at low nitrite ion concentrations and high aggressive species concentrations. PFs greater than 2 were indicative of a condition that is not expected to cause pitting. The PF for the 95 tests (i.e., initial PF) is shown in Equation 1,

$$PF = \frac{\text{Inhibitor Species}}{\text{Aggressive Species}} = \frac{8.52\,[OH^-]+2.41\,[NO_2^-]}{[NO_3^-]+19.6\,[\text{Halide}]} \qquad \textbf{Equation 1}$$

where halide concentration is the sum of the concentrations of chloride and fluoride. The use of halide, instead of chloride, was used as a conservative approach since fluoride concentration did not initially appear to be a significant variable. A primary reason is the low solubility of fluoride in the more concentrated solutions. However, in more dilute solutions, at low chloride levels, the fluoride is present and is a known pitting agent for carbon steel [6]. In order to separate the chloride and fluoride effects, fifteen tests were statistically selected for electrochemical experiments and historical CPP data with fluoride was analyzed with approximately 110 data points [7]. Logistic regression was performed with the results and with the additional experiments from tests at PF between 1 and 2. The resulting PF equation (i.e., final PF) with the individual contributions of chloride and fluoride was determined and is presented below (Equation 2),

$$PF = \frac{8.06\,[OH^-]+1.55\,[NO_2^-]}{[NO_3^-]+16.7\,[Cl^-]+5.7\,[Fl^-]} \qquad \textbf{Equation 2}$$

As calculated from Equation 2, the contribution of chloride resulted in around three times more significance than fluoride based on the coefficients. Based on the results, a review of historical pitting data, and coupon testing, it was demonstrated that carbon steel is not anticipated to be susceptible to pitting for pitting factors greater than 1.2. Additionally, for dilute solutions, a minimum nitrite concentration of 0.2 M was required. A complete summary of the PF equation rationale and implementation was summarized in a recent report [8].

2.2 Secondary Liner Corrosion

There are 28 DSTs at Hanford Site. Each DST consists of a primary liner (inner) surrounded by a secondary (outer) liner. The secondary liner rests on a concrete pad. A schematic diagram presented in Figure 2-1 for some DSTs (e.g., AY, AZ and SY Tank Farms), shows the concrete foundation and drain slots.

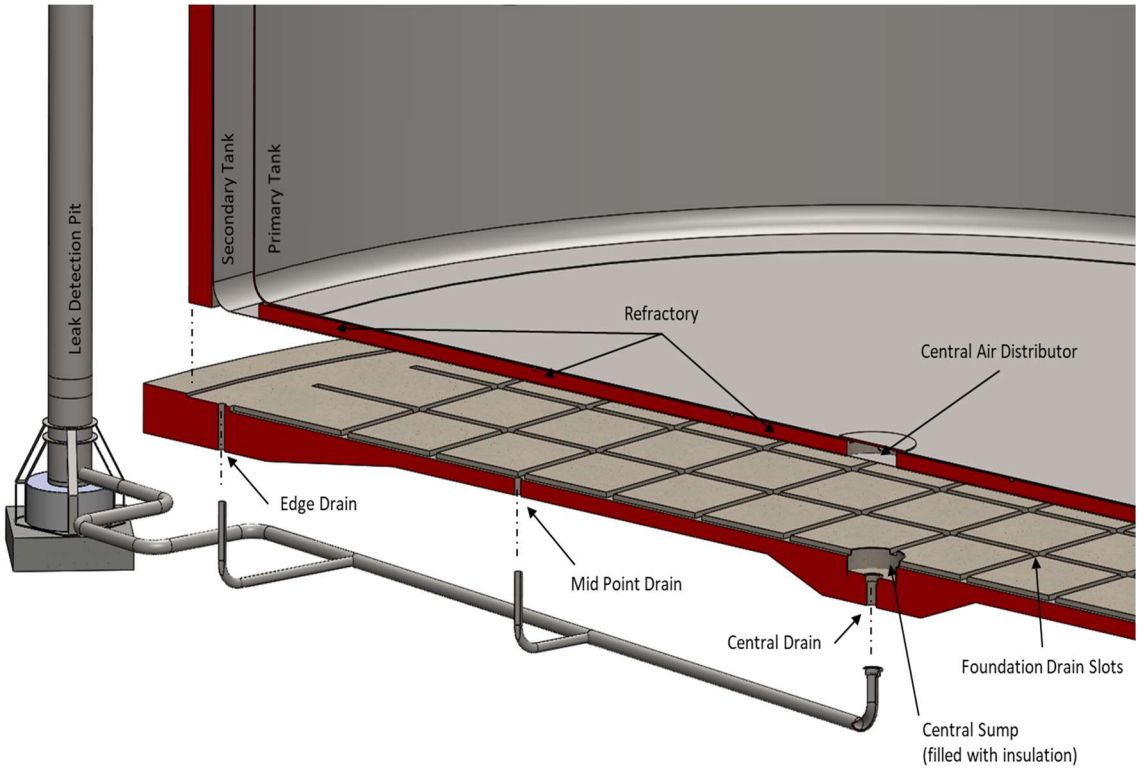


**Figure 2-1 Schematic of a double shell tank depicting primary and secondary tank shells, concrete foundation, and drain slots.**

Water is known to accumulate in the drain slots and cause corrosion on the exterior of the secondary liner. Ultrasonic inspection is confined to the annular space between the primary and secondary tanks, leaving a concern that corrosion is widespread on the underside of the bottom plate. Since the water level can vary in the drain slots based on accumulation, corrosion could be caused by direct contact with the accumulated water, or when the water level is below the underside of the tank bottom, VSC could also occur. Accumulated water is drained through the sumps into LDPs. The drained water was analyzed for its constituents, and two simulants were developed considering the chemical composition range of the accumulated water. The simulants were identified as LDP water and GW.

Testing with LDP and GW simulants for legacy carbon steel corrosion was started in FY14 with a long term immersion experiment in which the deleterious effects of these chemistries were observed, with mass loss corrosion rates obtained of approximately 10 mpy [9],[10]. During FY16 testing was focused on the inhibition strategies involving commercial VCI directly applied to the samples to mitigate VSC and other types of corrosion. Testing continued during FY17 and it was observed that by coating the samples with VCI, the corrosion inhibition was short-lived and did not significantly reduce carbon steel corrosion [5]. FY18 testing was conducted using three commercially available VCIs; two of the three VCIs were added to one solution. For this section, the objective is to find other VCI strategies that can effectively minimize corrosion of carbon steel exposed to LDP and GW.

## 2.3 Long-Term OCP Drift

Approximately 55 million gallons of radioactive waste is being stored in 177 carbon steel tanks at Hanford. Long-term performance and integrity of the tanks is partly dependent on modifying the waste chemistry such that risk of pitting and stress corrosion cracking (SCC) of the tank carbon steel are mitigated. To this end, CPP experiments are conducted to identify risk of pitting corrosion, and subsequently determine the

level of inhibition needed to mitigate pitting corrosion. One of the key parameters associated with the determination is the difference between the corrosion and repassivation potentials: if the corrosion potential is greater than repassivation potential, the risk of pitting corrosion exists. Corrosion potential is defined as steady-state value of OCP.

CPP data along with the waste chemistry compositions are used to develop the PF equation. PF predictions include waste chemistries where the likelihood of pitting corrosion is ambiguous, i.e., pitting corrosion could occur but is not certain. Such ambiguities in the pitting equation predictions arise because CPP data for some chemistries does not show clear delineation between pitting and no pitting (category 3). In such situations, i.e., ambiguous CPP responses, the difference between the corrosion and repassivation potentials is used to delineate differences between pitting and no pitting in the waste chemistry envelope: if the corrosion potential is greater than repassivation potential, the risk of pitting corrosion exists. Corrosion potential is defined as steady-state value of OCP. However, it has been observed that certain simulated waste chemistries lead to significant changes in OCP over time. A distinction is drawn between OCP and corrosion potential. At the corrosion potential, rates of anodic and cathodic reactions balance each other, and the metal surface is in steady equilibrium with the surrounding electrolyte. OCP is defined when the metal surface is in process of establishing equilibrium with the surrounding electrolyte, and rates of anodic and cathodic reactions are evolving, however, the reactions' rates balance each other even during the evolution. When the evolution reaches a steady-state (i.e., potential does not change more than +/- 10 mV/hr), OCP becomes the corrosion potential of a metal surface in a given electrolyte. The change in OCP during CPP tests could lead to underassessment of the risk especially when corrosion potential is below the repassivation potential, and difference between the two is sufficiently low such that an upward drift in OCP would increase the risk of corrosion potential exceeding the repassivation potential, and thereby, increasing the risk of localized corrosion in form of pitting corrosion. Therefore, to quantify the risk of pitting corrosion due to OCP drift, laboratory experiments were conducted with three waste simulant chemistries with pre-determined repassivation potentials in the CPP data.

Another key difference between laboratory testing using CPP and field conditions has been the surface condition of coupons used in the laboratory testing in comparison with the field condition of the tanks. CPP tests have been conducted using the bullet coupons with 600 grit polished surfaces [4],[5],[9],[10] whereas the tanks were constructed using steel with mill scale plus corrosion products. It is recognized that during the construction process, large sheets of the carbon-steel metal were welded together, and other processes associated with tank construction likely have disturbed the original mill-scale on portions of the tank liner. Considering this, a 600 grit polished coupon was utilized as one extreme of the surface condition whereas a coupon with mill-scale plus corrosion products is considered the other extreme. The surface condition of a newly constructed tank is expected to be somewhere between the two extremes. In addition, the tanks were put in service sometime after completion of construction. This would have resulted in the tank steel being exposed to ambient conditions and develop additional layers of corrosion products before being placed in service. Considering several possibilities of the surface conditions, the objective of the study also included determining effect of surface condition on evolution of OCP. The objective also included establishing conservatism of the CPP tests results, i.e., the tests results sufficiently bound the conclusions derived from the test data.

### 2.4 MIC Testing

The Hanford tank farm facility is seeking to understand the observations of accelerated corrosion on the exterior side of the secondary liner of several of the DSTs. One possibility is that the liner is in contact with stagnant water with high biological activity that induces microbiological corrosion. Two, 250 ml bottles of water from an LDP were sent to SRNL to determine the bacterial activity levels. This water was sampled because the LDP has communication with the exterior side of the secondary liner. Bacteria that can result

in MIC were of particular interest. MICkit® 5 and BART™ were the biological testing kits utilized for this determination. Both testers involve introducing the water to be tested into a container and observing visual changes.

## 3.0 Task Description and Activities

Several tasks were performed during FY19 and are described in the sections below.

### 3.1 Task 1: New Limits Pitting Corrosion Testing

For New Limits, the electrochemical testing was expanded to include elevated temperatures (i.e., up to 75 ºC). Since the temperature of the solution was not found to be statistically significant up to 50 ºC, the study of effect of higher temperature wanted to be studied to establish if temperature becomes a significant variable influencing pitting corrosion and quantify the effect of temperature on the PF equation. Twenty-one tests were statistically designed to evaluate the effect of temperature. In addition, the effect of concentrated hydroxide solutions up to 6 M was also studied with an additional thirteen tests. The high concentration of hydroxide was selected as it may contribute to localized corrosion effects. These two matrices were utilized to validate the PF equation at hydroxide concentrations up to 6 M and temperatures from 25 up to 75 ºC.

Historical data of about 300 tests was evaluated ranging from 25 to 75 ºC in temperature. A statistically designed matrix was established to test at a hydroxide concentration of 0.01 to 0.1 M (pH range of 12 to 13) due to the limited amount of data in this region. Twenty tests were statistically designed to address this pH range and check how the PF may change with additional five tests at pH range 13 to 13.5 to address that gap in the data as well.

### 3.2 Task 2: Secondary Liner Corrosion Testing

FY19 studies were conducted with commercially available VCIs at manufacturer recommended dosages, identified in this report as VCI-A and VCI-B. Three tests were conducted. In the first two tests, 100% of the recommended dosages of the two VCIs which were added to the GW solution mid-course of the tests. The third test was conducted at 10% of the recommended dosage of VCI-B. Prior studies with VCIs have shown that VCIs' effectiveness vanish at 10% of the recommended dosages for the aboveground tank bottom underside application [7]. Therefore, selection of 10% of the recommended dosage was to determine minimum VCI concentration needed for the secondary liner application. All three tests were conducted with twenty-four coupons for each experiment. Of these, six coupons were immersed, and the remaining eighteen coupons were placed in the vapor space of the vessel of each experiment. Twelve coupons were extracted from each experiment after 2 months. VCIs were added to the test solutions in each experiment at the time of extraction of the first twelve coupons. The remaining coupons were extracted after being exposed to the VCI treated solutions for an additional two months. The coupons were analyzed for both pitting and general corrosion rates. The corrosion rate data were used to determine performance of the VCIs on the weathered coupons and the effect of lower than recommended VCI dosages on corrosion mitigation. Electrical Resistance (ER) probes were also used for in-situ measurement of corrosion rates and VCI performance. ER probes were immersed in the electrolyte and positioned near the liquid and vapor space interface. ER probe data were continuously collected and analyzed to in-situ measure the corrosion mitigation performance of the VCI treated solutions.

3.3 Task 3: Long-Term OCP Drift Corrosion Testing

Three simplified chemistries were selected for the FY 2019 study. These chemistries were selected such that the corrosion behavior for the full range of anticipated pH and PF could be evaluated. Two coupons were placed in each solution. The first was a 600-grit surface polished bullet coupon representing an extreme of clean (freshly ground) metal on the tank wall. The other extreme was represented by a coupon containing mill scale plus corrosion products. While neither extreme represents the exact condition of the tank walls, these conditions should be bounding such that the actual condition of the tank wall in any given area falls between the two extremes. The tests were conducted at 35 °C. OCPs of the six coupons were monitored over a period of several months. Electrochemical impedance spectroscopy (EIS) measurements were conducted after the OCP measurements, followed finally by CPP measurements. The corrosion potential, EIS, and CPP data were used to determine changes in pitting corrosion risk due to evolution of corrosion potential and electrochemical properties of the metal surface.

3.4 Task 4: MIC Testing

For this task the objective was to evaluate the possibility and consequence of MIC on the secondary wall of the DSTs. The laboratory evaluation was performed by using viable bacteria determination kits: MICkit® 5 and BART. A sample of the water was added into the kits and depending on the response obtained, it can be assessed if bacteria that may result in MIC are present and if those bacteria are in sufficient concentration that they maybe aiding in the corrosion of the carbon steel.

## 4.0 Experimental Procedure

The material used for all corrosion testing is carbon steel selected from AAR TC-128 Rail Car Steel. This steel was selected for testing since it approximates the chemistry and microstructure of American Society for Testing and Materials (ASTM) A515, Grade 60 carbon steel, the steel from which some of the tanks were fabricated [13]. The chemical composition of the steel is shown in Table 4-1.

**Table 4-1 Chemical Composition of AAR TC-128 Rail Car Steel**

| | C | Mn | P | S | Si | Fe |
|---|---|---|---|---|---|---|
| **Specification (wt.%)** | 0.24 (max.) | 0.9 (max.) | 0.035 (max.) | 0.04 (max.) | 0.13 to 0.33 | Balance |
| **Measured (wt.%)** | 0.212 | 1.029 | 0.012 | 0.013 | 0.061 | Balance |

In the next pages are the experimental details and conditions in which the carbon steel was used and prepared for electrochemical testing and secondary liner corrosion testing.

4.1 Electrochemical Testing of Simulants

4.1.1 *Sample preparation*

The electrochemical testing was performed by using electrodes in “bullet” shape with dimensions: 0.188 inch in diameter and 1.25 inches long (Metal Samples Company part number EL-400). In Figure 4-1, a picture of the sample after being polished and rinsed is shown. Before testing, a drill was used to rotate the sample and grind it to a uniform 600 grit finish. After, the sample was rinsed with distilled water and acetone. The bullets were examined visually for any defect and to ensure that the sample had a uniform surface preparation. The sample was then attached to a stainless-steel rod protected by a glass holder. A

polytetrafluoroethylene (PTFE) fixture was used to prevent liquid contact with the stainless-steel rod and ensure electrical isolation.

**Figure 4-1 Side picture of the "bullet" shape sample**

For long-term potential drift testing, three samples were created by cutting 2 inches by 2 inches squares of plate AAR TC-128 metal mill-scale side with no further surface preparation. The plate was cut using an Electrical Discharge Machine (EDM). The samples were connected to a wire for electrical connection using silver epoxy, then mounted with a two-part clear epoxy solution (EpoKwick from Buehler) so that one face of the coupon was exposed. Figure 4-2 show an image of one of the coupons used for this task.

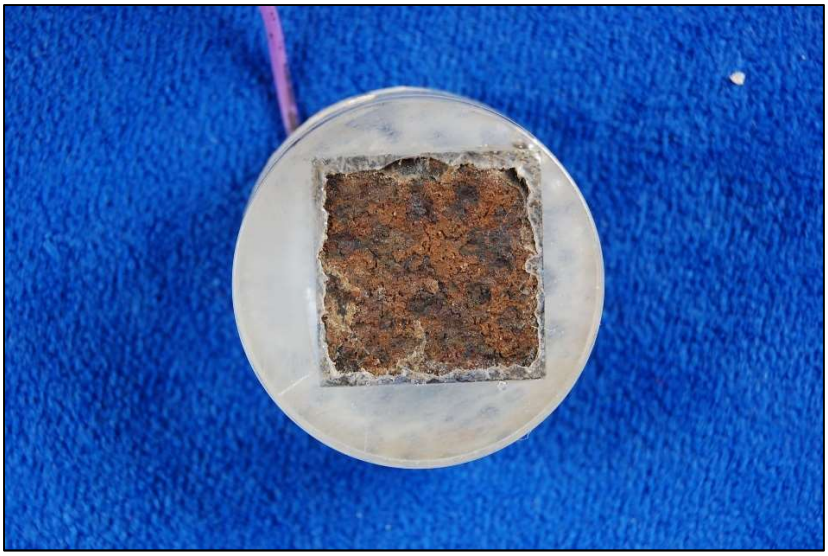

**Figure 4-2 Image of a coupon with mill-scale used to study evolution of OCP**

4.1.2 *Simulants*

For the New Limits Task, twenty-one simulants were statistically designed at a temperature of 75 ºC based on the changing concentration of significant species: nitrate, nitrite, hydroxide, chloride and fluoride, to see the effect of temperature on the predictive capabilities of the PF equation. The simulants are listed as tests in Table 4-2. All the constituents were mixed in distilled or deionized water. The sulfate concentration was also changed ranging from 0 to 0.2 M to see if with temperature the sulfate can become statistically significant. The total inorganic carbon (TIC) consisted of sodium carbonate and sodium bicarbonate for a total TIC concentration of 0.1 M. Sodium bicarbonate (up to 0.025 M) was only added at 0.0001 M hydroxide tests to adjust the pH to 10. Otherwise, sodium carbonate was added as TIC content in the simulant.

**Table 4-2 Simple chemistries simulants at a temperature of 75 ºC for elevated temperature testing (TIC was 0.1 M)**

| Test | Hydroxide (M) | Nitrite (M) | Nitrate (M) | Chloride (M) | Fluoride (M) | Sulfate (M) | PF |
|---|---|---|---|---|---|---|---|
| 1 | 0.0001 | 1.2 | 2.75 | 0 | 0 | 0.2 | 0.68 |
| 2 | 0.0001 | 0.48 | 3.3 | 0 | 0.3 | 0.12 | 0.15 |
| 3 | 0.0001 | 0 | 0 | 0.2 | 0.3 | 0.2 | 0.00 |
| 4 | 0.0001 | 0 | 5.5 | 0.4 | 0 | 0.1 | 0.00 |
| 5 | 0.0001 | 1.2 | 0 | 0.4 | 0.15 | 0 | 0.25 |
| 6 | 0.0001 | 1.2 | 5.5 | 0.4 | 0.3 | 0.2 | 0.13 |
| 7 | 0.24 | 0.72 | 2.2 | 0.16 | 0 | 0 | 0.63 |
| 8 | 0.48 | 0.96 | 5.5 | 0.32 | 0.06 | 0.2 | 0.48 |
| 9 | 0.6 | 0 | 0 | 0 | 0 | 0 | N/A |
| 10 | 0.6 | 0.6 | 2.75 | 0.2 | 0.15 | 0.1 | 0.83 |
| 11 | 0.6 | 0.6 | 2.75 | 0.2 | 0.15 | 0.1 | 0.83 |
| 12 | 0.6 | 0.6 | 2.75 | 0.2 | 0.15 | 0.1 | 0.83 |
| 13 | 0.6 | 0.6 | 2.75 | 0.2 | 0.15 | 0.1 | 0.83 |
| 14 | 0.72 | 0.24 | 0 | 0.4 | 0.12 | 0.16 | 0.84 |
| 15 | 0.96 | 0 | 4.4 | 0.24 | 0.24 | 0.04 | 0.79 |
| 16 | 1.2 | 0 | 5.5 | 0 | 0 | 0.2 | 1.76 |
| 17 | 1.2 | 1.2 | 0 | 0 | 0.3 | 0.1 | 6.74 |
| 18 | 1.2 | 1.2 | 1.1 | 0.08 | 0.18 | 0.08 | 3.33 |
| 19 | 1.2 | 1.2 | 5.5 | 0.2 | 0 | 0 | 1.30 |
| 20 | 1.2 | 0.6 | 0 | 0.4 | 0 | 0.2 | 1.59 |
| 21 | 1.2 | 0 | 2.75 | 0.4 | 0.3 | 0 | 0.87 |

Experiments were also performed with simple chemistry simulants to determine effects at hydroxide concentrations up to 6 M and at elevated temperatures. The simulant constituents were statistically selected and are listed in

Table 4-3.

**Table 4-3 Simulant chemistries for elevated hydroxide concentrations**

| Test | Temperature (°C) | Hydroxide (M) | Nitrite (M) | Nitrate (M) | Chloride (M) | Fluoride (M) | PF |
|---|---|---|---|---|---|---|---|
| 1 | 75 | 1.2 | 0.2 | 0.2 | 0 | 0.2 | 7.45 |
| 2 | 50 | 6 | 0.2 | 0.2 | 0.2 | 0.2 | 10.40 |
| 3 | 75 | 6 | 1.2 | 1.2 | 0.2 | 0.2 | 8.84 |
| 4 | 75 | 6 | 1.2 | 0.2 | 0 | 0 | 251.10 |
| 5 | 50 | 1.2 | 1.2 | 0.2 | 0.2 | 0 | 3.26 |
| 6 | 50 | 6 | 0.2 | 1.2 | 0 | 0 | 40.56 |
| 7 | 75 | 1.2 | 0.2 | 1.2 | 0.2 | 0 | 2.20 |
| 8 | 50 | 1.2 | 1.2 | 1.2 | 0 | 0.2 | 4.93 |
| 9 | 55 | 2.4 | 1.2 | 1.2 | 0 | 0.1 | 11.98 |
| 10 | 65 | 4.8 | 0.7 | 0.2 | 0.05 | 0 | 38.43 |
| 11 | 70 | 1.2 | 0.45 | 0.45 | 0.1 | 0.2 | 3.18 |
| 12 | 50 | 3.6 | 0.2 | 0.95 | 0.15 | 0.05 | 7.84 |
| 13 | 75 | 6 | 0.95 | 0.7 | 0.2 | 0.15 | 10.18 |

Additional testing in this task was performed based on historical data to address gaps in the data at hydroxide concentrations from 0.01 to 0.1 M. The simulants have a more complex chemistry including, in addition from the simple chemistry, formate, acetate, glycolate, oxalate and phosphate. The additional constituents represent previous historical data and were maintained as to not add additional variables. However, those species are in a low concentration and do not affect the statistical significance of the species toward pitting corrosion already established.

Table 4-4 lists the twenty-five statistically designed tests at different concentrations of hydroxide, nitrite, nitrate, chloride, fluoride, acetate and oxalate. The concentration of TIC, sulfate, formate, glycolate and phosphate was maintained at 0.1, 0.1, 0.03, 0.02 and 0.04 M, respectively.

**Table 4-4 Simple chemistries simulants at a temperature of 75 ºC for elevated temperature testing (TIC was 0.1 M)**

| Test | Temperature (ºC) | Hydroxide (M) | Nitrite (M) | Nitrate (M) | Chloride (M) | Fluoride (M) | Acetate (M) | Oxalate (M) | PF |
|---|---|---|---|---|---|---|---|---|---|
| 1 | 35 | 0.04 | 0.8 | 0.93 | 0.02 | 0.01 | 0.02 | 0.02 | 1.18 |
| 2 | 35 | 0.015 | 1.06 | 0.87 | 0.01 | 0.07 | 0.02 | 0.02 | 1.23 |
| 3 | 35 | 0.01 | 2.18 | 0.96 | 0.07 | 0.18 | 0.025 | 0.015 | 1.10 |
| 4 | 35 | 0.03 | 2.25 | 1.01 | 0.1 | 0.09 | 0.025 | 0.015 | 1.17 |
| 5 | 35 | 0.05 | 2.09 | 1.04 | 0.03 | 0.1 | 0.025 | 0.015 | 1.73 |
| 6 | 35 | 0.03 | 2.82 | 2.73 | 0.11 | 0.01 | 0.0325 | 0.075 | 1.00 |
| 7 | 35 | 0.02 | 2.2 | 0.78 | 0.04 | 0.11 | 0.025 | 0.015 | 1.72 |
| 8 | 35 | 0.02 | 0.75 | 1 | 0.01 | 0.01 | 0.02 | 0.02 | 1.08 |
| 9 | 35 | 0.09 | 1 | 1 | 0.04 | 0.04 | 0.02 | 0.02 | 1.20 |
| 10 | 35 | 0.06 | 1 | 1 | 0.04 | 0.06 | 0.02 | 0.02 | 1.01 |
| 11 | 35 | 0.05 | 0.7 | 1 | 0.01 | 0.04 | 0.02 | 0.02 | 1.07 |
| 12 | 35 | 0.075 | 0.5 | 1 | 0.01 | 0.01 | 0.02 | 0.02 | 1.13 |
| 13 | 75 | 0.01 | 1.06 | 0.87 | 0.01 | 0.07 | 0.02 | 0.02 | 1.20 |
| 14 | 75 | 0.03 | 2.25 | 1.01 | 0.1 | 0.09 | 0.025 | 0.015 | 1.17 |
| 15 | 75 | 0.05 | 2.09 | 1.04 | 0.03 | 0.1 | 0.025 | 0.015 | 1.73 |
| 16 | 75 | 0.09 | 1 | 1 | 0.04 | 0.04 | 0.02 | 0.02 | 1.20 |
| 17 | 75 | 0.06 | 1 | 1 | 0.04 | 0.06 | 0.02 | 0.02 | 1.01 |
| 18 | 75 | 0.02 | 0.75 | 1 | 0.01 | 0.01 | 0.02 | 0.02 | 1.08 |
| 19 | 75 | 0.05 | 0.7 | 1 | 0.01 | 0.04 | 0.02 | 0.02 | 1.07 |
| 20 | 75 | 0.01 | 2.18 | 0.96 | 0.07 | 0.04 | 0.025 | 0.015 | 1.47 |
| 21 | 75 | 0.125 | 1 | 1.25 | 0.05 | 0.04 | 0.025 | 0.015 | 1.11 |
| 22 | 75 | 0.175 | 1 | 1.25 | 0.05 | 0.04 | 0.025 | 0.015 | 1.28 |
| 23 | 75 | 0.225 | 0.75 | 1 | 0.075 | 0.04 | 0.025 | 0.015 | 1.20 |
| 24 | 75 | 0.25 | 0.75 | 1.25 | 0.075 | 0.04 | 0.025 | 0.015 | 1.16 |
| 25 | 75 | 0.15 | 1.25 | 1 | 0.05 | 0.04 | 0.025 | 0.015 | 1.53 |

For Long Term OCP drift testing, chemistries were chosen in which the previous results showed mixed hysteresis (category 3) in CPP experiments from FY18 work [7]. The simulant chemistries correspond to Test 3, 9 and 12 with simple chemistries that corresponded to PFs between 1 and 2. For test 12, the nitrite concentration was increased from 0 to 0.2 M. The chemical composition of these simulants is given in Table 4-5.

**Table 4-5 Chemical composition of the simple chemistry tests with PF between 1 and 2 test matrix used to test long term potential drift at 35 ºC (TIC 0.1 M, Sulfate 0.2 M)**

| Test | Hydroxide (M) | Nitrite (M) | Nitrate (M) | Chloride (M) | Fluoride (M) | PF |
|---|---|---|---|---|---|---|
| 3 | 0.0001 | 1.2 | 2 | 0 | 0 | 0.93 |
| 9 | 0.3 | 0.6 | 0.07 | 0.1 | 0 | 1.92 |
| 12 | 0.6 | 0.2 | 0.6 | 0.05 | 0 | 3.59 |

#### 4.1.3 *Testing Apparatus*

A glass corrosion cell with approximately 700 mL of simulant was used for electrochemical testing and long-term potential drift. A picture of the setup is shown in Figure 4-3. Two carbon rods connected by a jumper wire were used as the counter electrode. A saturated calomel electrode (SCE) was used as the reference electrode and placed in a bridge with a glass frit. Prior to each test, the electrode was checked against a standard (a SCE in 1 M KCl solution that was not used for testing) and several times during long term testing. The cell was placed on top of a hotplate with temperature control and the temperature was maintained by a thermocouple from the hotplate immersed in solution. REF600 and Interface E (Gamry) potentiostats were used in this study. Prior to initiating the electrochemical tests, ASTM G5 [14] was performed for quality assurance. ASTM G5 protocols were also run at the conclusion of testing. The standardized CPP protocol, shown in Table 2-2, was used to gather the data. In several instances, EIS scans were performed over a wide frequency range. At the end of testing, the standard CPP protocol was used to test the susceptibility to localized corrosion.

For long-term OCP drift testing, a multiplexer (Gamry) was used to obtain OCP values for each of the six coupons. Three corrosion cells were used, each with two working electrodes. OCP was measured every 10 seconds for the first week (i.e., 1-2 days) and then every hour for approximately 4 months.


**Figure 4-3 Image of the experimental setup used.**

4.2 Secondary Liner Corrosion Testing

4.2.1 *Materials*

Circular coupons of 1 inch diameter with a thickness of 0.125 inch and polished to a 600-grit finish on one side (procured from Metal Samples Company) were used for this task. A coated wire was placed in a lateral position to be able to hang the coupons with no electrical connection to the coupon. The coupons were mounted with a two-part clear epoxy solution (EpoKwick from Buehler) so that one face of the coupon was exposed. Prior to using the coupons, they were rinsed with distilled water, then acetone. A picture of a mounted coupon is shown in Figure 4-4.

**Figure 4-4 One coupon mounted in epoxy cold mount with wire**

4.2.2 *Simulants and VCIs*

GW simulant was used for the secondary liner corrosion studies. The composition of the GW simulant is provided in Table 4-6 and is presented in more detail in Appendix D. The pH of the simulant was adjusted using sodium carbonate and acetic acid to 7.6 after preparation. Several VCI formulations were mixed in GW for the study of VCI effects on corroded materials that were recommended by Cortec® using their VCI formulations: VpCI-337 (liquid), VpCI-649MF (liquid) and VpCI-609 (powder). The VCI recommended dosages are named VCI-A and VCI-B and are listed in Table 4-7.

**Table 4-6 Composition of GW Simulant**

| Chemical | Concentration (M) |
|---|---|
| Sodium bicarbonate | 1.750E-03 |
| Calcium hydroxide | 1.500E-03 |
| Potassium nitrate | 2.400E-04 |
| Strontium Nitrate | 2.874E-06 |
| Ferric sulfate | 6.250E-04 |
| Sodium Metasilicate, 5-hydrate | 6.000E-04 |
| Ferric chloride | 7.667E-05 |
| Manganese Chloride | 3.100E-04 |
| Acetic Acid | 3.000E-04 |
| pH adjusted using sodium carbonate and acetic acid | 7.6 |

**Table 4-7 VCI strategy with manufacturer recommended dosage**

| VCI strategy | VCI product used | Recommended dosage |
|---|---|---|
| VCI-A | VpCI-337 | 10% v/v VpCI-337 in GW simulant (100 mL in VpCI-337 plus 900 mL of GW simulant for 1 L) |
| VCI-B | VpCI-609 and VpCI-649MF | 10% wt. VpCI-609 in GW (100 g VpCI-609 in 1 L of GW) and 0.75% v/v VpCI-649MF in GW (7.5 mL in 1 L of GW) |

4.2.3 *Testing Apparatus*

Glass vessels of dimensions 3.3 ft tall and 5.5 inch diameter were used for each experiment. Approximately 1 to 2 L of simulant was added to a vessel for each experiment. Each vessel has a water jacket around the simulant holding area which was used to circulate warm water to maintain the simulant temperature at 45 ± 2 °C. Each vessel also has several ports, which were used to insert thermocouples and ER probes (only for two vessels). An image showing the three vessels used is presented in Figure 4-5(a). Coupons were exposed to the electrolyte and vapors of the electrolyte in each experiment by suspending them through a rod shown in Figure 4-5(b). The rods holding the coupons were placed inside the vessels. Coupons were suspended from stainless steel rings that are welded to a stainless-steel rod at three different locations. Three vessels were used and for these vessels six coupons were placed at the top, intermediate and low position. Also, six coupons were placed lower than the low position, so they can be immersed into the solution for a total of 24 coupons per vessel: 72 coupons overall. The coupons' positions, with respect to electrolyte in each vessel, simulated different vapor space conditions and water levels in the drain slots. These levels are described as follows.

Level 1: Bottom or low level. Coupons were dipped in the simulant for five minutes prior to testing. The coupons were hung at the bottom fixed ring of the rod shown in Figure 4-5(b). These coupons were suspended approximately 1 inch above the liquid level of the simulant. Every two weeks, the coupons were lowered into the simulant for 5 minutes. This level is representative of the situation when secondary liner bottom plate experienced periodic wetting/drying.

Level 2: Intermediate or middle level. Coupons were dipped in the simulant for five minutes prior to testing. The coupons were hung at the middle-fixed ring approximately 18 inches above the liquid simulant in each vessel. This level is representative of a vapor space region of the secondary liner bottom that at one time was exposed to water but has infrequent or no contact with the water. However, this region is exposed to the humidified air.

Level 3: Top or high level. This set of coupons was not exposed to the solution prior to testing. The coupons were suspended approximately 36 inches above the simulant. This level is representative of the secondary liner bottom plate region that is only exposed to the humidified air and any volatile species from the solution.


(a) (b)

**Figure 4-5 Images of the (a) experimental configuration, and (b) steel rod to suspend the coupons inside the vessel containing electrolyte.**

Table 4-8 shows the vessel and the corresponding VCI strategy used. Vessels 1 and 2 had 100% of the recommended dosage of VCI-A and VCI-B, respectively. Vessel 3 had 10% of the recommended dosage of VCI-B. ER probes were placed in Vessels 1 and 2, near the coupons at Level 1. ER probe data was collected periodically. Six coupons from each position were removed after two months. Then the corresponding VCI solution (VCI-A or VCI-B) was added and the rest of the coupons were exposed for additional two months. Coupons that were removed, were cleaned with Clarke's solution [15] to remove corrosion products and report accurate weight losses.

**Table 4-8 Experimental details of Vapor Space Corrosion Setup**

| Vessel | VCI strategy |
|---|---|
| 1 | GW + 100% of recommended dosage VCI-A |
| 2 | GW + 100% of recommended dosage VCI-B |
| 3 | GW + 10% of recommended dosage VCI-B |

4.3 MIC Testing

The two bottles of water received from Hanford from an LDP were analyzed using commercial MIC kits. The water samples were taken near DST AZ-101. All steps for performing the experiment are located within the BART™ User Manual (Droycon Bioconcepts, Inc) [16] and MICkit® 5 Instructions (BTI products LLC) [17]. All MICkit® and BART™ testers were labeled and put into the hood on a clean cloth. Approximately 15 ml of water sample was pipetted into each BART™ tester. This process was performed for both bottles of water. This process is known as serial dilution and it was used for all five bacteria types of both water bottles. The BART™ Tester samples were observed for changes in appearance on day one, two, three, eight, nine, and fifteen.

Figure 4-6 shows the changes in the BART™ solutions that may be observed during the growth of heterotrophic aerobic bacteria (HAB) (a), acid producing bacteria (APB) (b), and sulfate reducing bacteria (SRB) (c), respectively. Table 4-9 lists the projected range of bacteria depending on the day that changes are noted in the BART™ testers.

**Table 4-9 The range of bacteria population in each BART type.**

| **BART Potential HAB** | **Days** | **Population (cfu/ml)** |
|---|---|---|
| Aggressive | 1-2 | 575,000-5,400,000 |
| Moderate | 3-4 | 6,500-61,000 |
| Not Aggressive | 5-6 | <700 |
| **BART Potential APB** | **Days** | **Population (cfu/ml)** |
| Aggressive | 1-3 | 14,000-475,000 |
| Moderate | 4-6 | 75-4,500 |
| Not Aggressive | 7-8 | <10 |
| **BART Potential SRB** | **Days** | **Population (cfu/ml)** |
| Aggressive | 1-5 | 6,000-2,200,000 |
| Moderate | 6-8 | 75-1,400 |
| Not Aggressive | 9-11 | <20 |

For the MICkit® 1.0 ml of the water was withdrawn from bottle #1 with a syringe, and then placed into the rubber stopper for the first type of bacteria (e.g., low nutrient). The water was injected and withdrawn multiple times to mix the water. Then 1.0 ml of water was removed from bottle #1 and placed in bottle #2 mixing the water as done previously. Next 0.1 ml of sample was removed from bottle #2 and inserted in bottle #3. Finally,0.1 ml of solution from bottle #3 was mixed into bottle #4. MICkit® samples were observed for changes in appearance on days 1, 2, 3, 4, 8, 9, 15, 21, and 30. Figure 4-7 shows the changes in the MICkit® solutions that should be observed when low nutrient bacteria (LNB), iron-related bacteria (IRB), anerobic bacteria (ANA), APB, and SRB are formed respectively. Table 4-10 presents the correlation between the final MICkit® bottle number and the bacterial population. Colony-forming unit (cfu) is a measure of viable bacteria per ml of the volume in the test.

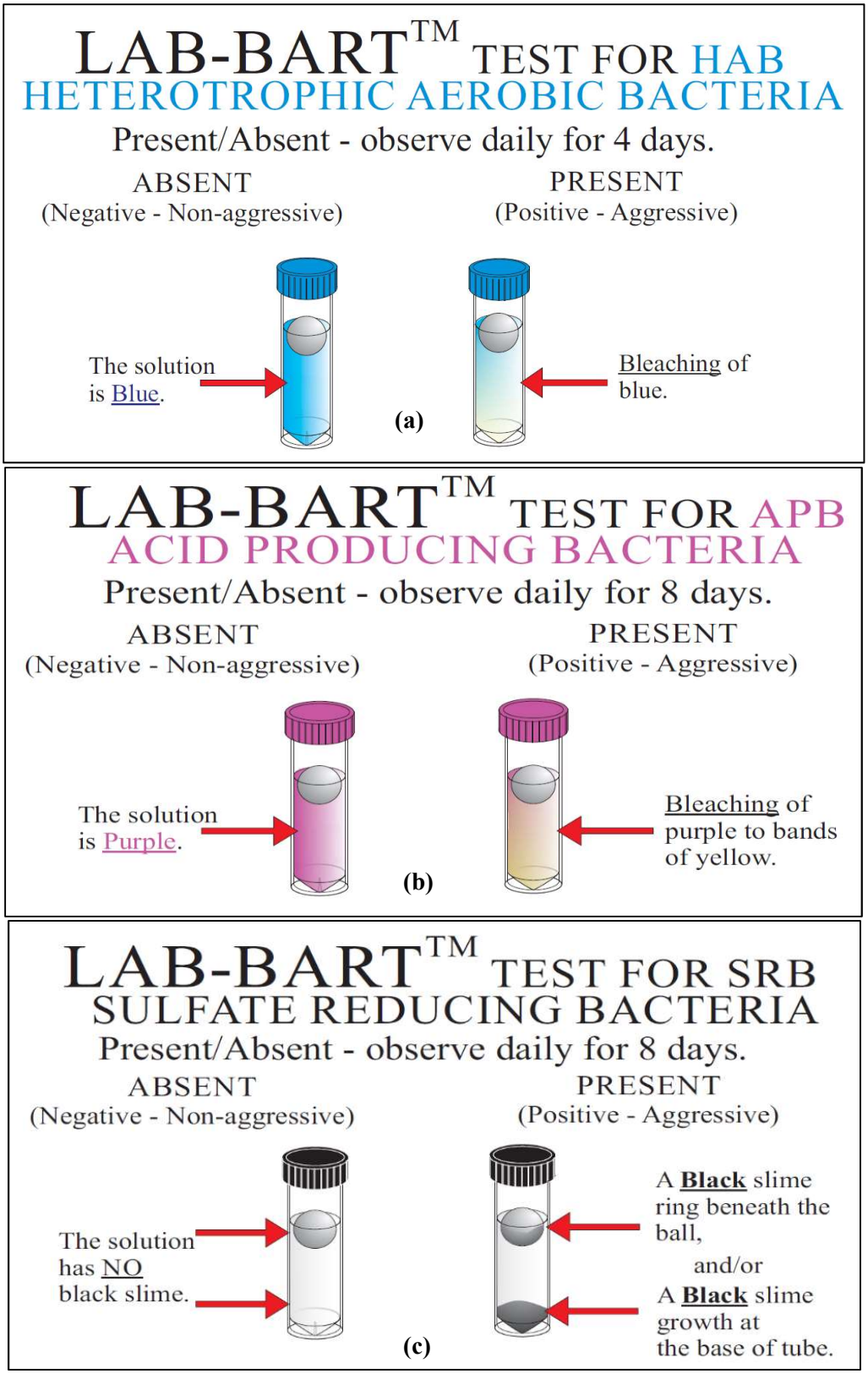


**Figure 4-6 Examples of the changes in solution noticed when (a) HAB [18], (b)APB [19] and (c) SRB [20] are active in solution.**

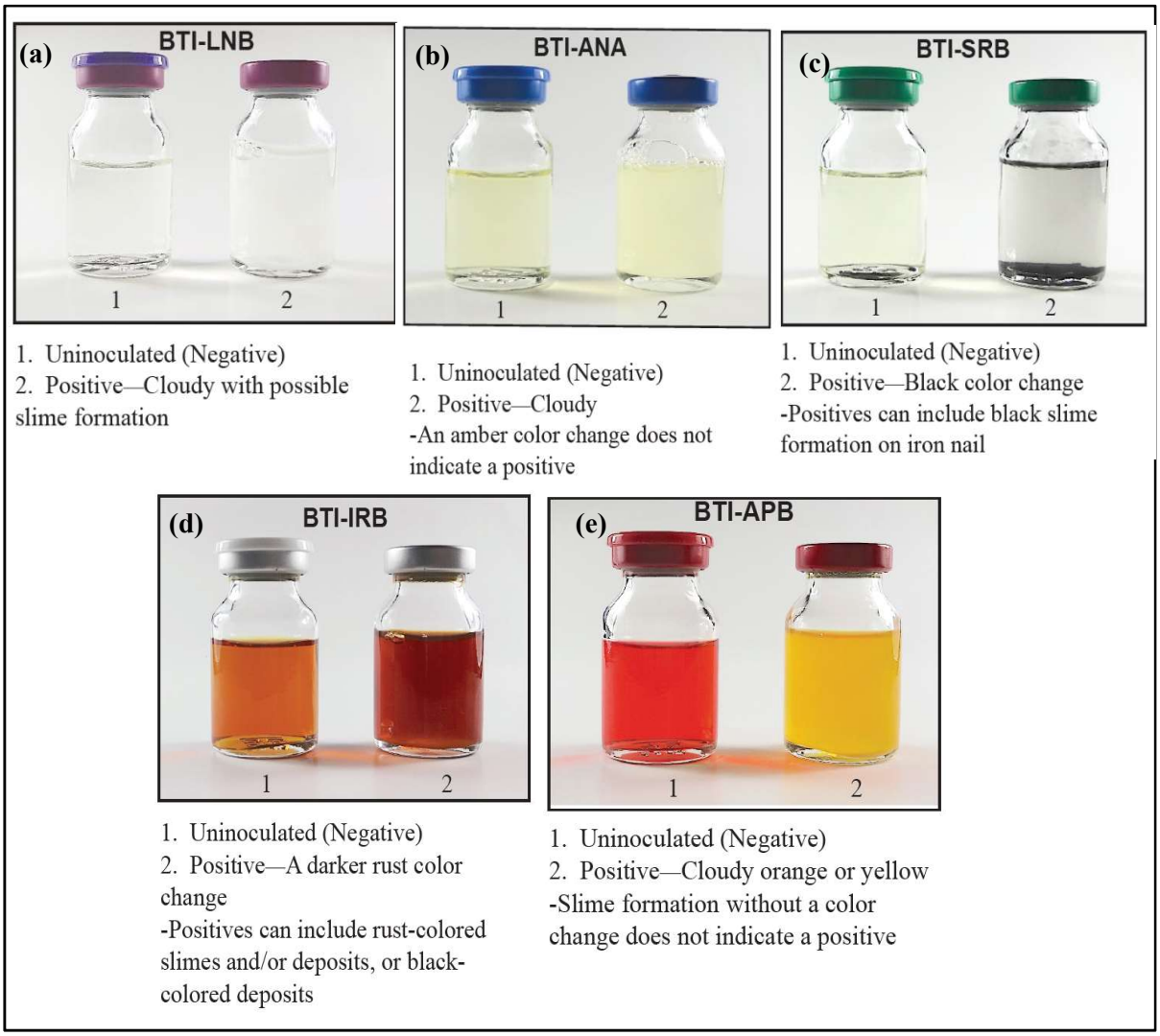


**Figure 4-7 Examples of the changes in solution noticed for when the five bacteria types: (a) LNB, (b) ANA, (c) SRB, (d) IRB and (e) APB are present in solution [17]**

**Table 4-10 The number of viable bacteria present per ml of solution.**

| Highest Bottle # to Turn Positive | Range of Viable Bacteria Per mL of Liquid Sample |
|---|---|
| 0 | 1-10 |
| 1 | 10-100 |
| 2 | 1,000-10,000 |
| 3 | 100,000-1,000,000 |
| 4 | >10,000,000 |

4.4 Quality Assurance

Data for all Tasks were recorded in the electronic laboratory notebook system, notebook number G8519-00126.

Requirements for performing reviews of technical reports and the extent of review are established in manual E7 2.60. SRNL documents the extent and type of review using the SRNL Technical Report Design Checklist contained in WSRC-IM-2002-00011, Rev. 2.

## 5.0 Results and Discussion

Simulant constituents of each tests as well as CPP results and pictures of the bullet coupon after test are shown in Appendix A for the New Limits pitting corrosion test at elevated temperatures only, in Appendix B at elevated temperatures and hydroxide concentrations and in Appendix C for testing between 0.01 to 0.1 M hydroxide to address gaps in historical data. Also included in these three appendices, are any modified ASTM G192 testing that was performed due to inconclusive results from CPP. Simulant constituents for Secondary Liner Corrosion tests are listed in a table in Appendix D. The pictures of the samples after exposure and cleaning for this task are shown in Appendix E. Additional OCP data plotted for each solution with different carbon steel surfaces: ground 600 grit and mill scale are presented in Appendix F The results and discussions for the report are enumerated by the corresponding task.

5.1 New Limits Pitting Corrosion Testing

New Limits Testing has focused on establishing the PF as an acceptable criterion for the development of a new waste chemistry envelope. The PF targets specific species of the waste that significantly influence pitting corrosion and by calculating a ratio of inhibitors versus aggressive species, it can predict susceptibility towards pitting corrosion. For FY19, the PF equation was addressed for elevated temperatures and for other conditions to continue validating the equation as a satisfactory metric to determine pitting corrosion susceptibility over a more complete range of potential exposure conditions. More information of the New Limits Testing and how it is being recommended to be used for updating the waste chemistry limits, as well as a summary of all the testing performed can be found in a recent report by Wiersma et al. [8].

A statistically designed matrix was developed in order to test the hypothesis that the PF model developed for test temperatures up to 50 ºC remained applicable at temperatures up to 75 ºC. The resulting matrix consisted of twenty-one tests. The standard CPP protocol was utilized for determining susceptibility towards localized corrosion. The CPP result was catalogued and a binary response of pass (“0”) or fail (“1”) designation for each test was adopted. More information on the categories are found in another report [21]. Category 1 and 2 are passes, category 4 and 5 are fails. The category 3, which indicates mixed hysteresis result is deemed inconclusive and the conditions are re-tested using a modified ASTM G192 test method developed by DNV-GL [22]. The modified ASTM G192 method provides a definitive categorization of pass or fail by measuring the repassivation potential. If the repassivation potential is observed and it is greater than 200 mV with respect to corrosion potential it is a pass (i.e., a category 2), while if the repassivation potential is less or equal than 200 mV with respect to corrosion potential it is a fail (i.e., a category 4 or 5).

Table 5-1 lists the temperature, resulting pH at room temperature, CPP category, a repassivation potential (if observed) and the binary result that indicates pass or fail for the twenty one tests.

**Table 5-1 Test conditions and results of testing from statistically designed matrix at 75 ºC.**

| Test | Category | Pitting on sample | Corrosion Potential (mV vs. SCE) | Repassivation Potential (mV vs. SCE) | Logistic Approach |
|---|---|---|---|---|---|
| 1 | 4 | Yes | -234 | -146 | 1 |
| 2 | 3 | Yes | -234 | No (G192) | 1 |
| 3 | 5 | Yes | -459 | N/A | 1 |
| 4 | 5 | Yes | -386 | N/A | 1 |
| 5 | 5 | Yes | -249 | N/A | 1 |
| 6 | 5 | Yes | -149 | N/A | 1 |
| 7 | 5 | Yes | -314 | N/A | 1 |
| 8 | 3 | Yes | -250 | No (G192) | 1 |
| 9 | 1 | Yes | -335 | N/A | 0 |
| 10 | 5 | Yes | -341 | N/A | 1 |
| 11 | 5 | Yes | -244 | N/A | 1 |
| 12 | 4 | Yes | -363 | -306 | 1 |
| 13 | 5 | Yes | -360 | N/A | 1 |
| 14 | 1 | Yes | -358 | N/A | 0 |
| 15 | 5 | Yes | -379 | N/A | 1 |
| 16 | 1 | No | -422 | N/A | 0 |
| 17 | 1 | No | -372 | N/A | 0 |
| 18 | 1 | No | -388 | N/A | 0 |
| 19 | 1 | No | -441 | N/A | 0 |
| 20 | 1 | No | -379 | N/A | 0 |
| 21 | 5 | Yes | -391 | N/A | 1 |

Of the twenty-one tests, ten showed positive hysteresis (category 5), seven negative hysteresis (category 1) and four mixed hysteresis (corresponding to category 3 and category 4 for two test each). By performing modified ASTM G192 tests for category 3 tests, no repassivation potential was obtained so were categorized as fails. By using the PF criterion as a cut-off of 1.2, the occurrence of pitting was accurately predicted. However, there was one case, Test 14, where initially appeared to be a contradiction. The CPP results and pictures for this test are shown in Figure 5-1. The CPP exhibited negative hysteresis, indicating a “pass”, however tiny pits were observed at the surface of the electrode. Pits such as these have been previously shown to be non-propagating [23] and thus this case was considered a “pass”. The model conservatively predicted that a condition was vulnerable to pitting (i.e., the PF was less than 1.2) when the test did not indicate the vulnerability for this case.

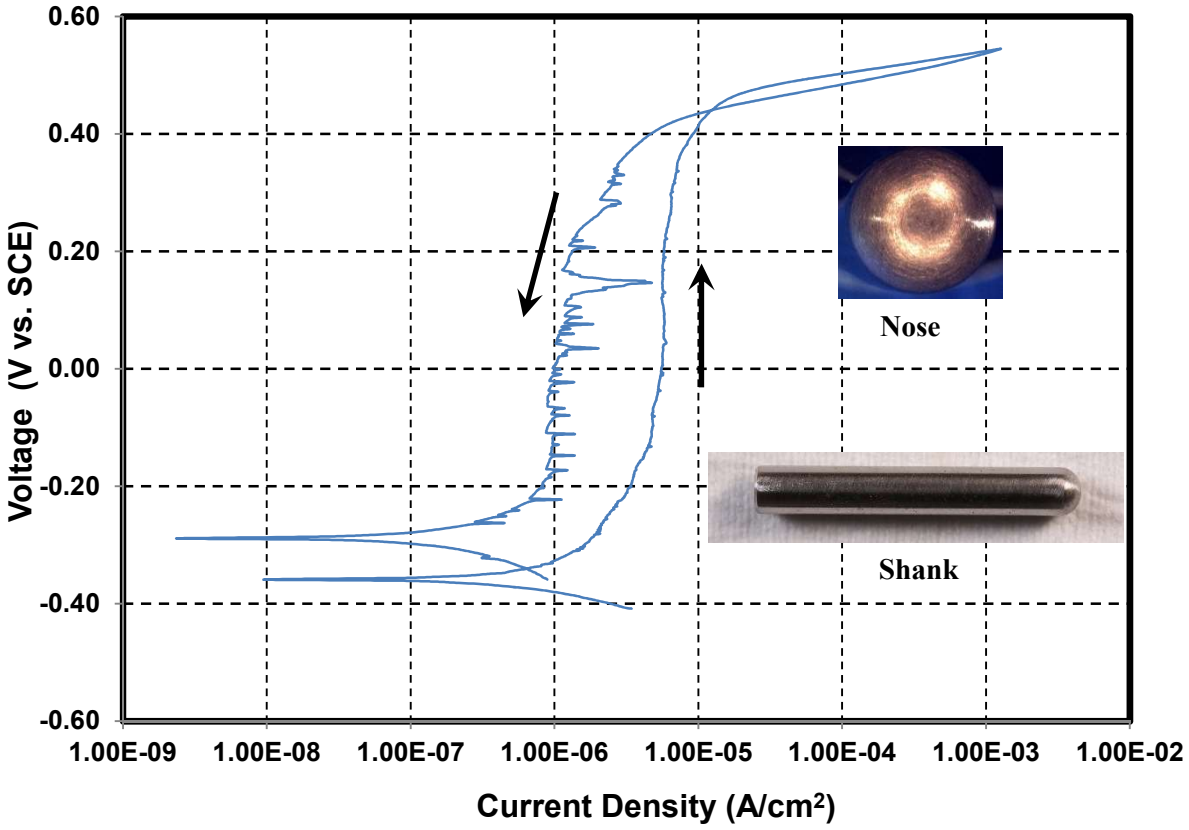


**Figure 5-1 CPP curve of Test 14 with after pictures of shank and nose of bullet coupon**

Additional tests at elevated temperatures and hydroxide concentration up to 6 M were performed. Additional tests at elevated temperatures and hydroxide concentration up to 6 M were performed. The elevated hydroxide concentration was used to address the maximum anticipated hydroxide concentration in the waste tank (6 M hydroxide). These concentrations can be representative of some DSTs. The CPP categories obtained are listed in Table 5-2 as well as temperature, corrosion potential from CPP and if pitting was observed on the samples. The corrosion potential became more negative as the hydroxide concentration was higher than 1.2 M and it reached more negative potentials (-900 mV vs. SCE) at 6 M hydroxide. All cases showed negative hystereses (category 1), except for Test 8 in which a mixed hysteresis (category 3) was observed. However, no pitting was observed, and after performing a modified G192 test, it resulted in a pass. There were several instances in which there was a discoloration in the sample, especially for high hydroxide (4.8 – 6 M) and nitrite concentration (0.7 to 1.2 M). A picture of the discoloration is presented in Figure 5-2 and is visually noticeable compared to a freshly polished surface (Figure 4-1). The discoloration is mostly uniform throughout the sample and by examination under a microscope, no pits were observed.

**Table 5-2 Test conditions and results of testing from statistically designed matrix for elevated temperatures up to 6 M hydroxide**

| Test | Temperature (°C) | Category | Pitting on sample | Corrosion Potential (mV vs. SCE) | Repassivation Potential (mV vs. SCE) | Logistic Approach |
|---|---|---|---|---|---|---|
| 1 | 75 | 1 | No | -366 | N/A | 0 |
| 2 | 50 | 1 | No | -953 | N/A | 0 |
| 3 | 75 | 1 | No (discolored) | -953 | N/A | 0 |
| 4 | 75 | 1 | No (discolored) | -914 | N/A | 0 |
| 5 | 50 | 1 | No | -346 | N/A | 0 |
| 6 | 50 | 1 | No (discolored) | -962 | N/A | 0 |
| 7 | 75 | 1 | No | -364 | N/A | 0 |
| 8 | 50 | 3 | No | -350 | 0.399 (G192) | 0 |
| 9 | 55 | 1 | No | -443 | N/A | 0 |
| 10 | 65 | 1 | No (discolored) | --634 | N/A | 0 |
| 11 | 70 | 1 | No | -372 | N/A | 0 |
| 12 | 50 | 1 | No | -475 | N/A | 0 |
| 13 | 75 | 1 | No (discolored) | -920 | N/A | 0 |

**Figure 5-2 After test picture of bullet coupon for Test 6 for shank (left) and nose (right)**

Supplemental testing to address gaps in historical data was performed for hydroxide concentrations of 0.01 to 0.1 M at low and elevated temperatures (i.e., 35 and 75 ºC) to verify the PF equation at these conditions [8]. The results of the twenty-five electrochemical tests are presented in Table 5-3. The corrosion potential range were from -211 to -340 mV vs. SCE. From the CPP responses, twenty resulted in negative hysteresis (category 1), one positive closed loop considered a pass (category 2) and three mixed hysteresis (category 3). Modified ASTM G192 test resulted in passes for these tests (i.e., repassivation potential obtained was over 200 mV vs. SCE). No pitting was observed in any of the samples.

**Table 5-3 Test conditions and results of testing for hydroxide concentrations between 0.01 to 0.1 M**

| Test | Temperature (°C) | Category | Pitting on sample | Corrosion Potential (mV vs. SCE) | Repassivation Potential (mV vs. SCE) | Logistic Approach |
|---|---|---|---|---|---|---|
| 1 | 35 | 3 | No | -249 | 446 (G192) | 0 |
| 2 | 35 | 1 | No | -273 | N/A | 0 |
| 3 | 35 | 1 | No | -257 | N/A | 0 |
| 4 | 35 | 1 | No | -256 | N/A | 0 |
| 5 | 35 | 1 | No | -259 | N/A | 0 |
| 6 | 35 | 1 | No | -291 | N/A | 0 |
| 7 | 35 | 1 | No | -269 | N/A | 0 |
| 8 | 35 | 1 | No | -309 | N/A | 0 |
| 9 | 35 | 1 | No | -211 | N/A | 0 |
| 10 | 35 | 1 | No | -239 | N/A | 0 |
| 11 | 35 | 1 | No | -255 | N/A | 0 |
| 12 | 35 | 1 | No | -252 | N/A | 0 |
| 13 | 75 | 1 | No | -274 | N/A | 0 |
| 14 | 75 | 3 | No | -214 | 433 (G192) | 0 |
| 15 | 75 | 1 | No | -298 | N/A | 0 |
| 16 | 75 | 1 | No | -328 | N/A | 0 |
| 17 | 75 | 1 | No | -285 | N/A | 0 |
| 18 | 75 | 1 | No | -292 | N/A | 0 |
| 19 | 75 | 2 | No | -265 | 301 | 0 |
| 20 | 75 | 1 | No | -274 | N/A | 0 |
| 21 | 75 | 1 | No | -237 | N/A | 0 |
| 22 | 75 | 3 | No | -318 | 470 | 0 |
| 23 | 75 | 1 | No | -321 | N/A | 0 |
| 24 | 75 | 1 | No | -340 | N/A | 0 |
| 25 | 75 | 3 | No | -307 | 497 (G192) | 0 |

An assessment of the PF model showed that the fifty nine tests performed in this campaign were accurately predicted except one (Test 14 from

Table 5-1) corresponding to a 98% prediction. In this case, the PF was less than 1.2, and the small pits that were observed were determined to be non-propagating. This means that, based on the preliminary results at elevated temperatures, the current PF equation can still predict the pitting susceptibility up to 75 ºC. Thus, no changes were required to the equation (Equation 2). Temperature remained a statistically non-contributing variable to the PF model for regions where the PF was greater than 1.2 [8]. Overall results from the New Limits Pitting Corrosion campaign that started in FY16 up until FY19 are shown in Figure 5-3 for the tests with PFs less than 4. A criterion of PF greater or equal than 1.2 was selected to indicate a region for no pitting susceptibility as defined by the CPP test. An orange line in Figure 5-3 at PF 1.2 emphasizes that this PF was selected as a boundary for the chemistry envelope and values lower than 1.2 can be considered as susceptible for localized corrosion [8]. All tests met this criterion except one (Test 4 from PF 1-2 & Tank Sim [8]). However, this test was conducted in a dilute solution with 0 M Nitrite. Other tests have shown that a minimum of 0.2 M nitrite should be used to provide adequate inhibition in the dilute solutions [8]. Overall, the model can conservatively predict a condition that can be vulnerable to pitting when the test did not show that vulnerability.

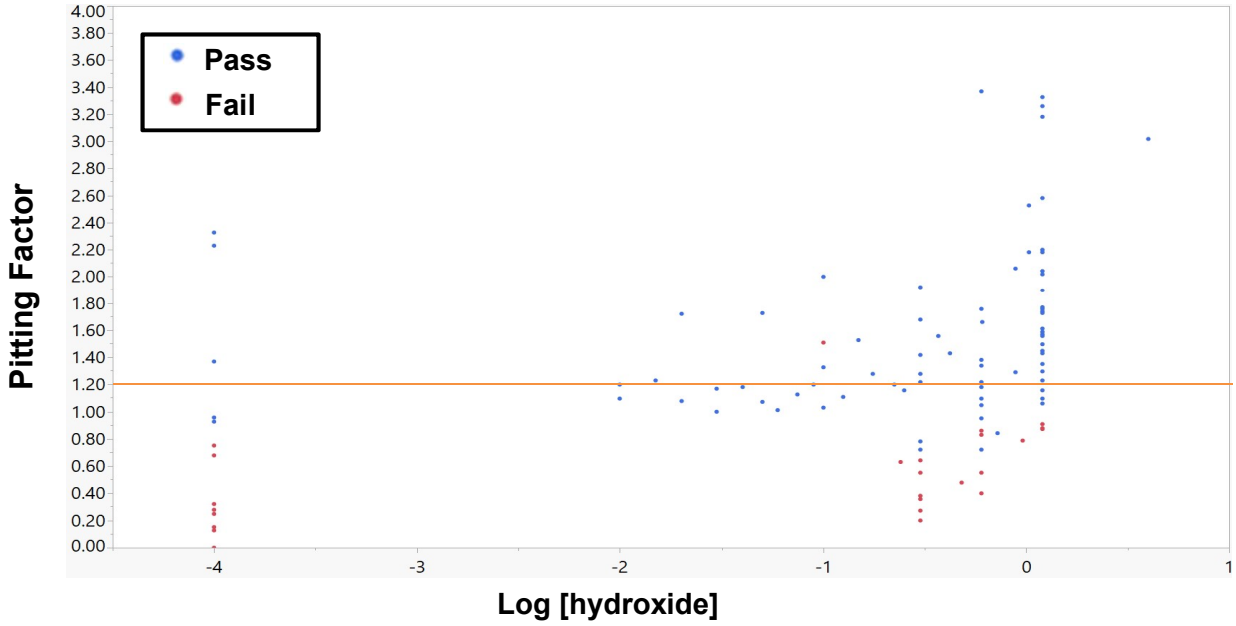


**Figure 5-3 All new limits testing since FY16 with a maximum PF of 4. The orange line indicates PF 1.2 which was selected as the boundary for the new chemistry envelope.**

## 5.2 Secondary Liner Corrosion

The corrosion rate data for the coupons treated with VCI-A in Vessel 1 and VCI-B in Vessel 2 are listed in Table 5-4 and Table 5-5, respectively. The corrosion rate data were obtained for each coupon: (i) surface average corrosion rate, and (ii) maximum pitting corrosion rate. The surface average corrosion rate for each coupon was obtained by recording mass loss and exposure time. The maximum pitting corrosion rate was obtained by measuring the deepest pit on each coupon. Table 5-4 has surface average and pitting corrosion rate data for the GW (2-month) and then GW plus 100% recommended dosage of VCI-A (4-month), and Table 5-5 has the data for the GW (2-month) and then GW plus 100% recommended dosage of VCI-B (4-month). The 2-month coupons were exposed to GW simulant whereas 4-month coupons were exposed to GW plus 100% VCI dosages. The tables' data also include average of surface average and pitting corrosion rates along with corresponding standard deviations. These average values and standard deviations are presented in Figure 5-4 (from Table 5-4 data) and Figure 5-5 (from Table 5-5 data). Vessels

1 and 2 also had ER probes, one immersed in electrolyte and another one just above the electrolyte interface in each vessel. The ER probe data are presented in Figure 5-6.

**Table 5-4. Corrosion Rate Data for Vessel 1 Coupons with Exposure to GW for First Two Months and then GW plus 100% VCI-A for an Additional Two Months**

| Corrosion Type | Corrosion Rate (µm/yr) | | | | | | | |
|---|---|---|---|---|---|---|---|---|
| | Immersed | | Level 1 | | Level 2 | | Level 3 | |
| | 2-month* | 4-month* | 2-month* | 4-month* | 2-month* | 4-month* | 2-month* | 4-month* |
| Surface Average Corrosion Rate | 170 | 79 | 69 | 48 | 5 | 3 | 107 | 25 |
| | 221 | 112 | 20 | 61 | 48 | 3 | 20 | 0 |
| | 97 | 91 | 74 | 76 | 51 | 5 | 23 | 23 |
| Average** ± std*** | 163 ± 63 | 94 ± 17 | 54 ± 29 | 62 ± 14 | 35 ± 26 | 3 ± 2 | 50 ± 49 | 16 ± 14 |
| Maximum Pitting Corrosion Rate | 569 | 251 | 757 | 368 | 813 | 216 | 516 | 330 |
| | 589 | 251 | 782 | 358 | 673 | 183 | 653 | 434 |
| | 480 | 114 | 620 | 1034 | 663 | 315 | 490 | 439 |
| Average** ± std*** | 546 ± 58 | 206 ± 79 | 720 ± 87 | 587 ± 387 | 716 ± 84 | 238 ± 69 | 553 ± 87 | 401 ± 62 |

*2-month: GW only exposure, 4-month: GW for first two months and GW+100% VCI-A thereafter
**Average values are calculated for 3 coupons
***std denotes standard deviation of the corrosion rate data used to calculate the average

**Table 5-5. Corrosion Rate Data for Vessel 2 Coupons with Exposure to GW for First Two Months and then GW plus 100% VCI-B for an Additional Two Months**

| Corrosion Type | Corrosion Rate (µm/yr) | | | | | | | |
|---|---|---|---|---|---|---|---|---|
| | Immersed | | Level 1 | | Level 2 | | Level 3 | |
| | 2-month* | 4-month* | 2-month* | 4-month* | 2-month* | 4-month* | 2-month* | 4-month* |
| Surface Average Corrosion Rate | 236 | 112 | 155 | 76 | 3 | 41 | 89 | 3 |
| | 43 | 117 | 102 | 99 | 5 | 3 | 3 | 13 |
| | 234 | 132 | 112 | 79 | 5 | 3 | 94 | 10 |
| Average** ± std*** | 171 ± 111 | 120 ± 11 | 123 ± 28 | 85 ± 13 | 4 ± 2 | 15 ± 22 | 62 ± 51 | 9 ± 5 |
| Maximum | 747 | 338 | 1351 | 620 | 0 | 310 | 445 | 269 |
| | 445 | 310 | 1143 | 218 | 475 | 0 | 287 | 315 |

| **Pitting Corrosion Rate** | 1016 | 302 | 787 | 572 | 351 | 462 | 625 | 282 |
|---|---|---|---|---|---|---|---|---|
| **Average** ± std*** | 736 ± 286 | 317 ± 19 | 1094 ± 285 | 470 ± 219 | 276 ± 246 | 257 ± 236 | 452 ± 169 | 289 ± 24 |

*2-month: GW only exposure, 4-month: GW for first two months and GW+100% VCI-A thereafter
**Average values are calculated for 3 coupons
***std denotes standard deviation of the corrosion rate data used to calculate the average

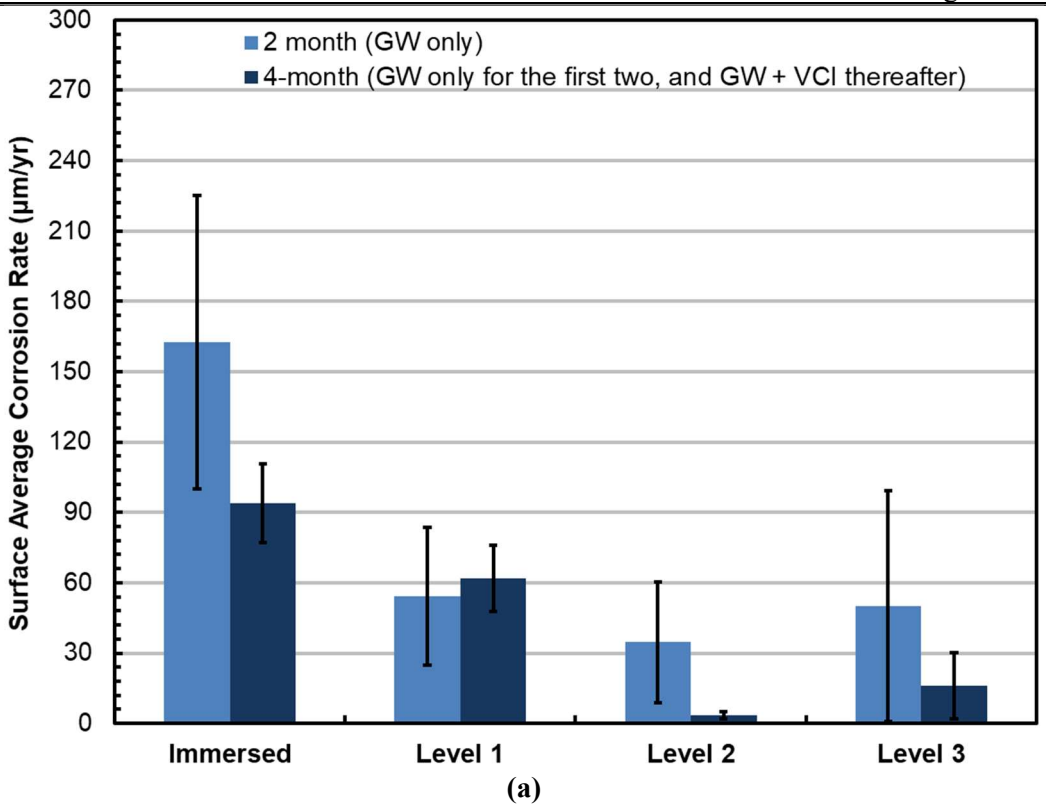


**(a)**

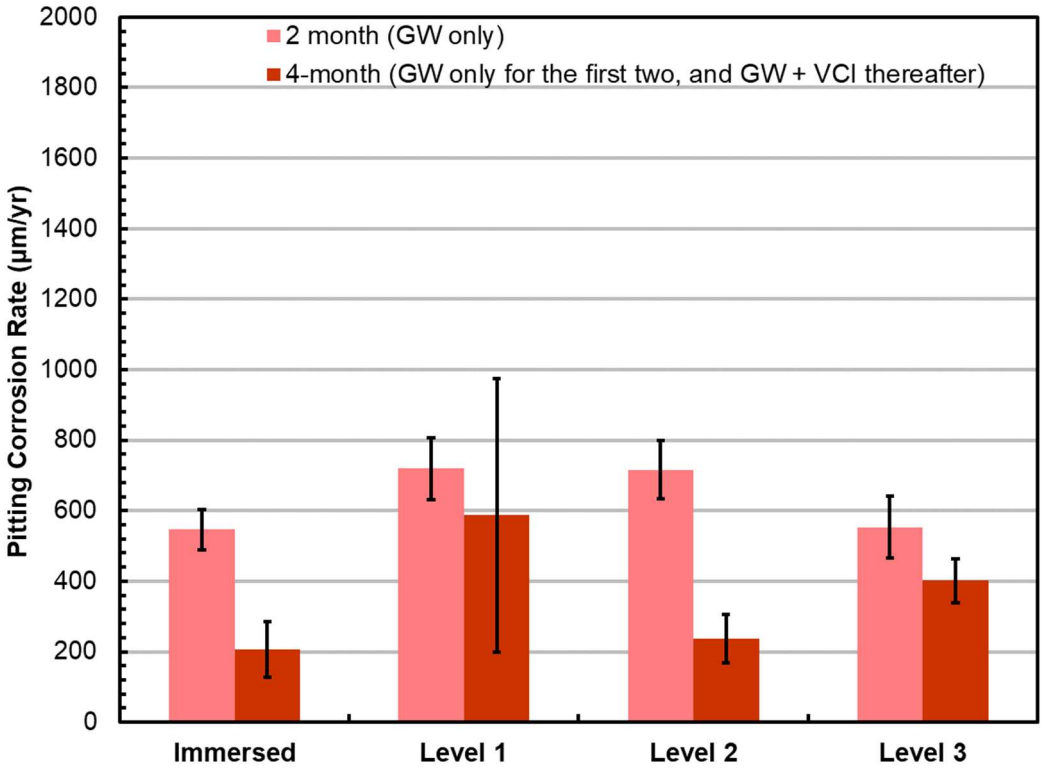


**(b)**

**Figure 5-4. Average of (a) surface average, and (b) pitting corrosion rates for coupons in Vessel 1 (GW, and then GW + 100% VCI-A). The black line in each bar represents the standard deviation.**

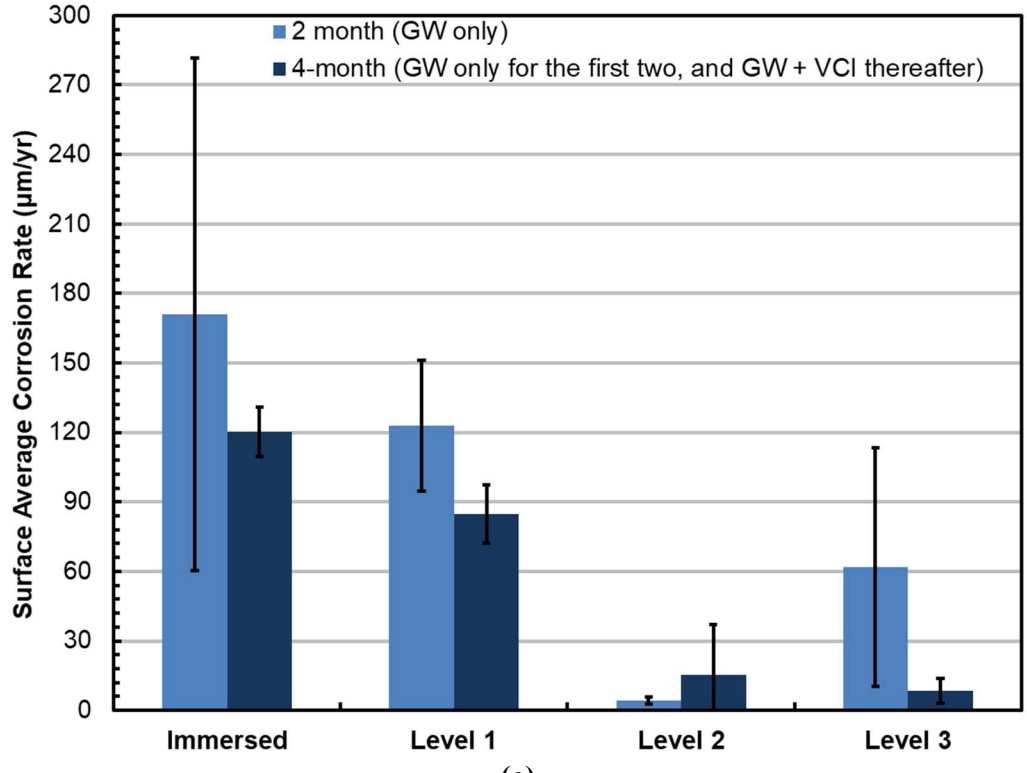


**(a)**

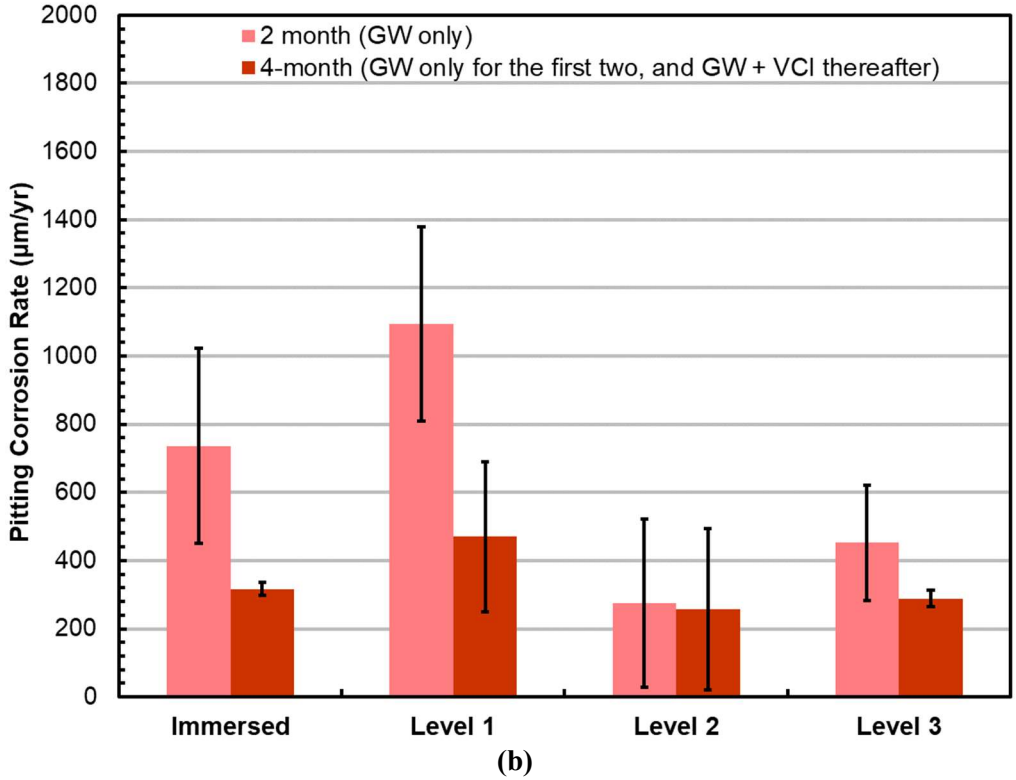


**(b)**

**Figure 5-5. Average of (a) surface average, and (b) pitting corrosion rates for coupons in Vessel 2 (GW, and then GW + 100% VCI-B). The black line in each bar represents the standard deviation.**

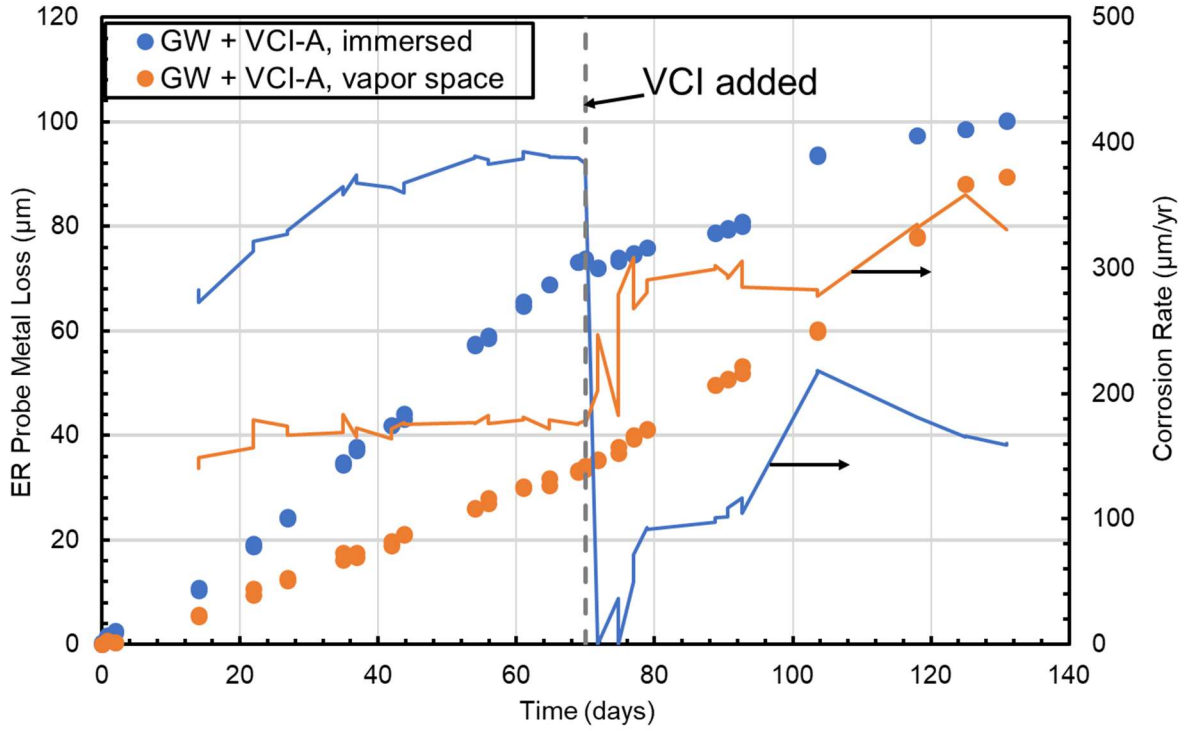


**(a)**

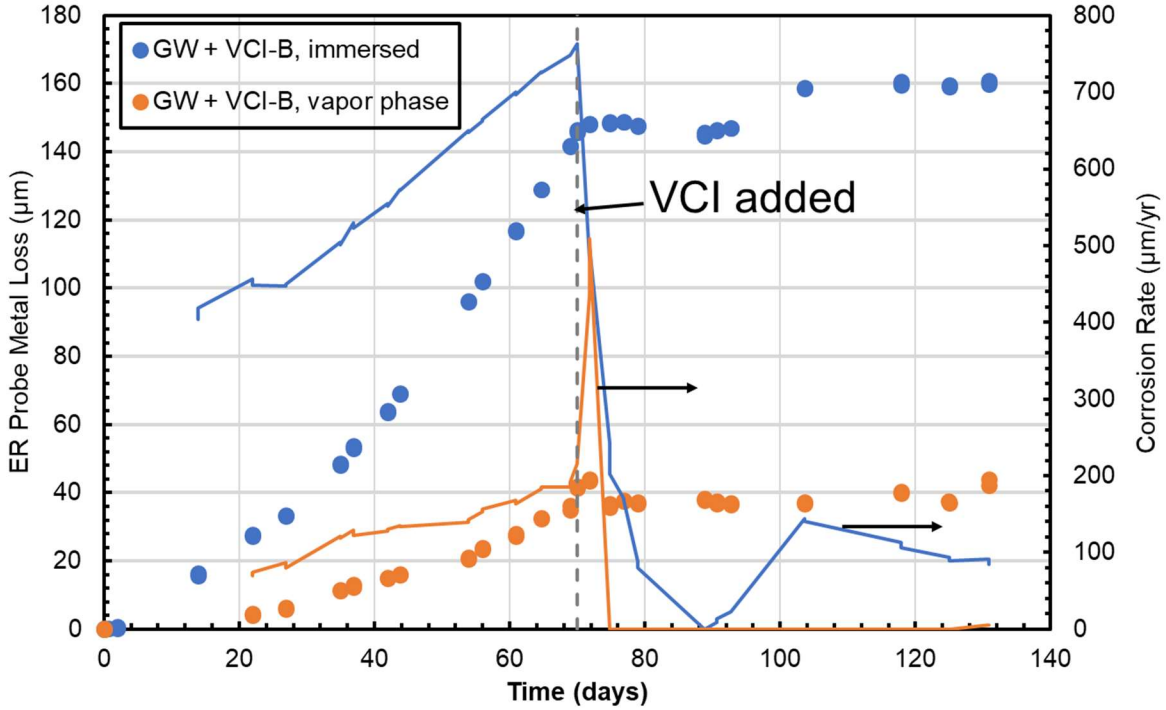


**(b)**

**Figure 5-6. (a) Vessel 1 and (b) Vessel 2 ER probe metal loss data and corresponding corrosion rates. The ER Probe data is represented by filled circles, and corrosion rates by solid lines.**

Vessel 1 corrosion rate data in Figure 5-4(a) show that VCI-A dosage lowered the corrosion rate except for the Level 1 coupons. Two ER probes were also placed in Vessel 1; one was immersed in the solution and another one at Level 1. The ER probe metal loss data and corresponding corrosion rates are presented in Figure 5-6(a). The Figure 5-4 (a) corrosion rate data are consistent with the ER probe data in Figure 5-6 (a). As per the ER probe data, the immersed coupons' corrosion rate should have decreased, and Level 1 coupons' corrosion rate should have increased after VCI-A addition. In Figure 5-4 (a), the 4-month immersed coupon corrosion rate is lower than the 2-month coupon, and 4-month Level 1 coupon corrosion rate is higher than the 2-month coupon, and thus, a consistency is observed between the ER probe and coupon data. It is, however, noted that the pitting corrosion rate decreased for all four sets, i.e., immersed and Levels 1-3, of coupons after VCI-A addition as seen in Figure 5-4 (b), indicating that addition of VCI-A helps arrest propagation of pitting corrosion.

Vessel 2 corrosion rate data in Figure 5-5(a) show that VCI-B dosage lowered the corrosion rate except for the Level 2 coupons. Two ER probes were also placed in Vessel 2; one was immersed in the solution and another one at Level 1. The ER probe metal loss data and corresponding corrosion rates are presented in Figure 5-6 (b). The Figure 5-5 (a) corrosion rate data are consistent with the ER probe data in Figure 5-6 (b). As per the ER probe data, the immersed and Level 1 coupons' corrosion rate should have decreased after VCI-B addition. In Figure 5-5 (a), the 4-month immersed and Level 1 coupons' corrosion rates are lower than the 2-month coupons, and thus, establish consistency between ER probe and coupon data. The addition of VCI-B also decreased pitting corrosion on the coupons, as seen in Figure 5-5 (b). A decrease in pitting corrosion was observed for immersed and Levels 1, 2 and 3 coupons.

The corrosion rate data for the coupons in Vessel 3 are listed in Table 5-6. The table has corrosion rate data, including surface average and pitting corrosion rates for the coupons exposed to GW and then GW plus 10 % recommended dosage of VCI-B. The 2-month coupons were exposed to GW simulant whereas 4-month coupons were exposed to GW plus 10% VCI-B dosage. Table 5-6 data also include average values of surface average and pitting corrosion rates and the corresponding standard deviations; the corrosion rates and standard deviations are presented in Figure 5-7. As seen in the figure, the average of the surface average corrosion rate of the immersed 4-month coupon is higher than the 2-month data. The same is observed in the surface average and pitting corrosion rates of the coupons that were at Level 2. This indicates that 10% VCI-B recommended dosage may not be enough to arrest the corrosion initiated by the GW simulant.

A statistical analysis was conducted to determine significance of the decrease in corrosion rate due to addition of 100% recommended dosages of VCI-A and VCI-B. The statistical method used was Student's t-test, which is based on the hypothesis that there is no statistically significant difference between the corrosion rates for the two electrolyte parameters used in the t-test—that is, that they are essentially identical to each other in terms of the coupon corrosion rates. The statistical result calculated by the test, P value, is the probability that the hypothesis is true. The higher the P-value, the greater the chance that the two sets of corrosion rates for the 2- and 4-month coupons are statistically similar. If the P-value is equal to or less than 0.05, it indicates that there is a less than 5% chance that the two sets of coupons have similar corrosion rates—that is, it means, with 95% confidence, that there is a statistically significant difference between the two 2- and 4-month coupons. The P-values are listed in Table 5-7.

Pitting corrosion is the main hazard for secondary tank failure. The P-values in Table 5-7, obtained by statistical analysis of the pitting corrosion rates, are discussed. The P-values for Vessel 1 immersed and Level 2 coupons are less than 0.05, and the P-value for Level 3 is 0.08, slightly above 0.05. This indicates with 95% confidence that immersed and Level 2 coupons' pitting corrosion were mitigated, however, there is only 92% confidence that Level 3 coupons' pitting corrosion was mitigated. In addition, Vessel 1 Level 1 coupons' pitting corrosion rates were not mitigated, as indicated by P-value of 0.62. In Vessel 2, the P-value for the Level 1 coupons is 0.04; there is 95% confidence that Level 1 coupons' pitting corrosion was mitigated. The P-values for immersed and Level 3 coupons are 0.13 and 0.23, respectively, this indicates

that the confidence levels in the reduction are 87 and 77% for the immersed and Level 3 coupons, respectively. Vessel 2 Level 2 coupons' pitting corrosion rates were not mitigated, as indicated by the P-value of 0.93. The P-values for Vessel 3 pitting corrosion are much higher than 0.05, indicating that there is high likelihood that pitting corrosion was not mitigated by the 10% VCI-B dosage.

**Table 5-6. Vessel 3 Corrosion Rate Data for Coupons with Exposure to GW for First Two Months and then GW plus 10% VCI-B for an Additional Two Months**

| Corrosion Type | Corrosion Rate (µm/yr) | | | | | | | |
|---|---|---|---|---|---|---|---|---|
| | Immersed | | Level 1 | | Level 2 | | Level 3 | |
| | 2-month* | 4-month* | 2-month* | 4-month* | 2-month* | 4-month* | 2-month* | 4-month* |
| Surface Average Corrosion Rate | 183 | 241 | 102 | 15 | 5 | 56 | 38 | 5 |
| | 147 | 218 | 64 | 25 | 3 | 3 | 99 | 0 |
| | 203 | 140 | 46 | 46 | 5 | 3 | 3 | 25 |
| Average** ± std*** | 178 ± 28 | 200 ± 53 | 70 ± 29 | 29 ± 16 | 4 ± 2 | 20 ± 31 | 49 ± 49 | 10 ± 13 |
| Maximum Pitting Corrosion Rate | 653 | 716 | 401 | 140 | 0 | 251 | 719 | 439 |
| | 318 | 452 | 861 | 310 | 0 | 307 | 594 | 0 |
| | 792 | 201 | 178 | 221 | 0 | 0 | 147 | 401 |
| Average** ± std*** | 588 ± 244 | 456 ± 258 | 480 ± 348 | 224 ± 85 | 0 ± 0 | 186 ± 164 | 487 ± 301 | 280 ± 243 |

*2-month: GW only exposure, 4-month: GW for first two months and GW+100% VCI-A thereafter
**Average values are calculated for 3 coupons
***std denotes standard deviation of the corrosion rate data used to calculate the average

**Table 5-7. Student's t-Test P-values* for Comparison Between Coupons Before and After VCI Treatment**

| Corrosion Cell | Corrosion Type | | | | | | | |
|---|---|---|---|---|---|---|---|---|
| | Surface Average Corrosion | | | | Maximum Pitting Corrosion | | | |
| | Immersed | Level 1 | Level 2 | Level 3 | Immersed | Level 1 | Level 2 | Level 3 |
| Vessel 1 (100% VCI-A) | 0.19 | 0.71 | 0.17 | 0.36 | 0.01 | 0.62 | 0.00 | 0.08 |
| Vessel 2 (100% VCI-B) | 0.51 | 0.13 | 0.48 | 0.21 | 0.13 | 0.04 | 0.93 | 0.23 |
| Vessel 3 (10% VCI-B) | 0.57 | 0.11 | 0.46 | 0.32 | 0.56 | 0.33 | 0.19 | 0.41 |

*P-values of 0.05 or less indicate statistically significant differences with 95% confidence

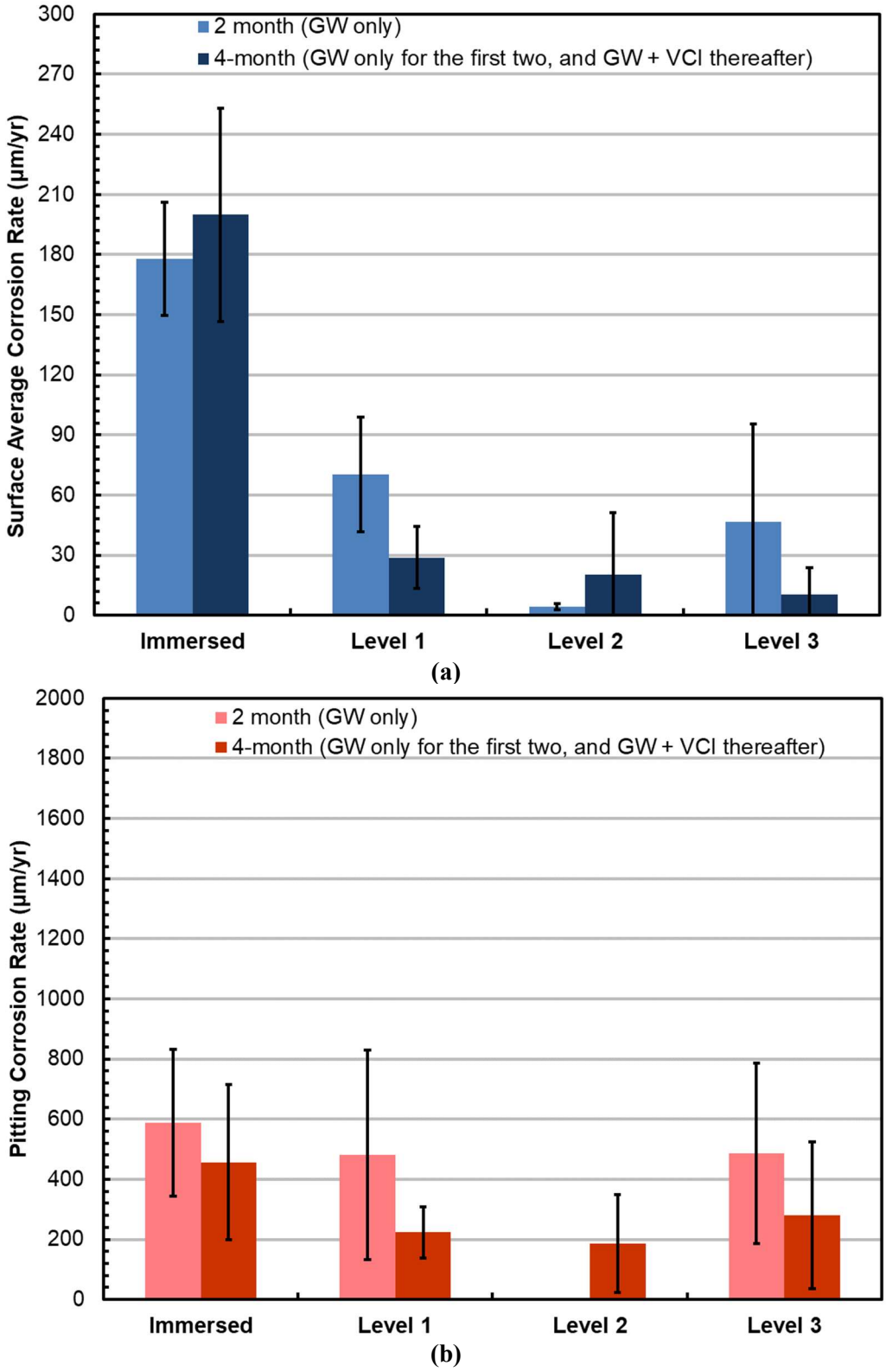


**Figure 5-7: Average of (a) surface average, and (b) pitting corrosion rates for coupons in Vessel 3 (GW, and then GW + 10% VCI-B). The black line in each bar represents the standard deviation.**

5.3 Long Term OCP Drift

As prepared chemical composition of the three solutions are listed in Table 5-8. The three electrolytes used for the OCP study are identified as Solution 3, Solution 9, and Solution 12.

**Table 5-8. As-prepared chemical compositions of the simulants for the OCP study**

| Simulant source salt | Concentration (M) | | |
|---|---|---|---|
| | **Solution 3** | **Solution 9** | **Solution 12** |
| Sodium hydroxide | 0.0001 | 0.3 | 0.6 |
| Sodium nitrite | 1.2 | 0.6 | 0.2 |
| Sodium nitrate | 2 | 0.07 | 0.6 |
| Sodium chloride | 0 | 0.1 | 0.05 |
| Sodium fluoride | 0 | 0 | 0 |
| Sodium sulfate | 0.2 | 0.2 | 0.2 |
| Sodium carbonate | 0.075 | 0.1 | 0.1 |
| Sodium bicarbonate | 0.025 | 0.0 | 0.0 |
| **Solution pH** | 10 | 13.3 | 13.3 |
| **PF** | 0.93 | 1.92 | 3.59 |

Initial CPP Measurements: Initial CPP data for two separate "bullet" coupons in Solution 3 and 9 are presented in Figure 5-8(a) and Figure 5-8 (b), respectively. As seen in Figure 5-8 (a), the CPP curve for the bullet coupon in Solution 3 exhibited Category 3 mixed response, i.e., a clear delineation between "pass" and "fail" for pitting corrosion cannot be made. However, as seen in Figure 5-8 (b), the CPP curve for the bullet coupon in Solution 9 exhibit Category 2 response, i.e., pitting corrosion of the coupon is unlikely in Solution 9. Images of the bullet coupons taken immediately after CPP data collection are presented in Figure 5-9. As seen in the figures, the coupons do not exhibit signs of pitting corrosion. The coupons' images are consistent with the CPP responses. CPP data in Figure 5-8 were collected using a separate set of experiments. Another set of experiments were setup to measure OCP drift, EIS and CPP.

OCP Drift: The OCP data for the bullet and mill-scale coupons were collected for almost 5 months. The data for the bullet coupons are presented in Figure 5-10; the initial OCPs of the three coupons are in the range of -370 to -410 mV vs. SCE. The OCPs quickly rose from initial values, and then slowly evolved with time. The initial and terminal OCPs values are listed in Table 5-9. The terminal OCPs for the bullet coupons in the three simulants are as follows: (a) 147 mV vs. SCE for Solution 3, (ii) -85 mV vs. SCE for Solution 9, and (iii) -176 mV vs. SCE for Solution 12. Overall shifts in the OCPs for the three simulants were: 520 mV for Solution 3, 300 mV for Solution 9, and 232 mV for Solution 12. The OCP data evolution for the bullet coupons in the three simulants were anodic, but the amount of change differed among the simulants, indicating that chemistries of the simulants affect extent of OCP drift.

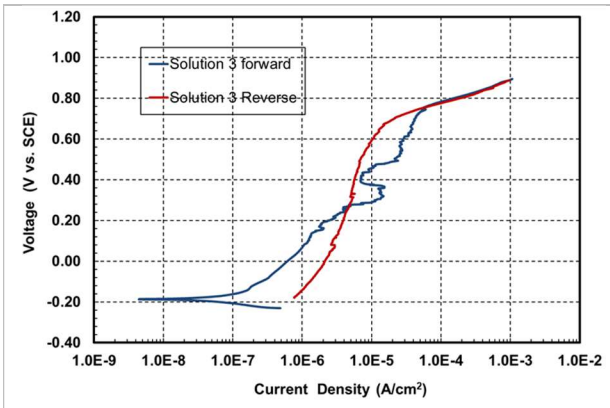


(a) Solution 3

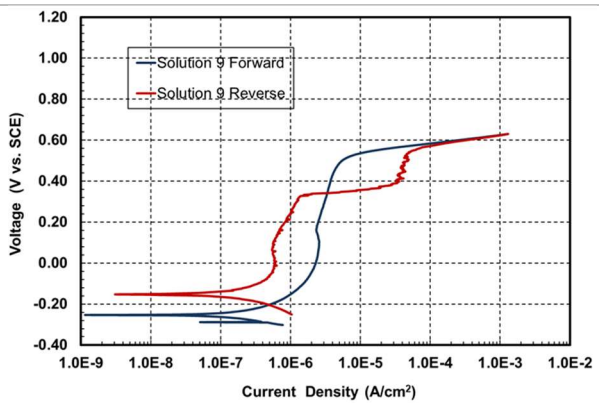


(b) Solution 9

**Figure 5-8. CPP data for the bullet coupons in (a) Solution 3, and (b) Solution 9**

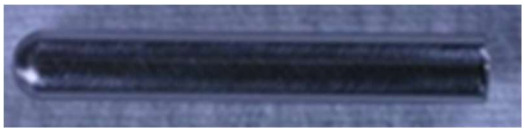

(a) Solution 3 bullet coupon side image

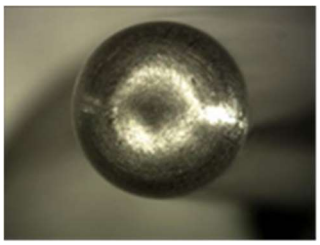

(b) Solution 3 bullet coupon nose image

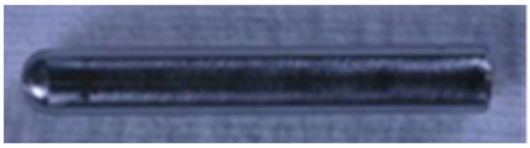

(c) Solution 12 bullet coupon side image

(d) Solution 9 bullet coupon nose image

**Figure 5-9. Images of the bullet coupons immediately after CPP tests**

OCP data for the mill-scale coupons are presented in Figure 5-11. As seen in the figure, the OCP data for the coupons with pre-existing surface conditions such as mill-scale plus corrosion products differed significantly compared to the bullet coupons with 600-grit polished surfaces. One key difference is the initial OCP values. In Figure 5-10, the initial OCPs were more cathodic compared to the OCPs evolved after 5 months. On other hand, the terminal OCPs are more cathodic compared to the initial values for mill-scale coupons except for the simulant labeled as Solution 12. The initial and terminal OCPs values for the mill-scale plus corrosion products coupons are listed in Table 5-9. The terminal OCPs for the mill-scale coupons in the three simulants are as follows: (i-11 mV vs. SCE for Solution 3, (ii) -141 mV vs. SCE for Solution 9, and (iii) -340 mV vs. SCE for Solution 12. Overall shifts in the OCPs for the three simulants were: -266 mV for Solution 3, -398 mV for Solution 9, and 101 mV for Solution 12. The OCP data evolution for the mill-scale plus corrosion products coupons in Solutions 3 and 9 was in cathodic direction, however, the evolution for Solution 12 was in anodic direction. Another point is noted that the differences between terminal OCPs for the bullet and mill-scale plus corrosion products coupons in each of the three simulants are: 524 mV for Solution 3, 454 mV for Solution 9, -65 mV for Solution 12.

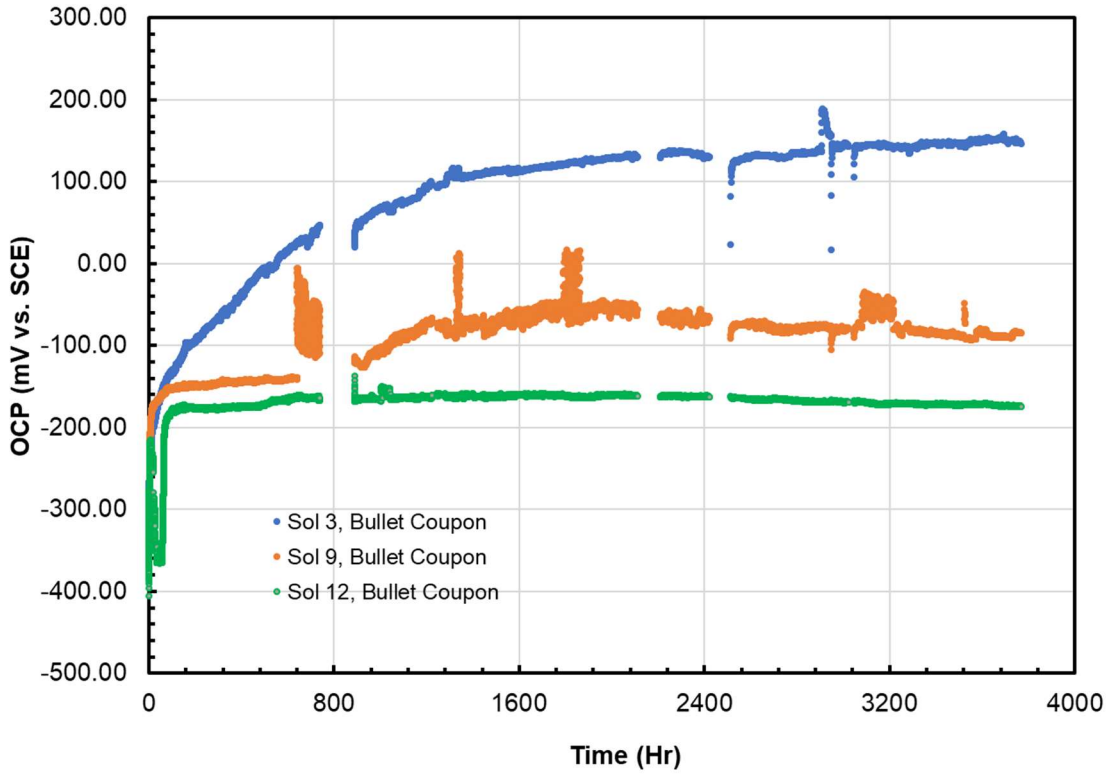


**Figure 5-10. OCP data for the bullet coupons (600-grit polished surface) in the three solutions**

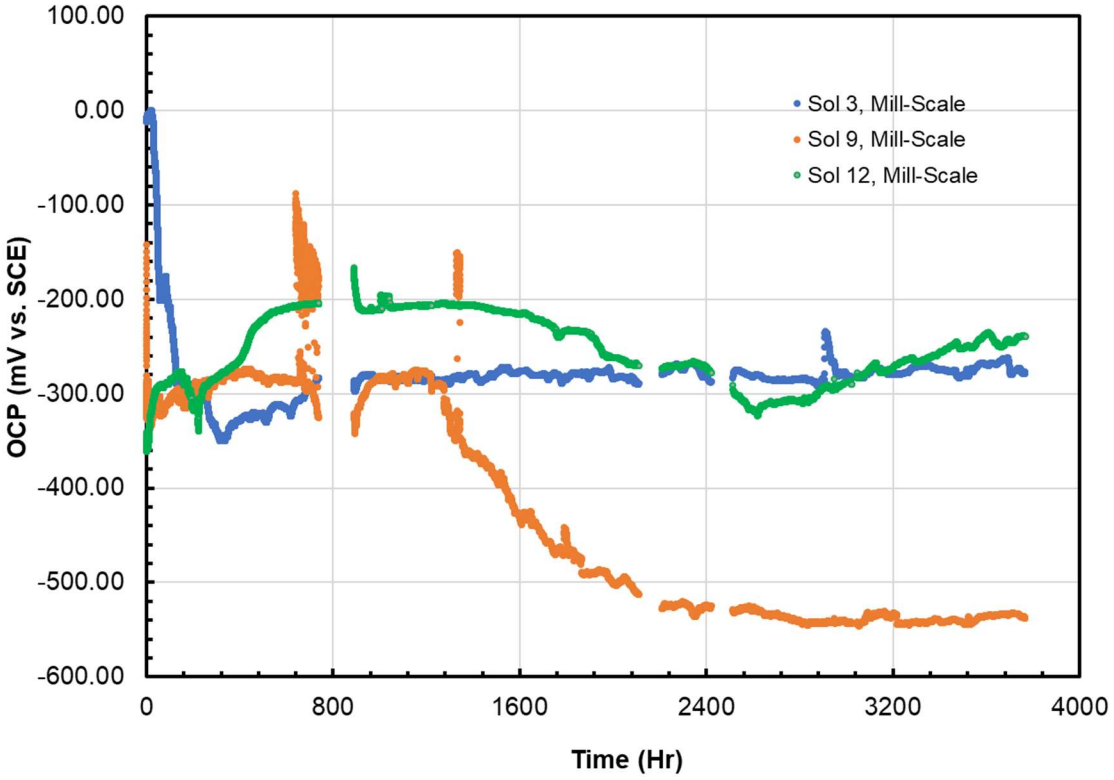


**Figure 5-11. OCP data for the mill-scale plus corrosion product coupons in the three solutions**

**Table 5-9. Initial and Terminal OCPs of Bullet and Mill-Scale Coupons**

| Electrolyte | Bullet Coupon OCP (mV vs. SCE) | | Mill-Scale Coupon OCP (mV vs. SCE) | |
|---|---|---|---|---|
| | Initial | Terminal | Initial | Terminal |
| **Solution 3** | -373 | 147 | -11 | -277 |
| **Solution 9** | -383 | -85 | -141 | -539 |
| **Solution 12** | -406 | -174 | -340 | -239 |

**EIS:** EIS data for the coupons are presented in Figure 5-12. EIS for the bullet coupons are in Figure 5-12 (a) and Figure 5-12 (b), and for mill-scale plus corrosion products coupons in Figure 5-12 (c) and Figure 5-12 (d). EIS measurements were conducted over the frequency range of $10^{5}$ to $10^{-5}$ Hz. Following observations are made in the impedance spectra of the coupons:

- Even at the low-end frequency spectra of the both sets of coupons, the asymptotic impedance values could not be measured, indicating that charge transfer resistances associated with the metal interface reactions are higher than the lowest frequency impedance values.

- For the bullet coupons, Solution 3 impedance spectra indicated the presence of one time constant, whereas Solutions 9 and 12 impedance spectra show presence of two separate time constants. The very low frequency time constant appears to occur below $10^{-5}$ Hz in the three coupons' spectra, however, for Solutions 9 and 12, the second time constant is observed in the frequency range of 0.1 to 10 Hz.

- For the mill-scale plus corrosion products coupons, Solution 12 impedance spectra indicated the presence of one time constant, whereas Solutions 3 and 9 impedance spectra show presence of two separate time constants. The very low frequency time constant appears to occur below $10^{-5}$ Hz in the three coupons' spectra, however, for Solutions 3 and 9, the second time constant is observed in the frequency range of $10^{-3}$ to 0.1 Hz. The change in the second time constant frequency range for the mill-scale coupons compared to the bullet coupons hints that presence of mill-scale plus corrosion products is likely to have shifted the zero frequency impedance values for the mill-scale plus corrosion products coupons. This further implies that asymptotic impedance for the mill-scale coupons would occur at frequencies lower than the bullet coupons, indicating that charge transfer resistance associated with the asymptotic impedance could be higher for the mill-scale plus corrosion products coupons than the bullet coupons.

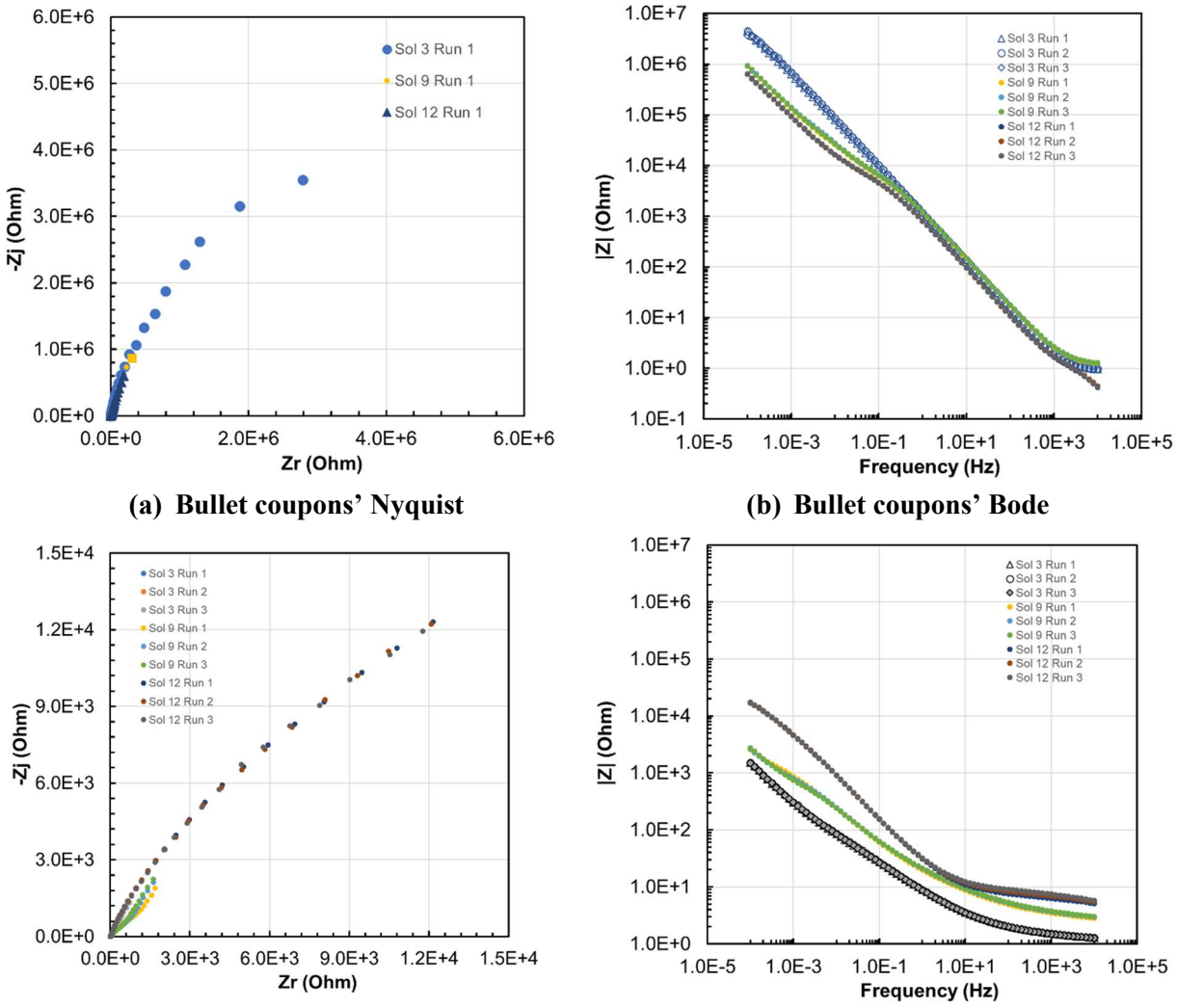


**(a) Bullet coupons' Nyquist** **(b) Bullet coupons' Bode**

**(c) Mill-scale coupons' Nyquist** **(d) Mill-scale coupons' Bode**

**Figure 5-12. EIS data for bullet and mill-scale coupons**

**CPP After OCP Hold:** CPP data and EIS measurements after OCP hold for approximately four months are presented in Figure 5-13, and the coupons' images post-exposure are presented in Figure 5-14. The CPP data for the bullet coupons show mixed response, i.e., no clear delineation between pitting and no-pitting can be made even after OCP evolution. This shows that even with the OCP evolutions, CPP data characteristics and corresponding deductions do not change. As seen in the Figure 5-13, the CPP responses for the mill-scale coupons are that of Category 1, i.e., pitting corrosion of the coupons is unlikely in the respective simulants. Images of the bullet coupons in Figure 5-14 show that pitting corrosion did not occur during CPP measurements; the same was observed for the mill-scale coupons, as seen in Figure 5-14(d), Figure 5-14(e), and Figure 5-14(f). A summary of the CPP data before and after OCP evolution is provided in Table 5-10. As listed in the table, CPP response of the mill-scale coupon is one level lower than that of bullet coupon, and the CPP responses of the bullet coupons in Solution 3 and 9 before and after OCP evolution are the same. In addition, as listed in Table 5-10, the mill-scale coupons' CPP responses are that of Category 1, and independent of electrolyte chemistry. These observations indicate that presence of the mill-scale and corrosion products lower pitting corrosion propensity of the metal in these three solutions.

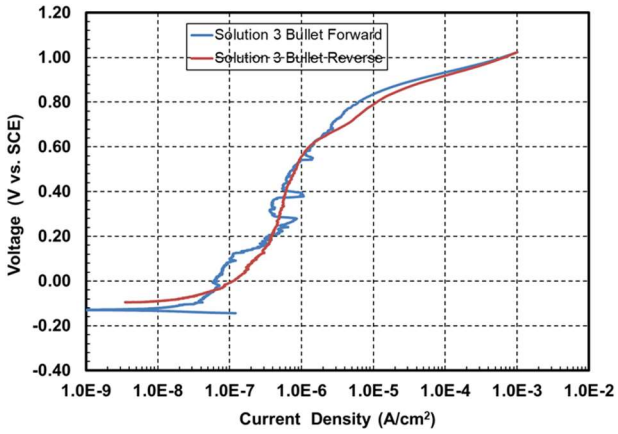


(a) Solution 3 Bullet Coupon

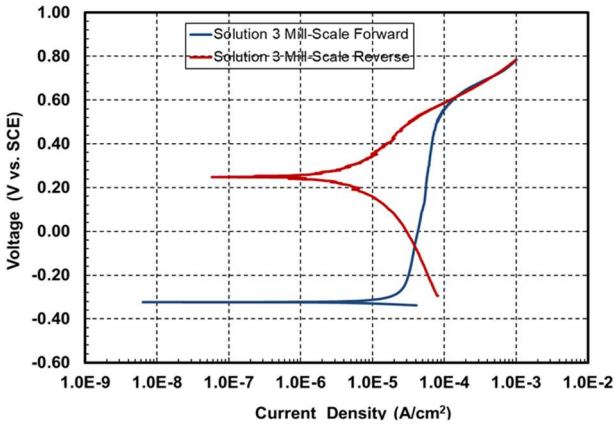


(b) Solution 3 Mill-Scale Coupon

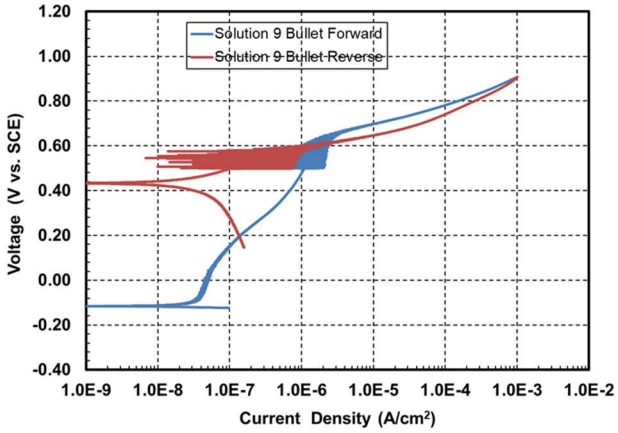


(c) Solution 9 Bullet Coupon

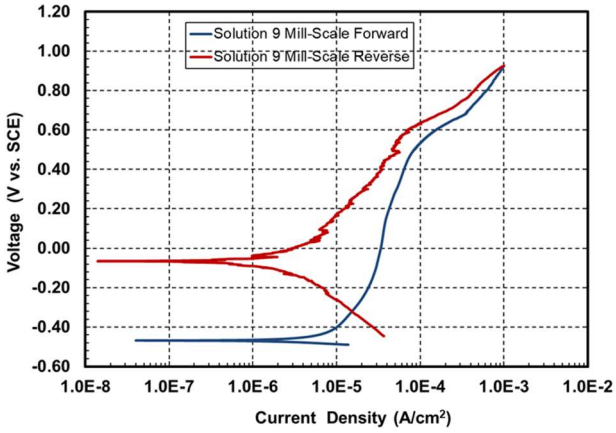


(d) Solution 9 Mill-Scale Coupon

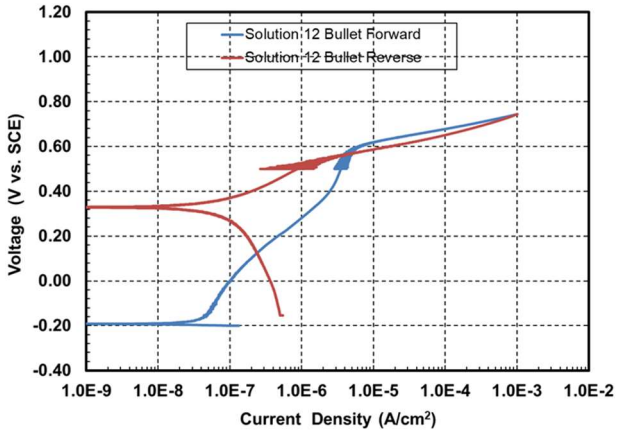


(e) Solution 12 Bullet Coupon

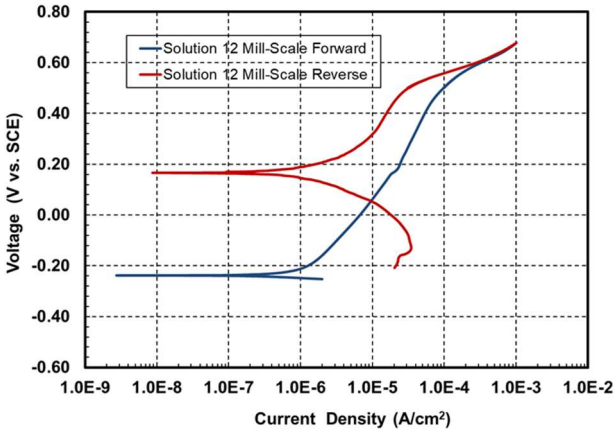


(f) Solution 12 Mill-Scale Coupon

**Figure 5-13. CPP Data after OCP hold for the Bullet and Mill-Scale Coupons**

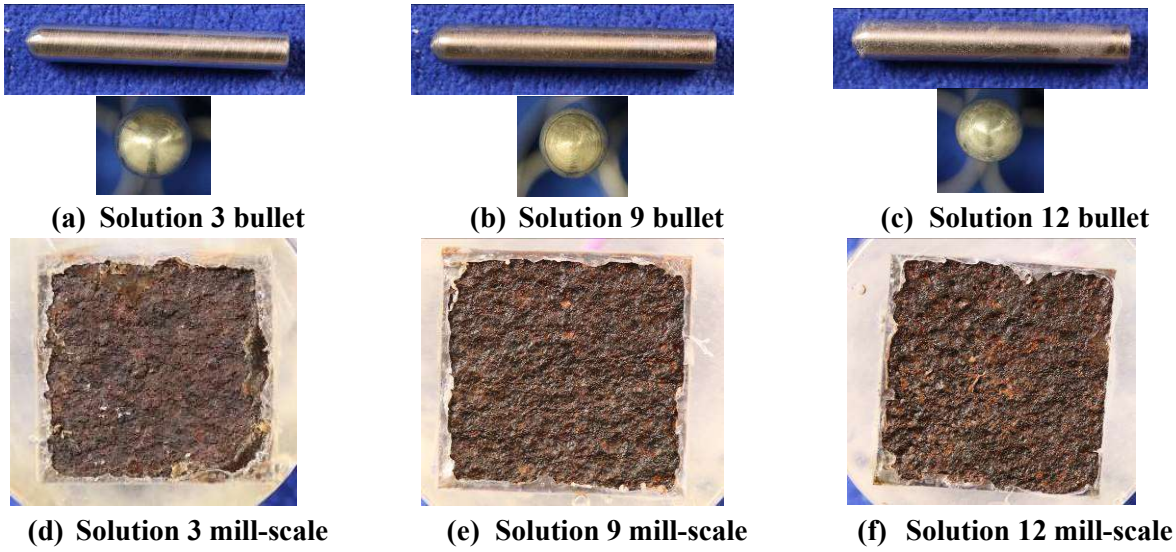

(a) Solution 3 bullet (b) Solution 9 bullet (c) Solution 12 bullet

(d) Solution 3 mill-scale (e) Solution 9 mill-scale (f) Solution 12 mill-scale

**Figure 5-14. Images of the bullet and mill-scale plus corrosion products coupons after OCP holds, CPP, and EIS measurements**

**Table 5-10. CPP Data Summary**

| Electrolyte | Bullet Coupon | | Mill-Scale | Notes |
|---|---|---|---|---|
| | Before OCP Evolution | After OCP Evolution | After OCP Evolution | |
| **Solution 3 (pH 10, PF 0.93)** | Category 3 (no clear "pass" or "fail") | Category 3 (no clear "pass" or "fail") | Category 1 (no pitting) | Pitting corrosion assessment risk decreased with use of mill-scale plus corrosion product coupons |
| **Solution 9 (pH 13.3, PF 1.92)** | Category 2 (no pitting) | Category 2 (no pitting) | Category 1 (no pitting) | |
| **Solution 12 (pH 13.3, PF 3.59)** | Not available | Category 2 (no pitting) | Category 1 (no pitting) | |

5.4 MIC Testing

The biological activity observed in the LDP water from a DST at Hanford differed by bacteria type. Differences between the two test kits were also observed. No large differences were noticed between the two bottles of the LDP water. The data is summarized in Table 5-11 and Table 5-12. The two bacteria types that the MICkit® and BART™ testers had in common were acid producing and sulfate reducing bacteria. Neither of these bacteria types were observed in either water bottle for either test. For sulfate reducing bacteria in the MICkit®, the water turned black, but no slime was formed on the metal, which indicated a negative test. The MICkit® indicated both water bottles had large populations of low-nutrient bacteria and significant populations of iron-related bacteria. Significantly, the MICkit® did not indicate any quantities of sulfate reducing bacteria or acid producing bacteria, which are commonly associated with MIC. The only bacteria that can sustain corrosion by itself is the sulfate reducing bacteria. Corrosion product and or sediment would also need to be analyzed to get more complete results. Testing the water indicates if there are bacteria, while testing the corrosion product determines if the bacteria is growing and if it can sustain

corrosion. It would be difficult to get corrosion product directly from the LDP. Alternatively, corrosion product could be observed by placing carbon steel coupons in the LDP water and then visually observing the corrosion product. This test would also need to be conducted on a routine basis, say every three months to get more representative results from the testing.

**Table 5-11 The change in bottle number as a function of bacteria type in the MICkit® testers.**

| Bottle | Bacteria | Day 1 | Day 2 | Day 3 | Day 4 | Day 8 | Day 9 | Day 15 | Day 21 | Day 30 |
|---|---|---|---|---|---|---|---|---|---|---|
| 2AZLDP-18-2A | Low Nutrient | 0 | 1 | 1 | 2 | 4 | 4 | 4 | 4 | 4 |
| | Iron-related | 0 | 0 | 0 | 0 | 0 | 0 | 0 | 3 | 4 |
| | Anaerobic | 0 | 0 | 1 | 1 | 1 | 1 | 1 | 1 | 1 |
| | Acid producing | 0 | 0 | 0 | 0 | 0 | 0 | 0 | 0 | 0 |
| | Sulfate reducing | 0 | 0 | 0 | 0 | 0 | 0 | 0 | 0 | 0 |
| 2AZLDP-18-2B | Low Nutrient | 0 | 0 | 0 | 2 | 4 | 4 | 4 | 4 | 4 |
| | Iron-related | 0 | 0 | 0 | 0 | 0 | 0 | 1 | 3 | 3 |
| | Anaerobic | 0 | 0 | 0 | 0 | 1 | 1 | 1 | 1 | 1 |
| | Acid producing | 0 | 0 | 0 | 0 | 0 | 0 | 0 | 0 | 0 |
| | Sulfate reducing | 0 | 0 | 0 | 0 | 0 | 0 | 0 | 0 | 0 |

**Table 5-12 The first day that a change was observed for each BART™ testers.**

| Bottle | Bacteria | Day 1 | Day 2 | Day 3 | Day 4 | Day 8 | Day 9 | Day 15 | Day 21 | Day 30 |
|---|---|---|---|---|---|---|---|---|---|---|
| 2AZLDP-18-2A | Heterotrophic aerobic | 0 | 0 | 0 | 0 | 0 | 0 | 1 | NR | NR |
| | Acid producing | 0 | 0 | 0 | 0 | 0 | 0 | 1 | NR | NR |
| | Sulfate reducing | 0 | 0 | 0 | 0 | 0 | 0 | 0 | NR | NR |
| 2AZLDP-18-2B | Heterotrophic aerobic | 0 | 0 | 0 | 0 | 0 | 0 | 0 | NR | NR |
| | Acid producing | 0 | 0 | 0 | 0 | 0 | 0 | 0 | NR | NR |
| | Sulfate reducing | 0 | 0 | 0 | 0 | 0 | 0 | 0 | NR | NR |

NR: Not Reported.

5.5 Summary of QEPAS study for ammonia detection

VSC may occur due to transport of aggressive species that condenses on the tank walls and within crevices. These aggressive species are present in tank waste, vapor space, and salt residues on the tank wall. Localized corrosion mechanisms such as pitting, and SCC may result [24].

Low concentrations of ammonia have been shown to inhibit VSC during laboratory testing [25],[26]. Ammonia is produced predominantly in the liquid waste through radiolysis of organics, nitrate/nitrite and water. The amount present in the vapor space of the tank is dependent on dissolved ammonia concentration in the supernate as well as the ventilation rate [10],[4],[5],[27].

During FY16, the investigation of an ammonia sensor technology for DSTs was initiated using a QEPAS sensor. QEPAS is a pass-through type method for measuring trace impurities in gas streams. In the simplest sense, QEPAS works by using a quartz-tuning fork (QTF) to detect optically generated sound in a gas

mixture that has been excited with a laser. Importantly, each gas target has a unique frequency mode(s) that can be vibrationally excited by the laser, therefore tuning the laser to specific modes allows for the detection of specific gases. Using off-the-shelf components, QEPAS systems can realize real-time detection limits in the low parts per million to parts per billion range for gaseous species such as $NH_3$, $N_2O$, $NO_2$, $CH_4$, CO, $CO_2$, HCl and $H_2S$ [28],[29]. Additionally, QEPAS can operate over 9 orders of magnitude of the acoustic signal, allowing it to cover large concentration ranges using extremely small sampling volumes. QEPAS sensor technology has already been applied for the detection of more than twelve different molecular species, both with near-IR and mid-IR laser excitation sources. Figure 5-15 shows the noise equivalent concentration with corresponding laser wavelength of the QEPAS.

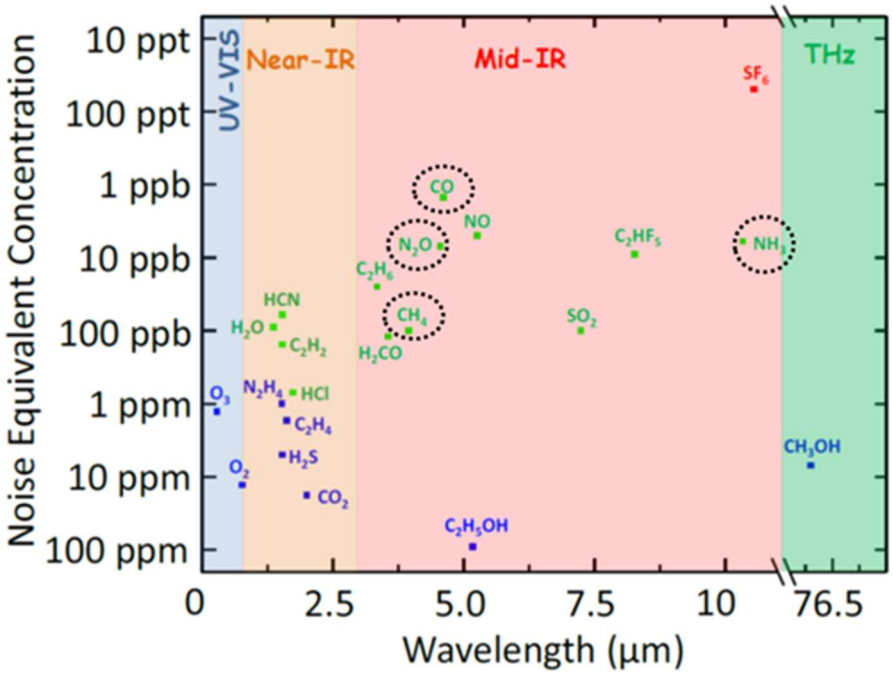


**Figure 5-15 Noise Equivalent Concentration QEPAS results with corresponding laser wavelength. The blue, green, and red symbols indicate values in the ppm, ppb, and ppt concentration ranges, respectively. [30]**

The QEPAS system at SRNL, displayed in Figure 5-16, has been designed to monitor both ammonia ($NH_3$) and methane ($CH_4$) in gas streams at varying pressures with detection limits as low as 2 ppm for $NH_3$ and 10ppm for $CH_4$. To date, the two-gas QEPAS detectors have been assembled and tested. The setup includes electronic cables, signal transfer cables, fiber optic cables for laser incorporation into the QEPAS QTF, and gas transfer lines to deliver the gas into the microresonator tube. The system was assembled as shown in Figure 5-16 a), b). Additionally, the software that controls the system has been installed on a control computer, and communication was established between the computer and the control electronics unit (CEU). The sensors that monitor the temperature, pressure, and humidity of the input gas have all been tested and shown to function properly. The final step in the checkout process involved connecting the detector to a calibration gas with a known ammonia concentration. A cylinder containing 550 ppm ammonia in air was chosen for this step. The system did not initially pass this test. However, after adjustments in the set-up and system parameters accurate measurements of the 550 ppm $NH_3$ gas stream were conducted.

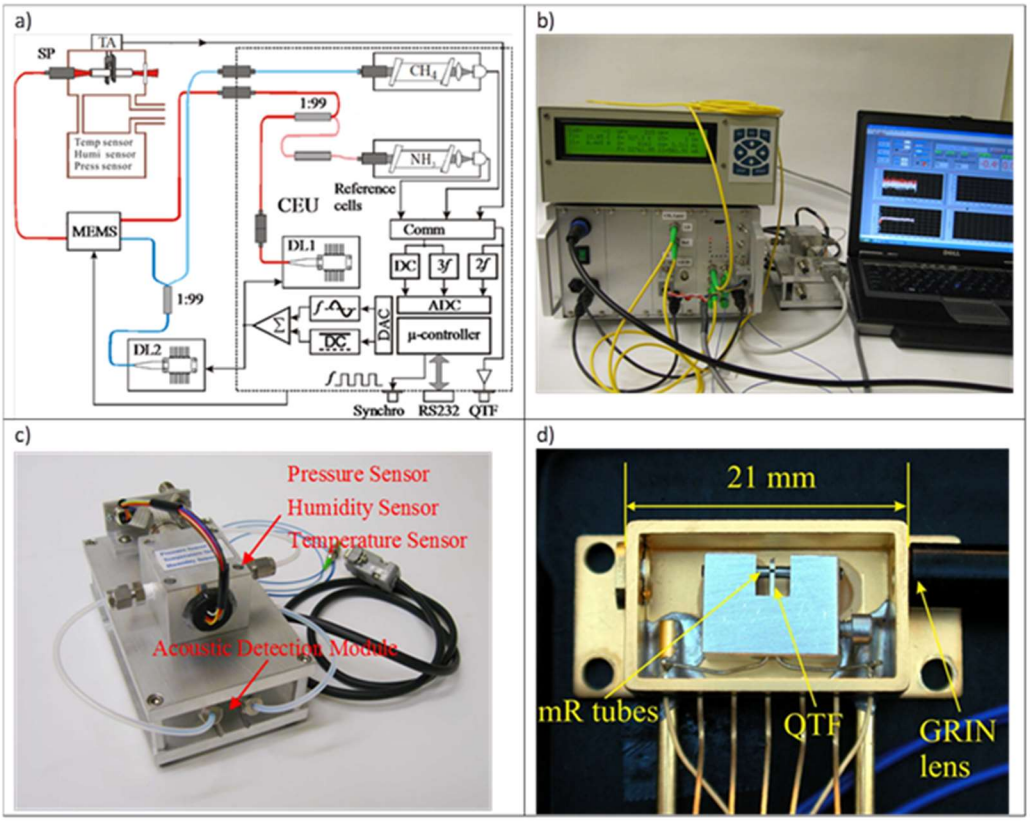


**Figure 5-16 a,b) Schematic and a photo of the near infrared diode laser based QEPAS sensor system for analyzing concentrations of two gases ($NH_3$ and $CH_4$), c) Sensor Head, and d) Close-up image of the fiber-coupled QEPAS acoustic detection module (ADM). [7]**

5.5.1 *Summary of progress*

*5.5.1.1 FY16 Summary*

The system was configured to allow a gas bottle to be connected directly to the inlet and a vacuum pump added to allow the system to be evacuated before and after testing. Baseline measurements were performed with the system under vacuum to determine the limit of detection (LOD) in the current configuration. Following the LOD measurements subsequent tests at approximately 1, 7, 12 and 50 ppm $NH_3$ in balance of air were conducted. These tests were all conducted at approximately 760 torr and a flow rate of 130 standard cubic centimeter per minute (sccm) to simulate conditions the system is expected to encounter in the field. These ammonia concentrations were first mixed on an external gas manifold equipped with a pressure gauge and vacuum system, which allowed for the complete evacuation of residual gases prior to the mixing of new concentrations. The use of the gas mixing system allowed for testing in a humid atmosphere to determine the effect of water on the accuracy of the system.

As shown in Figure 5-17, using 10 second data averages, the QEPAS system was able to detect all concentrations tested with relative accuracy (an error of approximately 6% was calculated when measuring the 50ppm $NH_3$ concentration). This error/noise was expected to decrease as the system is further tuned for its current operating environment.

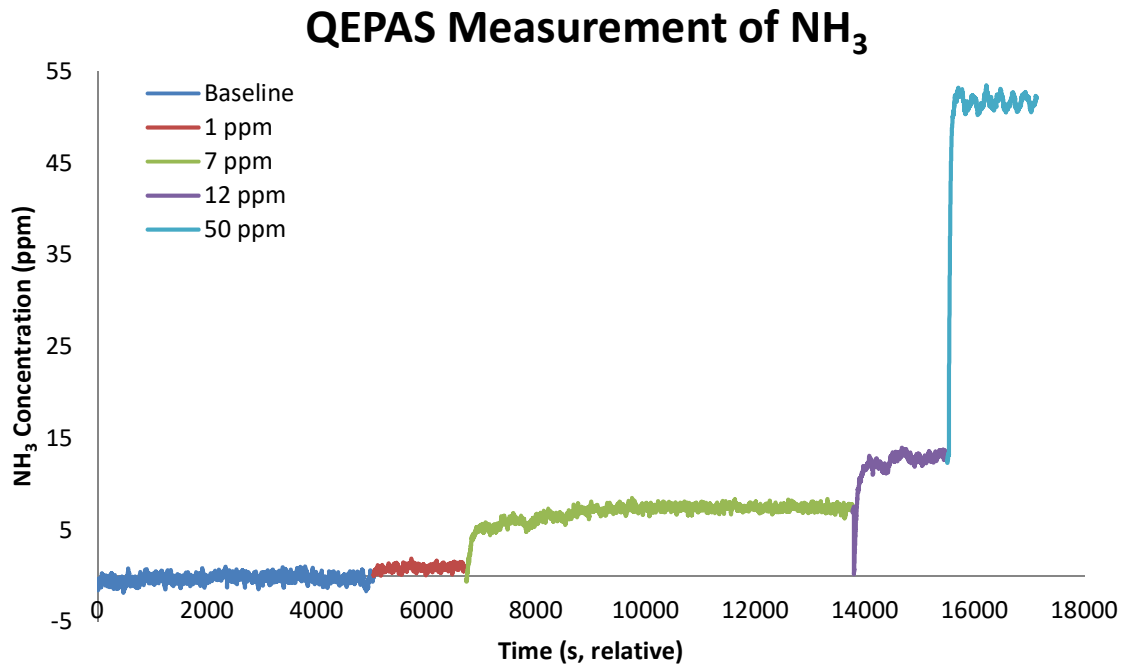


**Figure 5-17 QEPAS measurements of $NH_3$ at varying concentrations.**

*5.5.1.2 FY17 Summary*

For FY17, the QEPAS sensor was calibrated at various pressures and flow rates. Additionally, the effects of relative humidity levels higher than 90% were assessed by using different concentrations of ammonia in air. After calibration, the sensor was connected to the exhaust of the VSC apparatus. The equipment was in place for a determined amount of time to detect 50 and 550 ppm ammonia.

To accomplish these objectives, the QEPAS system was reconfigured, and by utilizing a calibrated $NH_3$ permeation tube, specific dilutions were made at different flow rates and changes in pressure that ranged from 200-650 Torr (~3 to 13 psia). Testing the response at varying pressures and flow rates allowed for determination of effects due to changing tank pressures on the system. It was determined during previous experiments that increases in pressure during $NH_3$ detection resulted in broadening of the absorption lines until two absorption lines merge at pressures above 600 Torr. Therefore, pressures above 650 Torr were not tested.

Figure 5-18 shows the effect of changes in pressure and flow rate on the QEPAS output signal. During testing, a constant 50 ppm $NH_3$ gas concentration was carried into the QEPAS system at a constant flow rate (varied between 50 – 200 sccm) while the total pressure within the cell was varied. As expected, variations in pressure resulted in a linear response of the $NH_3$ concentration as the number of $NH_3$ molecules present in the micro-resonator increased. As a result of these variations, it was determined that a constant pressure was required for accurate operation. However, because the variations in concentration were linear for specific flow rates, the pressure could be altered to match field requirements. Changes in flow also resulted in changes in the measured concentration. These changes in concentration, although not linear, were measurable and the sensor can be further calibrated to compensate for these variances. By installing a flow controller upstream and a pressure controller downstream of the QEPAS, more precise control over the flow and pressure within the QEPAS system was achieved.

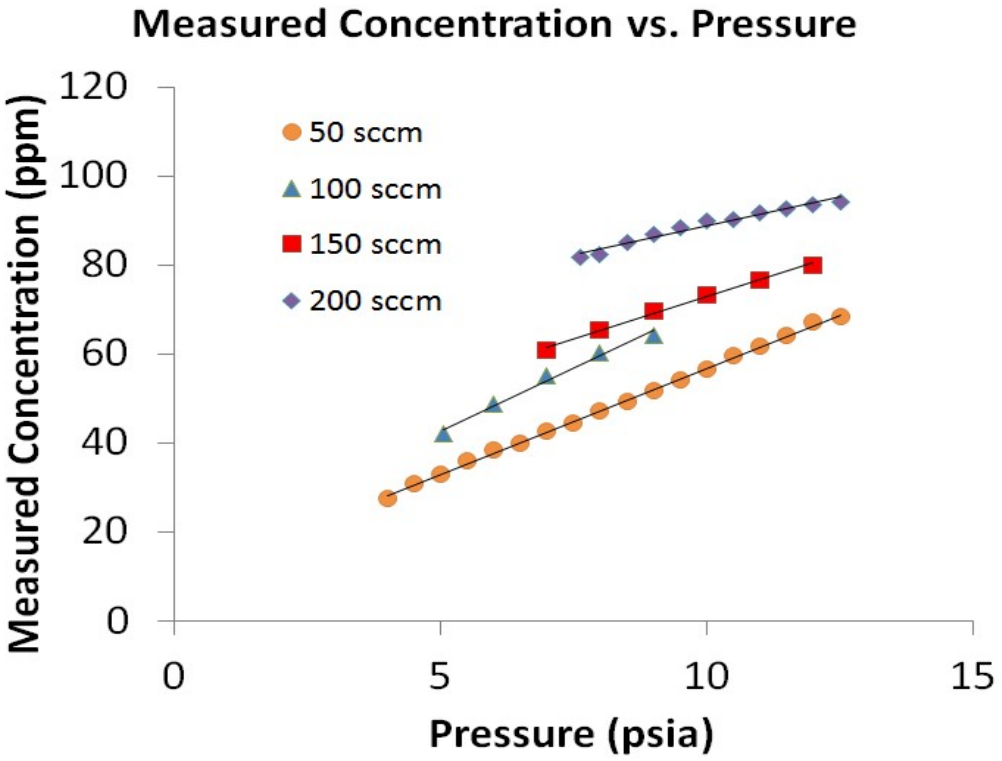


**Figure 5-18 Variations in measured ammonia concentrations under varying pressures and flow rates.**

The QEPAS system was placed at the exhaust of the VSC for humid ammonia in air concentration measurements. Figure 5-19 shows a picture of the setup attached to the exhaust of a vapor space corrosion testing system. Initial testing in a humid environment indicated that the $NH_3$ signal was unaffected by moisture. However, if moisture condenses onto the QTF sensor, dampening can be expected and may result in large variations in signal. Therefore, a constant flow should be maintained to limit the possibility of moisture condensation with the QEPAS cell.

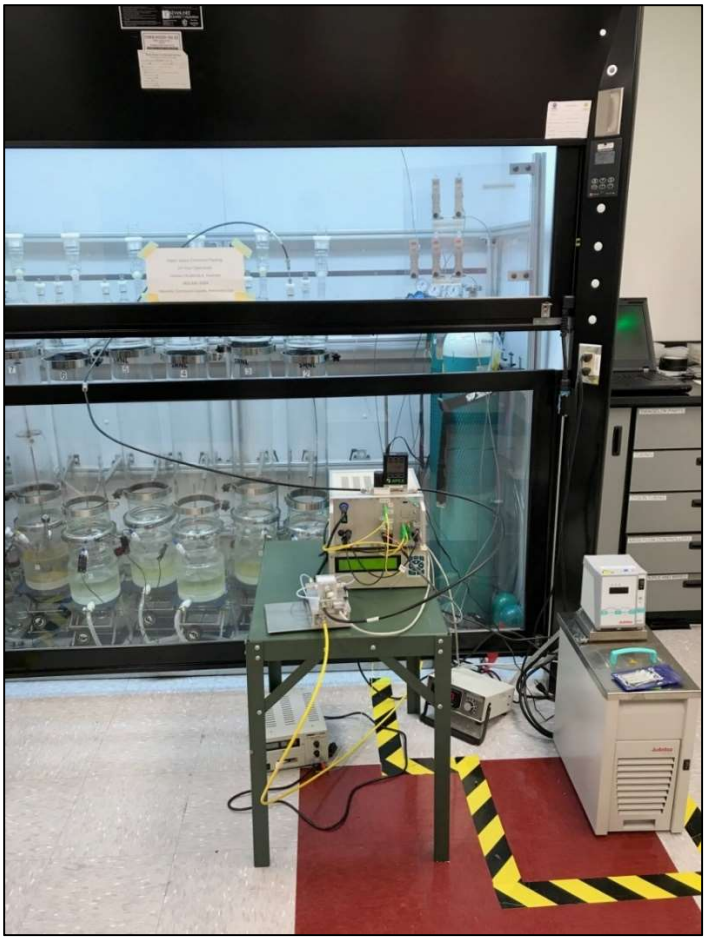

**Figure 5-19 Picture of QEPAS system attached to an exhaust of a VSC test system (first vessel from right to left).**

*5.5.1.3 FY18 Summary*

SRNL collaborated with Achray Photonics Inc. to design a new sensor specifically for the measurement of $NH_3$ in air. Achray fabricated the original sensor used in the SRNL QEPAS system which was optimized for use in a hydrogen environment. After replacement of the sensor, the system was recalibrated. The response of the sensor was calibrated with respect to concentration, system pressure, and humidity. Upon completion of the sensor setup, the system was connected to the exhaust of a blank VSC test setup as a first step in determining its efficacy in a head-space monitoring scenario. Finally, once confirmed, the system was moved to a live corrosion testing system to detect $NH_3$ in the exhausted gases.

A new Acoustic Detection Module (ADM) was purchased from Achray Photonics Inc. An ADM, shown in Figure 5-16 d), is the functioning portion of the QEPAS system. In the field, the ADM can be separated from the laser, CEU, and gas control if desired. The ADM is relatively small with a volume of ~1 cubic inch. As such, building a portable system would require the laser, CEU, and gas control systems to be optimized; however, the size of the ADM would not need to be changed. These components can be easily modified to fit within a small suitcase sized container, allowing for a completely portable system. Shown in Figure 5-20 is an example of a compact system designed by Viola et. al [31] that was able to maintain low limits of detection in the range of ppb.

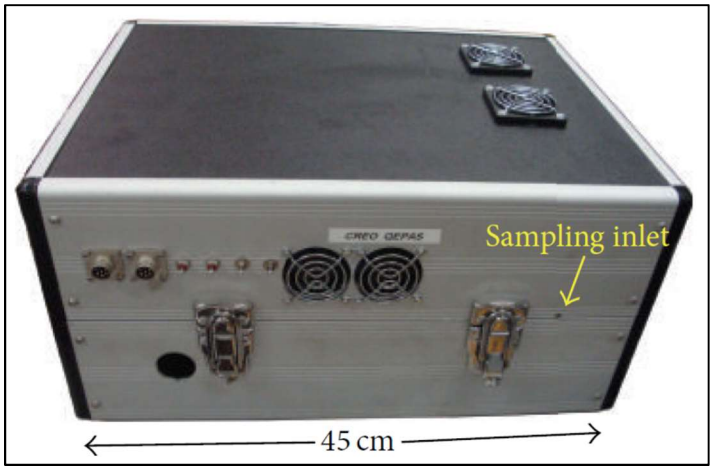


**Figure 5-20 Modular QEPAS sensor package developed by Viola et. al that measures approximately 17 in x 13 in x 9 in. [11]**

In FY18, a manifold was automated to perform the calibrations using LabView software from National Instruments™. The data analysis was also automated using Octave software. The process of a calibration included supplying a gas to the QEPAS sensor by a mixing manifold where test gas (a certified $NH_3$ cylinder) was diluted using clean dry nitrogen with mass flow controllers. In this way the concentration in the system can be stepped from 0 to the full concentration of the test gas as shown in Figure 5-21 (a), (b). In FY18 calibrations were performed over a wide range using two test gasses of 50 ppm $NH_3$ in air and 550 ppm $NH_3$ in air. The raw data is then reduced using an octave script to give measured concentration as a function of actual concentration as shown in Figure 5-21 (c), (d). The slope of this plot is the calibration factor in the QEPAS system.

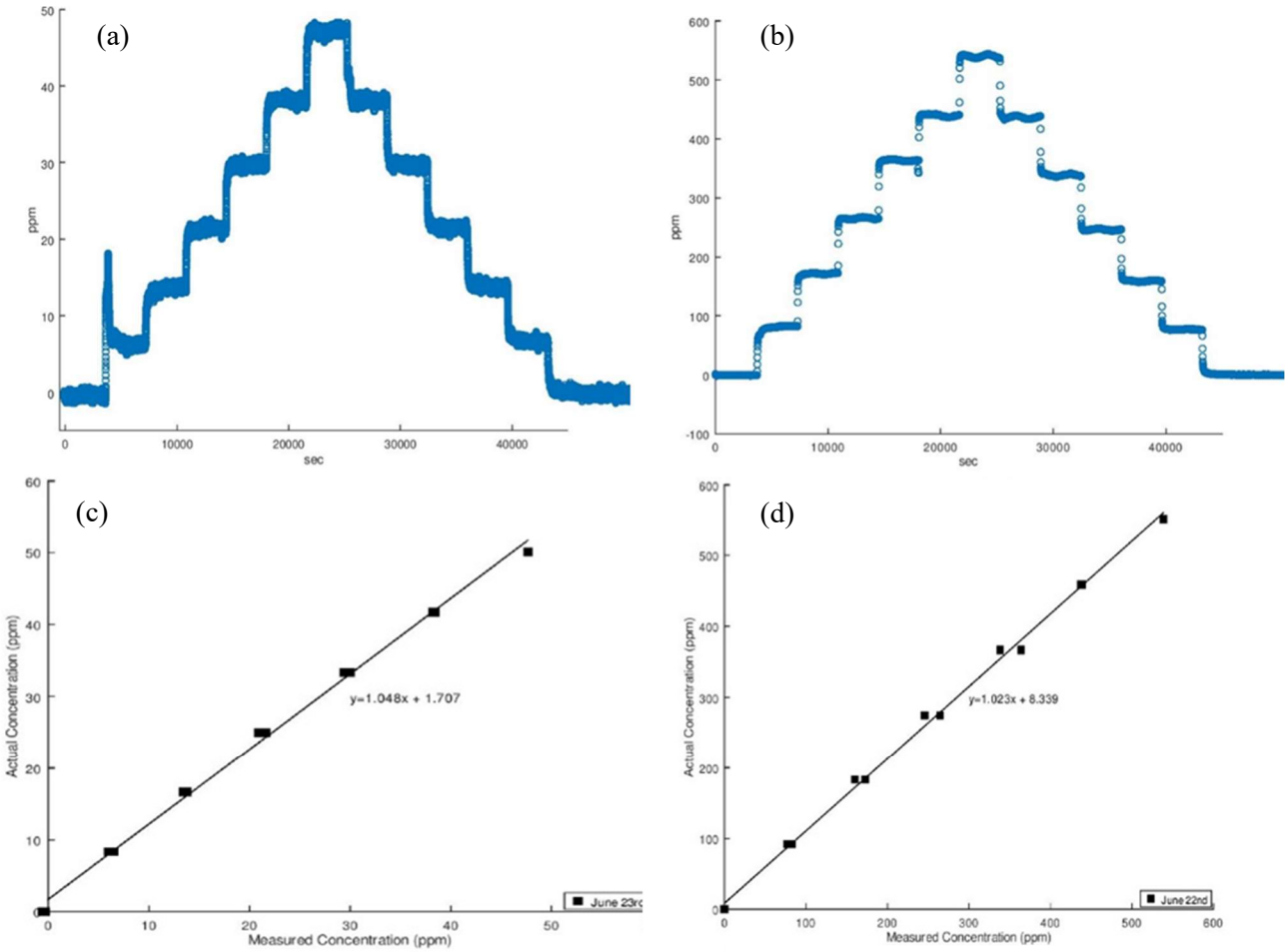


**Figure 5-21 ADM calibration data, (a) 50 ppm $NH_3$ raw calibration data, (b) 550 ppm $NH_3$ raw calibration data, (c) measured vs actual concentration plot for 50 ppm $NH_3$ test gas, and (d) measured vs actual concentration plot for 550 ppm $NH_3$ test gas.**

To test the effect of water on the QEPAS system the calibration manifold was modified to allow for mixing test gas ($NH_3$ in air) with humid nitrogen. Tests were run using the procedure described above for sensor calibrations. Figure 5-22 (a) shows the measured concentration as function of time for one of the humidity tests. Figure 5-22 (b) shows the humidity as a function of time for the same test. Figure 5-22 (c), (d) show the reduced data for humidity tests using 50 ppm and 550 ppm test gas, respectively. As can be seen in the figure, the variation between the dry calibrations and the humid atmosphere tests is quite small, less than the instrumental uncertainty for the 50 ppm case and only slightly larger in the 550 ppm test.

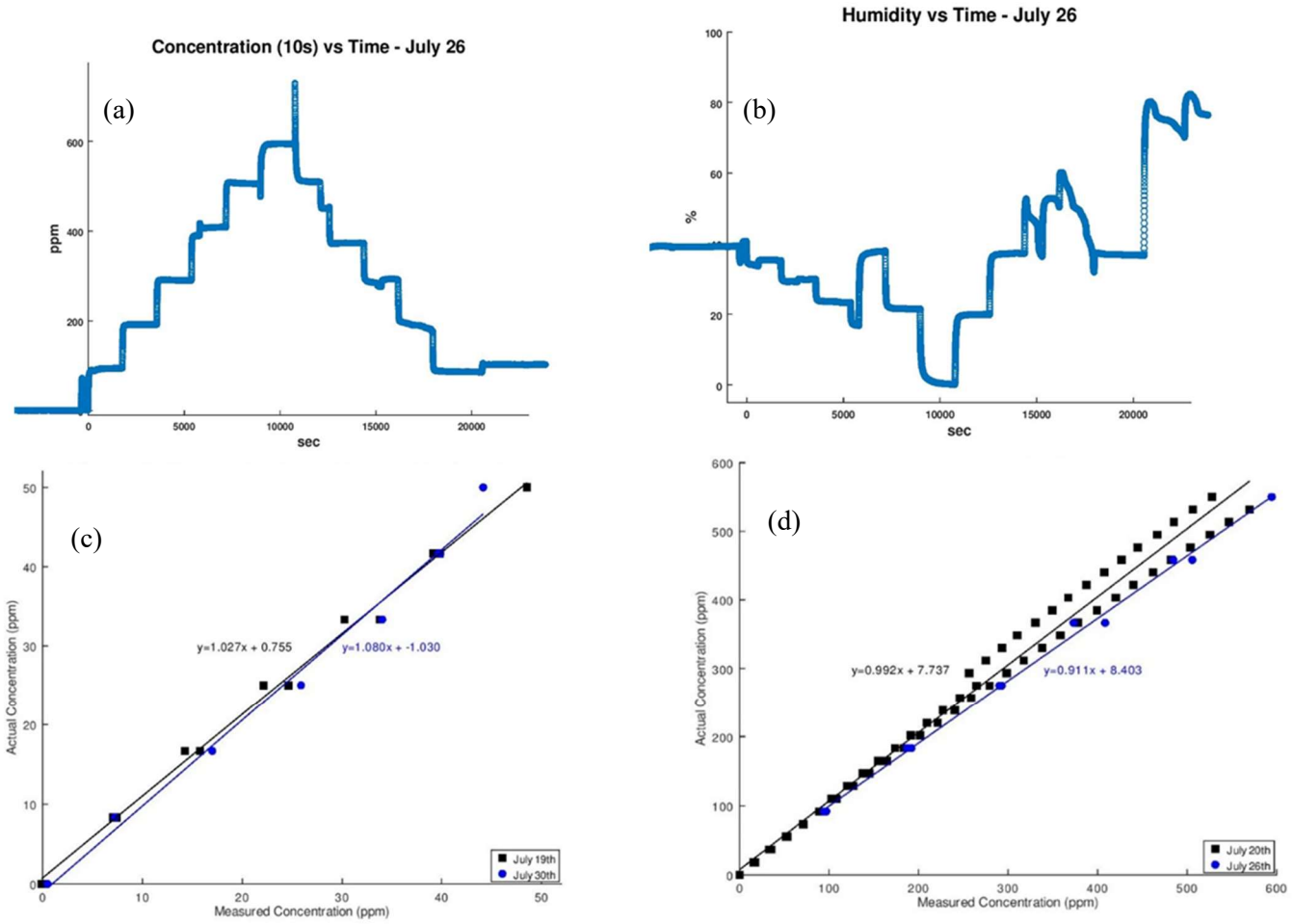


**Figure 5-22 Humidity data collected using humidified $N_2$ gas, (a) measured concentration using 550 ppm $NH_3$ and $N_2$ as humidified carrier gas, (b) measured humidity corresponding to the concentration values in figure a, (c) and (d) reduced concentration data showing actual vs measured $NH_3$ concentration using 50 ppm and 550 ppm $NH_3$ test gas, respectively.**

After calibrating the new sensor and verifying that humidity effects are small in the concentration range of interest, the SRNL QEPAS system was connected to the exhaust of a VSC cell (Figure 5-23). The system was configured to simulate a VSC test with the QEPAS probe connected to the exhaust. Additionally, a 1/4" diameter pipe was added to the plumbing of the QEPAS sensor to allow for measurement of the $NH_3$ concentration in the cell as a function of height. It is important to remember that the QEPAS sensor is maintained at sub atmospheric pressures during operation. This causes a pressure gradient from the cell to the sensor which drives gas flow. Flow into the QEPAS sensor is controlled by a mass flow controller.


**Figure 5-23 QEPAS system, gas control manifold, and VSC test setup, (A) electronics and laser housing, (B) QEPAS cell, housing the ADM, (C) gas control manifold, (D) gas input from $NH_3$ cylinder, and (E) $NH_3$ sampling probe for VSC measurements.**

VSC tests were performed using very small flow rates when compared to the flows used in the initial QEPAS scoping studies. The flow rate used in VSC tests at SRNL was 5-10 sccm, which leads to a very large residence time for gas in the VSC cell which has a volume of several liters. For this reason, it takes over 100 hours to fully replace the atmosphere in the VSC cell with the test gas and for measurements of the $NH_3$ concentration in the cell to reach steady state. Figure 5-24(a) shows the $NH_3$ concentration in an empty VSC cell as a function of time. Additionally, to determine if low flow rate issues caused variations in concentration throughout the vessel, samples were collected at varying heights within the vessel. Initial testing began with the probe at the lower position, nearest the bottom of the vessel and additional data was collected at heights in the middle and top of the VSC vessel. Data shown Figure 5-24(b) indicates that there is a small detectable variance in concentration through the height of the vessel. Upon completion of the initial height test, simulant VSC testing was conducted.

As shown in Figure 5-24(c), the measured $NH_3$ concentration in the vessel was significantly higher than the 50 ppm present in the test gas. This discrepancy can be attributed to the fact that the simulant solution was designed for a higher $NH_3$ concentration. The test solution was optimized for $NH_3$ concentrations of 550 ppm using ammonium nitrate. Figure 5-24(d) shows the data for the beginning of the measurements and highlights two important details. First, the time to reach steady state $NH_3$ concentration is relatively short when compared to the empty vessel, which suggests that the solution was the primary contributor to the $NH_3$ concentration in the headspace. Second, the discontinuities present every five hours are likely artifacts due to the internal system recalibration process. With that in mind, the uncertainty of the system over long time scales was largely dictated by the recalibration process, and therefore slightly larger than the ~5% uncertainty quoted for shorter runs. However, this uncertainty could likely be mitigated by optimizing the recalibration routine.

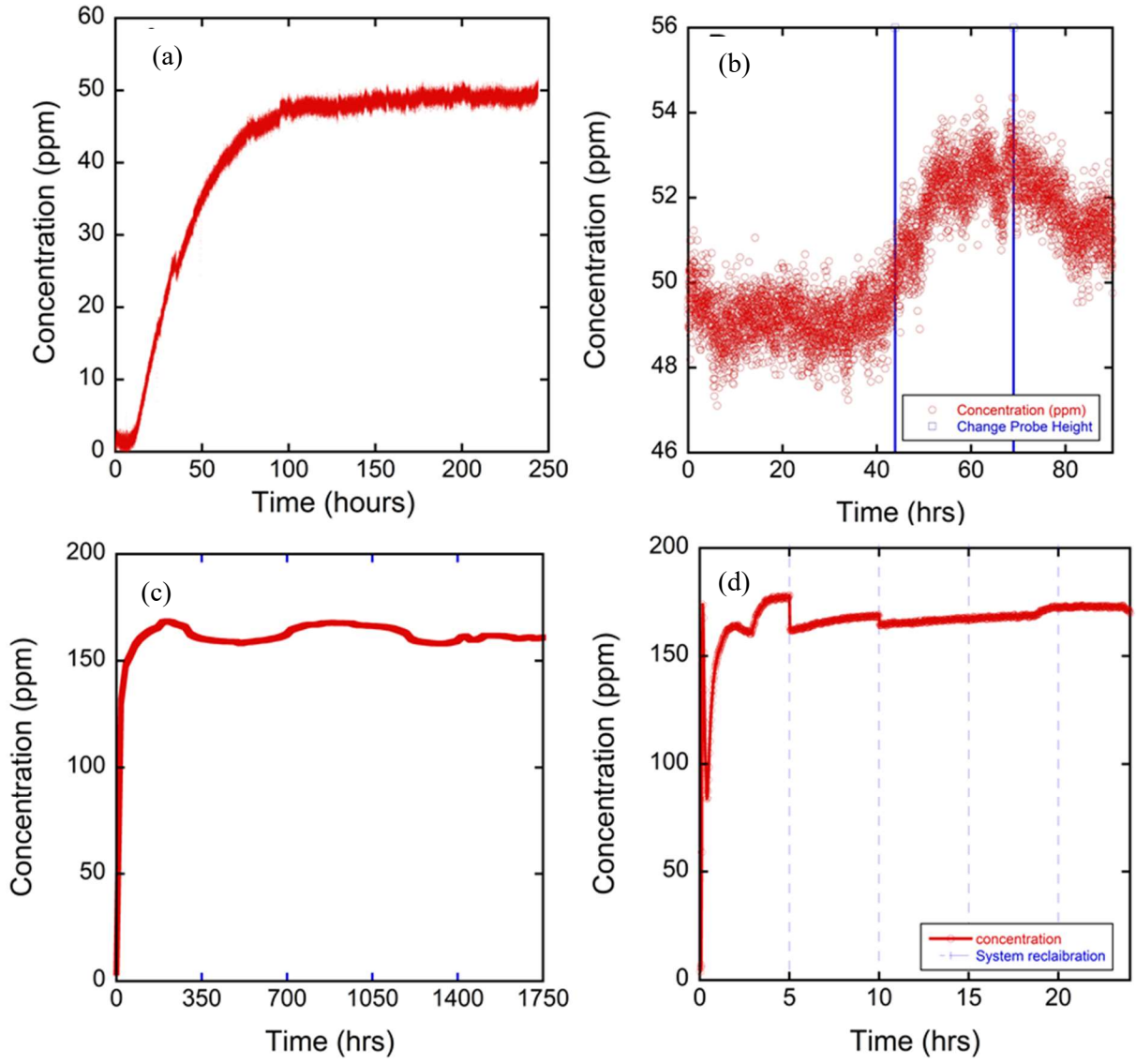


**Figure 5-24 VSC vessel testing, (a) VSC concentration over time during an empty vessel test using 50ppm $NH_3$, (b) variance in $NH_3$ concentration during probe height study, (c) VSC simulant test using 550 ppm $NH_3$ simulant and 50 ppm $NH_3$ gas, and (d) First 20 hours of VSC simulant with system recalibrations marked (blue-dashed lines)**

*5.5.1.4 FY19 Summary*

The current CEU and laser were designed to be modular, which limited their efficacy in studying gasses other than $NH_3$ and $CH_4$. In FY19 a benchtop QEPAS setup was assembled that allowed for QEPAS measurement of other analytes. Specific efforts were directed toward QEPAS detection of other VSC inhibitors being studied. Reference windows for gases other than ammonia were procured and installed in the bench top system. The plan initially called for detection of $SF_6$ gas. However, before that was initiated, WRPS communicated that they would not be pursuing the QEPAS technology in the near future. The following recommendations for future development of QEPAS were requested:

1. Design a mounted unit that can be placed in the field (e.g., the ventilation exhaust). The system can be miniaturized to adapt to various configurations.
2. The present system that is being tested was developed in 2011. Upgrades to the system design should be pursued.

## 6.0 Conclusions

Conclusions for each task that were performed for FY19 supporting Hanford DSTs are presented below in subsections.

6.1 New Limits Pitting Corrosion

Electrochemical testing was performed to expand the upper temperature limit for the PF equation from 50 to 75 ºC. Tests were performed at temperatures up to 75 ºC selected from a statistical designed matrix to determine the impact of temperature on predictive capabilities of the PF equation. Tests at elevated temperatures and hydroxide concentration up to 6 M were also performed. The elevated hydroxide concentration was used to cover cases in which the amount of hydroxide was increased and can be susceptible for SCC. Supplemental testing to address gaps in historical data was performed for hydroxide concentrations of 0.01 to 0.1 M at low and elevated temperatures (i.e., 35 and 75 ºC) and to verify the PF equation at these conditions. The results showed that for most tests, the PF equation for temperatures less than 50 °C, was able to accurately predict the results for tests performed at 75 ºC. It was shown that PFs greater than 1.2 predicted no pitting susceptibility, while PFs less than 1.2 were more likely to predict pitting susceptibility. However, in some cases "pass" conditions were observed for PF values less than 1.2. Generally, the model conservatively predicts whether carbon steel is vulnerable to pitting corrosion. Thus, at elevated temperatures the PF equation is still valid and can be used efficiently to predict vulnerability towards localized corrosion of carbon steel for liquid radioactive waste environments.

6.2 Secondary Liner Corrosion

VSC and immersion tests with commercially available VCIs were performed on the rail-road car carbon steel samples at specific concentrations mixed with the groundwater (GW) simulant. VCIs recommended dosages used for the study are:

- VCI-A: VpCI-337 – 10% v/v solution in GW simulant, i.e., 100 mL in VpCI-337 plus 900 mL of water for 1 L VCI formulation.
- VCI-B: 10% wt. VpCI-609 in GW simulant (100 g VpCI-609 in 1 liter) and 0.75% v/v VpCI-649MF (7.5 mL/L)

VCIs formulations were added during mid-course of experiments, i.e., after coupons had experienced corrosion in the untreated GW simulant. Three tests were conducted using VCI-A and VCI-B. The first two tests were conducted using 100% recommended dosages of VCI-A and VCI-B. The third test was

conducted at 10% of the recommended dosage of VCI-B. Following conclusions are made from the experimental data and results:

- The corrosion rate data indicated that 10% of the recommended dosage is not enough in mitigating corrosion. This observation is consistent with a prior study which also concluded that VCIs' effectiveness vanishes at 10% of the recommended dosages for the aboveground tank bottom underside application.

- The data also showed that 100% recommended dosages of VCI-A and VCI-B mitigated pitting corrosion of weathered coupons. Specifically, VCI-A mitigated pitting corrosion in immersed, Level 2, and Level 3 coupons, whereas VCI-B mitigated pitting corrosion in immersed, Level 1, and Level 3 coupons. Statistical significance of corrosion rate decrease in Level 1 coupons for 100% recommended dosage of VCI-A and Level 2 coupons for 100% recommended dosage of VCI-B could not be established; this may be due to choice of coupons' surface orientation being vertical during the tests, leading to limited and uneven weathering during groundwater only and groundwater plus VCI exposures.

6.3 Long-term OCP Drift

OCPs of carbon steel were measured in three Hanford waste tank simulants. Two sets of coupons, with three coupons in each set, were fabricated with differing surface conditions. The coupons' surface conditions included 600-grit polished surface, and surface with mill-scale plus corrosion products. Two coupons, one coupon from each set, were placed in each solution, and OCPs of the coupons were monitored for five months. OCPs of the coupons with polished surfaces evolved in the anodic direction with respect to the initial values, whereas OCPs of two of the three coupons with mill-scale plus corrosion products evolved in cathodic direction with respect to the initial values. Terminal OCP of one mill-scale plus corrosion products coupon was about 100 mV anodic with respect to the initial value. CPP data of the polished coupons before OCP evolutions showed mixed responses, i.e., a clear delineation between pitting and no-pitting cannot be made. CPP data after OCP evolutions remained mixed, indicating that change in OCP values do not affect CPP responses. Post OCP evolution, CPP data for the mill-scale plus corrosion products coupons in the three simulants showed negative hysteresis, which is a sign of no-pitting. The OCP and CPP data indicate that simulant chemistry and surface condition affect extent and direction of OCP evolution, however, OCP evolution does not affect CPP response. EIS spectra of the polished coupons differed compared to mill-scale plus corrosion product coupons in the three simulants. A qualitative analysis indicated that low-frequency asymptotic impedance values for the mill-scale plus corrosion products coupons are expected to be higher than the polished coupons. The EIS data indicate slower kinetics of the corrosion reactions at the mill-scale coupons compared the polished coupons.

6.4 MIC Testing

The Hanford tank farm facility observed significant corrosion degradation on the exterior side of the secondary liner of several DSTs. Two bottles of water from an LDP were analyzed to determine if MIC was a potential cause for this accelerated corrosion. MICkit® 5 and BART™ were used to determine the biological activity in the water bottles. The two testers showed similar negative results for sulfate reducing bacteria and acid producing bacteria which are commonly associated with MIC.

6.5 QEPAS

The current CEU and laser were designed to be modular, which limited their efficacy in studying gasses other than $NH_3$ and $CH_4$. In FY19 a benchtop QEPAS setup was assembled that allowed for QEPAS

measurement of other analytes. Specific efforts were directed toward QEPAS detection of other VSC inhibitors being studied. Reference windows for gases other than ammonia were procured and installed in the bench top system. The plan initially called for detection of $SF_6$ gas. However, before that was initiated, WRPS communicated that they would not be pursuing the QEPAS technology in the near future.

6.6 Recommendations

Recommendations for follow-on work are summarized on the next page. Some of these recommendations were incorporated into a proposal for FY20 activities.

New Limits Pitting Corrosion

- Historical review of slow strain rate tests to determine SCC conditions and identify gaps in the Hanford Site data.
- Perform statistical analysis of the historical SCC data and design experiments to address those gaps.

Secondary Liner

- Investigate corrosion mitigation of occluded areas of the secondary liner using VCIs.
- Use ER probe to monitor efficacy of the VCIs in mitigating vapor space corrosion.
- Perform the same test with the VCI concentration at less than the vendor recommended dosage to investigate the efficacy at depleted VCI conditions.

OCP Drift

- Utilizing coupons with various surface conditions, perform various electrochemical tests in three waste tanks simulants adding LPR tests intermittently during the course of the test.
- Identify source(s) of corrosion potential drift and quantify extent of drift as a function of simulant chemistry and metal surface condition, and;
- Determine the effect of the potential drift on the interpretation of pitting corrosion data.

MIC

- Testing would need to be done with kits as well as the testing of the corrosion products on carbon steel coupons in the LDP. Both tests should be done on a routine basis of every three months to get more representative data.

QEPAS

- Design a mounted unit that can be placed in the field (e.g., the ventilation exhaust). The system can be miniaturized to adapt to various configurations.
- The present system that is being tested was developed in 2011. Upgrades to the system design should be pursued.

## 7.0 References

[1] P. K. Shukla, R. E. Fuentes, "SRNL Task Technical and Quality Assurance Plan for Hanford Double Shell Waste Tank Corrosion Studies-FY19", SRNL-RP-2019-00100, Savannah River National Laboratory, Aiken, SC, February 2019.

[2] L. M. Stock, J. R. Follett, and E. C. Shallman, "Specifications for the Minimization of the Stress Corrosion Cracking Threat in Double-Shell Tank Wastes," RPP-RPT-47337, Washington River Protection Solutions, Richland, WA, March 2011.

[3] T. Martin, "Outcomes from the August 2013 Expert Panel Oversight Committee Meeting," RPP-ASMT-56781, Washington River Protection Solutions LLC, Richland, WA, February 2014.

[4] R. E. Fuentes, "Hanford Double Shell Waste Tank Corrosion Studies-Final Report FY16", SRNL-STI-2016-00721, Savannah River National Laboratory, Aiken, February 2017.
[5] R. E. Fuentes, "Hanford Double Shell Waste Tank Corrosion Studies-Final Report FY17", SRNL-STI-2018-00116, Savannah River National Laboratory, Aiken, April 2018.
[6] A. Macias and M. L. Escudero, "The Effect of Fluoride Ion on Corrosion of Reinforcing Steel in Alkaline Solutions", Corrosion Science, Vol. 36, No. 12, p. 2169.
[7] R. E. Fuentes, P. K. Shukla, B. Peters, D. A. Hitchcock, "Hanford Double Shell Waste Tank Corrosion Studies-Final Report FY2018", SRNL-STI-2019-00014, Savannah River National Laboratory, Aiken, August 2019.
[8] B. J. Wiersma, R. E. Fuentes, L. Stock, Chemistry Envelope for Pitting and Stress Corrosion Cracking Mitigation", SRNL-STI-2019-00217, Savannah River National Laboratory, Aiken, September 2019.
[9] R. E. Fuentes. B. J. Wiersma and K. Hicks, "Hanford Double Shell Waste Tank Corrosion Studies-Final Report FY14", SRNL-STI-2014-00616, Savannah River National Laboratory, Aiken, December 2014.
[10] R. E. Fuentes and R. B. Wyrwas, "Hanford Double Shell Waste Tank Corrosion Studies-Final Report FY15", SRNL-STI-2016-00117, Savannah River National Laboratory, Aiken, May 2016.
[11] J. W. Congdon, "Evaluation of Corrosion Inhibitors for Washed Precipitate – Coupon Test Results," DPST-86-721, Savannah River Laboratory, Aiken SC, October 1986.
[12] R. P. Anantatmula, "DST Pitting Annual Report," WHC-SD-WM-PRS-016, Rev. 0, Westinghouse Hanford Company, Richland, WA, September 1996.
[13] ASTM A515, "Standard Specification for Pressure Vessel Plates, Carbon Steel, for Intermediate- and Higher-Temperature Service", ASTM International, West Conshohocken, PA, 2003.
[14] ASTM G5-13 "Standard Reference Test Method for Making Potentiodynamic Anodic Polarization Measurements", ASTM International, West Conshohocken, PA, 2013.
[15] ASTM G1-03 "Standard Practice for Preparing, Cleaning, and Evaluating Corrosion Test Specimens", ASTM International, West Conshohocken, PA, 2011.
[16] Droycon Bioconcepts Inc., "Biological Activity Reaction Test BART User Manual", 2004 http://www.dbi.ca/BARTs/PDFs/Manual.pdf
[17] BTI Products, LLC. "MICkit 5 For the Detection of Problem-Causing Bacteria Involved in Microbiologically Influenced Corrosion (MIC)", 2018 https://www.bti-labs.com/resources/product-instructions/mickit-5-instructions/
[18] Droycon Bioconcepts Inc. "LAB-BART test for HAB Heterotrophic Aerobic Bacteria", 2014 https://www.dbi.ca/BARTs/PDFs/HAB-Lab.pdf
[19] Droycon Bioconcepts Inc. "LAB-BART test for APB Acid Producing Bacteria", 2014 https://www.dbi.ca/BARTs/PDFs/APB-Lab.pdf
[20] Droycon Bioconcepts Inc. "LAB-BART test for SRB Sulfate Reducing Bacteria", 2014 https://www.dbi.ca/BARTs/PDFs/SRB-Lab.pdf
[21] T. Martin, "Tank Integrity Expert Panel Corrosion Subgroup March 2016 Meeting Outcomes", RPP-ASMT-60833, Washington River Protection Solutions LLC, Richland, WA, May 2016.
[22] K. J. Evans, S. Chawla, K. M. Sherer, J. Gerst, J. Beavers, N. Sridhar and K. D. Boomer, "The Use of ASTM G192 to Evaluate the Susceptibility of Hanford Tank Steels to Pitting Corrosion", CORROSION/2016. Paper No. 51316-7688, NACE International, Houston, TX, 2016.
[23] R. B. Wyrwas, "SRNL Report for the Tank Waste Disposition Integrated Flowsheet: Corrosion Testing", SRNL-STI-2015-00506, Savannah River National Laboratory, Aiken, SC, September 2015

[24] M. T. Terry, "Expert Panel Workshop on Double-Shell Tank Vapor Space Corrosion Testing", RPP-RPT-31129, Rev. 0, September 2006.
[25] E. N. Hoffman, B. L. Garcia-Diaz, and T. B. Edwards, "Effect of Chloride and Sulfate Concentration on Probability Based Corrosion Control for Liquid Waste Tanks – Part IV", SRNL-STI-2011-00479, July 2012.
[26] J. R. Gray, B. L. Garcia-Diaz, T. H. Murphy, K. R. Hicks, "Vapor Space Corrosion Testing Simulating the Environment of Hanford Double-Shell Tanks", SRNL-STI-2013-00739, December 2013.
[27] R. B. Wyrwas, "Tank Waste Disposition Integrated Flowsheet: Corrosion Specification Development FY16 Interim Report", SRNL-RP-2016-00633, September, 2016.
[28] A.A. Kosterev, Yu. A. Bakhirkin, R.F. Curl, and F.K. Tittel, "Quartz-Enhanced photoacoustic spectroscopy", Optics Letters 27 p.1902, 2002.
[29] A.A. Kosterev, L. Dong, D. Thomazy, F.K. Tittel, S. Overby, "QEPAS for chemical analysis of multi-component gas mixtures", Appl Phys B 101, p. 649, 2010.
[30] Patimisco, G. Scamarco, F. Tittel, and V. Spagnolo, Sensors 14, 6165 (2014).
[31] R. Viola, N. Liberatore, D. Luciani and S. Mengali, "Quartz Enhanced Photoacoustic Spectroscopy for Detection of Improvised Explosive Devices and Precursors", Advances in Optical Technologies, vol. 2016, Article ID 5757361, 2016.

.

# Appendix A. Chemical Composition of New Limits Pitting Corrosion Task for Elevated Temperatures with CPP Results and Pictures after Test

## Table A-1 Test conditions and results of testing up to 75 ºC

| Test | Temperature (ºC) | Hydroxide (M) | Nitrite (M) | Nitrate (M) | Chloride (M) | Fluoride (M) | Sulfate (M) | Category | Pitting on Sample | Logistic approach |
|---|---|---|---|---|---|---|---|---|---|---|
| 1 | 75 | 0.0001 | 1.2 | 2.75 | 0 | 0 | 0.2 | 4 | Yes | 1 |
| 2 | 75 | 0.0001 | 0.48 | 3.3 | 0 | 0.3 | 0.12 | 3 | Yes | 1 |
| 3 | 75 | 0.0001 | 0 | 0 | 0.2 | 0.3 | 0.2 | 5 | Yes | 1 |
| 4 | 75 | 0.0001 | 0 | 5.5 | 0.4 | 0 | 0.1 | 5 | Yes | 1 |
| 5 | 75 | 0.0001 | 1.2 | 0 | 0.4 | 0.15 | 0 | 5 | Yes | 1 |
| 6 | 75 | 0.0001 | 1.2 | 5.5 | 0.4 | 0.3 | 0.2 | 5 | Yes | 1 |
| 7 | 75 | 0.24 | 0.72 | 2.2 | 0.16 | 0 | 0 | 5 | Yes | 1 |
| 8 | 75 | 0.48 | 0.96 | 5.5 | 0.32 | 0.06 | 0.2 | 3 | Yes | 1 |
| 9 | 75 | 0.6 | 0 | 0 | 0 | 0 | 0 | 1 | Yes | 0 |
| 10 | 75 | 0.6 | 0.6 | 2.75 | 0.2 | 0.15 | 0.1 | 5 | Yes | 1 |
| 11 | 75 | 0.6 | 0.6 | 2.75 | 0.2 | 0.15 | 0.1 | 5 | Yes | 1 |
| 12 | 75 | 0.6 | 0.6 | 2.75 | 0.2 | 0.15 | 0.1 | 4 | Yes | 1 |
| 13 | 75 | 0.6 | 0.6 | 2.75 | 0.2 | 0.15 | 0.1 | 5 | Yes | 1 |
| 14 | 75 | 0.72 | 0.24 | 0 | 0.4 | 0.12 | 0.16 | 1 | Yes | 0 |
| 15 | 75 | 0.96 | 0 | 4.4 | 0.24 | 0.24 | 0.04 | 5 | Yes | 1 |
| 16 | 75 | 1.2 | 0 | 5.5 | 0 | 0 | 0.2 | 1 | No | 0 |
| 17 | 75 | 1.2 | 1.2 | 0 | 0 | 0.3 | 0.1 | 1 | No | 0 |
| 18 | 75 | 1.2 | 1.2 | 1.1 | 0.08 | 0.18 | 0.08 | 1 | No | 0 |
| 19 | 75 | 1.2 | 1.2 | 5.5 | 0.2 | 0 | 0 | 1 | No | 0 |
| 20 | 75 | 1.2 | 0.6 | 0 | 0.4 | 0 | 0.2 | 1 | No | 0 |
| 21 | 75 | 1.2 | 0 | 2.75 | 0.4 | 0.3 | 0 | 5 | Yes | 1 |

*Additional chemicals added contributed to 0.2 M TIC in each test

## Test 1

### Composition of simulant

**Test 1**

| | | | |
|---|---|---|---|
| Temperature | 75 | °C | |
| pH at room temperature | 11.5 | Target | 10 |
| pH before testing (at temp.) | 10.2 | pH after testing (at temp.) | 10.0 |
| Volume | 0.7 | L | |

| Simulant Source | Formula | Molecular Weight (g/mol) | Concentration (M) | weight required (g) |
|---|---|---|---|---|
| Sodium hydroxide | NaOH | 40.0000 | 0.0001 | 0.0028 |
| Sodium nitrite | $NaNO_2$ | 69.0000 | 1.2 | 57.9600 |
| Sodium nitrate | $NaNO_3$ | 85.0000 | 2.75 | 163.6250 |
| Sodium chloride | NaCl | 58.4000 | 0 | 0.0000 |
| Sodium fluoride | NaF | 42.0000 | 0 | 0.0000 |
| Sodium sulfate | $Na_2SO_4$ | 142.0000 | 0.2 | 19.8800 |
| Sodium carbonate | $Na_2CO_3$ | 106.0000 | 0.075 | 5.5650 |
| Sodium bicarbonate | $NaHCO_3$ | 84.0100 | 0.025 | 1.4702 |

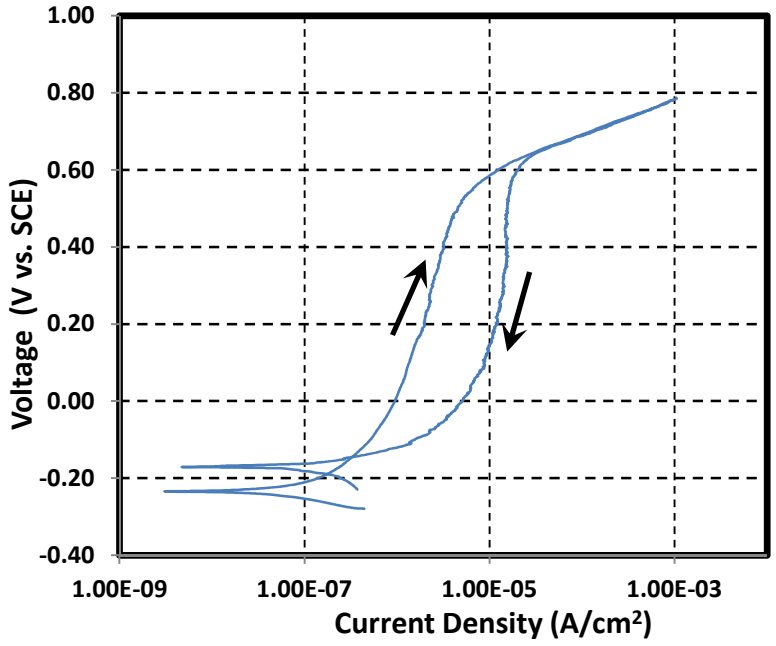


**Cyclic Potentiodynamic Polarization result**

**Images of bullet samples after test**

## Test 2

### Composition of simulant

**Test 2**

| | | | |
|---|---|---|---|
| Temperature | 50 | °C | |
| pH at room temperature | 11.6 | Target | 10 |
| pH before testing (at temp.) | 10.1 | pH after testing (at temp.) | 10.0 |
| Volume | 0.7 | L | |

| Simulant Source | Formula | Molecular Weight (g/mol) | Concentration (M) | weight required (g) |
|---|---|---|---|---|
| Sodium hydroxide | NaOH | 40.0000 | 0.0001 | 0.0028 |
| Sodium nitrite | $NaNO_2$ | 69.0000 | 0.48 | 23.1840 |
| Sodium nitrate | $NaNO_3$ | 85.0000 | 3.3 | 196.3500 |
| Sodium chloride | NaCl | 58.4000 | 0 | 0.0000 |
| Sodium fluoride | NaF | 42.0000 | 0.3 | 8.8200 |
| Sodium sulfate | $Na_2SO_4$ | 142.0000 | 0.12 | 11.9280 |
| Sodium carbonate | $Na_2CO_3$ | 106.0000 | 0.075 | 5.5650 |
| Sodium bicarbonate | $NaHCO_3$ | 84.0100 | 0.025 | 1.4702 |

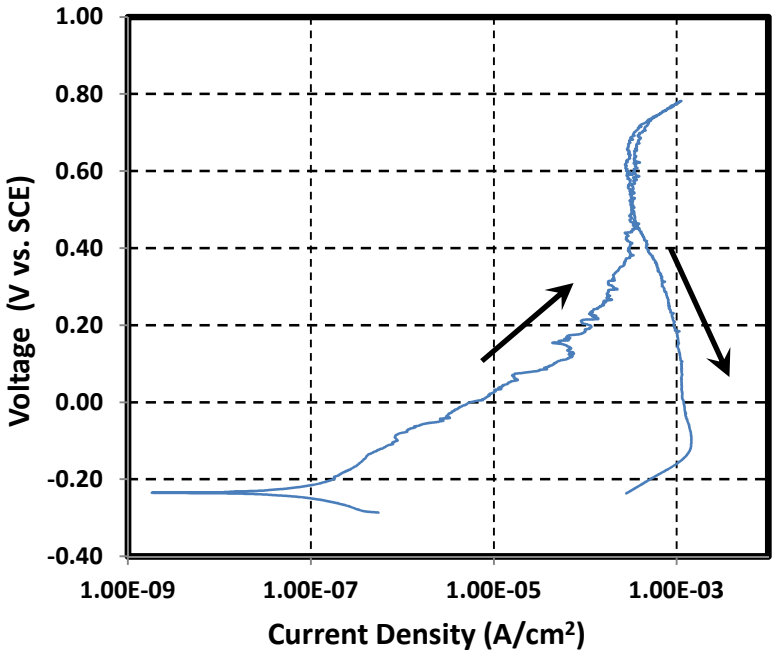


**Cyclic Potentiodynamic Polarization result**

**Images of bullet samples after test**

**ASTM G192 Plot**

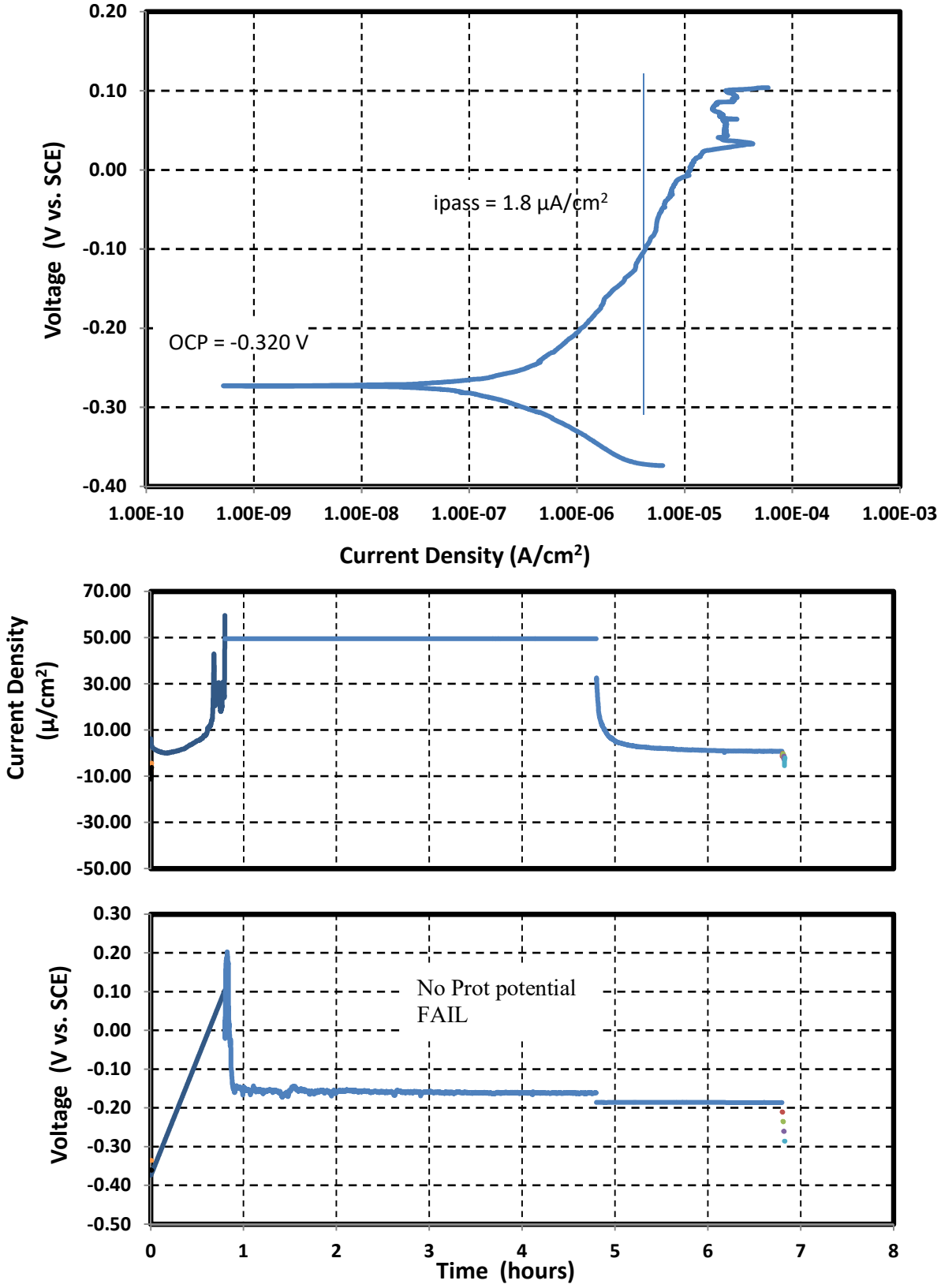

## Test 3

### Composition of simulant

**Test 3**

| | | | |
|---|---|---|---|
| Temperature | 75 | °C | |
| pH at room temperature | 11.8 | Target | 10 |
| pH before testing (at temp.) | 10.5 | pH after testing (at temp.) | 10.0 |
| Volume | 0.7 | L | |

| Simulant Source | Formula | Molecular Weight (g/mol) | Concentration (M) | weight required (g) |
|---|---|---|---|---|
| Sodium hydroxide | NaOH | 40.0000 | 0.0001 | 0.0028 |
| Sodium nitrite | $NaNO_2$ | 69.0000 | 0 | 0.0000 |
| Sodium nitrate | $NaNO_3$ | 85.0000 | 0 | 0.0000 |
| Sodium chloride | NaCl | 58.4000 | 0.2 | 8.1760 |
| Sodium fluoride | NaF | 42.0000 | 0.3 | 8.8200 |
| Sodium sulfate | $Na_2SO_4$ | 142.0000 | 0.2 | 19.8800 |
| Sodium carbonate | $Na_2CO_3$ | 106.0000 | 0.075 | 5.5650 |
| Sodium bicarbonate | $NaHCO_3$ | 84.0100 | 0.025 | 1.4702 |

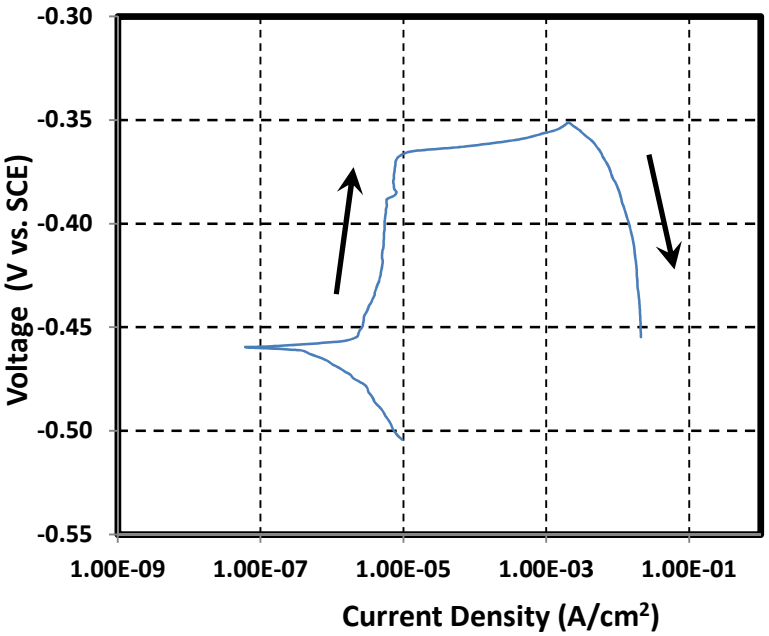


**Cyclic Potentiodynamic Polarization result**

**Images of bullet samples after test**

## Test 4

### Composition of simulant

**Test 4**

| | | | |
|---|---|---|---|
| Temperature | 75 | °C | |
| pH at room temperature | 11.16 | Target | 10 |
| pH before testing (at temp.) | 9.8 | pH after testing (at temp.) | 9.8 |
| Volume | 0.7 | L | |

| Simulant Source | Formula | Molecular Weight (g/mol) | Concentration (M) | weight required (g) |
|---|---|---|---|---|
| Sodium hydroxide | NaOH | 40.0000 | 0.0001 | 0.0028 |
| Sodium nitrite | $NaNO_2$ | 69.0000 | 0 | 0.0000 |
| Sodium nitrate | $NaNO_3$ | 85.0000 | 5.5 | 327.2500 |
| Sodium chloride | NaCl | 58.4000 | 0.4 | 16.3520 |
| Sodium fluoride | NaF | 42.0000 | 0 | 0.0000 |
| Sodium sulfate | $Na_2SO_4$ | 142.0000 | 0.1 | 9.9400 |
| Sodium carbonate | $Na_2CO_3$ | 106.0000 | 0.075 | 5.5650 |
| Sodium bicarbonate | $NaHCO_3$ | 84.0100 | 0.025 | 1.4702 |

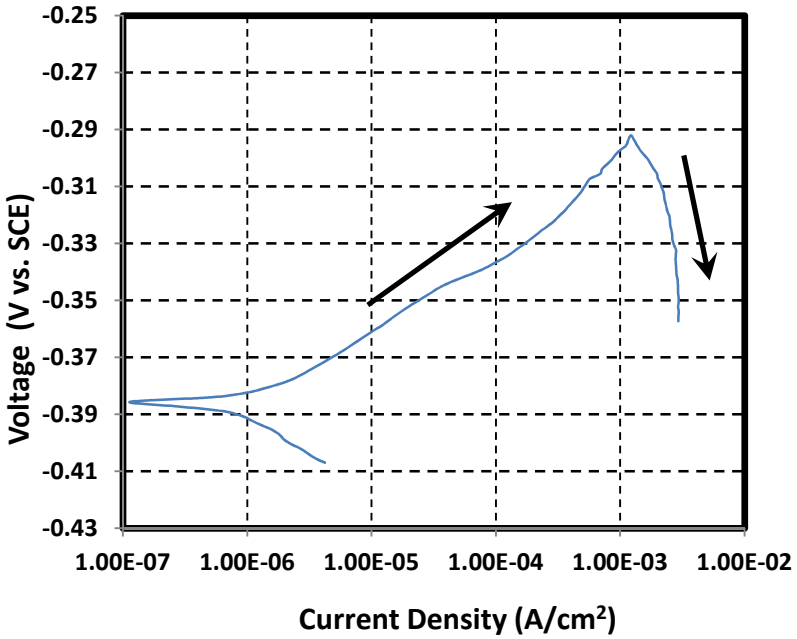


**Cyclic Potentiodynamic Polarization result**

**Images of bullet samples after test**

## Test 5

### Composition of simulant

**Test 5**

| | | | |
|---|---|---|---|
| Temperature | 50 | °C | |
| pH at room temperature | 11.1 | Target | 10 |
| pH before testing (at temp.) | 9.9 | pH after testing (at temp.) | 9.9 |
| Volume | 0.7 | L | |

| Simulant Source | Formula | Molecular Weight (g/mol) | Concentration (M) | weight required (g) |
|---|---|---|---|---|
| Sodium hydroxide | NaOH | 40.0000 | 0.0001 | 0.0028 |
| Sodium nitrite | $NaNO_2$ | 69.0000 | 1.2 | 57.9600 |
| Sodium nitrate | $NaNO_3$ | 85.0000 | 0 | 0.0000 |
| Sodium chloride | NaCl | 58.4000 | 0.4 | 16.3520 |
| Sodium fluoride | NaF | 42.0000 | 0.15 | 4.4100 |
| Sodium sulfate | $Na_2SO_4$ | 142.0000 | 0 | 0.0000 |
| Sodium carbonate | $Na_2CO_3$ | 106.0000 | 0.075 | 5.5650 |
| Sodium bicarbonate | $NaHCO_3$ | 84.0100 | 0.025 | 1.4702 |

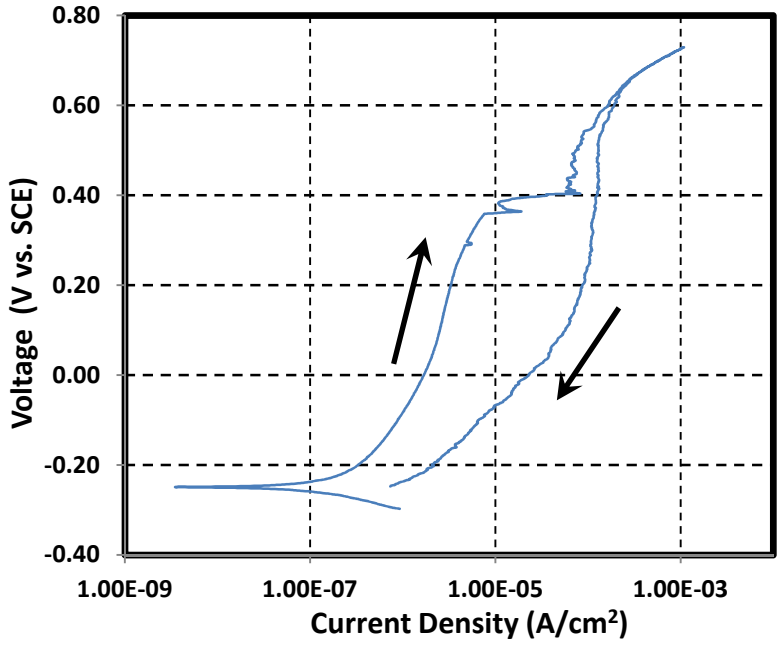


**Cyclic Potentiodynamic Polarization result**

**Images of bullet samples after test**

## Test 6

### Composition of simulant

**Test 6**

| | | | |
|---|---|---|---|
| Temperature | 50 | °C | |
| pH at room temperature | 11.2 | Target | 10 |
| pH before testing (at temp.) | 10.0 | pH after testing (at temp.) | 9.9 |
| Volume | 0.7 | L | |

| Simulant Source | Formula | Molecular Weight (g/mol) | Concentration (M) | weight required (g) |
|---|---|---|---|---|
| Sodium hydroxide | NaOH | 40.0000 | 0.0001 | 0.0028 |
| Sodium nitrite | $NaNO_2$ | 69.0000 | 1.2 | 57.9600 |
| Sodium nitrate | $NaNO_3$ | 85.0000 | 5.5 | 327.2500 |
| Sodium chloride | NaCl | 58.4000 | 0.4 | 16.3520 |
| Sodium fluoride | NaF | 42.0000 | 0.3 | 8.8200 |
| Sodium sulfate | $Na_2SO_4$ | 142.0000 | 0.2 | 19.8800 |
| Sodium carbonate | $Na_2CO_3$ | 106.0000 | 0.075 | 5.5650 |
| Sodium bicarbonate | $NaHCO_3$ | 84.0100 | 0.025 | 1.4702 |

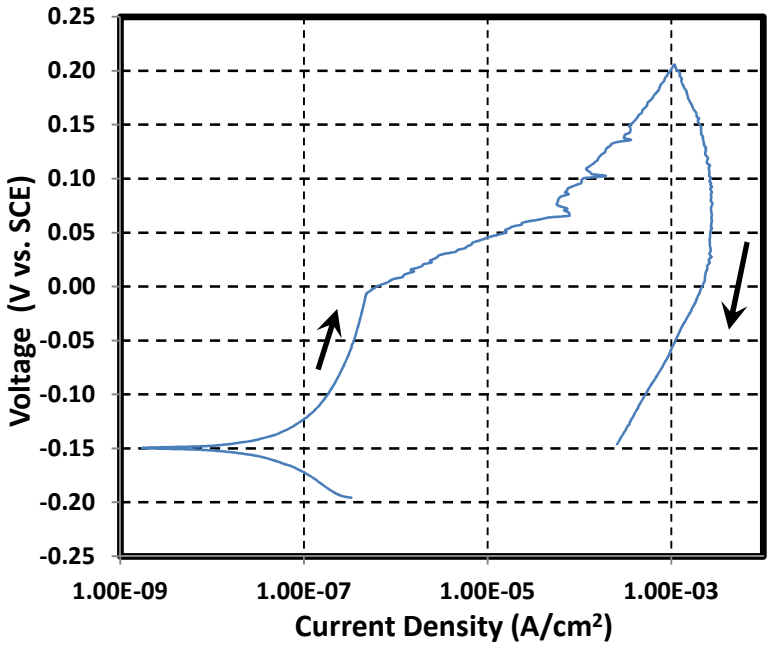


**Cyclic Potentiodynamic Polarization result**

**Images of bullet samples after test**

## Test 7

### Composition of simulant

**Test 7**

| | | | |
|---|---|---|---|
| Temperature | 75 °C | | |
| pH at room temperature | 13.0 | | |
| pH before testing (at temp.) | 11.4 | pH after testing (at temp.) | 11.3 |
| Volume | 0.7 L | | |

| Simulant Source | Formula | Molecular Weight (g/mol) | Concentration (M) | weight required (g) |
|---|---|---|---|---|
| Sodium hydroxide | NaOH | 40.0000 | 0.24 | 6.7200 |
| Sodium nitrite | $NaNO_2$ | 69.0000 | 0.72 | 34.7760 |
| Sodium nitrate | $NaNO_3$ | 85.0000 | 2.2 | 130.9000 |
| Sodium chloride | NaCl | 58.4000 | 0.16 | 6.5408 |
| Sodium fluoride | NaF | 42.0000 | 0 | 0.0000 |
| Sodium sulfate | $Na_2SO_4$ | 142.0000 | 0 | 0.0000 |
| Sodium carbonate | $Na_2CO_3$ | 106.0000 | 0.100 | 7.4200 |
| Sodium bicarbonate | $NaHCO_3$ | 84.0100 | 0.000 | 0.0000 |

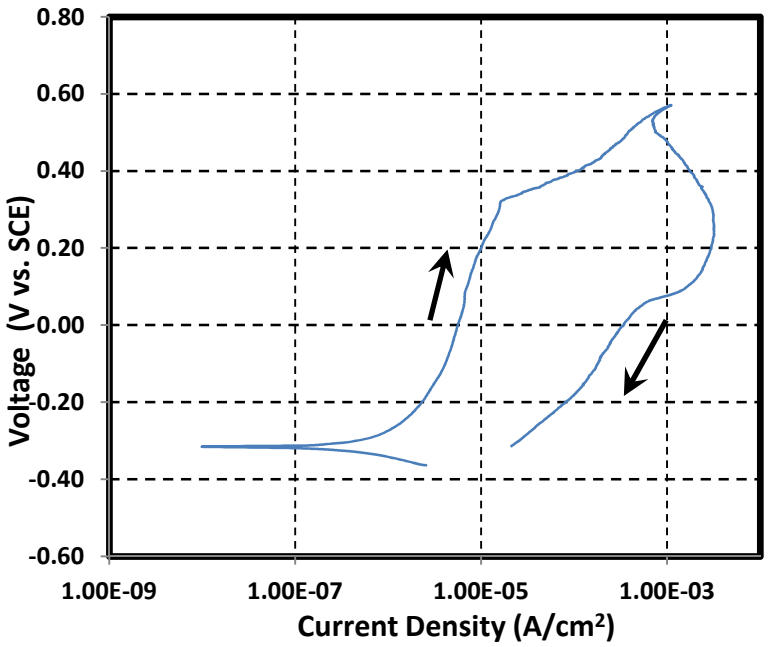


**Cyclic Potentiodynamic Polarization result**

**Images of bullet samples after test**

## Test 8

### Composition of simulant

**Test 8**

| | | | |
|---|---|---|---|
| Temperature | 50 | °C | |
| pH at room temperature | 13.5 | | |
| pH before testing (at temp.) | 11.8 | pH after testing (at temp.) | 11.7 |
| Volume | 0.7 | L | |

| Simulant Source | Formula | Molecular Weight (g/mol) | Concentration (M) | weight required (g) |
|---|---|---|---|---|
| Sodium hydroxide | NaOH | 40.0000 | 0.48 | 13.4400 |
| Sodium nitrite | $NaNO_2$ | 69.0000 | 0.96 | 46.3680 |
| Sodium nitrate | $NaNO_3$ | 85.0000 | 5.5 | 327.2500 |
| Sodium chloride | NaCl | 58.4000 | 0.32 | 13.0816 |
| Sodium fluoride | NaF | 42.0000 | 0.06 | 1.7640 |
| Sodium sulfate | $Na_2SO_4$ | 142.0000 | 0.2 | 19.8800 |
| Sodium carbonate | $Na_2CO_3$ | 106.0000 | 0.100 | 7.4200 |
| Sodium bicarbonate | $NaHCO_3$ | 84.0100 | 0.000 | 0.0000 |

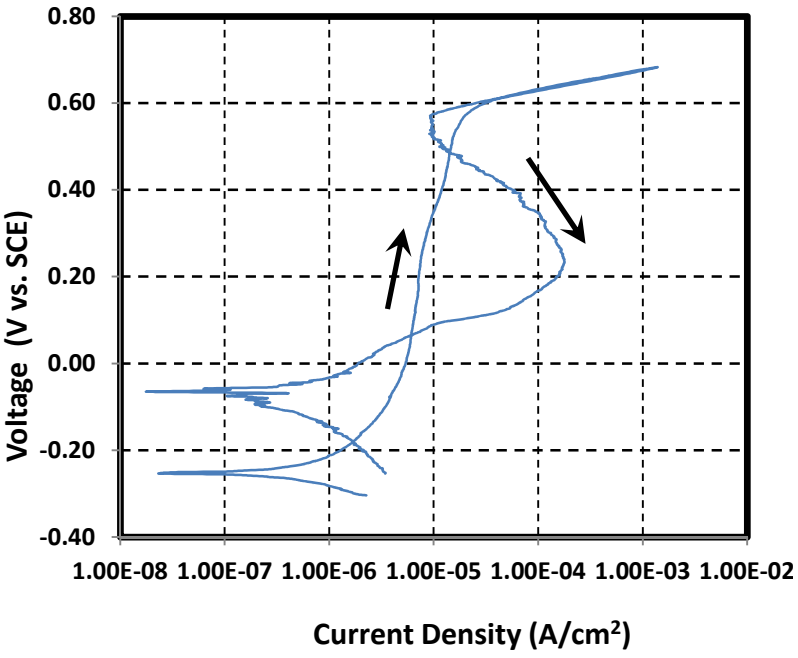


**Cyclic Potentiodynamic Polarization result**

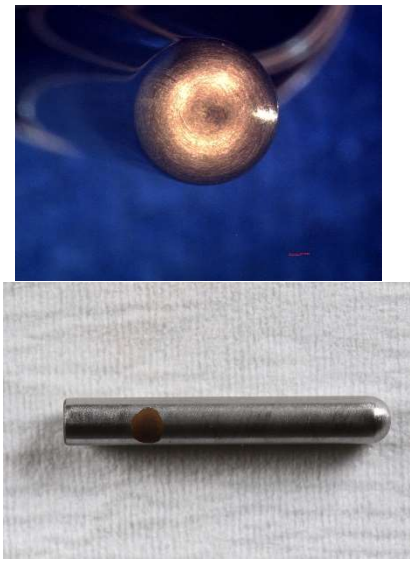

**Images of bullet samples after test**

**ASTM G192 Plot**

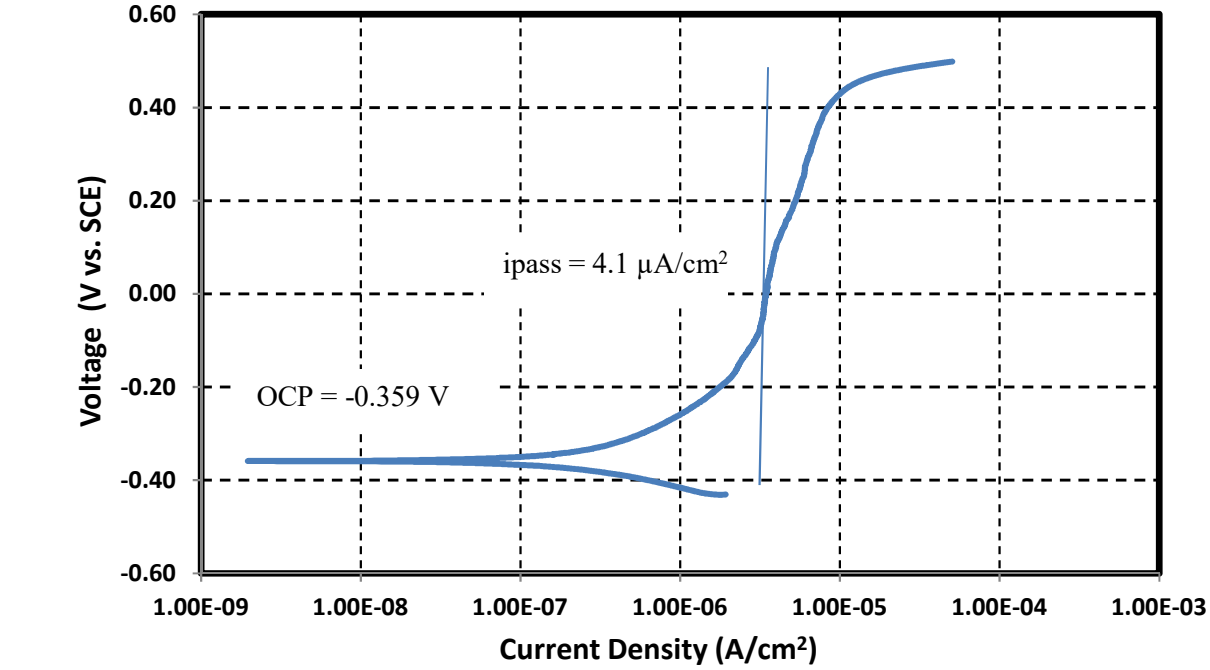


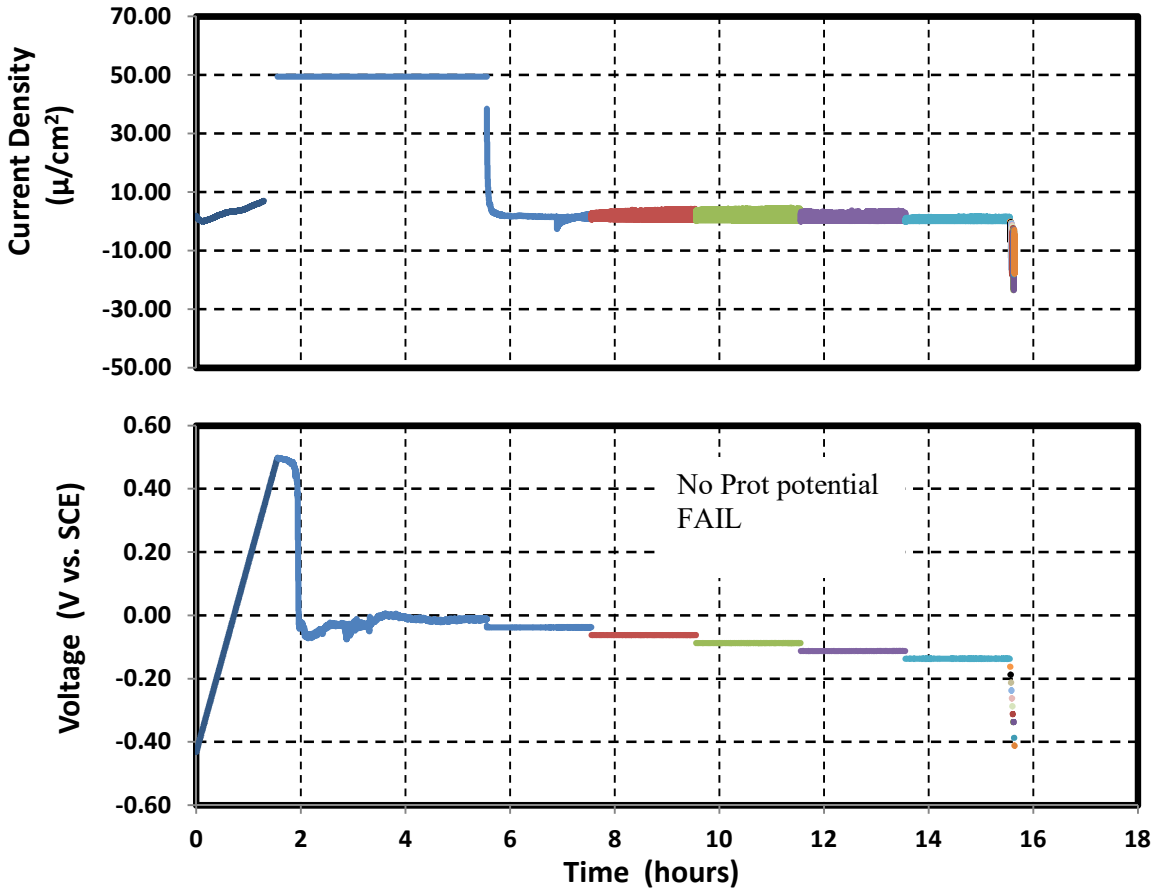

## Test 9

### Composition of simulant

**Test 9**

| | | | |
|---|---|---|---|
| Temperature | 55 | °C | |
| pH at room temperature | 13.8 | | |
| pH before testing (at temp.) | 11.6 | pH after testing (at temp.) | 11.4 |
| Volume | 0.7 | L | |

| Simulant Source | Formula | Molecular Weight (g/mol) | Concentration (M) | weight required (g) |
|---|---|---|---|---|
| Sodium hydroxide | NaOH | 40.0000 | 0.6 | 16.8000 |
| Sodium nitrite | $NaNO_2$ | 69.0000 | 0 | 0.0000 |
| Sodium nitrate | $NaNO_3$ | 85.0000 | 0 | 0.0000 |
| Sodium chloride | NaCl | 58.4000 | 0 | 0.0000 |
| Sodium fluoride | NaF | 42.0000 | 0 | 0.0000 |
| Sodium sulfate | $Na_2SO_4$ | 142.0000 | 0 | 0.0000 |
| Sodium carbonate | $Na_2CO_3$ | 106.0000 | 0.100 | 7.4200 |
| Sodium bicarbonate | $NaHCO_3$ | 84.0100 | 0.000 | 0.0000 |

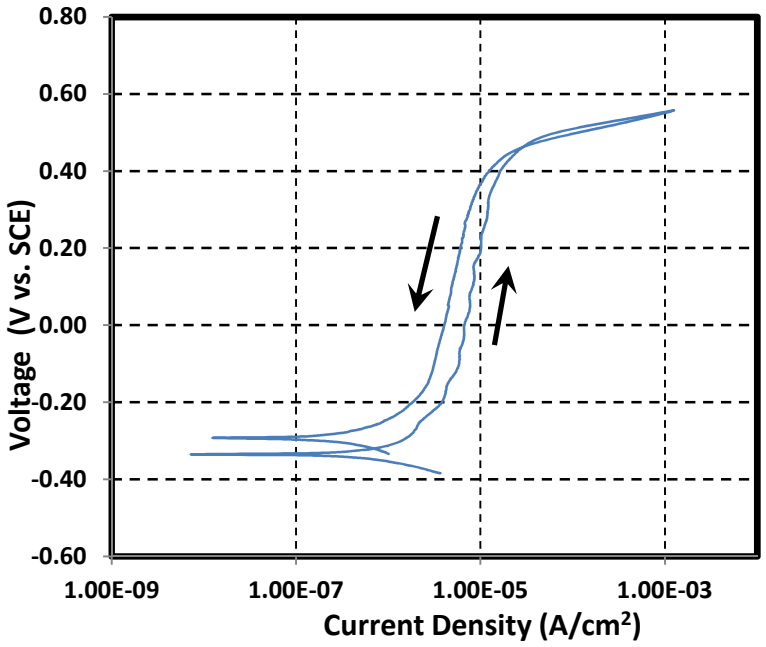


**Cyclic Potentiodynamic Polarization result**

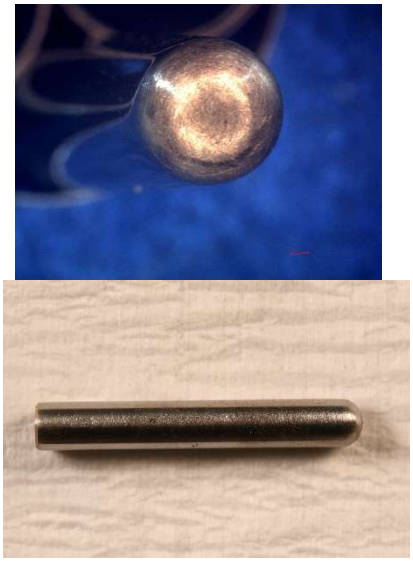

**Images of bullet samples after test**

## Test 10

### Composition of simulant

**Test 10**

| | | | |
|---|---|---|---|
| Temperature | 65 | °C | |
| pH at room temperature | 13.3 | | |
| pH before testing (at temp.) | 11.7 | pH after testing (at temp.) | 11.8 |
| Volume | 0.7 | L | |

| Simulant Source | Formula | Molecular Weight (g/mol) | Concentration (M) | weight required (g) |
|---|---|---|---|---|
| Sodium hydroxide | NaOH | 40.0000 | 0.6 | 16.8000 |
| Sodium nitrite | $NaNO_2$ | 69.0000 | 0.6 | 28.9800 |
| Sodium nitrate | $NaNO_3$ | 85.0000 | 2.75 | 163.6250 |
| Sodium chloride | NaCl | 58.4000 | 0.2 | 8.1760 |
| Sodium fluoride | NaF | 42.0000 | 0.15 | 4.4100 |
| Sodium sulfate | $Na_2SO_4$ | 142.0000 | 0.1 | 9.9400 |
| Sodium carbonate | $Na_2CO_3$ | 106.0000 | 0.100 | 7.4200 |
| Sodium bicarbonate | $NaHCO_3$ | 84.0100 | 0.000 | 0.0000 |

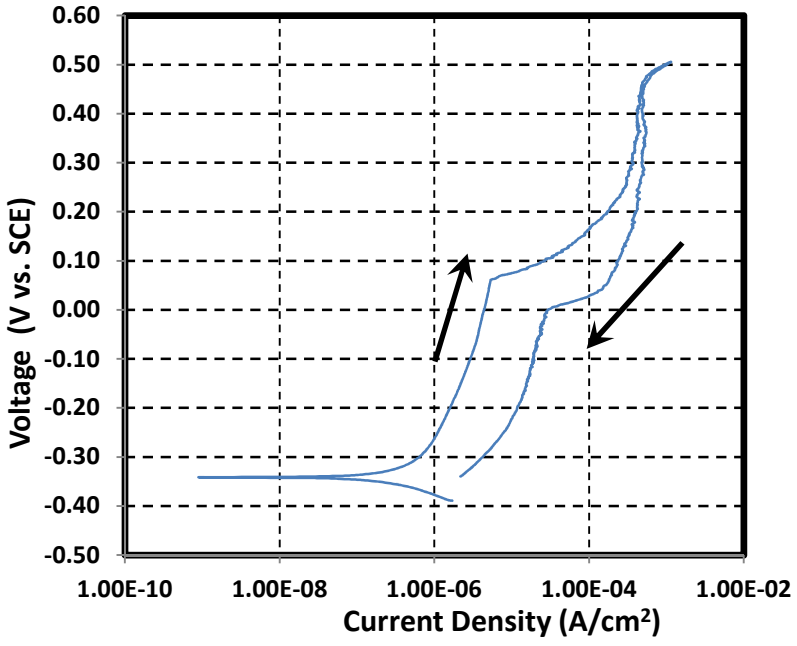


**Cyclic Potentiodynamic Polarization result**

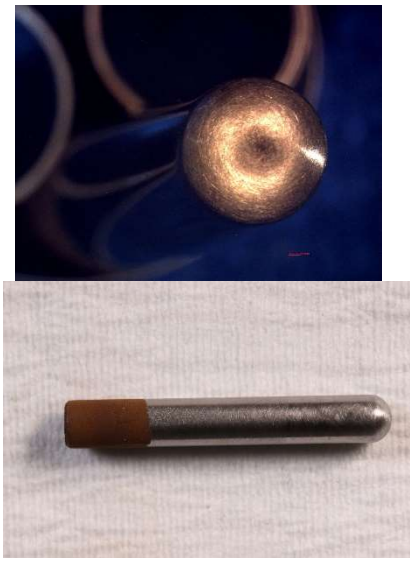

**Images of bullet samples after test**

## Test 11

### Composition of simulant

**Test 11**

| | | | |
|---|---|---|---|
| Temperature | 70 °C | | |
| pH at room temperature | 13.4 | | |
| pH before testing (at temp.) | 11.6 | pH after testing (at temp.) | 11.5 |
| Volume | 0.7 L | | |

| Simulant Source | Formula | Molecular Weight (g/mol) | Concentration (M) | weight required (g) |
|---|---|---|---|---|
| Sodium hydroxide | NaOH | 40.0000 | 0.6 | 16.8000 |
| Sodium nitrite | $NaNO_2$ | 69.0000 | 0.6 | 28.9800 |
| Sodium nitrate | $NaNO_3$ | 85.0000 | 2.75 | 163.6250 |
| Sodium chloride | NaCl | 58.4000 | 0.2 | 8.1760 |
| Sodium fluoride | NaF | 42.0000 | 0.15 | 4.4100 |
| Sodium sulfate | $Na_2SO_4$ | 142.0000 | 0.1 | 9.9400 |
| Sodium carbonate | $Na_2CO_3$ | 106.0000 | 0.100 | 7.4200 |
| Sodium bicarbonate | $NaHCO_3$ | 84.0100 | 0.000 | 0.0000 |

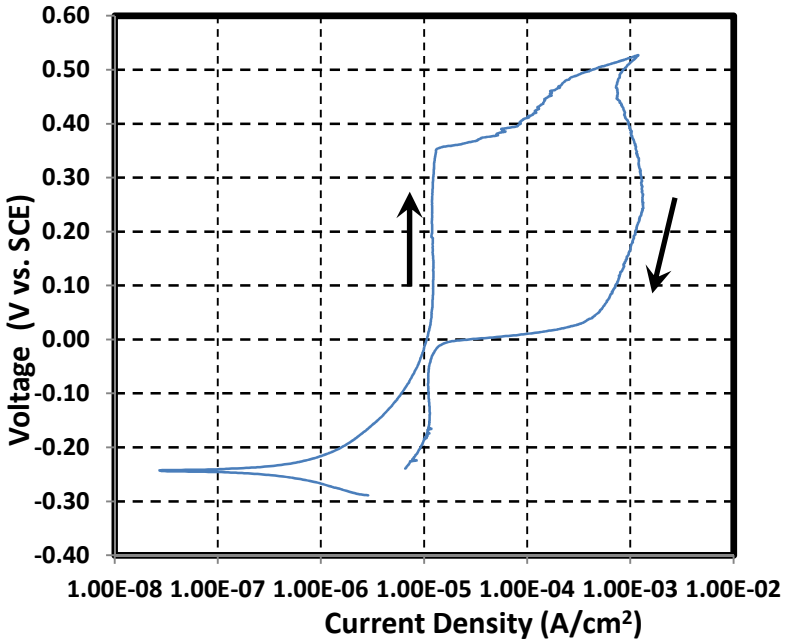


**Cyclic Potentiodynamic Polarization result**

**Images of bullet samples after test**

## Test 12

### Composition of simulant

**Test 12**

| | | | |
|---|---|---|---|
| Temperature | 50 °C | | |
| pH at room temperature | 13.4 | | |
| pH before testing (at temp.) | 11.4 | pH after testing (at temp.) | 11.4 |
| Volume | 0.7 L | | |

| Simulant Source | Formula | Molecular Weight (g/mol) | Concentration (M) | weight required (g) |
|---|---|---|---|---|
| Sodium hydroxide | NaOH | 40.0000 | 0.6 | 16.8000 |
| Sodium nitrite | $NaNO_2$ | 69.0000 | 0.6 | 28.9800 |
| Sodium nitrate | $NaNO_3$ | 85.0000 | 2.75 | 163.6250 |
| Sodium chloride | NaCl | 58.4000 | 0.2 | 8.1760 |
| Sodium fluoride | NaF | 42.0000 | 0.15 | 4.4100 |
| Sodium sulfate | $Na_2SO_4$ | 142.0000 | 0.1 | 9.9400 |
| Sodium carbonate | $Na_2CO_3$ | 106.0000 | 0.100 | 7.4200 |
| Sodium bicarbonate | $NaHCO_3$ | 84.0100 | 0.000 | 0.0000 |

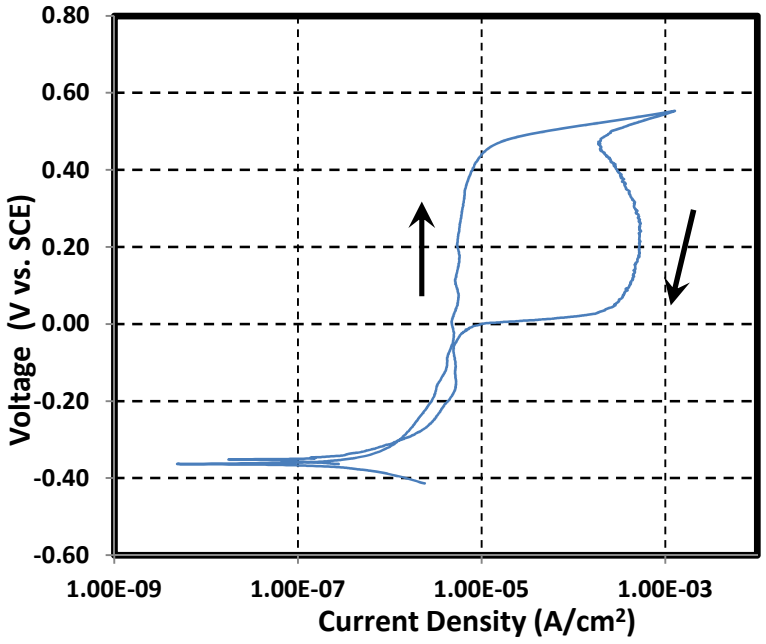


**Cyclic Potentiodynamic Polarization result**

**Images of bullet samples after test**

## Test 13

### Composition of simulant

**Test 13**

| | | | |
|---|---|---|---|
| Temperature | 75 | °C | |
| pH at room temperature | 13.8 | | |
| pH before testing (at temp.) | 12.2 | pH after testing (at temp.) | 12.0 |
| Volume | 0.7 | L | |

| Simulant Source | Formula | Molecular Weight (g/mol) | Concentration (M) | weight required (g) |
|---|---|---|---|---|
| Sodium hydroxide | NaOH | 40.0000 | 0.6 | 16.8000 |
| Sodium nitrite | $NaNO_2$ | 69.0000 | 0.6 | 28.9800 |
| Sodium nitrate | $NaNO_3$ | 85.0000 | 2.75 | 163.6250 |
| Sodium chloride | NaCl | 58.4000 | 0.2 | 8.1760 |
| Sodium fluoride | NaF | 42.0000 | 0.15 | 4.4100 |
| Sodium sulfate | $Na_2SO_4$ | 142.0000 | 0.1 | 9.9400 |
| Sodium carbonate | $Na_2CO_3$ | 106.0000 | 0.100 | 7.4200 |
| Sodium bicarbonate | $NaHCO_3$ | 84.0100 | 0.000 | 0.0000 |

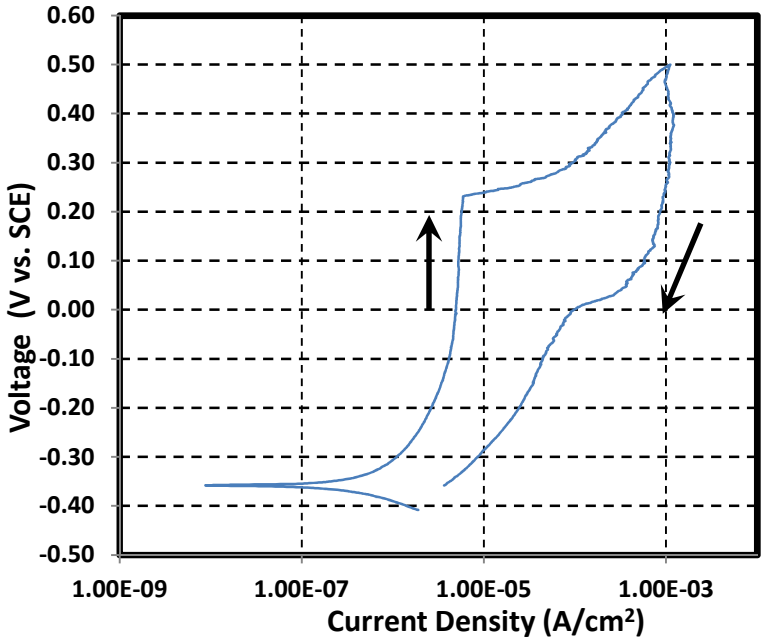


**Cyclic Potentiodynamic Polarization result**

**Images of bullet samples after test**

## Test 14

### Composition of simulant

**Test 14**

| | | | |
|---|---|---|---|
| Temperature | 75 °C | | |
| pH at room temperature | 13.9 | | |
| pH before testing (at temp.) | 11.5 | pH after testing (at temp.) | 11.5 |
| Volume | 0.7 L | | |

| Simulant Source | Formula | Molecular Weight (g/mol) | Concentration (M) | weight required (g) |
|---|---|---|---|---|
| Sodium hydroxide | NaOH | 40.0000 | 0.72 | 20.1600 |
| Sodium nitrite | $NaNO_2$ | 69.0000 | 0.24 | 11.5920 |
| Sodium nitrate | $NaNO_3$ | 85.0000 | 0 | 0.0000 |
| Sodium chloride | NaCl | 58.4000 | 0.4 | 16.3520 |
| Sodium fluoride | NaF | 42.0000 | 0.12 | 3.5280 |
| Sodium sulfate | $Na_2SO_4$ | 142.0000 | 0.16 | 15.9040 |
| Sodium carbonate | $Na_2CO_3$ | 106.0000 | 0.100 | 7.4200 |
| Sodium bicarbonate | $NaHCO_3$ | 84.0100 | 0.000 | 0.0000 |

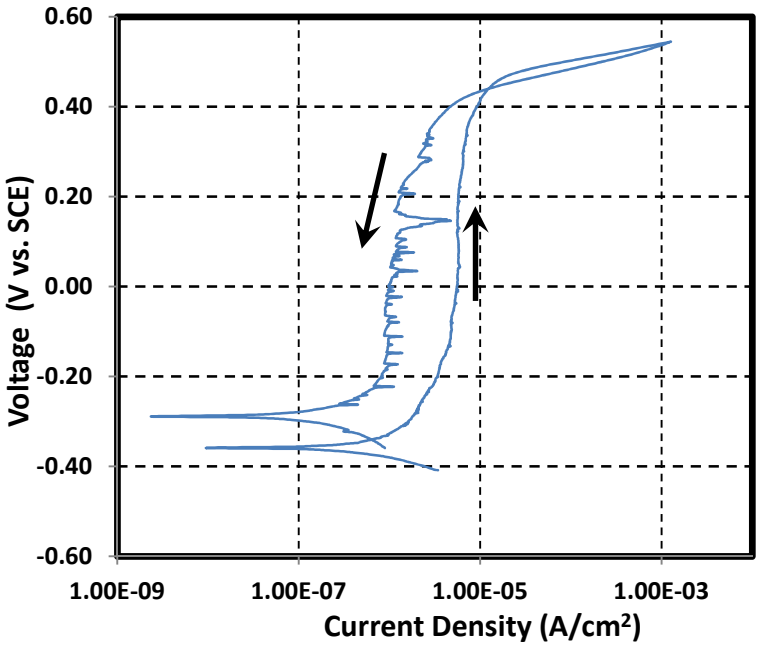


**Cyclic Potentiodynamic Polarization result**

**Images of bullet samples after test**

**ASTM G192 Plot**

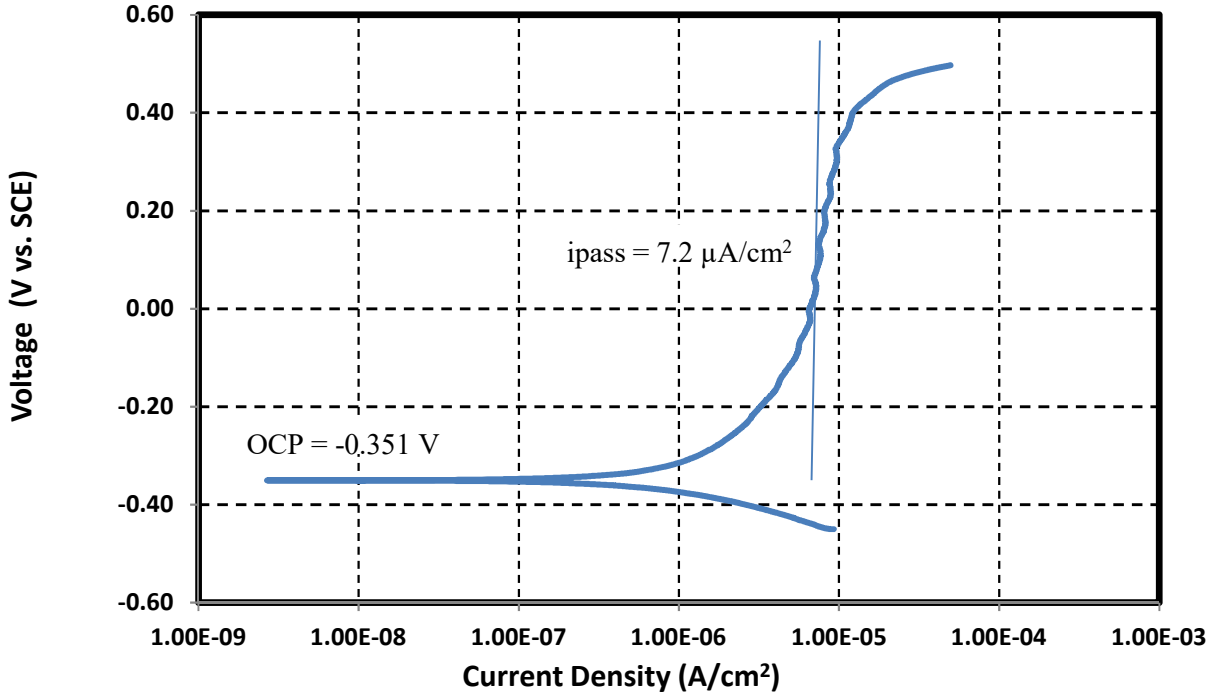


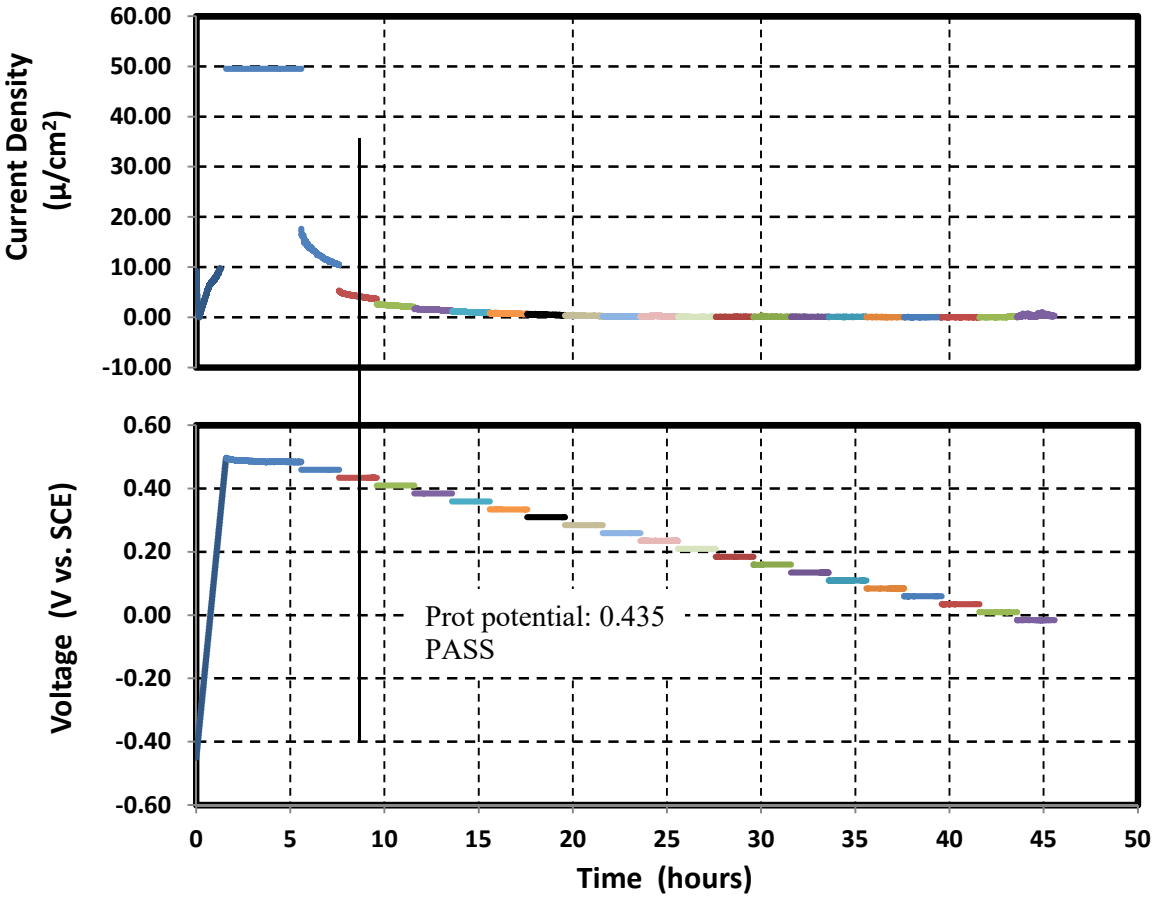

## Test 15

### Composition of simulant

**Test 15**

| | | | |
|---|---|---|---|
| Temperature | 75 °C | | |
| pH at room temperature | 14.0 | | |
| pH before testing (at temp.) | 12.2 | pH after testing (at temp.) | 12.0 |
| Volume | 0.7 L | | |

| Simulant Source | Formula | Molecular Weight (g/mol) | Concentration (M) | weight required (g) |
|---|---|---|---|---|
| Sodium hydroxide | NaOH | 40.0000 | 0.96 | 26.8800 |
| Sodium nitrite | $NaNO_2$ | 69.0000 | 0 | 0.0000 |
| Sodium nitrate | $NaNO_3$ | 85.0000 | 4.4 | 261.8000 |
| Sodium chloride | NaCl | 58.4000 | 0.24 | 9.8112 |
| Sodium fluoride | NaF | 42.0000 | 0.24 | 7.0560 |
| Sodium sulfate | $Na_2SO_4$ | 142.0000 | 0.04 | 3.9760 |
| Sodium carbonate | $Na_2CO_3$ | 106.0000 | 0.100 | 7.4200 |
| Sodium bicarbonate | $NaHCO_3$ | 84.0100 | 0.000 | 0.0000 |

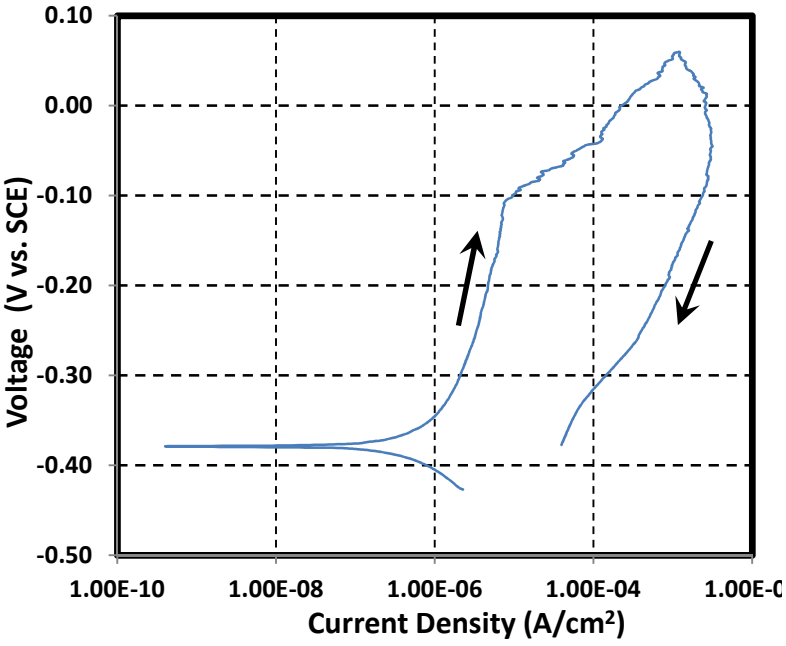


**Cyclic Potentiodynamic Polarization result**

**Images of bullet samples after test**

## Test 16

### Composition of simulant

**Test 16**

| | | | |
|---|---|---|---|
| Temperature | 75 °C | | |
| pH at room temperature | 14.0 | Target | 12 - 13 |
| pH before testing (at temp.) | 12.2 | pH after testing (at temp.) | 12.0 |
| Volume | 0.7 L | | |

| Simulant Source | Formula | Molecular Weight (g/mol) | Concentration (M) | weight required (g) |
|---|---|---|---|---|
| Sodium hydroxide | NaOH | 40.0000 | 1.2 | 33.6000 |
| Sodium nitrite | $NaNO_2$ | 69.0000 | 0 | 0.0000 |
| Sodium nitrate | $NaNO_3$ | 85.0000 | 5.5 | 327.2500 |
| Sodium chloride | NaCl | 58.4000 | 0 | 0.0000 |
| Sodium fluoride | NaF | 42.0000 | 0 | 0.0000 |
| Sodium sulfate | $Na_2SO_4$ | 142.0000 | 0.2 | 19.8800 |
| Sodium carbonate | $Na_2CO_3$ | 106.0000 | 0.100 | 7.4200 |
| Sodium bicarbonate | $NaHCO_3$ | 84.0100 | 0.000 | 0.0000 |

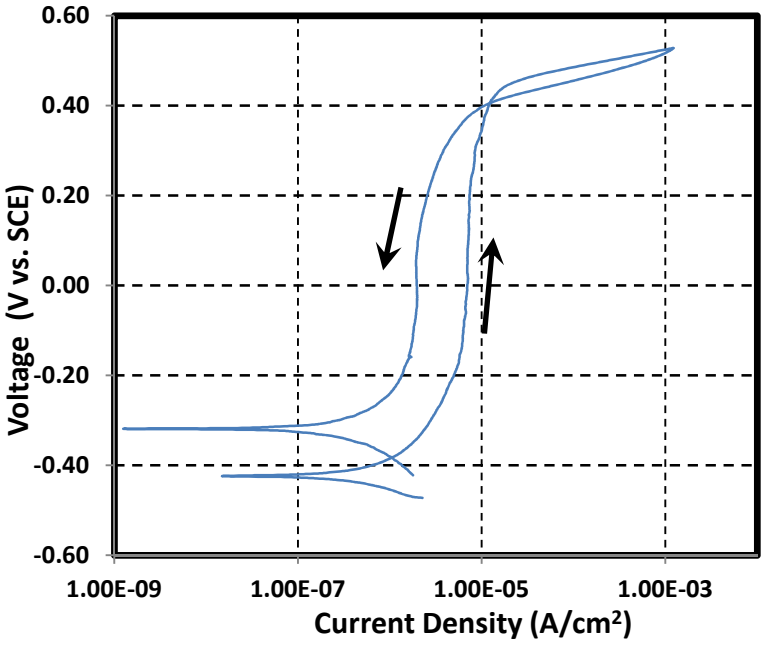


**Cyclic Potentiodynamic Polarization result**

**Images of bullet samples after test**

## Test 17

### Composition of simulant

**Test 17**

| | | | |
|---|---|---|---|
| Temperature | 75 °C | | |
| pH at room temperature | 13.8 | | |
| pH before testing (at temp.) | 12.2 | pH after testing (at temp.) | 12.0 |
| Volume | 0.7 L | | |

| Simulant Source | Formula | Molecular Weight (g/mol) | Concentration (M) | weight required (g) |
|---|---|---|---|---|
| Sodium hydroxide | NaOH | 40.0000 | 1.2 | 33.6000 |
| Sodium nitrite | $NaNO_2$ | 69.0000 | 1.2 | 57.9600 |
| Sodium nitrate | $NaNO_3$ | 85.0000 | 0 | 0.0000 |
| Sodium chloride | NaCl | 58.4000 | 0 | 0.0000 |
| Sodium fluoride | NaF | 42.0000 | 0.3 | 8.8200 |
| Sodium sulfate | $Na_2SO_4$ | 142.0000 | 0.1 | 9.9400 |
| Sodium carbonate | $Na_2CO_3$ | 106.0000 | 0.100 | 7.4200 |
| Sodium bicarbonate | $NaHCO_3$ | 84.0100 | 0.000 | 0.0000 |

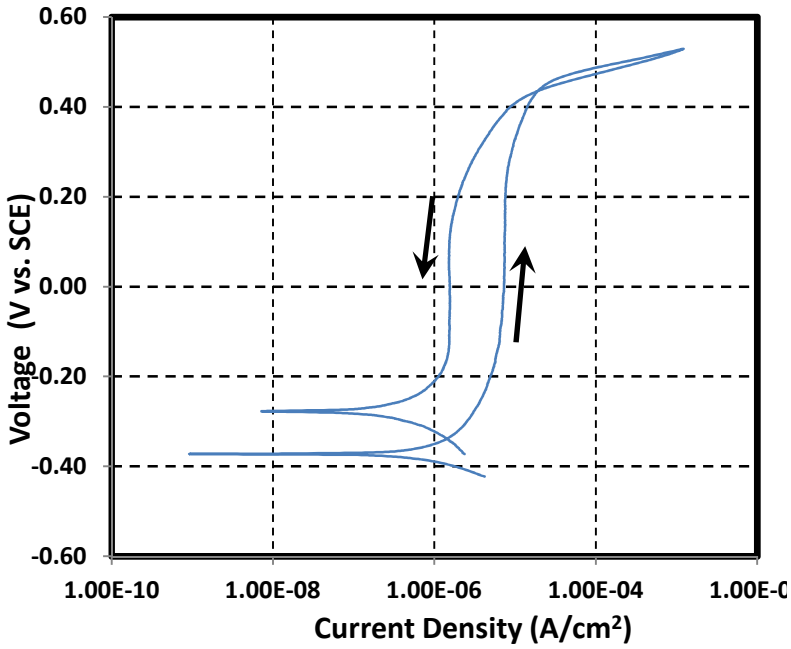


**Cyclic Potentiodynamic Polarization result**

**Images of bullet samples after test**

## Test 18

### Composition of simulant

**Test 18**

| | | | |
|---|---|---|---|
| Temperature | 75 °C | | |
| pH at room temperature | 13.8 | | |
| pH before testing (at temp.) | 12.1 | pH after testing (at temp.) | 11.9 |
| Volume | 0.7 L | | |

| Simulant Source | Formula | Molecular Weight (g/mol) | Concentration (M) | weight required (g) |
|---|---|---|---|---|
| Sodium hydroxide | NaOH | 40.0000 | 1.2 | 33.6000 |
| Sodium nitrite | $NaNO_2$ | 69.0000 | 1.2 | 57.9600 |
| Sodium nitrate | $NaNO_3$ | 85.0000 | 1.1 | 65.4500 |
| Sodium chloride | NaCl | 58.4000 | 0.08 | 3.2704 |
| Sodium fluoride | NaF | 42.0000 | 0.18 | 5.2920 |
| Sodium sulfate | $Na_2SO_4$ | 142.0000 | 0.08 | 7.9520 |
| Sodium carbonate | $Na_2CO_3$ | 106.0000 | 0.100 | 7.4200 |
| Sodium bicarbonate | $NaHCO_3$ | 84.0100 | 0.000 | 0.0000 |

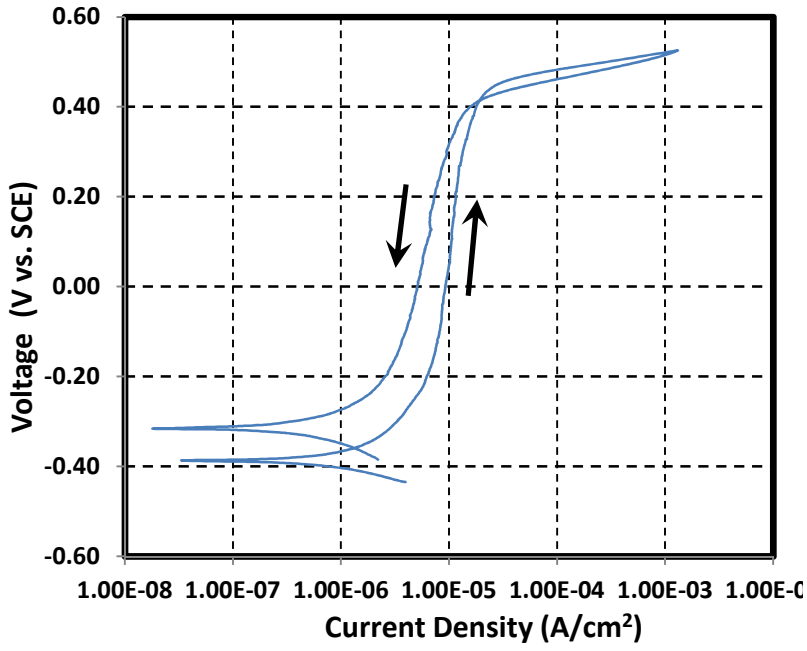


**Cyclic Potentiodynamic Polarization result**

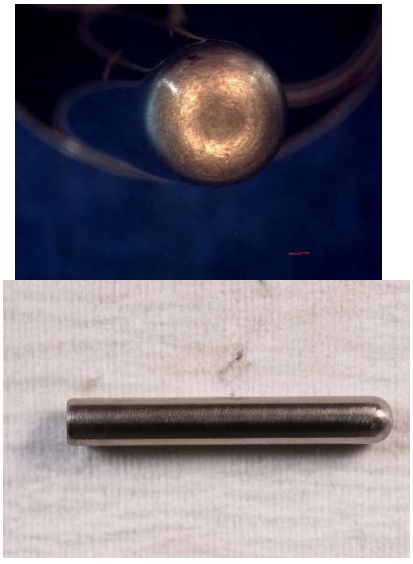

**Images of bullet samples after test**

## Test 19

### Composition of simulant

**Test 19**

| | | | |
|---|---|---|---|
| Temperature | 75 °C | | |
| pH at room temperature | 13.8 | | |
| pH before testing (at temp.) | 11.9 | pH after testing (at temp.) | 11.9 |
| Volume | 0.7 L | | |

| Simulant Source | Formula | Molecular Weight (g/mol) | Concentration (M) | weight required (g) |
|---|---|---|---|---|
| Sodium hydroxide | NaOH | 40.0000 | 1.2 | 33.6000 |
| Sodium nitrite | $NaNO_2$ | 69.0000 | 1.2 | 57.9600 |
| Sodium nitrate | $NaNO_3$ | 85.0000 | 5.5 | 327.2500 |
| Sodium chloride | NaCl | 58.4000 | 0.2 | 8.1760 |
| Sodium fluoride | NaF | 42.0000 | 0 | 0.0000 |
| Sodium sulfate | $Na_2SO_4$ | 142.0000 | 0 | 0.0000 |
| Sodium carbonate | $Na_2CO_3$ | 106.0000 | 0.100 | 7.4200 |
| Sodium bicarbonate | $NaHCO_3$ | 84.0100 | 0.000 | 0.0000 |

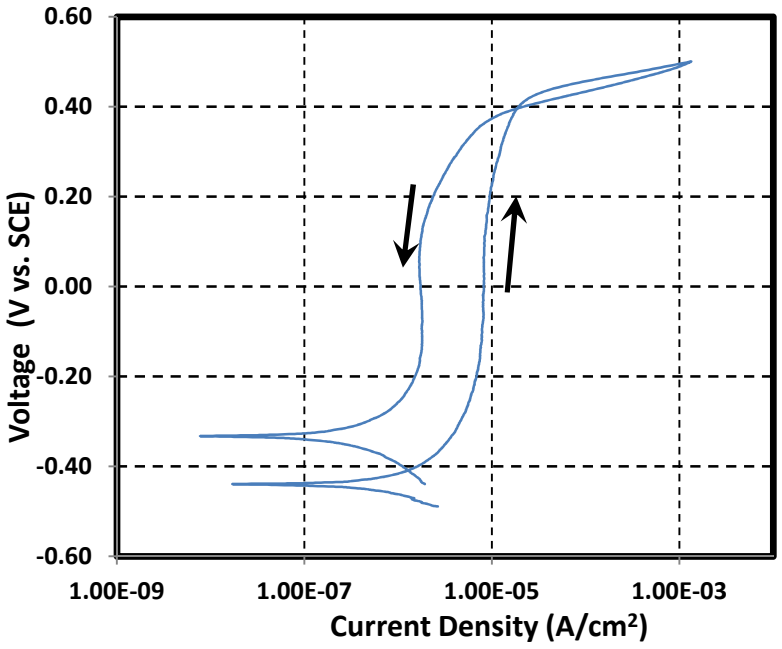


**Cyclic Potentiodynamic Polarization result**

**Images of bullet samples after test**

## Test 20

### Composition of simulant

**Test 20**

| | | | |
|---|---|---|---|
| Temperature | 75 °C | | |
| pH at room temperature | 13.7 | | |
| pH before testing (at temp.) | 11.9 | pH after testing (at temp.) | 11.8 |
| Volume | 0.7 L | | |

| Simulant Source | Formula | Molecular Weight (g/mol) | Concentration (M) | weight required (g) |
|---|---|---|---|---|
| Sodium hydroxide | NaOH | 40.0000 | 1.2 | 33.6000 |
| Sodium nitrite | $NaNO_2$ | 69.0000 | 0.6 | 28.9800 |
| Sodium nitrate | $NaNO_3$ | 85.0000 | 0 | 0.0000 |
| Sodium chloride | NaCl | 58.4000 | 0.4 | 16.3520 |
| Sodium fluoride | NaF | 42.0000 | 0 | 0.0000 |
| Sodium sulfate | $Na_2SO_4$ | 142.0000 | 0.2 | 19.8800 |
| Sodium carbonate | $Na_2CO_3$ | 106.0000 | 0.100 | 7.4200 |
| Sodium bicarbonate | $NaHCO_3$ | 84.0100 | 0.000 | 0.0000 |

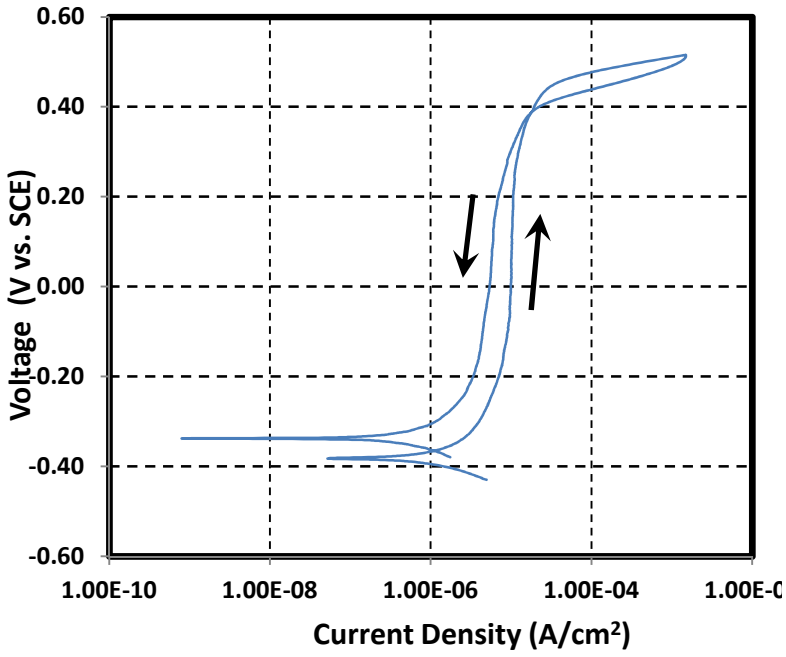


**Cyclic Potentiodynamic Polarization result**

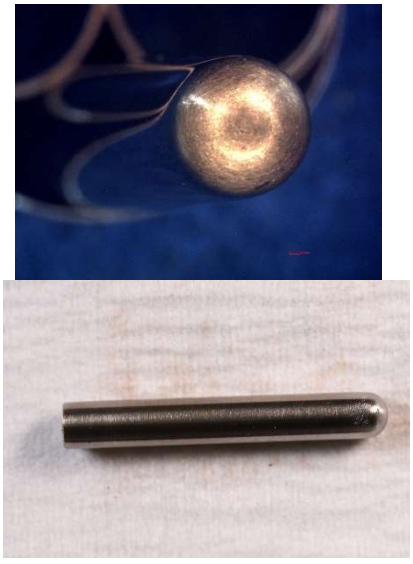

**Images of bullet samples after test**

## Test 21

### Composition of simulant

**Test 21**

| | | | |
|---|---|---|---|
| Temperature | 75 °C | | |
| pH at room temperature | 13.7 | | |
| pH before testing (at temp.) | 11.9 | pH after testing (at temp.) | 11.8 |
| Volume | 0.7 L | | |

| Simulant Source | Formula | Molecular Weight (g/mol) | Concentration (M) | weight required (g) |
|---|---|---|---|---|
| Sodium hydroxide | NaOH | 40.0000 | 1.2 | 33.6000 |
| Sodium nitrite | $NaNO_2$ | 69.0000 | 0 | 0.0000 |
| Sodium nitrate | $NaNO_3$ | 85.0000 | 2.75 | 163.6250 |
| Sodium chloride | NaCl | 58.4000 | 0.4 | 16.3520 |
| Sodium fluoride | NaF | 42.0000 | 0.3 | 8.8200 |
| Sodium sulfate | $Na_2SO_4$ | 142.0000 | 0 | 0.0000 |
| Sodium carbonate | $Na_2CO_3$ | 106.0000 | 0.100 | 7.4200 |
| Sodium bicarbonate | $NaHCO_3$ | 84.0100 | 0.000 | 0.0000 |

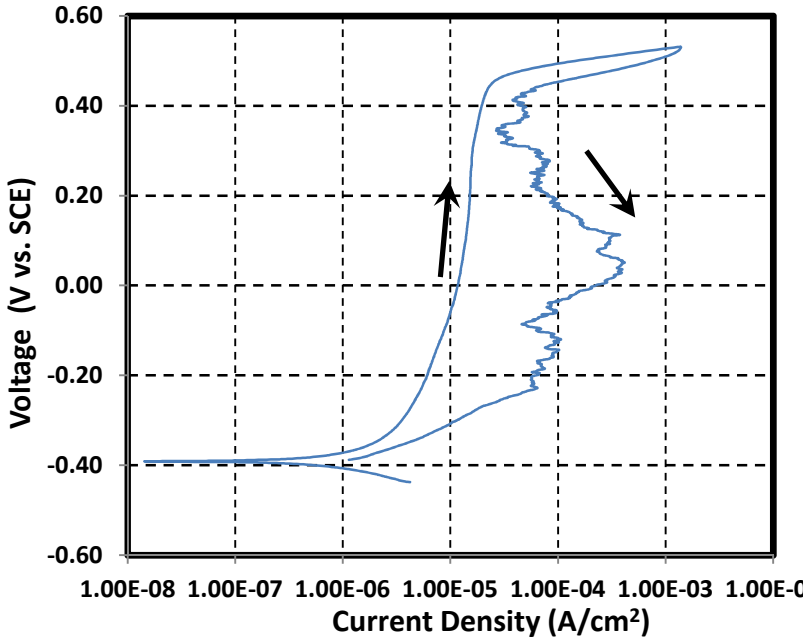


**Cyclic Potentiodynamic Polarization Result**

**Images of bullet samples after test**

# Appendix B Chemical Composition of New Limits Pitting Corrosion Task for up to 6 M Hydroxide with Cyclic Potentiodynamic Polarization Results and Pictures after Test

**Table B-1. Test conditions and results of testing up to 6 M Hydroxide**

| Test | Temperature (°C) | Hydroxide (M) | Nitrite (M) | Nitrate (M) | Chloride (M) | Fluoride (M) | Sulfate (M) | Category | Pitting on Sample | Logistic approach |
|---|---|---|---|---|---|---|---|---|---|---|
| 1 | 75 | 1.2 | 0.2 | 0.2 | 0 | 0.2 | 0.2 | 1 | No | 0 |
| 2 | 50 | 6 | 0.2 | 0.2 | 0.2 | 0.2 | 0.2 | 1 | No | 0 |
| 3 | 75 | 6 | 1.2 | 1.2 | 0.2 | 0.2 | 0.2 | 1 | No (discolored) | 0 |
| 4 | 75 | 6 | 1.2 | 0.2 | 0 | 0 | 0.2 | 1 | No (discolored) | 0 |
| 5 | 50 | 1.2 | 1.2 | 0.2 | 0.2 | 0 | 0.2 | 1 | No | 0 |
| 6 | 50 | 6 | 0.2 | 1.2 | 0 | 0 | 0.2 | 1 | No (discolored) | 0 |
| 7 | 75 | 1.2 | 0.2 | 1.2 | 0.2 | 0 | 0.2 | 1 | No | 0 |
| 8 | 50 | 1.2 | 1.2 | 1.2 | 0 | 0.2 | 0.2 | 3 | No | 0 |
| 9 | 55 | 2.4 | 1.2 | 1.2 | 0 | 0.1 | 0.2 | 1 | No | 0 |
| 10 | 65 | 4.8 | 0.7 | 0.2 | 0.05 | 0 | 0.2 | 1 | No (discolored) | 0 |
| 11 | 70 | 1.2 | 0.45 | 0.45 | 0.1 | 0.2 | 0.2 | 1 | No | 0 |
| 12 | 50 | 3.6 | 0.2 | 0.95 | 0.15 | 0.05 | 0.2 | 1 | No | 0 |
| 13 | 75 | 6 | 0.95 | 0.7 | 0.2 | 0.15 | 0.2 | 1 | No (discolored) | 0 |

*Additional chemicals added contributed to 0.2 M TIC in each test

## Test 1

### Composition of simulant

**Test 1**

| | | | |
|---|---|---|---|
| Temperature | 75 °C | | |
| pH at room temperature | 13.8 | | |
| pH before testing (at temp.) | 11.6 | pH after testing (at temp.) | 11.5 |
| Volume | 0.7 L | | |

| Simulant Source | Formula | Molecular Weight (g/mol) | Concentration (M) | weight required (g) |
|---|---|---|---|---|
| Sodium hydroxide | NaOH | 40.0000 | 1.2 | 33.6000 |
| Sodium nitrite | $NaNO_2$ | 69.0000 | 0.2 | 9.6600 |
| Sodium nitrate | $NaNO_3$ | 85.0000 | 0.2 | 11.9000 |
| Sodium chloride | NaCl | 58.4000 | 0 | 0.0000 |
| Sodium fluoride | NaF | 42.0000 | 0.2 | 5.8800 |
| Sodium sulfate | $Na_2SO_4$ | 142.0000 | 0.2 | 19.8800 |
| Sodium carbonate | $Na_2CO_3$ | 106.0000 | 0.100 | 7.4200 |
| Sodium bicarbonate | $NaHCO_3$ | 84.0100 | 0.000 | 0.0000 |

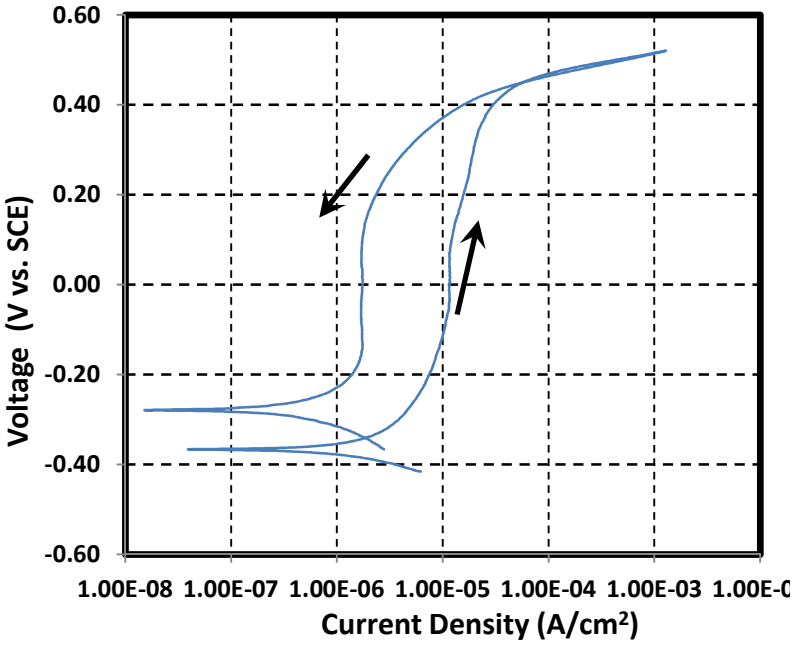


**Cyclic Potentiodynamic Polarization result**

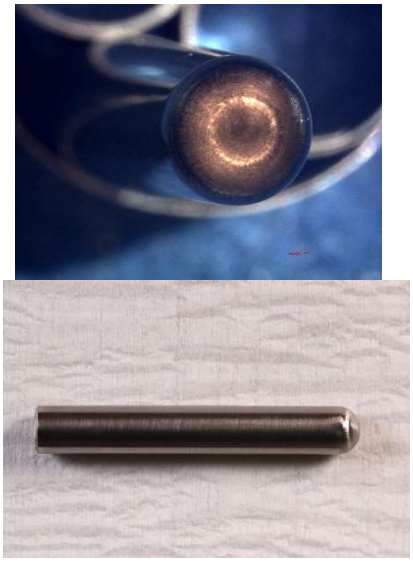

**Images of bullet samples after test**

## Test 2

### Composition of simulant

**Test 2**

| | | | |
|---|---|---|---|
| Temperature | 50 | °C | |
| pH at room temperature | 14.3 | | |
| pH before testing (at temp.) | 12.5 | pH after testing (at temp.) | 12.6 |
| Volume | 0.7 | L | |

| Simulant Source | Formula | Molecular Weight (g/mol) | Concentration (M) | weight required (g) |
|---|---|---|---|---|
| Sodium hydroxide | NaOH | 40.0000 | 6 | 168.0000 |
| Sodium nitrite | $NaNO_2$ | 69.0000 | 0.2 | 9.6600 |
| Sodium nitrate | $NaNO_3$ | 85.0000 | 0.2 | 11.9000 |
| Sodium chloride | NaCl | 58.4000 | 0.2 | 8.1760 |
| Sodium fluoride | NaF | 42.0000 | 0.2 | 5.8800 |
| Sodium sulfate | $Na_2SO_4$ | 142.0000 | 0.2 | 19.8800 |
| Sodium carbonate | $Na_2CO_3$ | 106.0000 | 0.100 | 7.4200 |
| Sodium bicarbonate | $NaHCO_3$ | 84.0100 | 0.000 | 0.0000 |

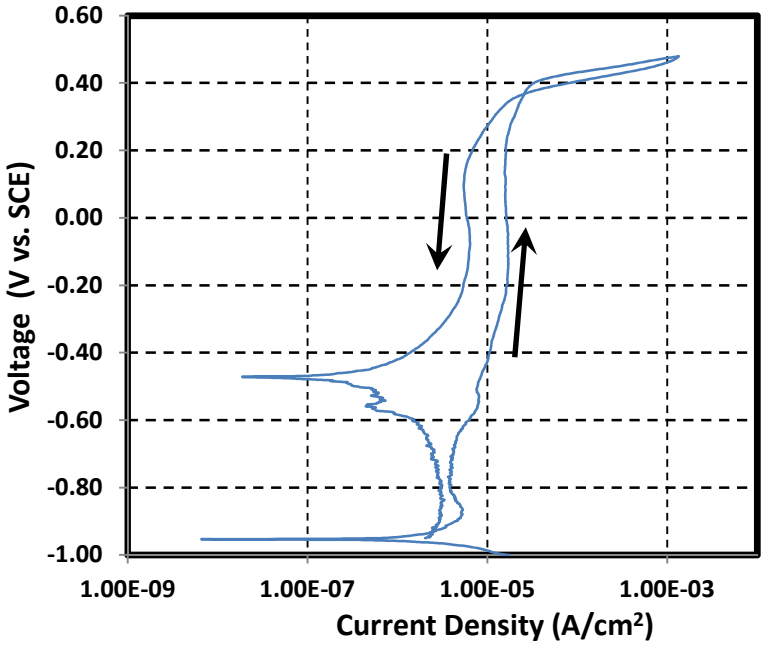


**Cyclic Potentiodynamic Polarization result**

**Images of bullet samples after test**

## Test 3

### Composition of simulant

**Test 3**

| | | | |
|---|---|---|---|
| Temperature | 75 | °C | |
| pH at room temperature | 14.3 | | |
| pH before testing (at temp.) | 12.8 | pH after testing (at temp.) | 12.4 |
| Volume | 0.7 | L | |

| Simulant Source | Formula | Molecular Weight (g/mol) | Concentration (M) | weight required (g) |
|---|---|---|---|---|
| Sodium hydroxide | NaOH | 40.0000 | 6 | 168.0000 |
| Sodium nitrite | $NaNO_2$ | 69.0000 | 1.2 | 57.9600 |
| Sodium nitrate | $NaNO_3$ | 85.0000 | 1.2 | 71.4000 |
| Sodium chloride | NaCl | 58.4000 | 0.2 | 8.1760 |
| Sodium fluoride | NaF | 42.0000 | 0.2 | 5.8800 |
| Sodium sulfate | $Na_2SO_4$ | 142.0000 | 0.2 | 19.8800 |
| Sodium carbonate | $Na_2CO_3$ | 106.0000 | 0.100 | 7.4200 |
| Sodium bicarbonate | $NaHCO_3$ | 84.0100 | 0.000 | 0.0000 |

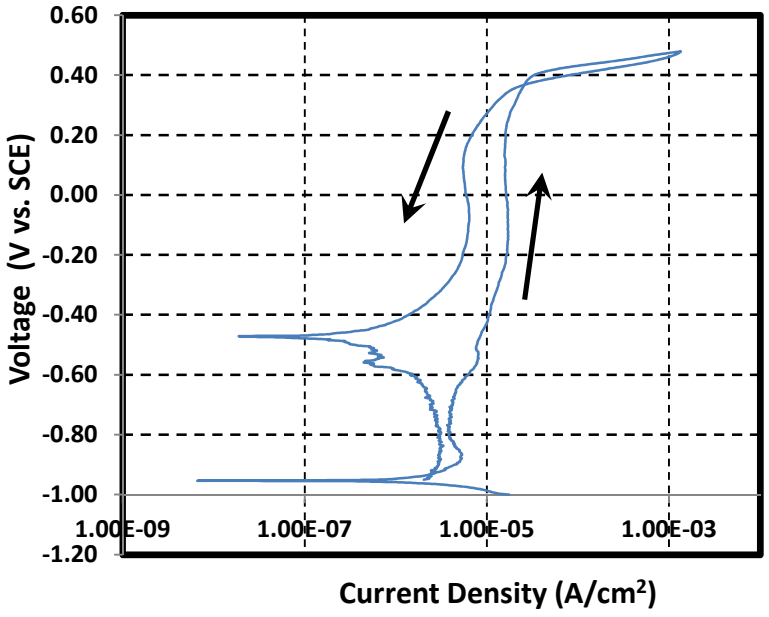


**Cyclic Potentiodynamic Polarization result**

**Images of bullet samples after test**

## Test 4

### Composition of simulant

**Test 4**

| | | | |
|---|---|---|---|
| Temperature | 75 °C | | |
| pH at room temperature | 14.5 | | |
| pH before testing (at temp.) | 11.0 | pH after testing (at temp.) | 11.1 |
| Volume | 0.7 L | | |

| Simulant Source | Formula | Molecular Weight (g/mol) | Concentration (M) | weight required (g) |
|---|---|---|---|---|
| Sodium hydroxide | NaOH | 40.0000 | 6 | 168.0000 |
| Sodium nitrite | $NaNO_2$ | 69.0000 | 1.2 | 57.9600 |
| Sodium nitrate | $NaNO_3$ | 85.0000 | 0.2 | 11.9000 |
| Sodium chloride | NaCl | 58.4000 | 0 | 0.0000 |
| Sodium fluoride | NaF | 42.0000 | 0 | 0.0000 |
| Sodium sulfate | $Na_2SO_4$ | 142.0000 | 0.2 | 19.8800 |
| Sodium carbonate | $Na_2CO_3$ | 106.0000 | 0.100 | 7.4200 |
| Sodium bicarbonate | $NaHCO_3$ | 84.0100 | 0.000 | 0.0000 |

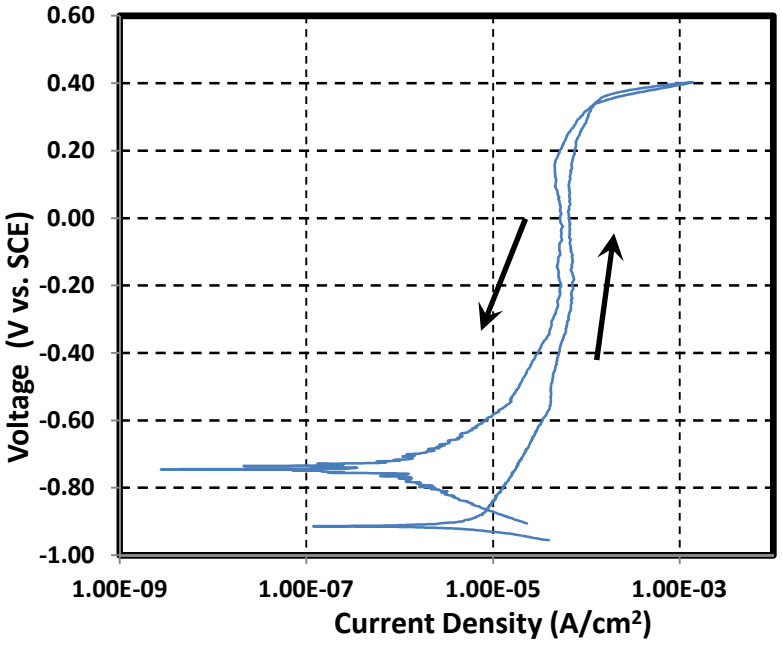


**Cyclic Potentiodynamic Polarization result**

**Images of bullet samples after test**

## Test 5

### Composition of simulant

**Test 5**

| | | | |
|---|---|---|---|
| Temperature | 50 °C | | |
| pH at room temperature | 13.7 | | |
| pH before testing (at temp.) | 11.4 | pH after testing (at temp.) | 12.1 |
| Volume | 0.7 L | | |

| Simulant Source | Formula | Molecular Weight (g/mol) | Concentration (M) | weight required (g) |
|---|---|---|---|---|
| Sodium hydroxide | NaOH | 40.0000 | 1.2 | 33.6000 |
| Sodium nitrite | $NaNO_2$ | 69.0000 | 1.2 | 57.9600 |
| Sodium nitrate | $NaNO_3$ | 85.0000 | 0.2 | 11.9000 |
| Sodium chloride | NaCl | 58.4000 | 0.2 | 8.1760 |
| Sodium fluoride | NaF | 42.0000 | 0 | 0.0000 |
| Sodium sulfate | $Na_2SO_4$ | 142.0000 | 0.2 | 19.8800 |
| Sodium carbonate | $Na_2CO_3$ | 106.0000 | 0.100 | 7.4200 |
| Sodium bicarbonate | $NaHCO_3$ | 84.0100 | 0.000 | 0.0000 |

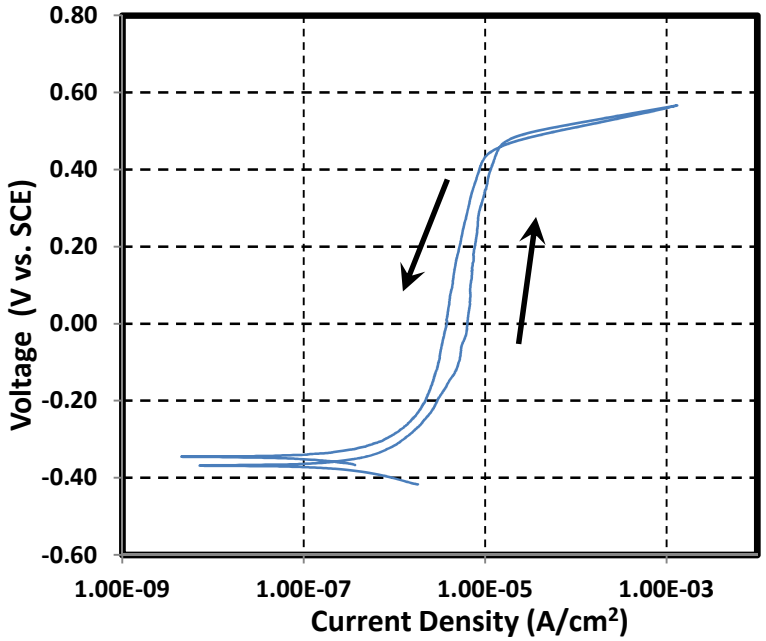


**Cyclic Potentiodynamic Polarization result**

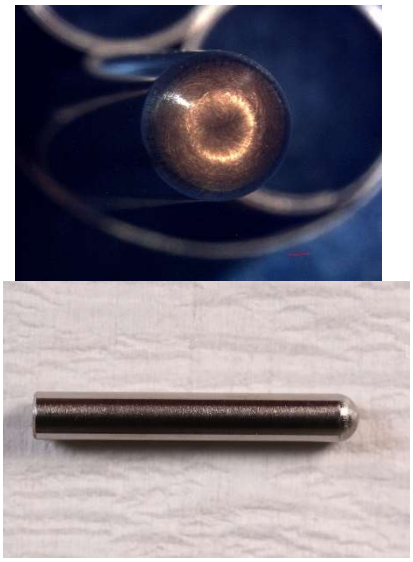

**Images of bullet samples after test**

## Test 6

### Composition of simulant

**Test 6**

| | | | |
|---|---|---|---|
| Temperature | 50 °C | | |
| pH at room temperature | 14.0 | | |
| pH before testing (at temp.) | 11.5 | pH after testing (at temp.) | 11.6 |
| Volume | 0.7 L | | |

| Simulant Source | Formula | Molecular Weight (g/mol) | Concentration (M) | weight required (g) |
|---|---|---|---|---|
| Sodium hydroxide | NaOH | 40.0000 | 6 | 168.0000 |
| Sodium nitrite | $NaNO_2$ | 69.0000 | 0.2 | 9.6600 |
| Sodium nitrate | $NaNO_3$ | 85.0000 | 1.2 | 71.4000 |
| Sodium chloride | NaCl | 58.4000 | 0 | 0.0000 |
| Sodium fluoride | NaF | 42.0000 | 0 | 0.0000 |
| Sodium sulfate | $Na_2SO_4$ | 142.0000 | 0.2 | 19.8800 |
| Sodium carbonate | $Na_2CO_3$ | 106.0000 | 0.100 | 7.4200 |
| Sodium bicarbonate | $NaHCO_3$ | 84.0100 | 0.000 | 0.0000 |

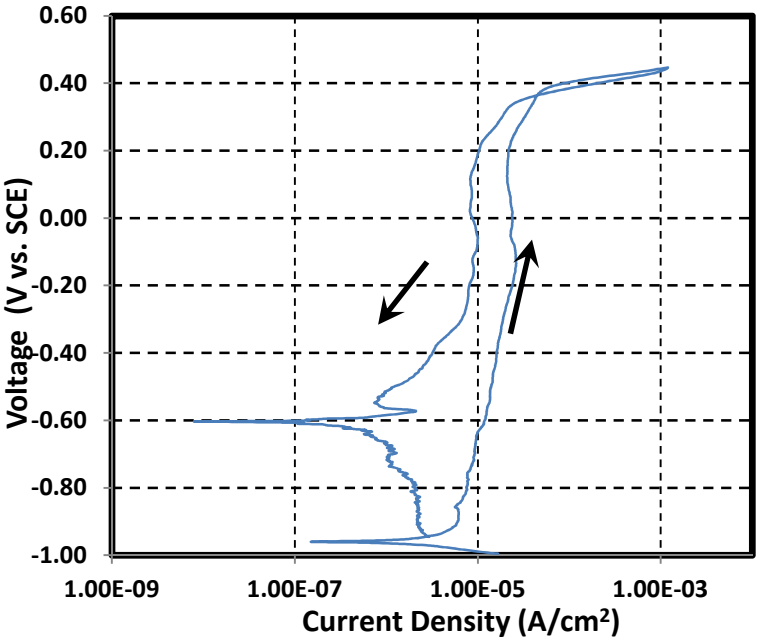


**Cyclic Potentiodynamic Polarization result**

**Images of bullet samples after test**

## Test 7

### Composition of simulant

**Test 7**

| | | | |
|---|---|---|---|
| Temperature | 75 °C | | |
| pH at room temperature | 13.6 | | |
| pH before testing (at temp.) | 11.1 | pH after testing (at temp.) | 11.2 |
| Volume | 0.7 L | | |

| Simulant Source | Formula | Molecular Weight (g/mol) | Concentration (M) | weight required (g) |
|---|---|---|---|---|
| Sodium hydroxide | NaOH | 40.0000 | 1.2 | 33.6000 |
| Sodium nitrite | $NaNO_2$ | 69.0000 | 0.2 | 9.6600 |
| Sodium nitrate | $NaNO_3$ | 85.0000 | 1.2 | 71.4000 |
| Sodium chloride | NaCl | 58.4000 | 0.2 | 8.1760 |
| Sodium fluoride | NaF | 42.0000 | 0 | 0.0000 |
| Sodium sulfate | $Na_2SO_4$ | 142.0000 | 0.2 | 19.8800 |
| Sodium carbonate | $Na_2CO_3$ | 106.0000 | 0.100 | 7.4200 |
| Sodium bicarbonate | $NaHCO_3$ | 84.0100 | 0.000 | 0.0000 |

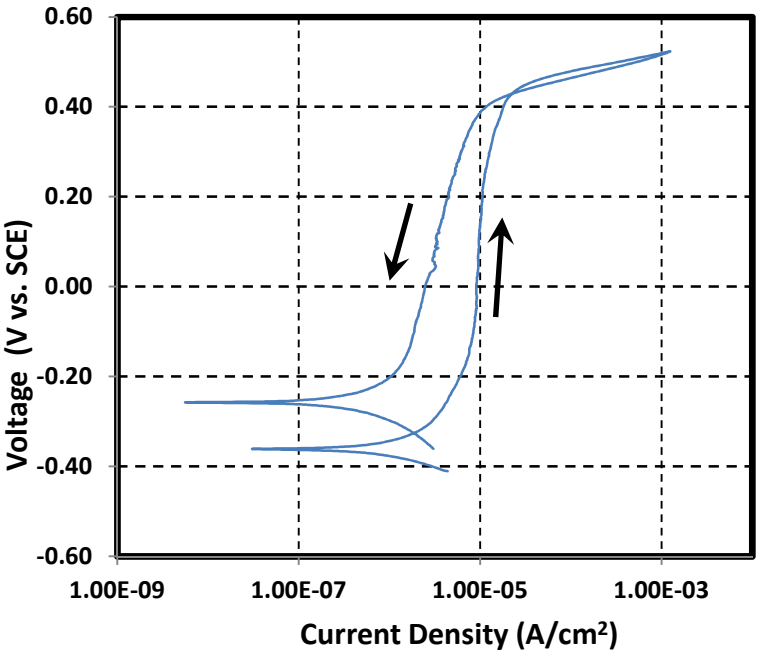


**Cyclic Potentiodynamic Polarization result**

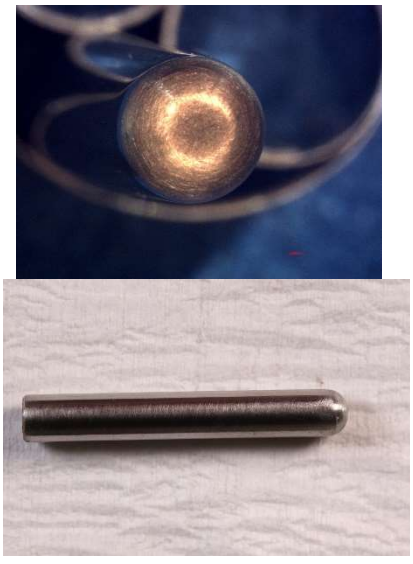

**Images of bullet samples after test**

## Test 8

### Composition of simulant

**Test 8**

| | | | |
|---|---|---|---|
| Temperature | 50 °C | | |
| pH at room temperature | 13.4 | | |
| pH before testing (at temp.) | 11.6 | pH after testing (at temp.) | 12.4 |
| Volume | 0.7 L | | |

| Simulant Source | Formula | Molecular Weight (g/mol) | Concentration (M) | weight required (g) |
|---|---|---|---|---|
| Sodium hydroxide | NaOH | 40.0000 | 1.2 | 33.6000 |
| Sodium nitrite | $NaNO_2$ | 69.0000 | 1.2 | 57.9600 |
| Sodium nitrate | $NaNO_3$ | 85.0000 | 1.2 | 71.4000 |
| Sodium chloride | NaCl | 58.4000 | 0 | 0.0000 |
| Sodium fluoride | NaF | 42.0000 | 0.2 | 5.8800 |
| Sodium sulfate | $Na_2SO_4$ | 142.0000 | 0.2 | 19.8800 |
| Sodium carbonate | $Na_2CO_3$ | 106.0000 | 0.100 | 7.4200 |
| Sodium bicarbonate | $NaHCO_3$ | 84.0100 | 0.000 | 0.0000 |

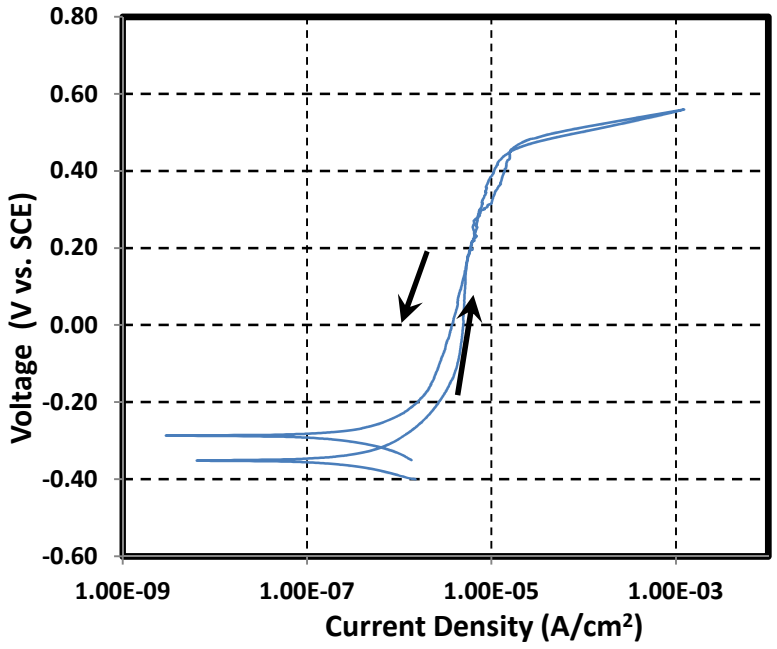


**Cyclic Potentiodynamic Polarization result**

**Images of bullet samples after test**

**ASTM G192 Plot**

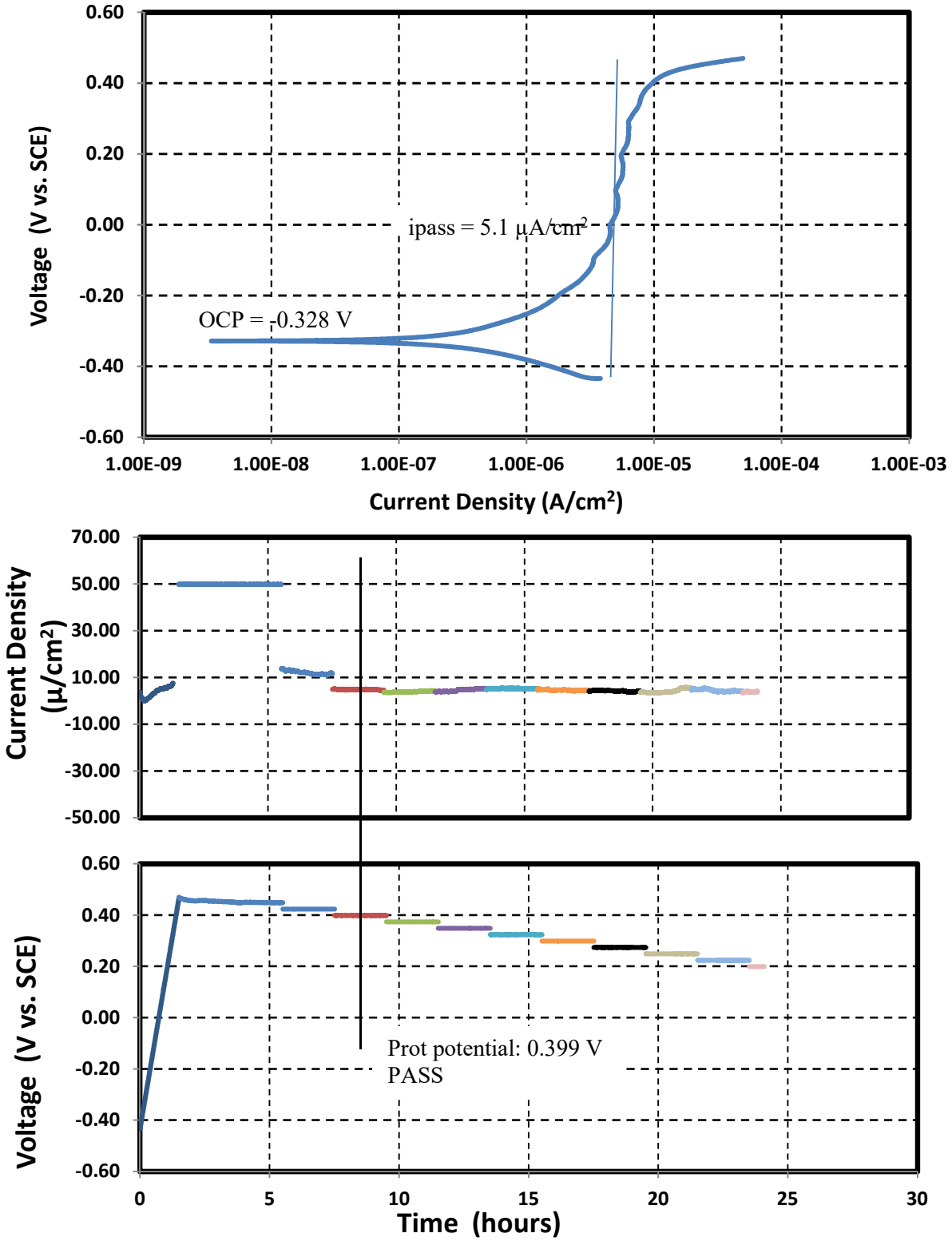

## Test 9

### Composition of simulant

**Test 9**

| | | | |
|---|---|---|---|
| Temperature | 55 | °C | |
| pH at room temperature | 13.5 | | |
| pH before testing (at temp.) | 11.6 | pH after testing (at temp.) | 12.1 |
| Volume | 0.7 | L | |

| Simulant Source | Formula | Molecular Weight (g/mol) | Concentration (M) | weight required (g) |
|---|---|---|---|---|
| Sodium hydroxide | NaOH | 40.0000 | 2.4 | 67.2000 |
| Sodium nitrite | $NaNO_2$ | 69.0000 | 1.2 | 57.9600 |
| Sodium nitrate | $NaNO_3$ | 85.0000 | 1.2 | 71.4000 |
| Sodium chloride | NaCl | 58.4000 | 0 | 0.0000 |
| Sodium fluoride | NaF | 42.0000 | 0.1 | 2.9400 |
| Sodium sulfate | $Na_2SO_4$ | 142.0000 | 0.2 | 19.8800 |
| Sodium carbonate | $Na_2CO_3$ | 106.0000 | 0.100 | 7.4200 |
| Sodium bicarbonate | $NaHCO_3$ | 84.0100 | 0.000 | 0.0000 |

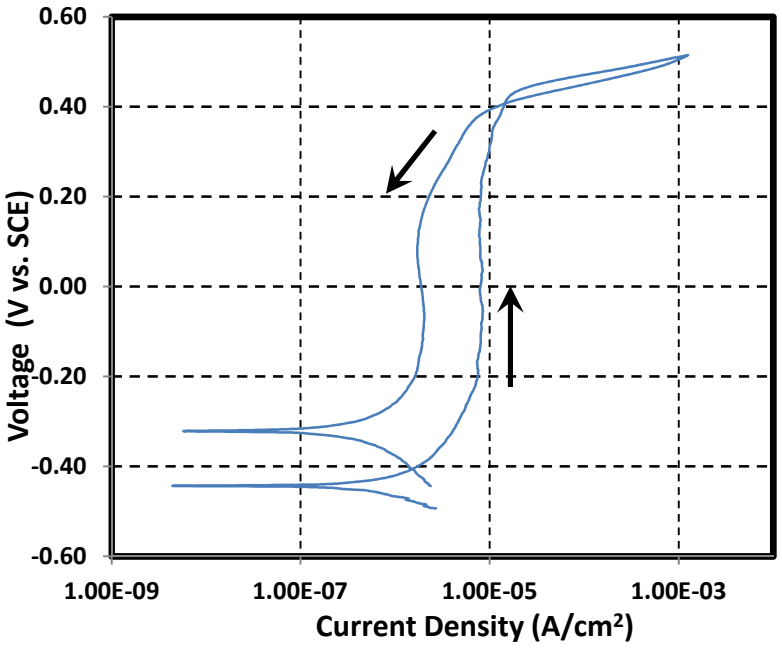


**Cyclic Potentiodynamic Polarization result**

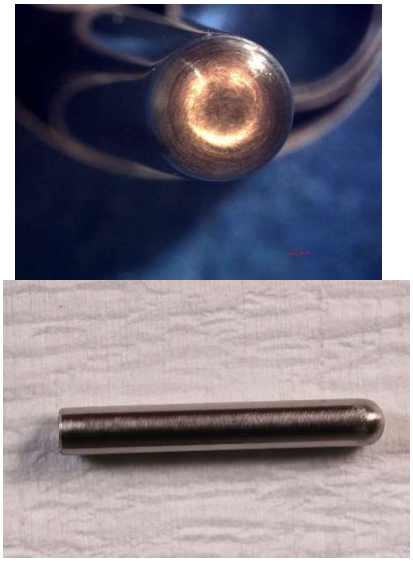

**Images of bullet samples after test**

## Test 10

### Composition of simulant

**Test 10**

| | | | |
|---|---|---|---|
| Temperature | 65 | °C | |
| pH at room temperature | 13.5 | | |
| pH before testing (at temp.) | 11.5 | pH after testing (at temp.) | 11.5 |
| Volume | 0.7 | L | |

| Simulant Source | Formula | Molecular Weight (g/mol) | Concentration (M) | weight required (g) |
|---|---|---|---|---|
| Sodium hydroxide | NaOH | 40.0000 | 4.8 | 134.4000 |
| Sodium nitrite | $NaNO_2$ | 69.0000 | 0.7 | 33.8100 |
| Sodium nitrate | $NaNO_3$ | 85.0000 | 0.2 | 11.9000 |
| Sodium chloride | NaCl | 58.4000 | 0.05 | 2.0440 |
| Sodium fluoride | NaF | 42.0000 | 0 | 0.0000 |
| Sodium sulfate | $Na_2SO_4$ | 142.0000 | 0.2 | 19.8800 |
| Sodium carbonate | $Na_2CO_3$ | 106.0000 | 0.100 | 7.4200 |
| Sodium bicarbonate | $NaHCO_3$ | 84.0100 | 0.000 | 0.0000 |

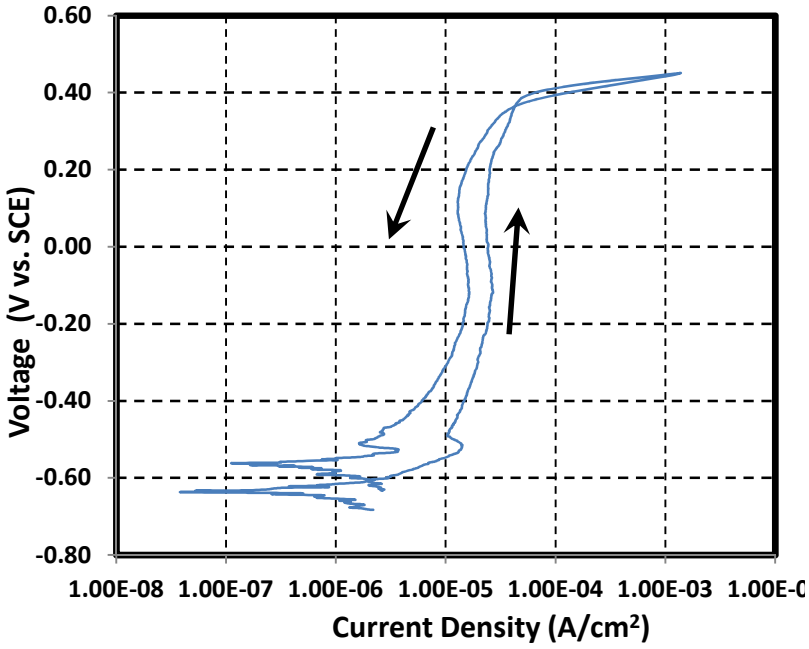


**Cyclic Potentiodynamic Polarization result**

**Images of bullet samples after test**

## Test 11

### Composition of simulant

**Test 11**

| | | | |
|---|---|---|---|
| Temperature | 70 °C | | |
| pH at room temperature | 13.5 | | |
| pH before testing (at temp.) | 11.6 | pH after testing (at temp.) | 11.4 |
| Volume | 0.7 L | | |

| Simulant Source | Formula | Molecular Weight (g/mol) | Concentration (M) | weight required (g) |
|---|---|---|---|---|
| Sodium hydroxide | NaOH | 40.0000 | 1.2 | 33.6000 |
| Sodium nitrite | $NaNO_2$ | 69.0000 | 0.45 | 21.7350 |
| Sodium nitrate | $NaNO_3$ | 85.0000 | 0.45 | 26.7750 |
| Sodium chloride | NaCl | 58.4000 | 0.1 | 4.0880 |
| Sodium fluoride | NaF | 42.0000 | 0.2 | 5.8800 |
| Sodium sulfate | $Na_2SO_4$ | 142.0000 | 0.2 | 19.8800 |
| Sodium carbonate | $Na_2CO_3$ | 106.0000 | 0.100 | 7.4200 |
| Sodium bicarbonate | $NaHCO_3$ | 84.0100 | 0.000 | 0.0000 |

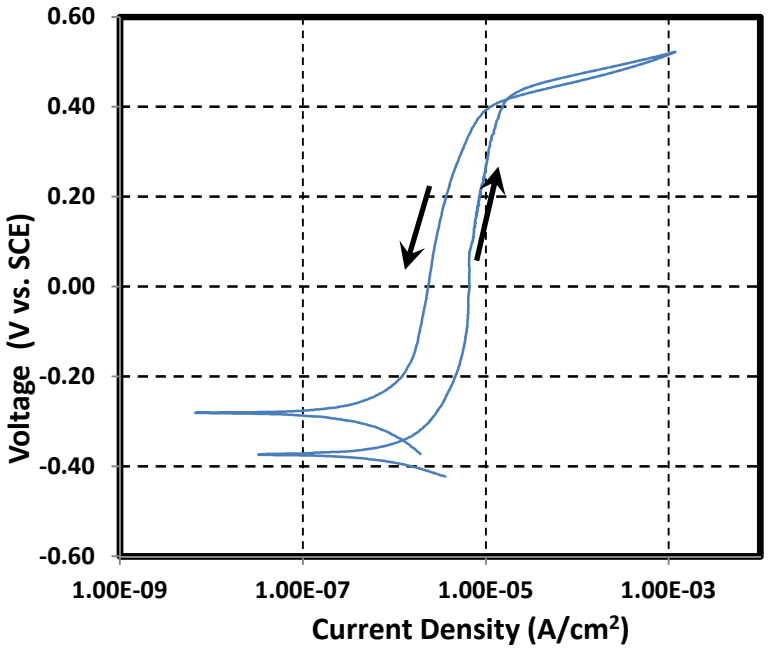


**Cyclic Potentiodynamic Polarization result**

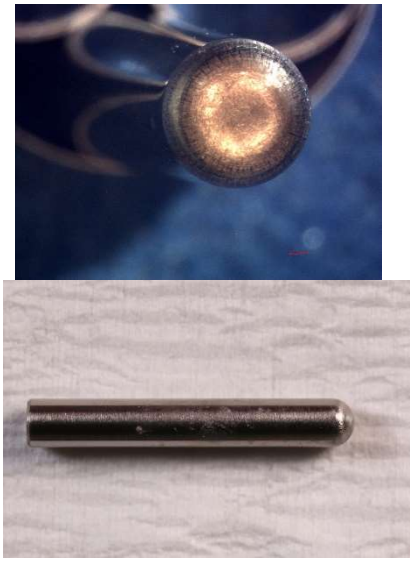

**Images of bullet samples after test**

## Test 12

### Composition of simulant

**Test 12**

| | | | |
|---|---|---|---|
| Temperature | 50 °C | | |
| pH at room temperature | 13.9 | | |
| pH before testing (at temp.) | 12.3 | pH after testing (at temp.) | 12.2 |
| Volume | 0.7 L | | |

| Simulant Source | Formula | Molecular Weight (g/mol) | Concentration (M) | weight required (g) |
|---|---|---|---|---|
| Sodium hydroxide | NaOH | 40.0000 | 3.6 | 100.8000 |
| Sodium nitrite | $NaNO_2$ | 69.0000 | 0.2 | 9.6600 |
| Sodium nitrate | $NaNO_3$ | 85.0000 | 0.95 | 56.5250 |
| Sodium chloride | NaCl | 58.4000 | 0.15 | 6.1320 |
| Sodium fluoride | NaF | 42.0000 | 0.05 | 1.4700 |
| Sodium sulfate | $Na_2SO_4$ | 142.0000 | 0.2 | 19.8800 |
| Sodium carbonate | $Na_2CO_3$ | 106.0000 | 0.100 | 7.4200 |
| Sodium bicarbonate | $NaHCO_3$ | 84.0100 | 0.000 | 0.0000 |

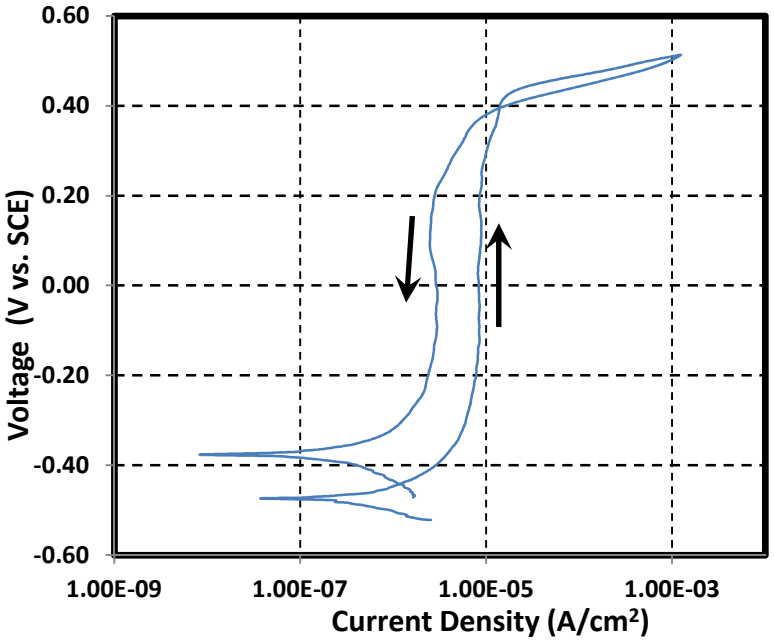


**Cyclic Potentiodynamic Polarization result**

**Images of bullet samples after test**

## Test 13

### Composition of simulant

**Test 13**

| | | | |
|---|---|---|---|
| Temperature | 75 °C | | |
| pH at room temperature | 13.9 | | |
| pH before testing (at temp.) | 11.7 | pH after testing (at temp.) | 11.0 |
| Volume | 0.7 L | | |

| Simulant Source | Formula | Molecular Weight (g/mol) | Concentration (M) | weight required (g) |
|---|---|---|---|---|
| Sodium hydroxide | NaOH | 40.0000 | 6 | 168.0000 |
| Sodium nitrite | $NaNO_2$ | 69.0000 | 0.95 | 45.8850 |
| Sodium nitrate | $NaNO_3$ | 85.0000 | 0.7 | 41.6500 |
| Sodium chloride | NaCl | 58.4000 | 0.2 | 8.1760 |
| Sodium fluoride | NaF | 42.0000 | 0.15 | 4.4100 |
| Sodium sulfate | $Na_2SO_4$ | 142.0000 | 0.2 | 19.8800 |
| Sodium carbonate | $Na_2CO_3$ | 106.0000 | 0.100 | 7.4200 |
| Sodium bicarbonate | $NaHCO_3$ | 84.0100 | 0.000 | 0.0000 |

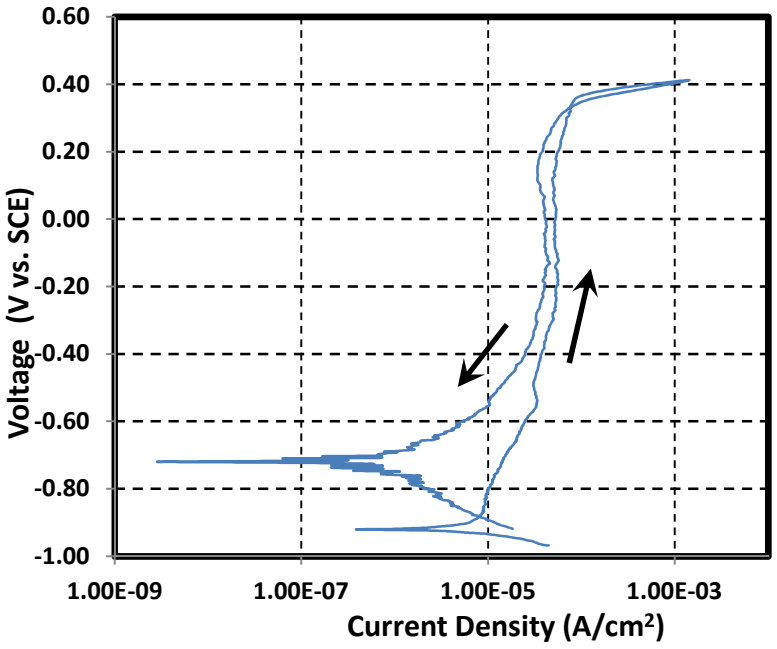


**Cyclic Potentiodynamic Polarization result**

**Images of bullet samples after test**

# Appendix C Chemical Composition of New Limits Pitting Corrosion Task for fluoride effects with Cyclic Potentiodynamic Polarization Results and Pictures after Test

**Table C-1. Test conditions and results of testing with low hydroxide**

| Test | Temperature (ºC) | Hydroxide (M) | Nitrite (M) | Nitrate (M) | Chloride (M) | Fluoride (M) | Acetate (M) | Oxalate (M) | Category | Pitting on Sample | Logistic approach |
|---|---|---|---|---|---|---|---|---|---|---|---|
| 1 | 35 | 0.04 | 0.8 | 0.93 | 0.02 | 0.01 | 0.02 | 0.02 | 3 | No | 0 |
| 2 | 35 | 0.015 | 1.06 | 0.87 | 0.01 | 0.07 | 0.02 | 0.02 | 1 | No | 0 |
| 3 | 35 | 0.01 | 2.18 | 0.96 | 0.07 | 0.18 | 0.025 | 0.015 | 1 | No | 0 |
| 4 | 35 | 0.03 | 2.25 | 1.01 | 0.1 | 0.09 | 0.025 | 0.015 | 1 | No | 0 |
| 5 | 35 | 0.05 | 2.09 | 1.04 | 0.03 | 0.1 | 0.025 | 0.015 | 1 | No | 0 |
| 6 | 35 | 0.03 | 2.82 | 2.73 | 0.11 | 0.01 | 0.0325 | 0.075 | 1 | No | 0 |
| 7 | 35 | 0.02 | 2.2 | 0.78 | 0.04 | 0.11 | 0.025 | 0.015 | 1 | No | 0 |
| 8 | 35 | 0.02 | 0.75 | 1 | 0.01 | 0.01 | 0.02 | 0.02 | 1 | No | 0 |
| 9 | 35 | 0.09 | 1 | 1 | 0.04 | 0.04 | 0.02 | 0.02 | 1 | No | 0 |
| 10 | 35 | 0.06 | 1 | 1 | 0.04 | 0.06 | 0.02 | 0.02 | 1 | No | 0 |
| 11 | 35 | 0.05 | 0.7 | 1 | 0.01 | 0.04 | 0.02 | 0.02 | 1 | No | 0 |
| 12 | 35 | 0.075 | 0.5 | 1 | 0.01 | 0.01 | 0.02 | 0.02 | 1 | No | 0 |
| 13 | 75 | 0.01 | 1.06 | 0.87 | 0.01 | 0.07 | 0.02 | 0.02 | 1 | No | 0 |
| 14 | 75 | 0.03 | 2.25 | 1.01 | 0.1 | 0.09 | 0.025 | 0.015 | 3 | No | 0 |
| 15 | 75 | 0.05 | 2.09 | 1.04 | 0.03 | 0.1 | 0.025 | 0.015 | 1 | No | 0 |
| 16 | 75 | 0.09 | 1 | 1 | 0.04 | 0.04 | 0.02 | 0.02 | 1 | No | 0 |
| 17 | 75 | 0.06 | 1 | 1 | 0.04 | 0.06 | 0.02 | 0.02 | 1 | No | 0 |
| 18 | 75 | 0.02 | 0.75 | 1 | 0.01 | 0.01 | 0.02 | 0.02 | 1 | No | 0 |
| 19 | 75 | 0.05 | 0.7 | 1 | 0.01 | 0.04 | 0.02 | 0.02 | 2 | No | 0 |
| 20 | 75 | 0.01 | 2.18 | 0.96 | 0.07 | 0.04 | 0.025 | 0.015 | 1 | No | 0 |
| 21 | 75 | 0.125 | 1 | 1.25 | 0.05 | 0.04 | 0.025 | 0.015 | 1 | No | 0 |
| 22 | 75 | 0.175 | 1 | 1.25 | 0.05 | 0.04 | 0.025 | 0.015 | 3 | No | 0 |
| 23 | 75 | 0.225 | 0.75 | 1 | 0.075 | 0.04 | 0.025 | 0.015 | 1 | No | 0 |
| 24 | 75 | 0.25 | 0.75 | 1.25 | 0.075 | 0.04 | 0.025 | 0.015 | 1 | No | 0 |
| 25 | 75 | 0.15 | 1.25 | 1 | 0.05 | 0.04 | 0.025 | 0.015 | 3 | No | 0 |

*Additional chemicals added were 0.1 M Sulfate, 0.02 M glycolate, 0.04 M Phosphate and chemicals that contributed 0.2 M TIC in each test.

## Test 1 Composition of simulant

**Test 1**

| | | | |
|---|---|---|---|
| Temperature | 35 | °C | |
| pH at room temperature | 12.6 | | |
| pH before testing (at temp.) | 12.3 | pH after testing (at temp.) | 12.3 |
| Volume | 0.7 | L | |

| Simulant Source | Formula | Molecular Weight (g/mol) | Concentration (M) | weight required (g) |
|---|---|---|---|---|
| Sodium chloride | NaCl | 58.4000 | 0.02 | 0.8176 |
| Sodium fluoride | NaF | 42.0000 | 0.01 | 0.2940 |
| Sodium sulfate | $Na_2SO_4$ | 142.0000 | 0.1 | 9.9400 |
| Sodium phosphate, 12-hydrate | $Na_3PO_4.12H_2O$ | 380.0000 | 0.04 | 10.6400 |
| Sodium hydroxide* | NaOH | 40.0000 | 0.06 | 1.6800 |
| Sodium acetate, 3-hydrate | $Na(C_2H_3O_2).3H_2O$ | 136.0000 | 0.02 | 1.9040 |
| Sodium formate | $Na(CHO_2)$ | 68.0000 | 0.03 | 1.4280 |
| Glycolic acid | $C_2H_4O_3$ | 76.1000 | 0.02 | 1.0654 |
| Sodium oxalate | $Na_2C_2O_4$ | 134.0000 | 0.02 | 1.8760 |
| Sodium nitrite | $NaNO_2$ | 69.0000 | 0.8 | 38.6400 |
| Sodium nitrate | $NaNO_3$ | 85.0000 | 0.93 | 55.3350 |
| Sodium carbonate | $Na_2CO_3$ | 106.0000 | 0.194 | 14.3948 |
| Sodium bicarbonate | $NaHCO_3$ | 84.0100 | 0.006 | 0.3528 |

* additional sodium hydroxide to neutralize acid.

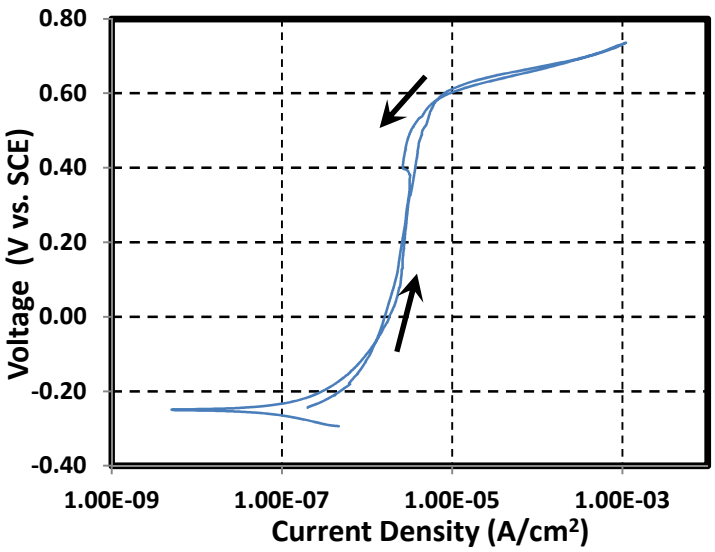


**Cyclic Potentiodynamic Polarization result**

**Images of bullet samples after test**

**ASTM G192 Plot**

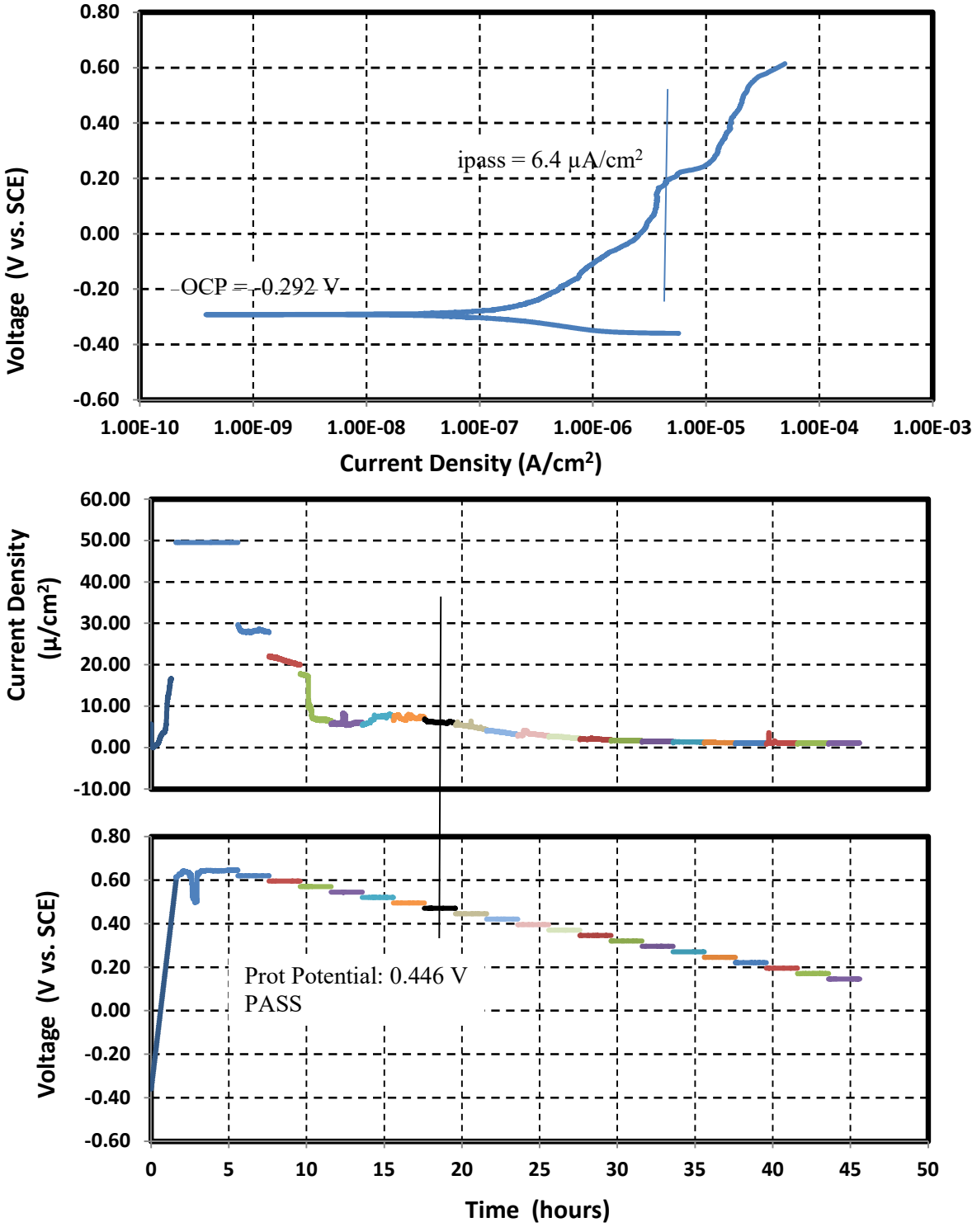

## Test 2 Composition of simulant

**Test 2**

| | | | |
|---|---|---|---|
| Temperature | 35 °C | | |
| pH at room temperature | 12.3 | | |
| pH before testing (at temp.) | 11.6 | pH after testing (at temp.) | 11.7 |
| Volume | 0.7 L | | |

| Simulant Source | Formula | Molecular Weight (g/mol) | Concentration (M) | weight required (g) |
|---|---|---|---|---|
| Sodium chloride | NaCl | 58.4000 | 0.01 | 0.4088 |
| Sodium fluoride | NaF | 42.0000 | 0.07 | 2.0580 |
| Sodium sulfate | $Na_2SO_4$ | 142.0000 | 0.1 | 9.9400 |
| Sodium phosphate, 12-hydrate | $Na_3PO_4.12H_2O$ | 380.0000 | 0.04 | 10.6400 |
| Sodium hydroxide* | NaOH | 40.0000 | 0.035 | 0.9800 |
| Sodium acetate, 3-hydrate | $Na(C_2H_3O_2).3H_2O$ | 136.0000 | 0.02 | 1.9040 |
| Sodium formate | $Na(CHO_2)$ | 68.0000 | 0.03 | 1.4280 |
| Glycolic acid | $C_2H_4O_3$ | 76.1000 | 0.02 | 1.0654 |
| Sodium oxalate | $Na_2C_2O_4$ | 134.0000 | 0.02 | 1.8760 |
| Sodium nitrite | $NaNO_2$ | 69.0000 | 1.06 | 51.1980 |
| Sodium nitrate | $NaNO_3$ | 85.0000 | 0.87 | 51.7650 |
| Sodium carbonate | $Na_2CO_3$ | 106.0000 | 0.198 | 14.6916 |
| Sodium bicarbonate | $NaHCO_3$ | 84.0100 | 0.002 | 0.1176 |

* additional sodium hydroxide to neutralize acid

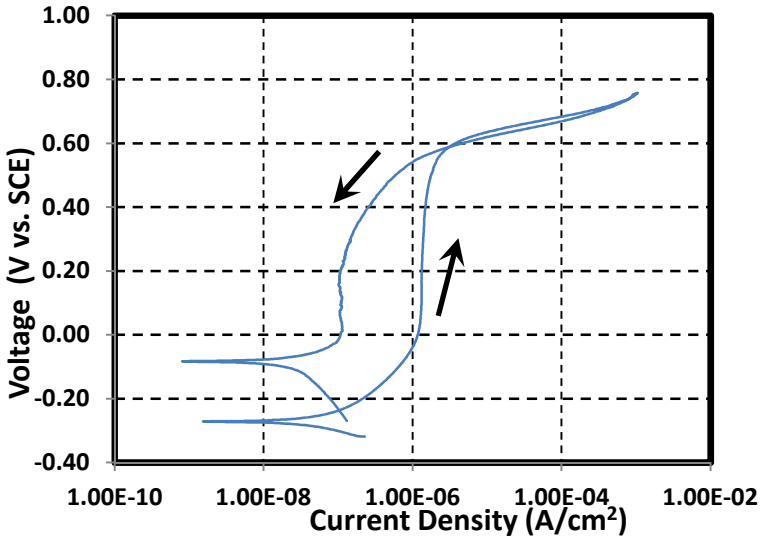


**Cyclic Potentiodynamic Polarization result**

**Images of bullet samples after test**

## Test 3 Composition of simulant

**Test 3**

| | | | |
|---|---|---|---|
| Temperature | 35 °C | | |
| pH at room temperature | 12.1 | | |
| pH before testing (at temp.) | 11.7 | pH after testing (at temp.) | 11.7 |
| Volume | 0.7 L | | |

| Simulant Source | Formula | Molecular Weight (g/mol) | Concentration (M) | weight required (g) |
|---|---|---|---|---|
| Sodium chloride | NaCl | 58.4000 | 0.07 | 2.8616 |
| Sodium fluoride | NaF | 42.0000 | 0.18 | 5.2920 |
| Sodium sulfate | $Na_2SO_4$ | 142.0000 | 0.1 | 9.9400 |
| Sodium phosphate, 12-hydrate | $Na_3PO_4.12H_2O$ | 380.0000 | 0.04 | 10.6400 |
| Sodium hydroxide* | NaOH | 40.0000 | 0.03 | 0.8400 |
| Sodium acetate, 3-hydrate | $Na(C_2H_3O_2).3H_2O$ | 136.0000 | 0.025 | 2.3800 |
| Sodium formate | $Na(CHO_2)$ | 68.0000 | 0.03 | 1.4280 |
| Glycolic acid | $C_2H_4O_3$ | 76.1000 | 0.02 | 1.0654 |
| Sodium oxalate | $Na_2C_2O_4$ | 134.0000 | 0.015 | 1.4070 |
| Sodium nitrite | $NaNO_2$ | 69.0000 | 2.18 | 105.2940 |
| Sodium nitrate | $NaNO_3$ | 85.0000 | 0.96 | 57.1200 |
| Sodium carbonate | $Na_2CO_3$ | 106.0000 | 0.1985 | 14.7287 |
| Sodium bicarbonate | $NaHCO_3$ | 84.0100 | 0.0015 | 0.0882 |

* additional sodium hydroxide to neutralize acid

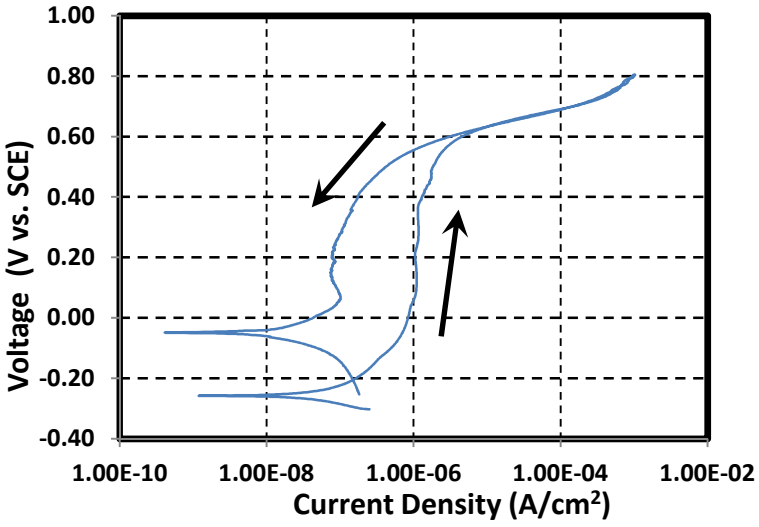


**Cyclic Potentiodynamic Polarization result**

**Images of bullet samples after test**

## Test 4 Composition of simulant

**Test 4**

| | | | |
|---|---|---|---|
| Temperature | 35 °C | | |
| pH at room temperature | 12.6 | | |
| pH before testing (at temp.) | 12.0 | pH after testing (at temp.) | 12.0 |
| Volume | 0.7 L | | |

| Simulant Source | Formula | Molecular Weight (g/mol) | Concentration (M) | weight required (g) |
|---|---|---|---|---|
| Sodium chloride | NaCl | 58.4000 | 0.1 | 4.0880 |
| Sodium fluoride | NaF | 42.0000 | 0.09 | 2.6460 |
| Sodium sulfate | $Na_2SO_4$ | 142.0000 | 0.1 | 9.9400 |
| Sodium phosphate, 12-hydrate | $Na_3PO_4.12H_2O$ | 380.0000 | 0.04 | 10.6400 |
| Sodium hydroxide* | NaOH | 40.0000 | 0.05 | 1.4000 |
| Sodium acetate, 3-hydrate | $Na(C_2H_3O_2).3H_2O$ | 136.0000 | 0.025 | 2.3800 |
| Sodium formate | $Na(CHO_2)$ | 68.0000 | 0.03 | 1.4280 |
| Glycolic acid | $C_2H_4O_3$ | 76.1000 | 0.02 | 1.0654 |
| Sodium oxalate | $Na_2C_2O_4$ | 134.0000 | 0.015 | 1.4070 |
| Sodium nitrite | $NaNO_2$ | 69.0000 | 2.25 | 108.6750 |
| Sodium nitrate | $NaNO_3$ | 85.0000 | 1.01 | 60.0950 |
| Sodium carbonate | $Na_2CO_3$ | 106.0000 | 0.1995 | 14.8029 |
| Sodium bicarbonate | $NaHCO_3$ | 84.0100 | 0.0005 | 0.0294 |

* additional sodium hydroxide to neutralize acid

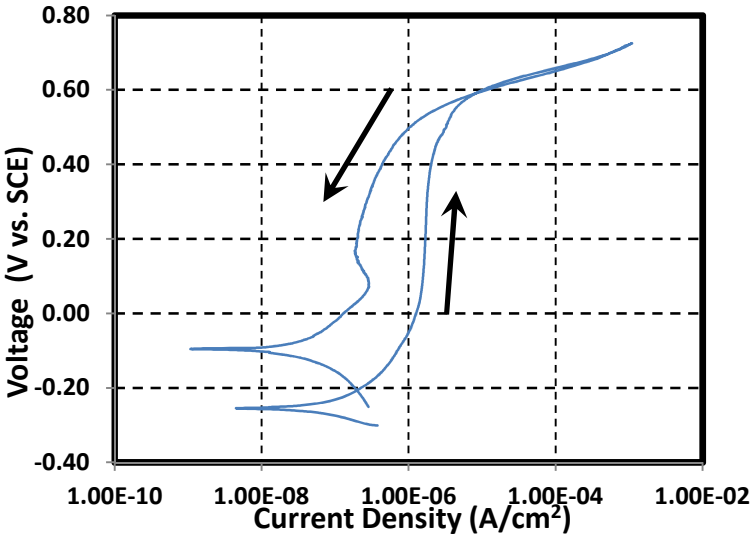


**Cyclic Potentiodynamic Polarization result**

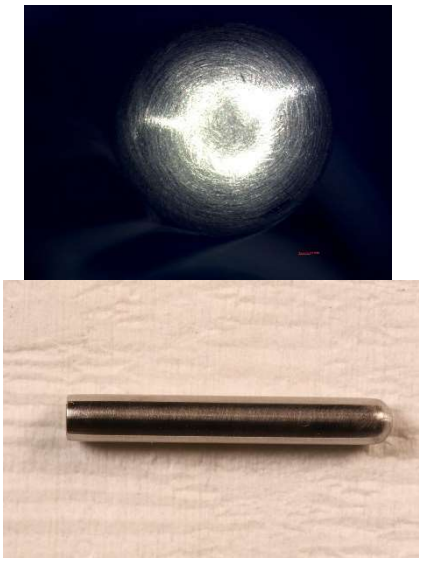

**Images of bullet samples after test**

## Test 5 Composition of simulant

**Test 5**

| | | | |
|---|---|---|---|
| Temperature | 35 | °C | |
| pH at room temperature | 12.6 | | |
| pH before testing (at temp.) | 12.2 | pH after testing (at temp.) | 12.2 |
| Volume | 0.7 | L | |

| Simulant Source | Formula | Molecular Weight (g/mol) | Concentration (M) | weight required (g) |
|---|---|---|---|---|
| Sodium chloride | NaCl | 58.4000 | 0.03 | 1.2264 |
| Sodium fluoride | NaF | 42.0000 | 0.1 | 2.9400 |
| Sodium sulfate | $Na_2SO_4$ | 142.0000 | 0.1 | 9.9400 |
| Sodium phosphate, 12-hydrate | $Na_3PO_4.12H_2O$ | 380.0000 | 0.04 | 10.6400 |
| Sodium hydroxide* | NaOH | 40.0000 | 0.07 | 1.9600 |
| Sodium acetate, 3-hydrate | $Na(C_2H_3O_2).3H_2O$ | 136.0000 | 0.025 | 2.3800 |
| Sodium formate | $Na(CHO_2)$ | 68.0000 | 0.03 | 1.4280 |
| Glycolic acid | $C_2H_4O_3$ | 76.1000 | 0.02 | 1.0654 |
| Sodium oxalate | $Na_2C_2O_4$ | 134.0000 | 0.015 | 1.4070 |
| Sodium nitrite | $NaNO_2$ | 69.0000 | 2.09 | 100.9470 |
| Sodium nitrate | $NaNO_3$ | 85.0000 | 1.04 | 61.8800 |
| Sodium carbonate | $Na_2CO_3$ | 106.0000 | 0.1997 | 14.8177 |
| Sodium bicarbonate | $NaHCO_3$ | 84.0100 | 0.0003 | 0.0176 |

* additional sodium hydroxide to neutralize acid

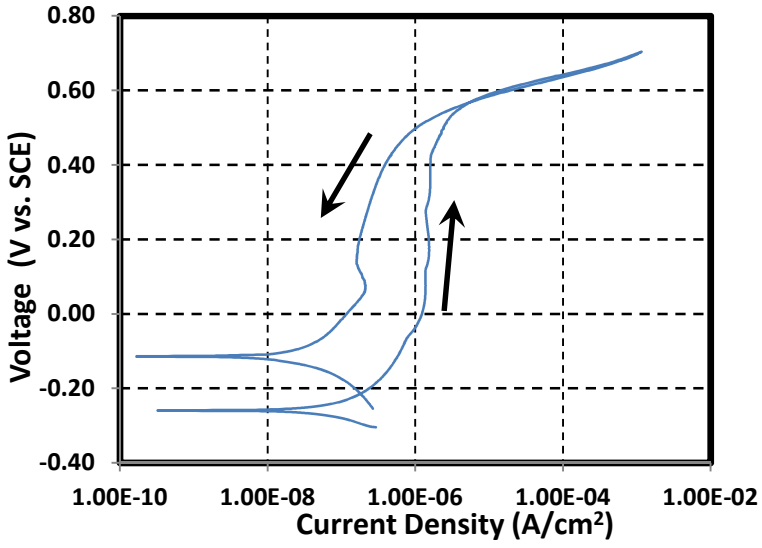


**Cyclic Potentiodynamic Polarization result**

**Images of bullet samples after test**

## Test 6 Composition of simulant

**Test 6**

| | | | |
|---|---|---|---|
| Temperature | 35 °C | | |
| pH at room temperature | 12.3 | | |
| pH before testing (at temp.) | 12.1 | pH after testing (at temp.) | 11.9 |
| Volume | 0.7 L | | |

| Simulant Source | Formula | Molecular Weight (g/mol) | Concentration (M) | weight required (g) |
|---|---|---|---|---|
| Sodium chloride | NaCl | 58.4000 | 0.11 | 4.4968 |
| Sodium fluoride | NaF | 42.0000 | 0.01 | 0.2940 |
| Sodium sulfate | $Na_2SO_4$ | 142.0000 | 0.1 | 9.9400 |
| Sodium phosphate, 12-hydrate | $Na_3PO_4.12H_2O$ | 380.0000 | 0.04 | 10.6400 |
| Sodium hydroxide* | NaOH | 40.0000 | 0.05 | 1.4000 |
| Sodium acetate, 3-hydrate | $Na(C_2H_3O_2).3H_2O$ | 136.0000 | 0.0325 | 3.0940 |
| Sodium formate | $Na(CHO_2)$ | 68.0000 | 0.03 | 1.4280 |
| Glycolic acid | $C_2H_4O_3$ | 76.1000 | 0.02 | 1.0654 |
| Sodium oxalate | $Na_2C_2O_4$ | 134.0000 | 0.075 | 7.0350 |
| Sodium nitrite | $NaNO_2$ | 69.0000 | 2.82 | 136.2060 |
| Sodium nitrate | $NaNO_3$ | 85.0000 | 2.73 | 162.4350 |
| Sodium carbonate | $Na_2CO_3$ | 106.0000 | 0.2 | 14.8400 |
| Sodium bicarbonate | $NaHCO_3$ | 84.0100 | 0 | 0.0000 |

* additional sodium hydroxide to neutralize acid

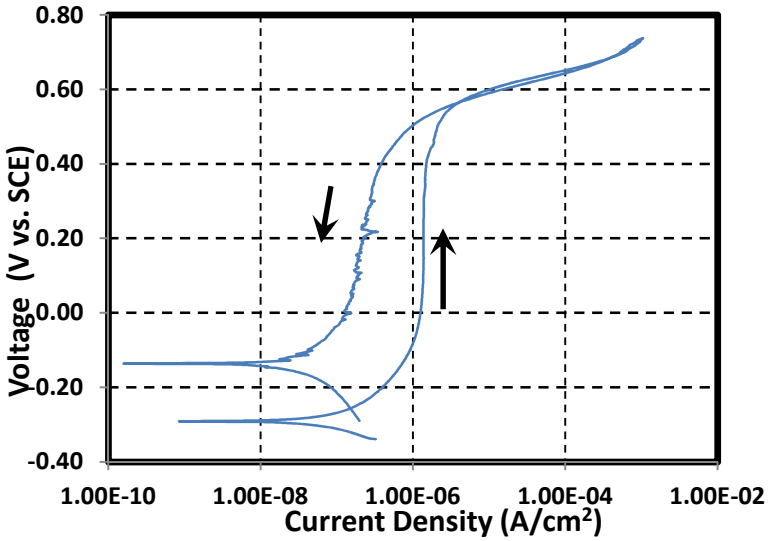


**Cyclic Potentiodynamic Polarization result**

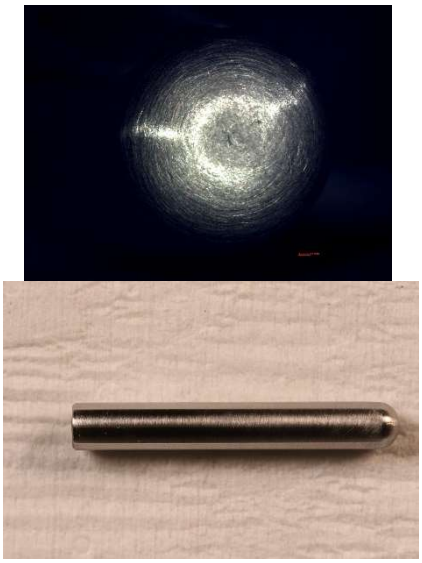

**Images of bullet samples after test**

## Test 7 Composition of simulant

**Test 7**

| | | | |
|---|---|---|---|
| Temperature | 35 | °C | |
| pH at room temperature | 12.2 | | |
| pH before testing (at temp.) | 11.8 | pH after testing (at temp.) | 11.8 |
| Volume | 0.7 | L | |
| Temperature | 25 | °C | |

| Simulant Source | Formula | Molecular Weight (g/mol) | Concentration (M) | weight required (g) |
|---|---|---|---|---|
| Sodium chloride | NaCl | 58.4000 | 0.04 | 1.6352 |
| Sodium fluoride | NaF | 42.0000 | 0.11 | 3.2340 |
| Sodium sulfate | $Na_2SO_4$ | 142.0000 | 0.1 | 9.9400 |
| Sodium phosphate, 12-hydrate | $Na_3PO_4.12H_2O$ | 380.0000 | 0.04 | 10.6400 |
| Sodium hydroxide* | NaOH | 40.0000 | 0.04 | 1.1200 |
| Sodium acetate, 3-hydrate | $Na(C_2H_3O_2).3H_2O$ | 136.0000 | 0.025 | 2.3800 |
| Sodium formate | $Na(CHO_2)$ | 68.0000 | 0.03 | 1.4280 |
| Glycolic acid | $C_2H_4O_3$ | 76.1000 | 0.02 | 1.0654 |
| Sodium oxalate | $Na_2C_2O_4$ | 134.0000 | 0.015 | 1.4070 |
| Sodium nitrite | $NaNO_2$ | 69.0000 | 2.2 | 106.2600 |
| Sodium nitrate | $NaNO_3$ | 85.0000 | 0.78 | 46.4100 |
| Sodium carbonate | $Na_2CO_3$ | 106.0000 | 0.1992 | 14.7806 |
| Sodium bicarbonate | $NaHCO_3$ | 84.0100 | 0.0008 | 0.0470 |

* additional sodium hydroxide to neutralize acid

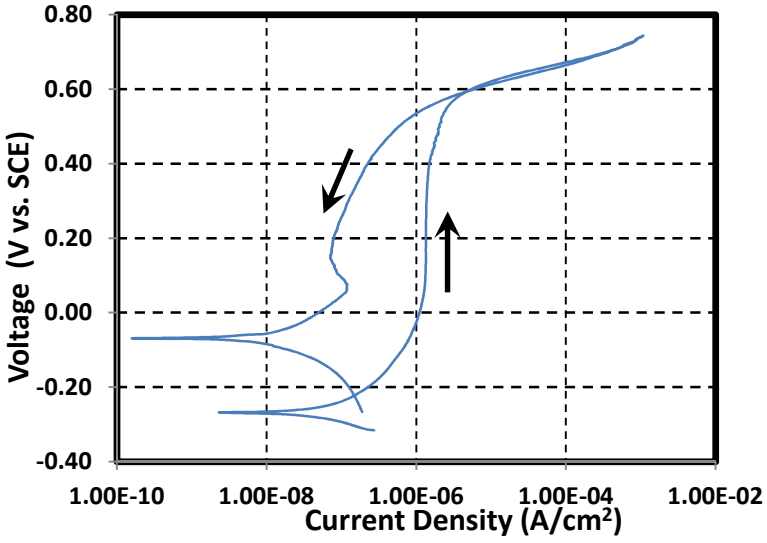


**Cyclic Potentiodynamic Polarization result**

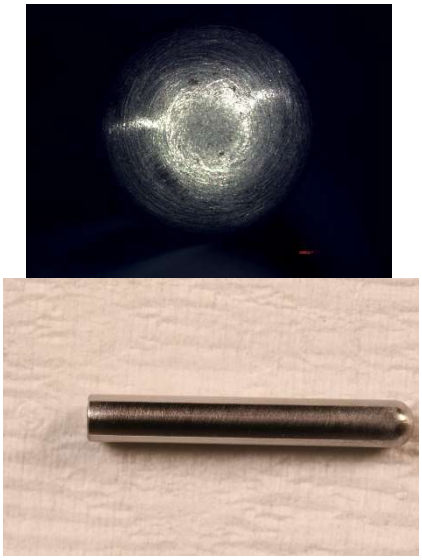

**Images of bullet samples after test**

## Test 8 Composition of simulant

**Test 8**

| | | | |
|---|---|---|---|
| Temperature | 35 | °C | |
| pH at room temperature | 12.2 | | |
| pH before testing (at temp.) | 11.8 | pH after testing (at temp.) | 11.8 |
| Volume | 0.7 | L | |

| Simulant Source | Formula | Molecular Weight (g/mol) | Concentration (M) | weight required (g) |
|---|---|---|---|---|
| Sodium chloride | NaCl | 58.4000 | 0.01 | 0.4088 |
| Sodium fluoride | NaF | 42.0000 | 0.01 | 0.2940 |
| Sodium sulfate | $Na_2SO_4$ | 142.0000 | 0.1 | 9.9400 |
| Sodium phosphate, 12-hydrate | $Na_3PO_4.12H_2O$ | 380.0000 | 0.04 | 10.6400 |
| Sodium hydroxide* | NaOH | 40.0000 | 0.04 | 1.1200 |
| Sodium acetate, 3-hydrate | $Na(C_2H_3O_2).3H_2O$ | 136.0000 | 0.02 | 1.9040 |
| Sodium formate | $Na(CHO_2)$ | 68.0000 | 0.03 | 1.4280 |
| Glycolic acid | $C_2H_4O_3$ | 76.1000 | 0.02 | 1.0654 |
| Sodium oxalate | $Na_2C_2O_4$ | 134.0000 | 0.02 | 1.8760 |
| Sodium nitrite | $NaNO_2$ | 69.0000 | 0.75 | 36.2250 |
| Sodium nitrate | $NaNO_3$ | 85.0000 | 1 | 59.5000 |
| Sodium carbonate | $Na_2CO_3$ | 106.0000 | 0.1983 | 14.7139 |
| Sodium bicarbonate | $NaHCO_3$ | 84.0100 | 0.0017 | 0.1000 |

* additional sodium hydroxide to neutralize acid

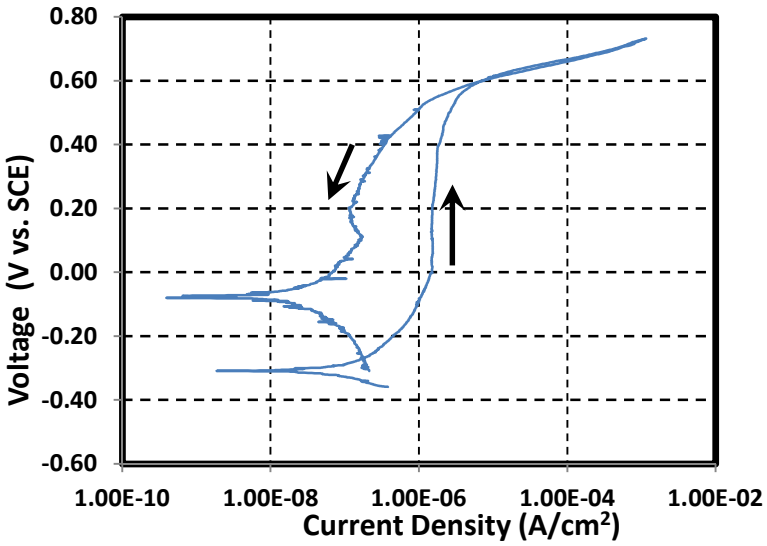


**Cyclic Potentiodynamic Polarization result**

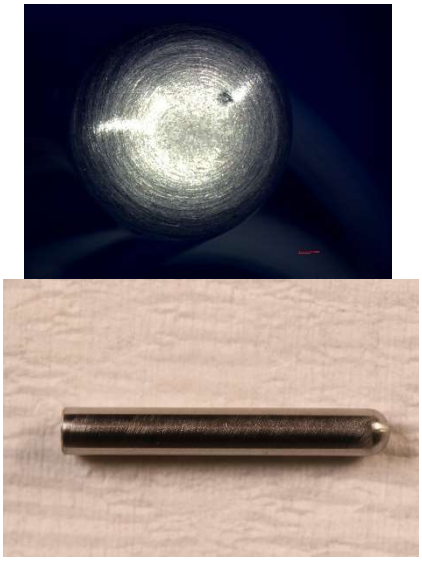

**Images of bullet samples after test**

## Test 9 Composition of simulant

**Test 9**

| | | | |
|---|---|---|---|
| Temperature | 35 °C | | |
| pH at room temperature | 12.9 | | |
| pH before testing (at temp.) | 12.5 | pH after testing (at temp.) | 12.4 |
| Volume | 0.7 L | | |

| Simulant Source | Formula | Molecular Weight (g/mol) | Concentration (M) | weight required (g) |
|---|---|---|---|---|
| Sodium chloride | NaCl | 58.4000 | 0.04 | 1.6352 |
| Sodium fluoride | NaF | 42.0000 | 0.04 | 1.1760 |
| Sodium sulfate | $Na_2SO_4$ | 142.0000 | 0.1 | 9.9400 |
| Sodium phosphate, 12-hydrate | $Na_3PO_4.12H_2O$ | 380.0000 | 0.04 | 10.6400 |
| Sodium hydroxide | NaOH | 40.0000 | 0.11 | 3.0800 |
| Sodium acetate, 3-hydrate | $Na(C_2H_3O_2).3H_2O$ | 136.0000 | 0.02 | 1.9040 |
| Sodium formate | $Na(CHO_2)$ | 68.0000 | 0.03 | 1.4280 |
| Glycolic acid | $C_2H_4O_3$ | 76.1000 | 0.02 | 1.0654 |
| Sodium oxalate | $Na_2C_2O_4$ | 134.0000 | 0.02 | 1.8760 |
| Sodium nitrite | $NaNO_2$ | 69.0000 | 1 | 48.3000 |
| Sodium nitrate | $NaNO_3$ | 85.0000 | 1 | 59.5000 |
| Sodium carbonate | $Na_2CO_3$ | 106.0000 | 0.1997 | 14.8177 |
| Sodium bicarbonate | $NaHCO_3$ | 84.0100 | 0.0003 | 0.0176 |

* additional sodium hydroxide to neutralize acid

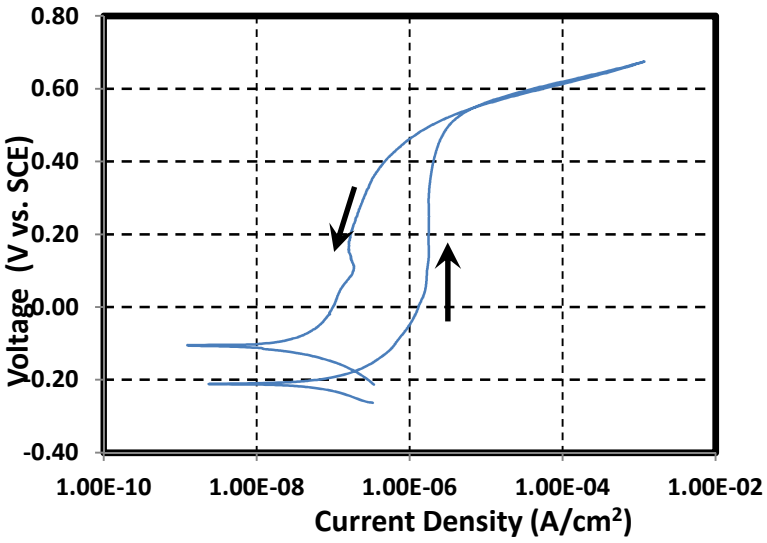


**Cyclic Potentiodynamic Polarization result**

**Images of bullet samples after test**

## Test 10 Composition of simulant

**Test 10**

| | | | |
|---|---|---|---|
| Temperature | 35 | °C | |
| pH at room temperature | 12.7 | | |
| pH before testing (at temp.) | 12.3 | pH after testing (at temp.) | 12.3 |
| Volume | 0.7 | L | |

| Simulant Source | Formula | Molecular Weight (g/mol) | Concentration (M) | weight required (g) |
|---|---|---|---|---|
| Sodium chloride | NaCl | 58.4000 | 0.04 | 1.6352 |
| Sodium fluoride | NaF | 42.0000 | 0.06 | 1.7640 |
| Sodium sulfate | $Na_2SO_4$ | 142.0000 | 0.1 | 9.9400 |
| Sodium phosphate, 12-hydrate | $Na_3PO_4.12H_2O$ | 380.0000 | 0.04 | 10.6400 |
| Sodium hydroxide* | NaOH | 40.0000 | 0.08 | 2.2400 |
| Sodium acetate, 3-hydrate | $Na(C_2H_3O_2).3H_2O$ | 136.0000 | 0.02 | 1.9040 |
| Sodium formate | $Na(CHO_2)$ | 68.0000 | 0.03 | 1.4280 |
| Glycolic acid | $C_2H_4O_3$ | 76.1000 | 0.02 | 1.0654 |
| Sodium oxalate | $Na_2C_2O_4$ | 134.0000 | 0.02 | 1.8760 |
| Sodium nitrite | $NaNO_2$ | 69.0000 | 1 | 48.3000 |
| Sodium nitrate | $NaNO_3$ | 85.0000 | 1 | 59.5000 |
| Sodium carbonate | $Na_2CO_3$ | 106.0000 | 0.1997 | 14.8177 |
| Sodium bicarbonate | $NaHCO_3$ | 84.0100 | 0.003 | 0.1764 |

* additional sodium hydroxide to neutralize acid

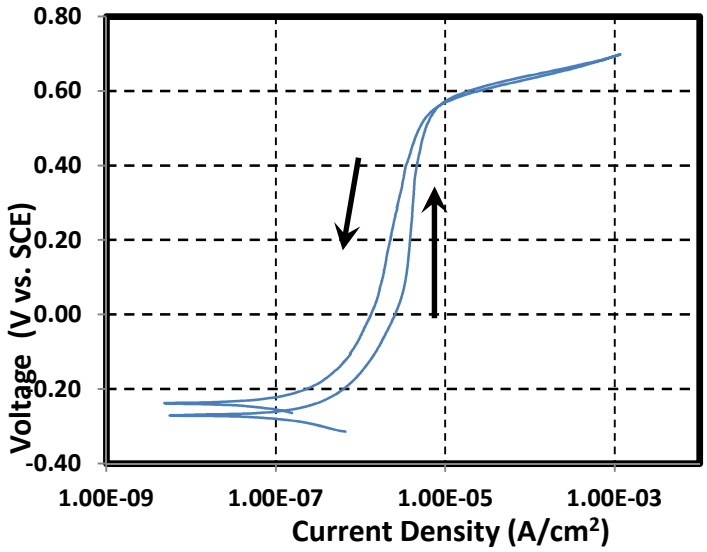


**Cyclic Potentiodynamic Polarization result**

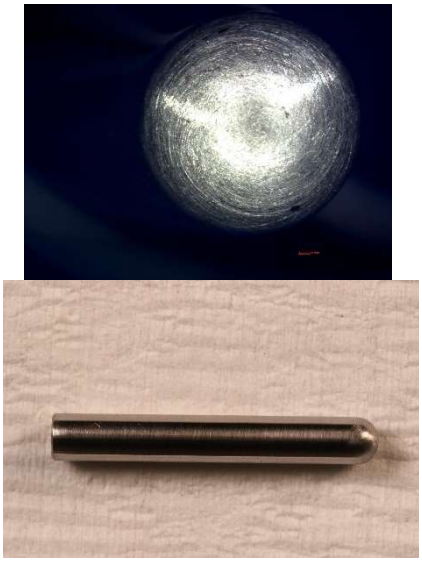

**Images of bullet samples after test**

## Test 11 Composition of simulant

**Test 11**

| | | | |
|---|---|---|---|
| Temperature | 35 °C | | |
| pH at room temperature | 12.8 | | |
| pH before testing (at temp.) | 12.3 | pH after testing (at temp.) | 12.2 |
| Volume | 0.7 L | | |
| Temperature | 25 °C | | |

| Simulant Source | Formula | Molecular Weight (g/mol) | Concentration (M) | weight required (g) |
|---|---|---|---|---|
| Sodium chloride | NaCl | 58.4000 | 0.01 | 0.4088 |
| Sodium fluoride | NaF | 42.0000 | 0.04 | 1.1760 |
| Sodium sulfate | $Na_2SO_4$ | 142.0000 | 0.1 | 9.9400 |
| Sodium phosphate, 12-hydrate | $Na_3PO_4.12H_2O$ | 380.0000 | 0.04 | 10.6400 |
| Sodium hydroxide* | NaOH | 40.0000 | 0.07 | 1.9600 |
| Sodium acetate, 3-hydrate | $Na(C_2H_3O_2).3H_2O$ | 136.0000 | 0.02 | 1.9040 |
| Sodium formate | $Na(CHO_2)$ | 68.0000 | 0.03 | 1.4280 |
| Glycolic acid | $C_2H_4O_3$ | 76.1000 | 0.02 | 1.0654 |
| Sodium oxalate | $Na_2C_2O_4$ | 134.0000 | 0.02 | 1.8760 |
| Sodium nitrite | $NaNO_2$ | 69.0000 | 0.7 | 33.8100 |
| Sodium nitrate | $NaNO_3$ | 85.0000 | 1 | 59.5000 |
| Sodium carbonate | $Na_2CO_3$ | 106.0000 | 0.1993 | 14.7881 |
| Sodium bicarbonate | $NaHCO_3$ | 84.0100 | 0.0007 | 0.0412 |

* additional sodium hydroxide to neutralize acid

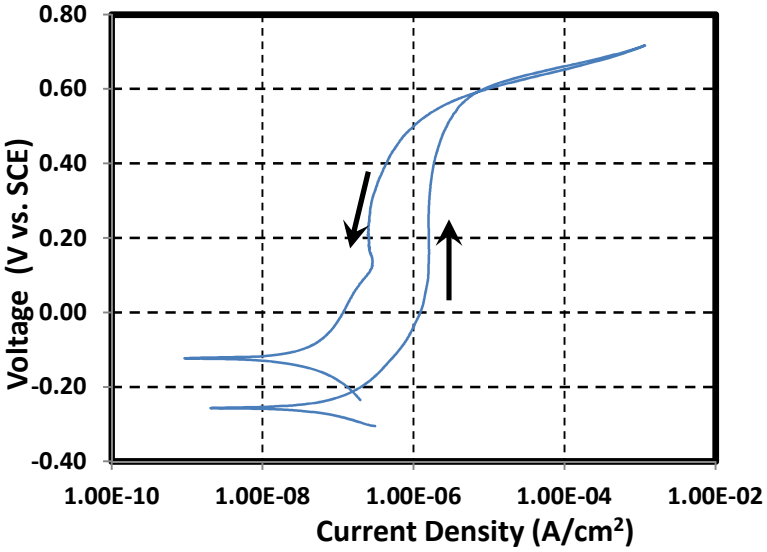


**Cyclic Potentiodynamic Polarization result**

**Images of bullet samples after test**

## Test 12 Composition of simulant

**Test 12**

| | | | |
|---|---|---|---|
| Temperature | 35 | °C | |
| pH at room temperature | 12.8 | | |
| pH before testing (at temp.) | 12.3 | pH after testing (at temp.) | 12.2 |
| Volume | 0.7 | L | |
| Temperature | 25 | °C | |

| Simulant Source | Formula | Molecular Weight (g/mol) | Concentration (M) | weight required (g) |
|---|---|---|---|---|
| Sodium chloride | NaCl | 58.4000 | 0.01 | 0.4088 |
| Sodium fluoride | NaF | 42.0000 | 0.01 | 0.2940 |
| Sodium sulfate | $Na_2SO_4$ | 142.0000 | 0.1 | 9.9400 |
| Sodium phosphate, 12-hydrate | $Na_3PO_4.12H_2O$ | 380.0000 | 0.04 | 10.6400 |
| Sodium hydroxide | NaOH | 40.0000 | 0.095 | 2.6600 |
| Sodium acetate, 3-hydrate | $Na(C_2H_3O_2).3H_2O$ | 136.0000 | 0.02 | 1.9040 |
| Sodium formate | $Na(CHO_2)$ | 68.0000 | 0.03 | 1.4280 |
| Glycolic acid | $C_2H_4O_3$ | 76.1000 | 0.02 | 1.0654 |
| Sodium oxalate | $Na_2C_2O_4$ | 134.0000 | 0.02 | 1.8760 |
| Sodium nitrite | $NaNO_2$ | 69.0000 | 0.5 | 24.1500 |
| Sodium nitrate | $NaNO_3$ | 85.0000 | 1 | 59.5000 |
| Sodium carbonate | $Na_2CO_3$ | 106.0000 | 0.1995 | 14.8029 |
| Sodium bicarbonate | $NaHCO_3$ | 84.0100 | 0.0005 | 0.0294 |

* additional sodium hydroxide to neutralize acid

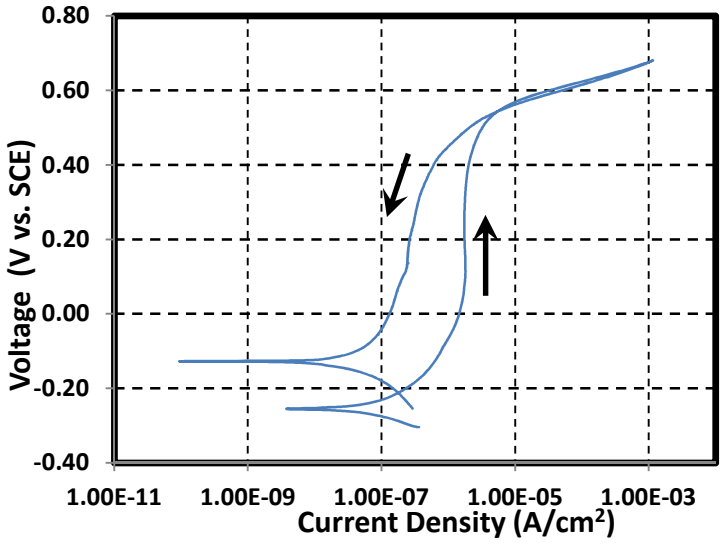


**Cyclic Potentiodynamic Polarization result**

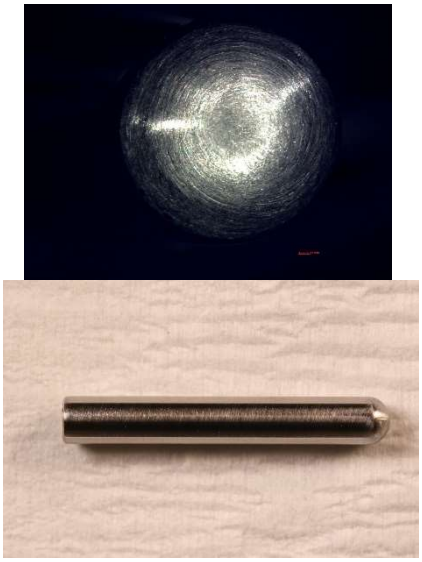

**Images of bullet samples after test**

## Test 13 Composition of simulant

**Test 13**

| | | | |
|---|---|---|---|
| Temperature | 75 | °C | |
| pH at room temperature | 12.1 | | |
| pH before testing (at temp.) | 10.7 | pH after testing (at temp.) | 10.5 |
| Volume | 0.7 | L | |

| Simulant Source | Formula | Molecular Weight (g/mol) | Concentration (M) | weight required (g) |
|---|---|---|---|---|
| Sodium chloride | NaCl | 58.4000 | 0.01 | 0.4088 |
| Sodium fluoride | NaF | 42.0000 | 0.07 | 2.0580 |
| Sodium sulfate | $Na_2SO_4$ | 142.0000 | 0.1 | 9.9400 |
| Sodium phosphate, 12-hydrate | $Na_3PO_4.12H_2O$ | 380.0000 | 0.04 | 10.6400 |
| Sodium hydroxide* | NaOH | 40.0000 | 0.03 | 0.8400 |
| Sodium acetate, 3-hydrate | $Na(C_2H_3O_2).3H_2O$ | 136.0000 | 0.02 | 1.9040 |
| Sodium formate | $Na(CHO_2)$ | 68.0000 | 0.03 | 1.4280 |
| Glycolic acid | $C_2H_4O_3$ | 76.1000 | 0.02 | 1.0654 |
| Sodium oxalate | $Na_2C_2O_4$ | 134.0000 | 0.02 | 1.8760 |
| Sodium nitrite | $NaNO_2$ | 69.0000 | 1.06 | 51.1980 |
| Sodium nitrate | $NaNO_3$ | 85.0000 | 0.87 | 51.7650 |
| Sodium carbonate | $Na_2CO_3$ | 106.0000 | 0.1971 | 14.6248 |
| Sodium bicarbonate | $NaHCO_3$ | 84.0100 | 0.0029 | 0.1705 |

* additional sodium hydroxide to neutralize acid

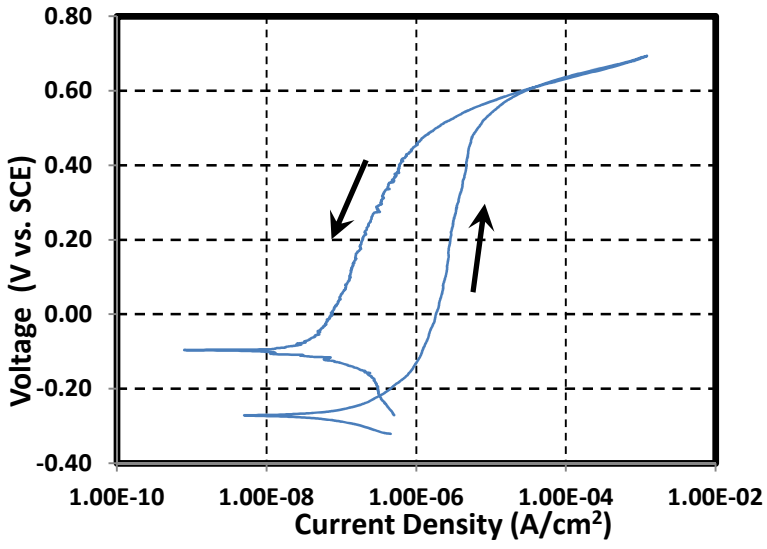


**Cyclic Potentiodynamic Polarization result**

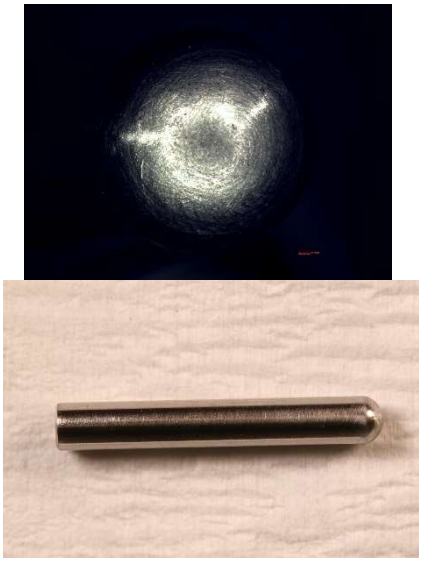

**Images of bullet samples after test**

## Test 14 Composition of simulant

**Test 14**

| | | | |
|---|---|---|---|
| Temperature | 75 | °C | |
| pH at room temperature | 12.4 | | |
| pH before testing (at temp.) | 10.9 | pH after testing (at temp.) | 10.8 |
| Volume | 0.7 | L | |

| Simulant Source | Formula | Molecular Weight (g/mol) | Concentration (M) | weight required (g) |
|---|---|---|---|---|
| Sodium chloride | NaCl | 58.4000 | 0.1 | 4.0880 |
| Sodium fluoride | NaF | 42.0000 | 0.09 | 2.6460 |
| Sodium sulfate | $Na_2SO_4$ | 142.0000 | 0.1 | 9.9400 |
| Sodium phosphate, 12-hydrate | $Na_3PO_4.12H_2O$ | 380.0000 | 0.04 | 10.6400 |
| Sodium hydroxide* | NaOH | 40.0000 | 0.05 | 1.4000 |
| Sodium acetate, 3-hydrate | $Na(C_2H_3O_2).3H_2O$ | 136.0000 | 0.025 | 2.3800 |
| Sodium formate | $Na(CHO_2)$ | 68.0000 | 0.03 | 1.4280 |
| Glycolic acid | $C_2H_4O_3$ | 76.1000 | 0.02 | 1.0654 |
| Sodium oxalate | $Na_2C_2O_4$ | 134.0000 | 0.015 | 1.4070 |
| Sodium nitrite | $NaNO_2$ | 69.0000 | 2.25 | 108.6750 |
| Sodium nitrate | $NaNO_3$ | 85.0000 | 1.01 | 60.0950 |
| Sodium carbonate | $Na_2CO_3$ | 106.0000 | 0.1995 | 14.8029 |
| Sodium bicarbonate | $NaHCO_3$ | 84.0100 | 0.0005 | 0.0294 |

* additional sodium hydroxide to neutralize acid

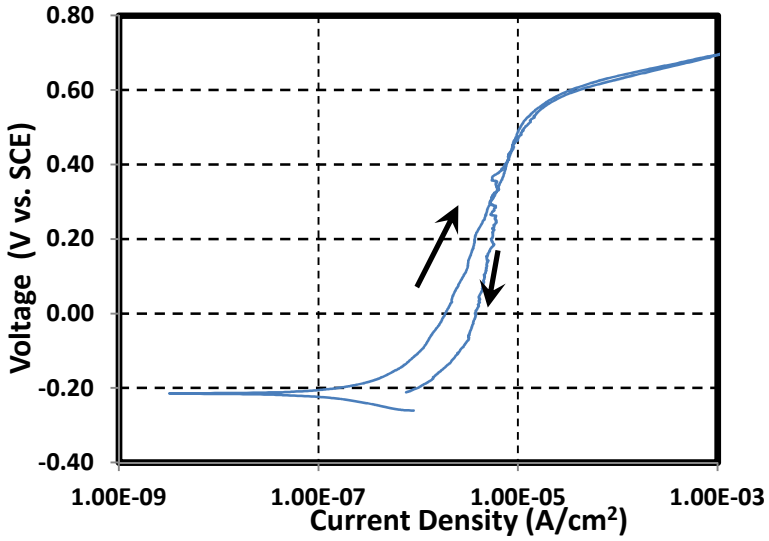


**Cyclic Potentiodynamic Polarization result**

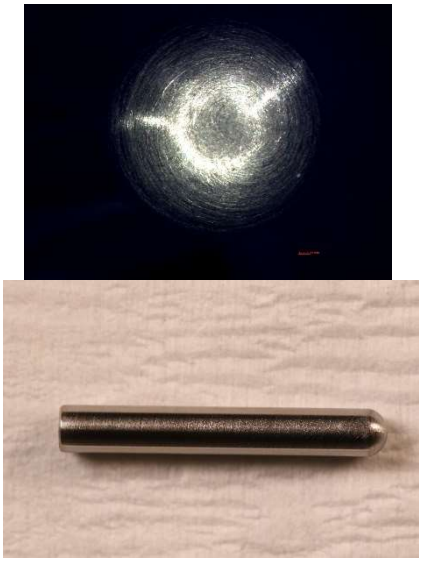

**Images of bullet samples after test**

**ASTM G192 Plot**

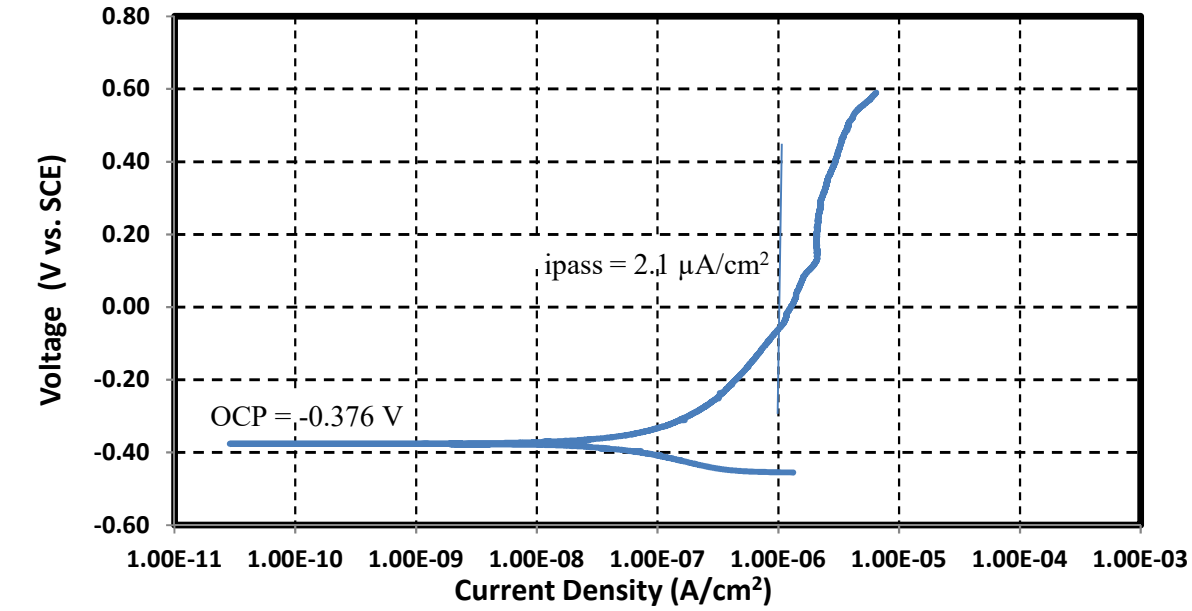


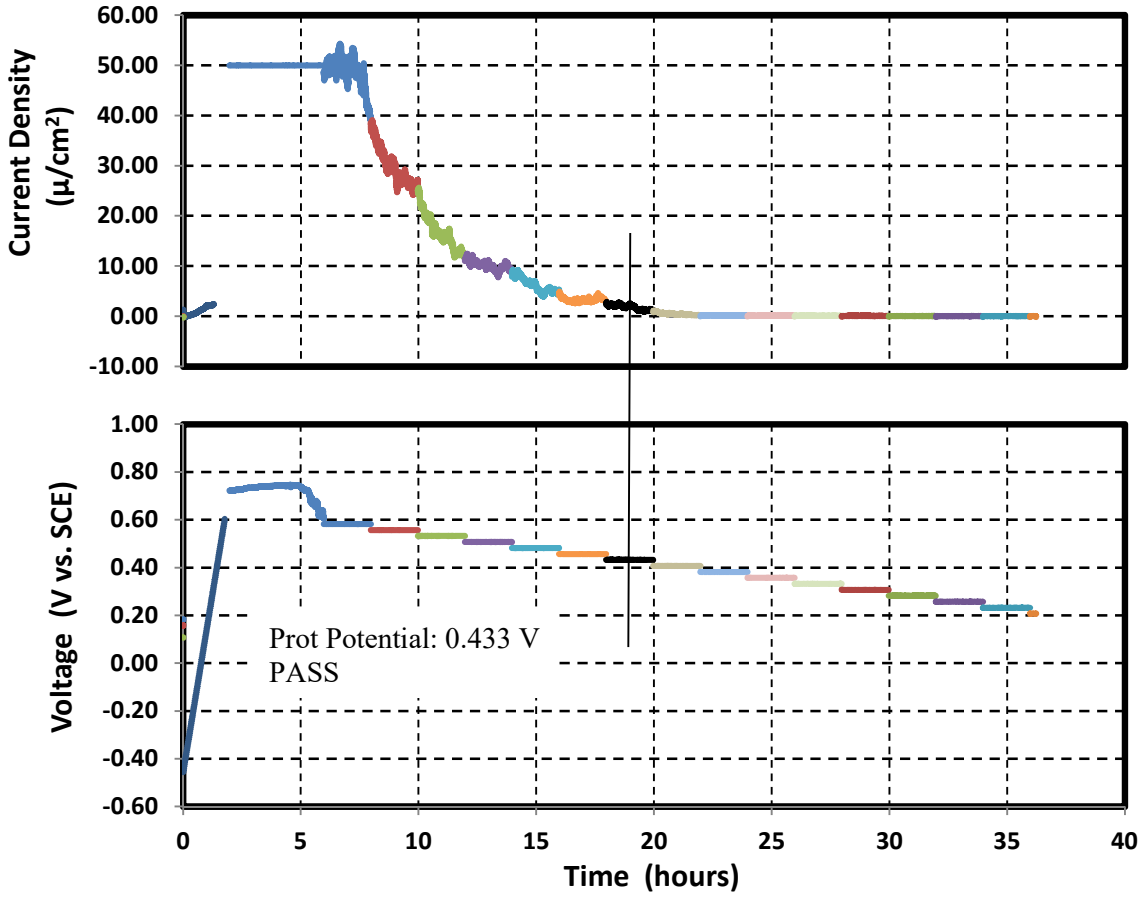

## Test 15 Composition of simulant

**Test 15**

| | | | |
|---|---|---|---|
| Temperature | 75 | °C | |
| pH at room temperature | 12.5 | | |
| pH before testing (at temp.) | 11.0 | pH after testing (at temp.) | 10.8 |
| Volume | 0.7 | L | |

| Simulant Source | Formula | Molecular Weight (g/mol) | Concentration (M) | weight required (g) |
|---|---|---|---|---|
| Sodium chloride | NaCl | 58.4000 | 0.03 | 1.2264 |
| Sodium fluoride | NaF | 42.0000 | 0.1 | 2.9400 |
| Sodium sulfate | $Na_2SO_4$ | 142.0000 | 0.1 | 9.9400 |
| Sodium phosphate, 12-hydrate | $Na_3PO_4.12H_2O$ | 380.0000 | 0.04 | 10.6400 |
| Sodium hydroxide* | NaOH | 40.0000 | 0.07 | 1.9600 |
| Sodium acetate, 3-hydrate | $Na(C_2H_3O_2).3H_2O$ | 136.0000 | 0.025 | 2.3800 |
| Sodium formate | $Na(CHO_2)$ | 68.0000 | 0.03 | 1.4280 |
| Glycolic acid | $C_2H_4O_3$ | 76.1000 | 0.02 | 1.0654 |
| Sodium oxalate | $Na_2C_2O_4$ | 134.0000 | 0.015 | 1.4070 |
| Sodium nitrite | $NaNO_2$ | 69.0000 | 2.09 | 100.9470 |
| Sodium nitrate | $NaNO_3$ | 85.0000 | 1.04 | 61.8800 |
| Sodium carbonate | $Na_2CO_3$ | 106.0000 | 0.1997 | 14.8177 |
| Sodium bicarbonate | $NaHCO_3$ | 84.0100 | 0.0003 | 0.0176 |

* additional sodium hydroxide to neutralize acid

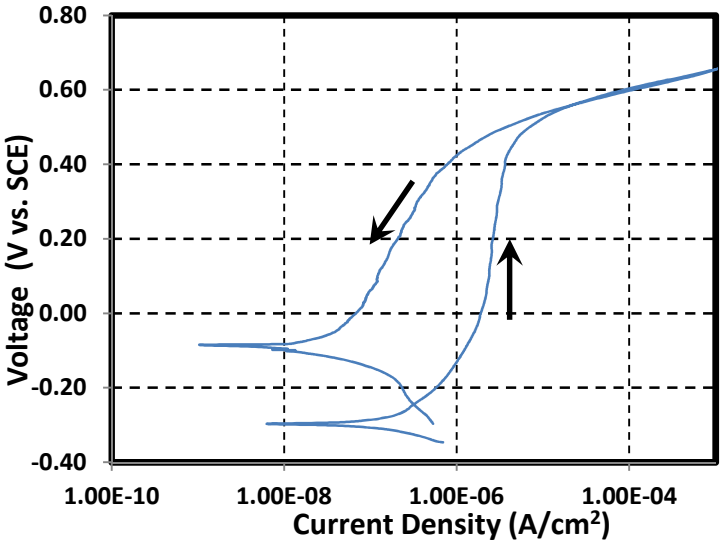


**Cyclic Potentiodynamic Polarization result**

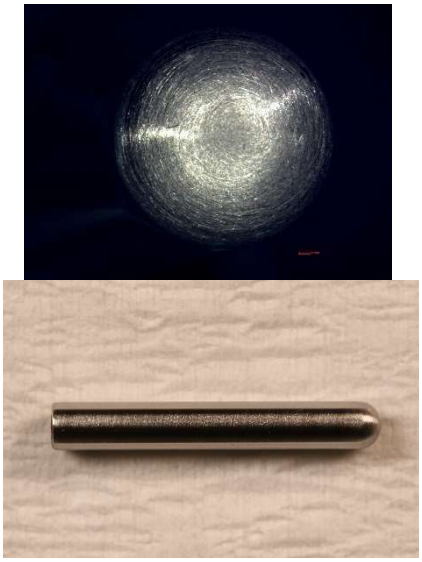

**Images of bullet samples after test**

## Test 16 Composition of simulant

**Test 16**

| | | | |
|---|---|---|---|
| Temperature | 75 | °C | |
| pH at room temperature | 12.7 | | |
| pH before testing (at temp.) | 11.1 | pH after testing (at temp.) | 10.9 |
| Volume | 0.7 | L | |

| Simulant Source | Formula | Molecular Weight (g/mol) | Concentration (M) | weight required (g) |
|---|---|---|---|---|
| Sodium chloride | NaCl | 58.4000 | 0.04 | 1.6352 |
| Sodium fluoride | NaF | 42.0000 | 0.04 | 1.1760 |
| Sodium sulfate | $Na_2SO_4$ | 142.0000 | 0.1 | 9.9400 |
| Sodium phosphate, 12-hydrate | $Na_3PO_4.12H_2O$ | 380.0000 | 0.04 | 10.6400 |
| Sodium hydroxide* | NaOH | 40.0000 | 0.11 | 3.0800 |
| Sodium acetate, 3-hydrate | $Na(C_2H_3O_2).3H_2O$ | 136.0000 | 0.02 | 1.9040 |
| Sodium formate | $Na(CHO_2)$ | 68.0000 | 0.03 | 1.4280 |
| Glycolic acid | $C_2H_4O_3$ | 76.1000 | 0.02 | 1.0654 |
| Sodium oxalate | $Na_2C_2O_4$ | 134.0000 | 0.02 | 1.8760 |
| Sodium nitrite | $NaNO_2$ | 69.0000 | 1 | 48.3000 |
| Sodium nitrate | $NaNO_3$ | 85.0000 | 1 | 59.5000 |
| Sodium carbonate | $Na_2CO_3$ | 106.0000 | 0.1997 | 14.8177 |
| Sodium bicarbonate | $NaHCO_3$ | 84.0100 | 0.0003 | 0.0176 |

* additional sodium hydroxide to neutralize acid

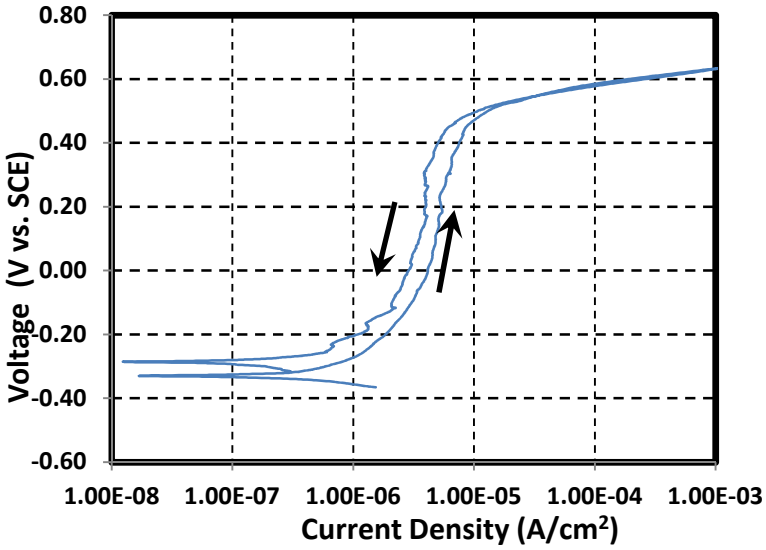


**Cyclic Potentiodynamic Polarization result**

**Images of bullet samples after test**

## Test 17 Composition of simulant

**Test 17**

| | | | |
|---|---|---|---|
| Temperature | 75 | °C | |
| pH at room temperature | 12.5 | | |
| pH before testing (at temp.) | 10.9 | pH after testing (at temp.) | 10.7 |
| Volume | 0.7 | L | |

| Simulant Source | Formula | Molecular Weight (g/mol) | Concentration (M) | weight required (g) |
|---|---|---|---|---|
| Sodium chloride | NaCl | 58.4000 | 0.04 | 1.6352 |
| Sodium fluoride | NaF | 42.0000 | 0.06 | 1.7640 |
| Sodium sulfate | $Na_2SO_4$ | 142.0000 | 0.1 | 9.9400 |
| Sodium phosphate, 12-hydrate | $Na_3PO_4.12H_2O$ | 380.0000 | 0.04 | 10.6400 |
| Sodium hydroxide* | NaOH | 40.0000 | 0.08 | 2.2400 |
| Sodium acetate, 3-hydrate | $Na(C_2H_3O_2).3H_2O$ | 136.0000 | 0.02 | 1.9040 |
| Sodium formate | $Na(CHO_2)$ | 68.0000 | 0.03 | 1.4280 |
| Glycolic acid | $C_2H_4O_3$ | 76.1000 | 0.02 | 1.0654 |
| Sodium oxalate | $Na_2C_2O_4$ | 134.0000 | 0.02 | 1.8760 |
| Sodium nitrite | $NaNO_2$ | 69.0000 | 1 | 48.3000 |
| Sodium nitrate | $NaNO_3$ | 85.0000 | 1 | 59.5000 |
| Sodium carbonate | $Na_2CO_3$ | 106.0000 | 0.1995 | 14.8029 |
| Sodium bicarbonate | $NaHCO_3$ | 84.0100 | 0.0005 | 0.0294 |

* additional sodium hydroxide to neutralize acid

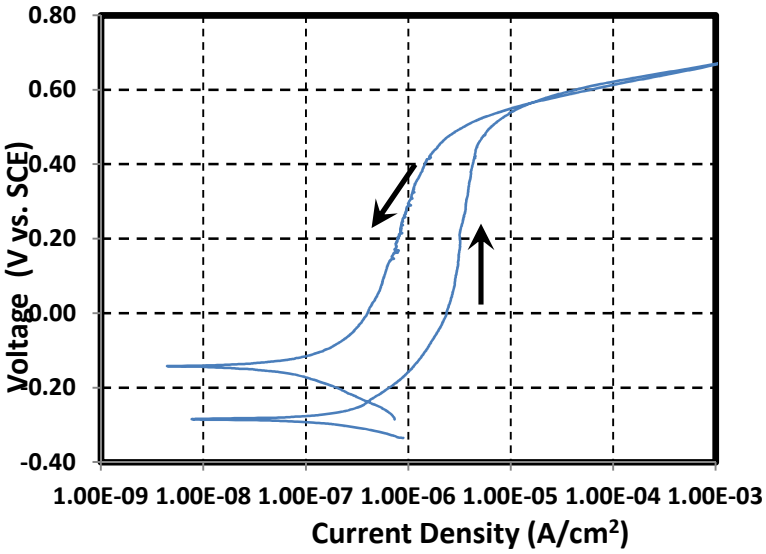


**Cyclic Potentiodynamic Polarization result**

**Images of bullet samples after test**

## Test 18 Composition of simulant

**Test 18**

| | | | |
|---|---|---|---|
| Temperature | 75 | °C | |
| pH at room temperature | 12.2 | | |
| pH before testing (at temp.) | 10.5 | pH after testing (at temp.) | 10.4 |
| Volume | 0.7 | L | |

| Simulant Source | Formula | Molecular Weight (g/mol) | Concentration (M) | weight required (g) |
|---|---|---|---|---|
| Sodium chloride | NaCl | 58.4000 | 0.01 | 0.4088 |
| Sodium fluoride | NaF | 42.0000 | 0.01 | 0.2940 |
| Sodium sulfate | $Na_2SO_4$ | 142.0000 | 0.1 | 9.9400 |
| Sodium phosphate, 12-hydrate | $Na_3PO_4.12H_2O$ | 380.0000 | 0.04 | 10.6400 |
| Sodium hydroxide | NaOH | 40.0000 | 0.04 | 1.1200 |
| Sodium acetate, 3-hydrate | $Na(C_2H_3O_2).3H_2O$ | 136.0000 | 0.02 | 1.9040 |
| Sodium formate | $Na(CHO_2)$ | 68.0000 | 0.03 | 1.4280 |
| Glycolic acid | $C_2H_4O_3$ | 76.1000 | 0.02 | 1.0654 |
| Sodium oxalate | $Na_2C_2O_4$ | 134.0000 | 0.02 | 1.8760 |
| Sodium nitrite | $NaNO_2$ | 69.0000 | 0.75 | 36.2250 |
| Sodium nitrate | $NaNO_3$ | 85.0000 | 1 | 59.5000 |
| Sodium carbonate | $Na_2CO_3$ | 106.0000 | 0.1983 | 14.7139 |
| Sodium bicarbonate | $NaHCO_3$ | 84.0100 | 0.0017 | 0.1000 |

* additional sodium hydroxide to neutralize acid

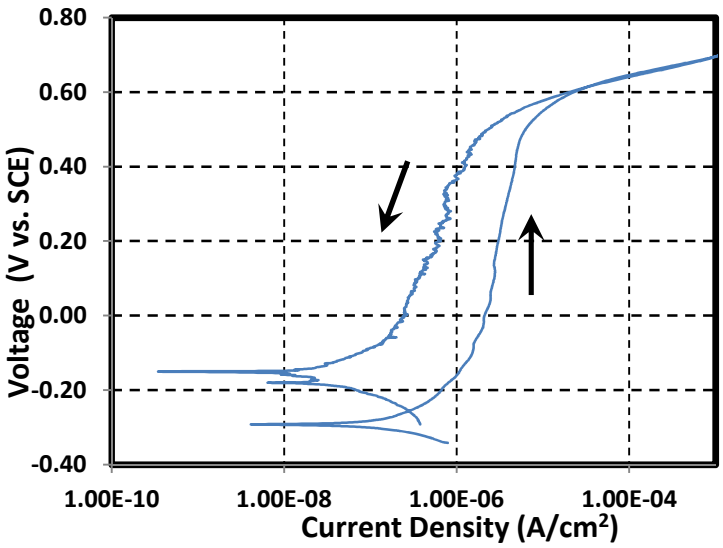


**Cyclic Potentiodynamic Polarization result**

**Images of bullet samples after test**

## Test 19 Composition of simulant

**Test 19**

| | | | |
|---|---|---|---|
| Temperature | 75 | °C | |
| pH at room temperature | 12.5 | | |
| pH before testing (at temp.) | 10.8 | pH after testing (at temp.) | 10.7 |
| Volume | 0.7 | L | |

| Simulant Source | Formula | Molecular Weight (g/mol) | Concentration (M) | weight required (g) |
|---|---|---|---|---|
| Sodium chloride | NaCl | 58.4000 | 0.01 | 0.4088 |
| Sodium fluoride | NaF | 42.0000 | 0.04 | 1.1760 |
| Sodium sulfate | $Na_2SO_4$ | 142.0000 | 0.1 | 9.9400 |
| Sodium phosphate, 12-hydrate | $Na_3PO_4.12H_2O$ | 380.0000 | 0.04 | 10.6400 |
| Sodium hydroxide* | NaOH | 40.0000 | 0.07 | 1.9600 |
| Sodium acetate, 3-hydrate | $Na(C_2H_3O_2).3H_2O$ | 136.0000 | 0.02 | 1.9040 |
| Sodium formate | $Na(CHO_2)$ | 68.0000 | 0.03 | 1.4280 |
| Glycolic acid | $C_2H_4O_3$ | 76.1000 | 0.02 | 1.0654 |
| Sodium oxalate | $Na_2C_2O_4$ | 134.0000 | 0.02 | 1.8760 |
| Sodium nitrite | $NaNO_2$ | 69.0000 | 0.7 | 33.8100 |
| Sodium nitrate | $NaNO_3$ | 85.0000 | 1 | 59.5000 |
| Sodium carbonate | $Na_2CO_3$ | 106.0000 | 0.1993 | 14.7881 |
| Sodium bicarbonate | $NaHCO_3$ | 84.0100 | 0.0007 | 0.0412 |

* additional sodium hydroxide to neutralize acid

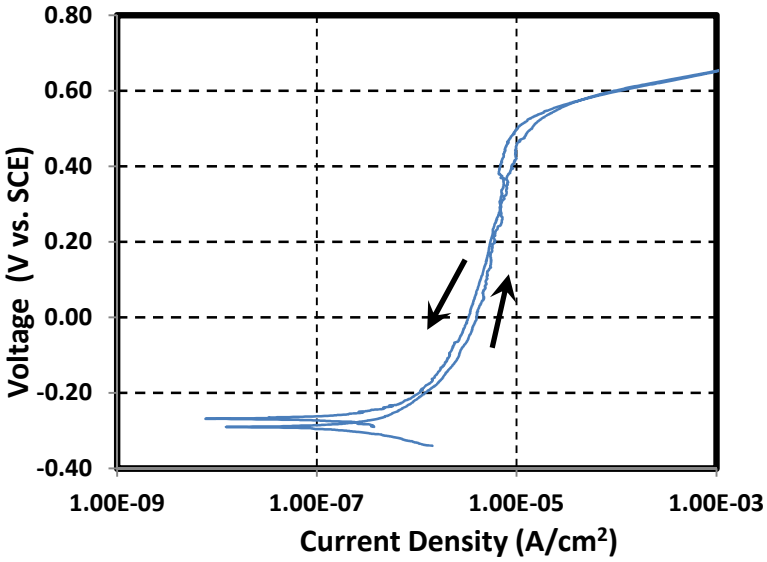


**Cyclic Potentiodynamic Polarization result**

**Images of bullet samples after test**

## Test 20 Composition of simulant

**Test 20**

| | | | |
|---|---|---|---|
| Temperature | 75 | °C | |
| pH at room temperature | 11.9 | | |
| pH before testing (at temp.) | 10.3 | pH after testing (at temp.) | 10.2 |
| Volume | 0.7 | L | |

| Simulant Source | Formula | Molecular Weight (g/mol) | Concentration (M) | weight required (g) |
|---|---|---|---|---|
| Sodium chloride | NaCl | 58.4000 | 0.07 | 2.8616 |
| Sodium fluoride | NaF | 42.0000 | 0.04 | 1.1760 |
| Sodium sulfate | $Na_2SO_4$ | 142.0000 | 0.1 | 9.9400 |
| Sodium phosphate, 12-hydrate | $Na_3PO_4.12H_2O$ | 380.0000 | 0.04 | 10.6400 |
| Sodium hydroxide* | NaOH | 40.0000 | 0.03 | 0.8400 |
| Sodium acetate, 3-hydrate | $Na(C_2H_3O_2).3H_2O$ | 136.0000 | 0.025 | 2.3800 |
| Sodium formate | $Na(CHO_2)$ | 68.0000 | 0.03 | 1.4280 |
| Glycolic acid | $C_2H_4O_3$ | 76.1000 | 0.02 | 1.0654 |
| Sodium oxalate | $Na_2C_2O_4$ | 134.0000 | 0.015 | 1.4070 |
| Sodium nitrite | $NaNO_2$ | 69.0000 | 2.18 | 105.2940 |
| Sodium nitrate | $NaNO_3$ | 85.0000 | 0.96 | 57.1200 |
| Sodium carbonate | $Na_2CO_3$ | 106.0000 | 0.1985 | 14.7287 |
| Sodium bicarbonate | $NaHCO_3$ | 84.0100 | 0.0015 | 0.0882 |

* additional sodium hydroxide to neutralize acid

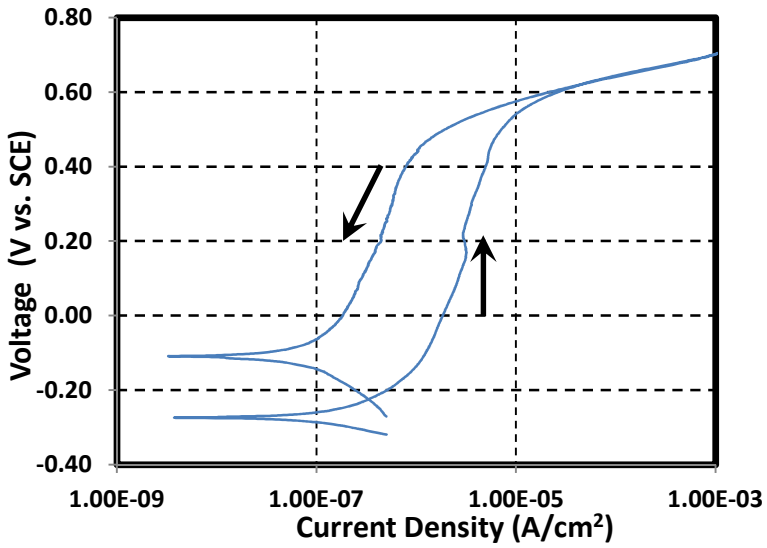


**Cyclic Potentiodynamic Polarization result**

**Images of bullet samples after test**

## Test 21 Composition of simulant

**Test 21**

| | | | |
|---|---|---|---|
| Temperature | 75 | °C | |
| pH at room temperature | 13.6 | | |
| pH before testing (at temp.) | 11.2 | pH after testing (at temp.) | 11.0 |
| Volume | 0.7 | L | |

| Simulant Source | Formula | Molecular Weight (g/mol) | Concentration (M) | weight required (g) |
|---|---|---|---|---|
| Sodium chloride | NaCl | 58.4000 | 0.05 | 2.0440 |
| Sodium fluoride | NaF | 42.0000 | 0.04 | 1.1760 |
| Sodium sulfate | $Na_2SO_4$ | 142.0000 | 0.1 | 9.9400 |
| Sodium phosphate, 12-hydrate | $Na_3PO_4.12H_2O$ | 380.0000 | 0.04 | 10.6400 |
| Sodium hydroxide* | NaOH | 40.0000 | 0.145 | 4.0600 |
| Sodium acetate, 3-hydrate | $Na(C_2H_3O_2).3H_2O$ | 136.0000 | 0.025 | 2.3800 |
| Sodium formate | $Na(CHO_2)$ | 68.0000 | 0.03 | 1.4280 |
| Glycolic acid | $C_2H_4O_3$ | 76.1000 | 0.02 | 1.0654 |
| Sodium oxalate | $Na_2C_2O_4$ | 134.0000 | 0.015 | 1.4070 |
| Sodium nitrite | $NaNO_2$ | 69.0000 | 1 | 48.3000 |
| Sodium nitrate | $NaNO_3$ | 85.0000 | 1.25 | 74.3750 |
| Sodium carbonate | $Na_2CO_3$ | 106.0000 | 0.2 | 14.8400 |
| Sodium bicarbonate | $NaHCO_3$ | 84.0100 | 0 | 0.0000 |

* additional sodium hydroxide to neutralize acid

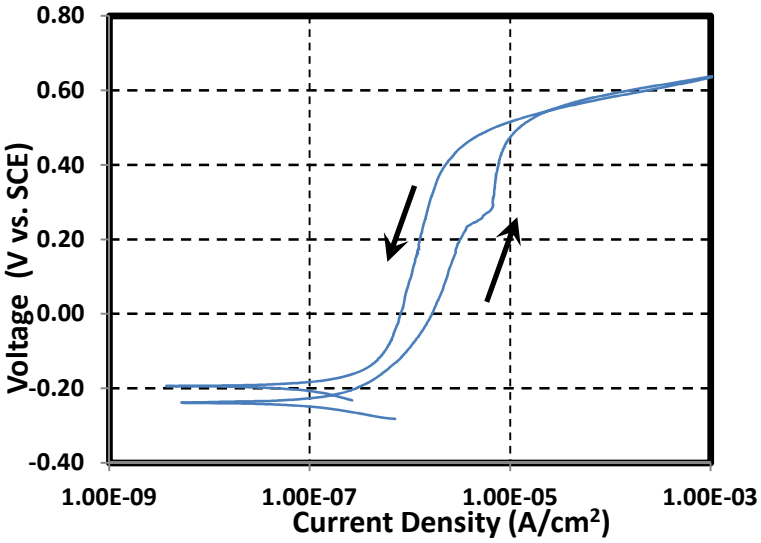


**Cyclic Potentiodynamic Polarization result**

**Images of bullet samples after test**

## Test 22 Composition of simulant

**Test 22**

| | | | |
|---|---|---|---|
| Temperature | 75 | °C | |
| pH at room temperature | 12.9 | | |
| pH before testing (at temp.) | 11.0 | pH after testing (at temp.) | 10.9 |
| Volume | 0.7 | L | |

| Simulant Source | Formula | Molecular Weight (g/mol) | Concentration (M) | weight required (g) |
|---|---|---|---|---|
| Sodium chloride | NaCl | 58.4000 | 0.05 | 2.0440 |
| Sodium fluoride | NaF | 42.0000 | 0.04 | 1.1760 |
| Sodium sulfate | $Na_2SO_4$ | 142.0000 | 0.1 | 9.9400 |
| Sodium phosphate, 12-hydrate | $Na_3PO_4.12H_2O$ | 380.0000 | 0.04 | 10.6400 |
| Sodium hydroxide* | NaOH | 40.0000 | 0.195 | 5.4600 |
| Sodium acetate, 3-hydrate | $Na(C_2H_3O_2).3H_2O$ | 136.0000 | 0.025 | 2.3800 |
| Sodium formate | $Na(CHO_2)$ | 68.0000 | 0.03 | 1.4280 |
| Glycolic acid | $C_2H_4O_3$ | 76.1000 | 0.02 | 1.0654 |
| Sodium oxalate | $Na_2C_2O_4$ | 134.0000 | 0.015 | 1.4070 |
| Sodium nitrite | $NaNO_2$ | 69.0000 | 1 | 48.3000 |
| Sodium nitrate | $NaNO_3$ | 85.0000 | 1.25 | 74.3750 |
| Sodium carbonate | $Na_2CO_3$ | 106.0000 | 0.2 | 14.8400 |
| Sodium bicarbonate | $NaHCO_3$ | 84.0100 | 0 | 0.0000 |

* additional sodium hydroxide to neutralize acid

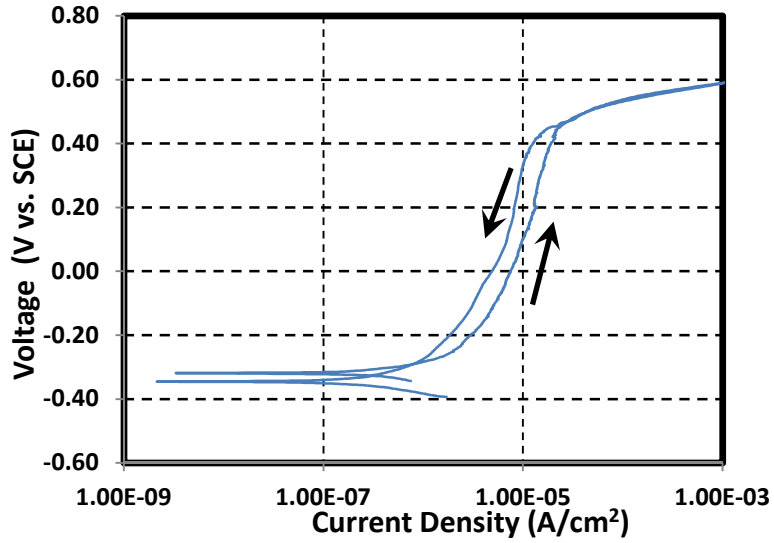


**Cyclic Potentiodynamic Polarization result**

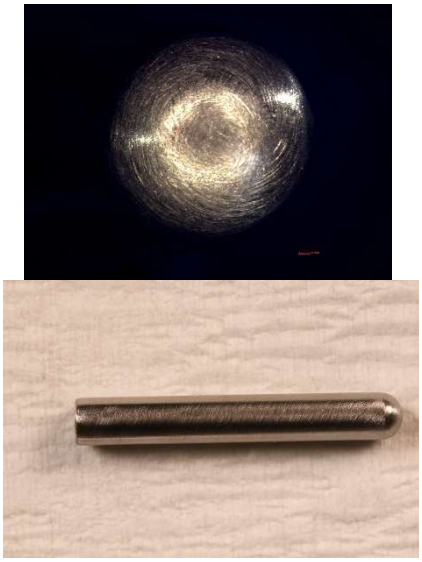

**Images of bullet samples after test**

## Test 23 Composition of simulant

**Test 23**

| | | | |
|---|---|---|---|
| Temperature | 75 | °C | |
| pH at room temperature | 13.1 | | |
| pH before testing (at temp.) | 11.2 | pH after testing (at temp.) | 11.0 |
| Volume | 0.7 | L | |

| Simulant Source | Formula | Molecular Weight (g/mol) | Concentration (M) | weight required (g) |
|---|---|---|---|---|
| Sodium chloride | NaCl | 58.4000 | 0.075 | 3.0660 |
| Sodium fluoride | NaF | 42.0000 | 0.04 | 1.1760 |
| Sodium sulfate | $Na_2SO_4$ | 142.0000 | 0.1 | 9.9400 |
| Sodium phosphate, 12-hydrate | $Na_3PO_4.12H_2O$ | 380.0000 | 0.04 | 10.6400 |
| Sodium hydroxide* | NaOH | 40.0000 | 0.245 | 6.8600 |
| Sodium acetate, 3-hydrate | $Na(C_2H_3O_2).3H_2O$ | 136.0000 | 0.025 | 2.3800 |
| Sodium formate | $Na(CHO_2)$ | 68.0000 | 0.03 | 1.4280 |
| Glycolic acid | $C_2H_4O_3$ | 76.1000 | 0.02 | 1.0654 |
| Sodium oxalate | $Na_2C_2O_4$ | 134.0000 | 0.015 | 1.4070 |
| Sodium nitrite | $NaNO_2$ | 69.0000 | 0.75 | 36.2250 |
| Sodium nitrate | $NaNO_3$ | 85.0000 | 1 | 59.5000 |
| Sodium carbonate | $Na_2CO_3$ | 106.0000 | 0.2 | 14.8400 |
| Sodium bicarbonate | $NaHCO_3$ | 84.0100 | 0 | 0.0000 |

* additional sodium hydroxide to neutralize acid

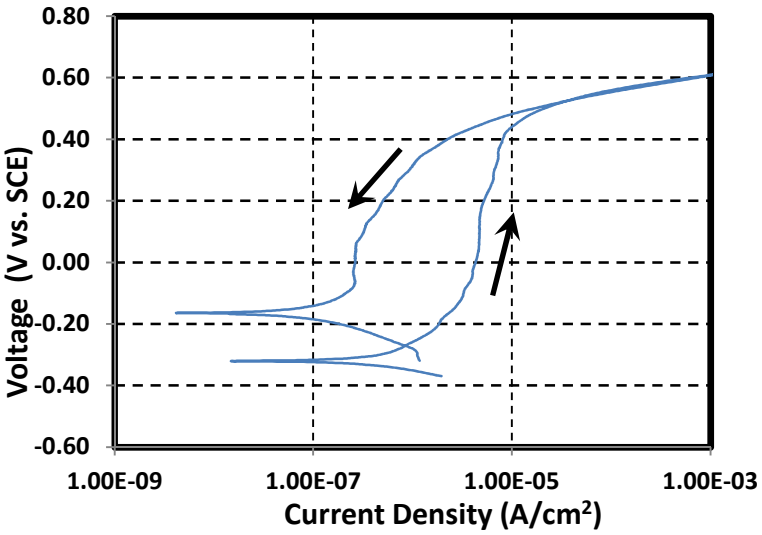


**Cyclic Potentiodynamic Polarization result**

**Images of bullet samples after test**

## Test 24 Composition of simulant

**Test 24**

| | | | |
|---|---|---|---|
| Temperature | 75 | °C | |
| pH at room temperature | 13.3 | | |
| pH before testing (at temp.) | 11.1 | pH after testing (at temp.) | 11.1 |
| Volume | 0.7 | L | |

| Simulant Source | Formula | Molecular Weight (g/mol) | Concentration (M) | weight required (g) |
|---|---|---|---|---|
| Sodium chloride | NaCl | 58.4000 | 0.075 | 3.0660 |
| Sodium fluoride | NaF | 42.0000 | 0.04 | 1.1760 |
| Sodium sulfate | $Na_2SO_4$ | 142.0000 | 0.1 | 9.9400 |
| Sodium phosphate, 12-hydrate | $Na_3PO_4.12H_2O$ | 380.0000 | 0.04 | 10.6400 |
| Sodium hydroxide* | NaOH | 40.0000 | 0.27 | 7.5600 |
| Sodium acetate, 3-hydrate | $Na(C_2H_3O_2).3H_2O$ | 136.0000 | 0.025 | 2.3800 |
| Sodium formate | $Na(CHO_2)$ | 68.0000 | 0.03 | 1.4280 |
| Glycolic acid | $C_2H_4O_3$ | 76.1000 | 0.02 | 1.0654 |
| Sodium oxalate | $Na_2C_2O_4$ | 134.0000 | 0.015 | 1.4070 |
| Sodium nitrite | $NaNO_2$ | 69.0000 | 0.75 | 36.2250 |
| Sodium nitrate | $NaNO_3$ | 85.0000 | 1.25 | 74.3750 |
| Sodium carbonate | $Na_2CO_3$ | 106.0000 | 0.2 | 14.8400 |
| Sodium bicarbonate | $NaHCO_3$ | 84.0100 | 0 | 0.0000 |

* additional sodium hydroxide to neutralize acid

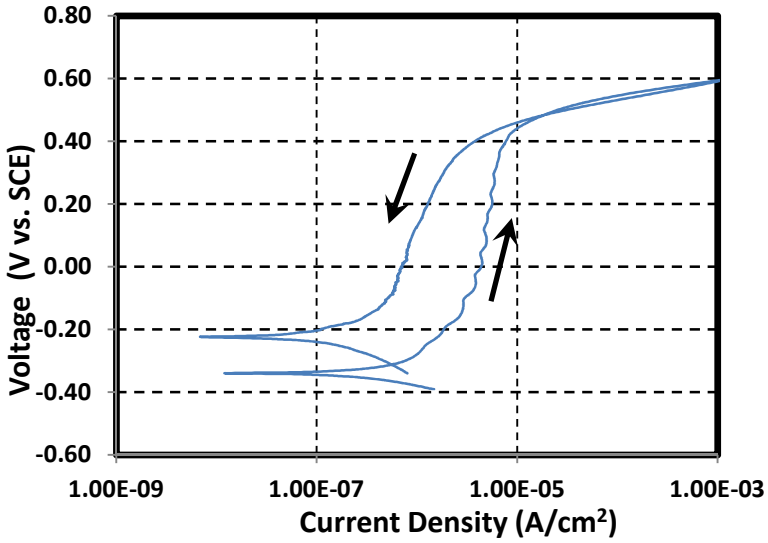


**Cyclic Potentiodynamic Polarization result**

**Images of bullet samples after test**

## Test 25 Composition of simulant

**Test 25**

| | | | |
|---|---|---|---|
| Temperature | 75 | °C | |
| pH at room temperature | 13.0 | | |
| pH before testing (at temp.) | 10.9 | pH after testing (at temp.) | 10.8 |
| Volume | 0.7 | L | |

| Simulant Source | Formula | Molecular Weight (g/mol) | Concentration (M) | weight required (g) |
|---|---|---|---|---|
| Sodium chloride | NaCl | 58.4000 | 0.05 | 2.0440 |
| Sodium fluoride | NaF | 42.0000 | 0.04 | 1.1760 |
| Sodium sulfate | $Na_2SO_4$ | 142.0000 | 0.1 | 9.9400 |
| Sodium phosphate, 12-hydrate | $Na_3PO_4.12H_2O$ | 380.0000 | 0.04 | 10.6400 |
| Sodium hydroxide* | NaOH | 40.0000 | 0.17 | 4.7600 |
| Sodium acetate, 3-hydrate | $Na(C_2H_3O_2).3H_2O$ | 136.0000 | 0.025 | 2.3800 |
| Sodium formate | $Na(CHO_2)$ | 68.0000 | 0.03 | 1.4280 |
| Glycolic acid | $C_2H_4O_3$ | 76.1000 | 0.02 | 1.0654 |
| Sodium oxalate | $Na_2C_2O_4$ | 134.0000 | 0.015 | 1.4070 |
| Sodium nitrite | $NaNO_2$ | 69.0000 | 1.25 | 60.3750 |
| Sodium nitrate | $NaNO_3$ | 85.0000 | 1 | 59.5000 |
| Sodium carbonate | $Na_2CO_3$ | 106.0000 | 0.2 | 14.8400 |
| Sodium bicarbonate | $NaHCO_3$ | 84.0100 | 0 | 0.0000 |

* additional sodium hydroxide to neutralize acid

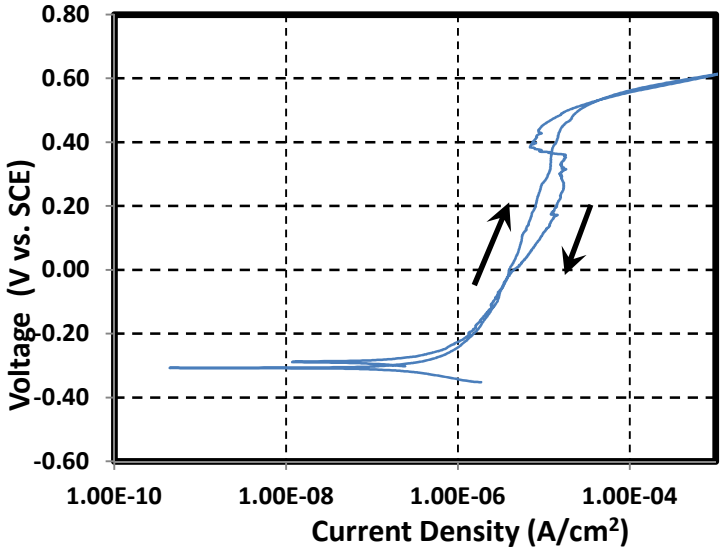


**Cyclic Potentiodynamic Polarization result**

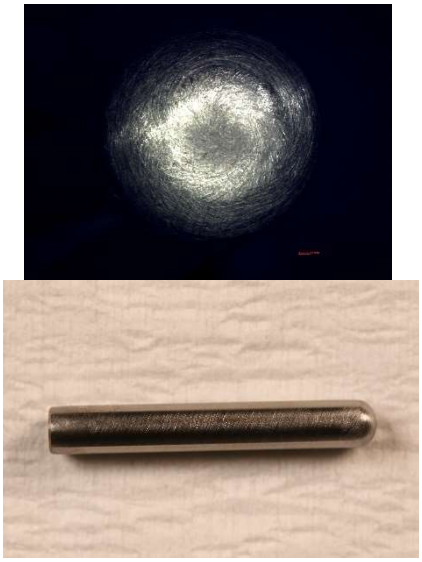

**Images of bullet samples after test**

**ASTM G192 Plot**

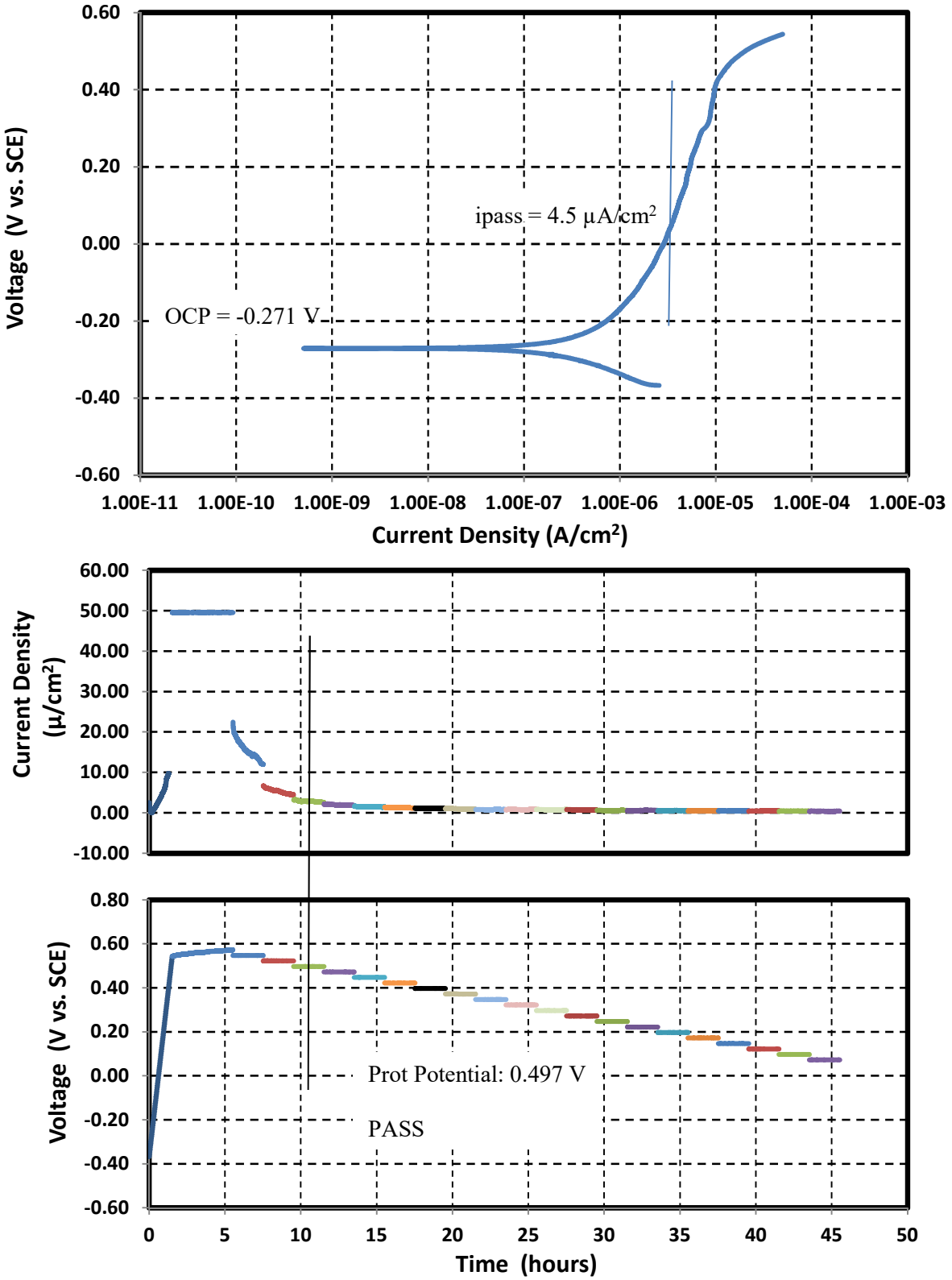

# Appendix D Chemical Composition of Simulants used in Secondary Liner Corrosion Testing

**Table D-1 Composition for GW simulant**

| | | |
|---|---|---|
| Temperature | 45 | °C |
| pH adjusted | 7.6 | |
| Volume | 2 | L |

| Simulant Source | Formula | Concentration (M) | Weight required (g) |
|---|---|---|---|
| Sodium bicarbonate | $NaHCO_3$ | 1.750E-03 | 0.2940 |
| Calcium hydroxide | $Ca(OH)_2$ | 1.500E-03 | 0.2223 |
| Potassium nitrate | $KNO_3$ | 2.400E-04 | 0.0485 |
| Ferric sulfate | $Fe_2(SO_4)_3$ | 6.250E-04 | 0.4999 |
| Ferric chloride | $FeCl_3$ | 7.667E-05 | 0.0249 |
| Strontium Nitrate | $Sr(NO_3)_2$ | 2.874E-06 | 0.0012 |
| Sodium Metasilicate, 5-hydrate | $Na_2SiO_3.5H_2O$ | 6.000E-04 | 0.2546 |
| Magnesium Chloride | $MgCl_2$ | 3.100E-04 | 0.0590 |
| Acetic Acid | $C_2H_4O_2$ | 3.000E-04 | 0.0360 |

## Appendix E Pictures of Secondary Liner Corrosion Testing Samples after Test

## After removal of cold mount

### Vessel 1: Level 3
2 months


Front 25 Back Front 26 Back Front 27 Back

### Vessel 1: Level 3
4 months


Front 28 Back Front 29 Back Front 30 Back

### Vessel 1: Level 2
2 months


Front 31 Back Front 32 Back Front 33 Back

### Vessel 1: Level 2
4 months


Front 34 Back Front 35 Back Front 36 Back

,

**Vessel 1: Level 1**
**2 months**

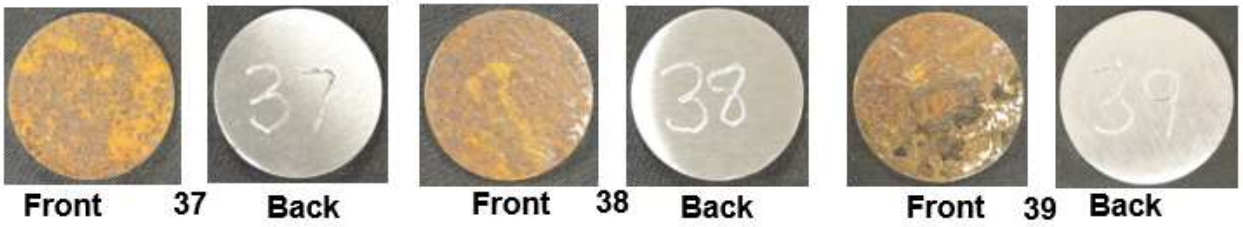


Front 37 Back Front 38 Back Front 39 Back

**Vessel 1: Level 1**
**4 months**


Front 40 Back Front 41 Back Front 42 Back

**Vessel 1: Immersed**
**2 months**


Front 43 Back Front 44 Back Front 45 Back

**Vessel 1: Immersed**
**4 months**


Front 46 Back Front 47 Back Front 48 Back

## After cleaning with Clarke's solution

### Vessel 1: Level 3

2 months | 4 months

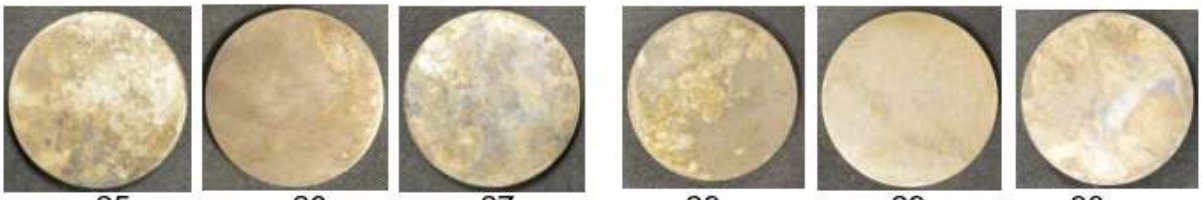

25 26 27 28 29 30

### Vessel 1: Level 2

2 months | 4 months

31 32 33 34 35 36

### Vessel 1: Level 1

2 months | 4 months

37 38 39 40 41 42

### Vessel 1: Immersed

2 months | 4 months

43 44 45 46 47 48

**Samples cold mounted**

**Vessel 2: Level 3**


**Vessel 2: Level 2**


**Vessel 2: Level 1**


**Vessel 2: Immersed**

## After removal of cold mount

### Vessel 2: Level 3
2 months

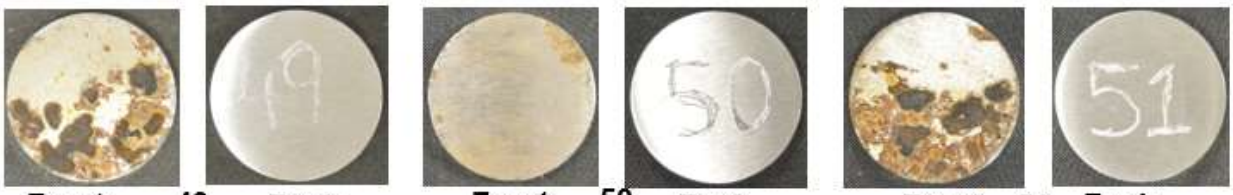


### Vessel 2: Level 3
4 months

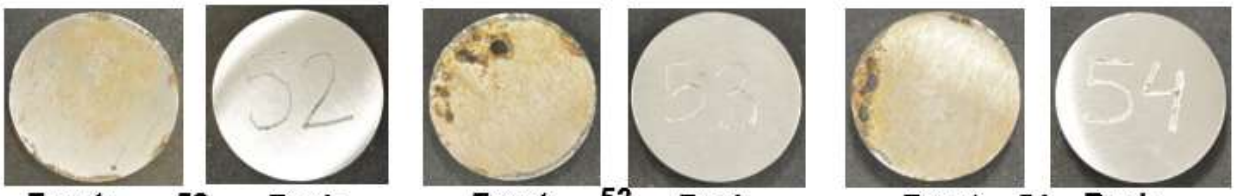


### Vessel 2: Level 2
2 months

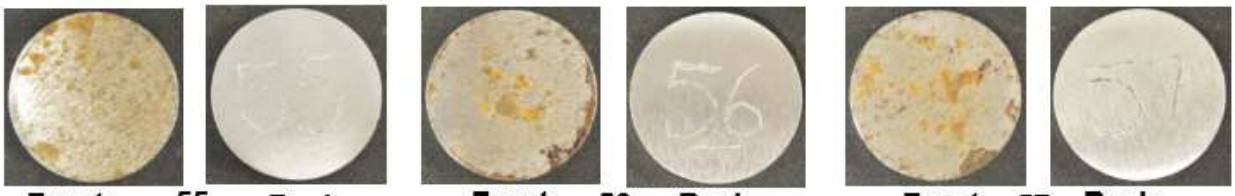


### Vessel 2: Level 2
4 months

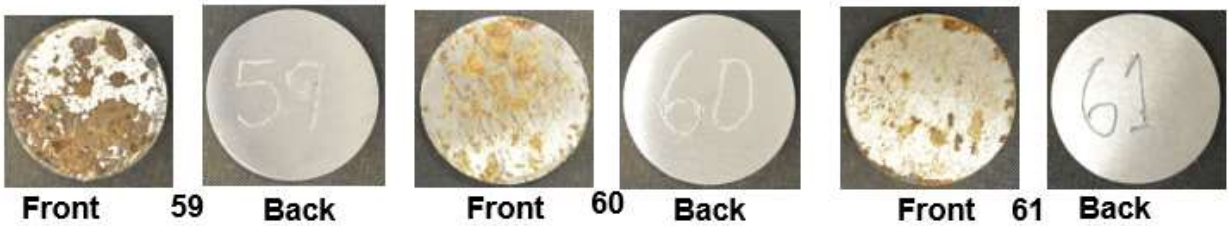

**Vessel 2: Level 1**
**2 months**

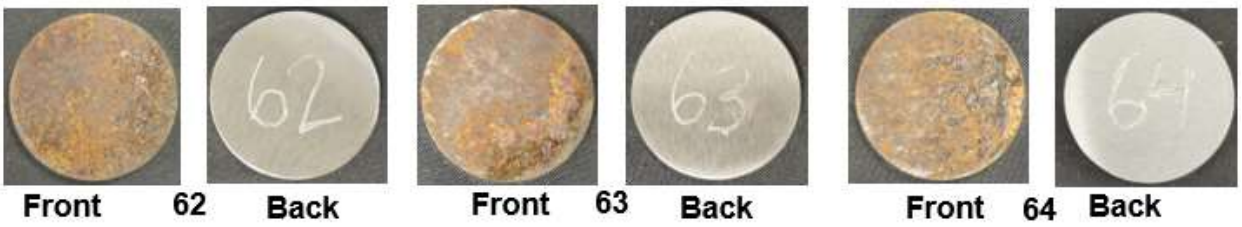


**Vessel 2: Level 1**
**4 months**

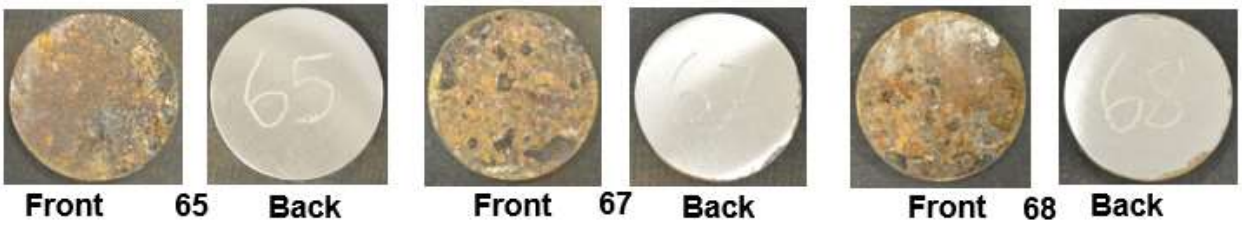


**Vessel 2: Immersed**
**2 months**


**Vessel 2: Immersed**
**4 months**

## After cleaning with Clarke's solution

### Vessel 2: Level 3

2 months | 4 months

49 50 51 52 53 54

### Vessel 2: Level 2

2 months | 4 months

55 56 57 59 60 61

### Vessel 2: Level 1

2 months | 4 months

62 63 64 65 67 68

### Vessel 2: Immersed

2 months | 4 months

70 71 72 73 74 75

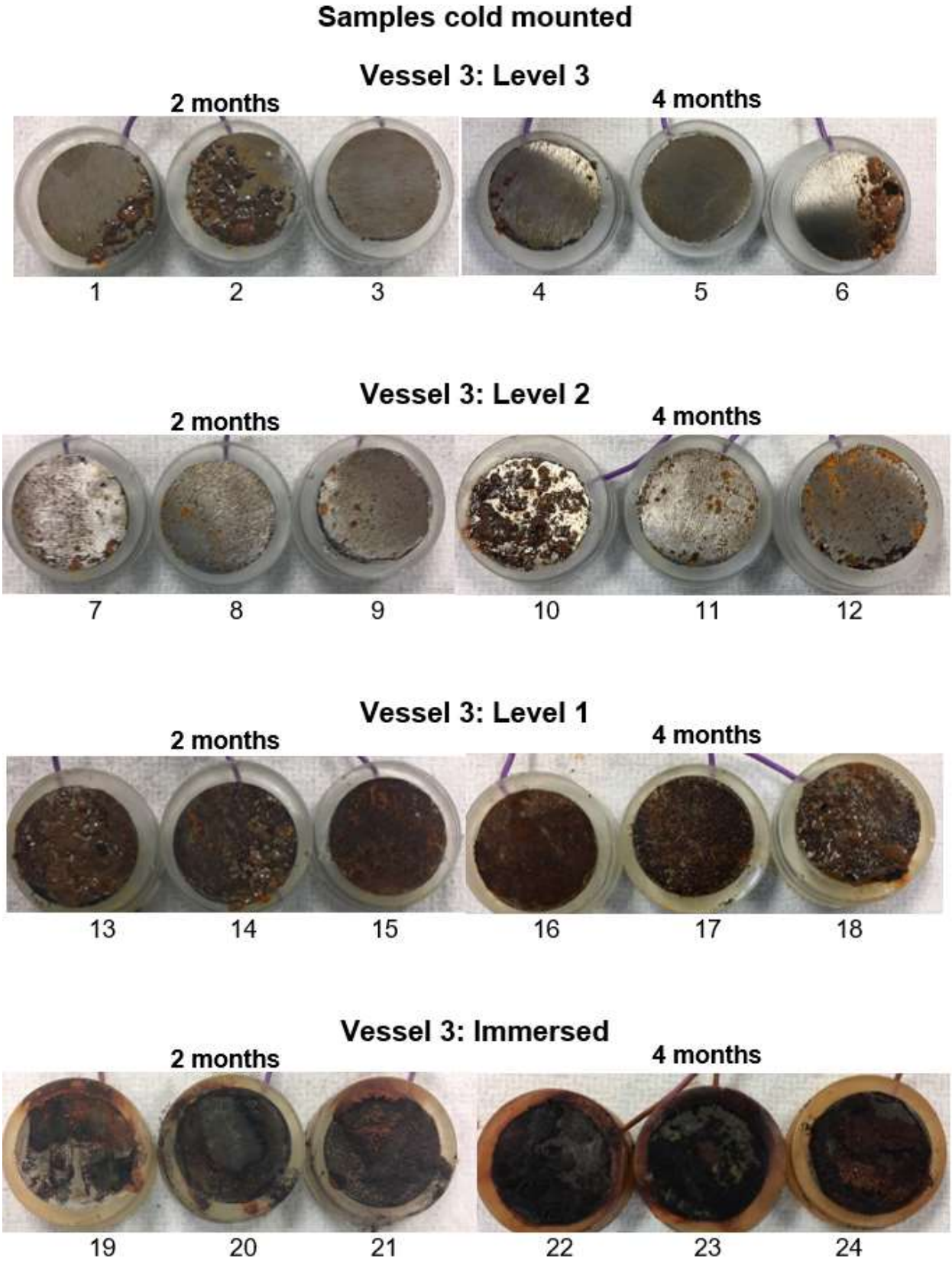
Samples cold mounted
Vessel 3: Level 3
2 months
4 months
1
2
3
4
5
6
Vessel 3: Level 2
2 months
4 months
7
8
9
10
11
12
Vessel 3: Level 1
2 months
4 months
13
14
15
16
17
18
Vessel 3: Immersed
2 months
4 months
19
20
21
22
23
24

## After removal of cold mount

### Vessel 3: Level 3
2 months

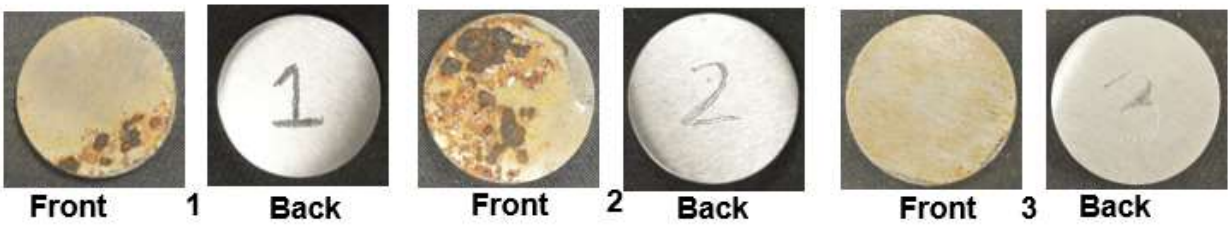


### Vessel 3: Level 3
4 months

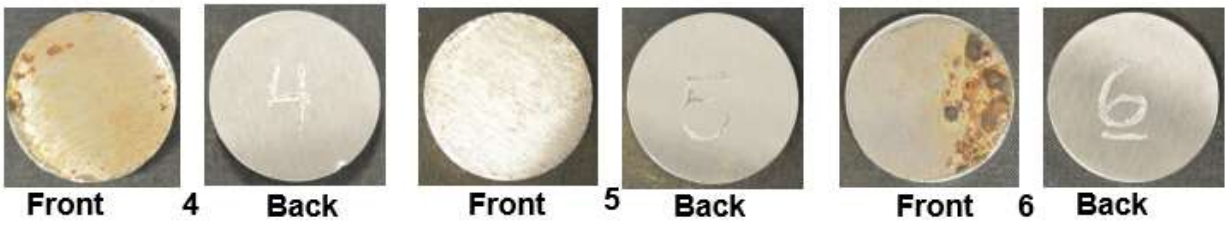


### Vessel 3: Level 2
2 months

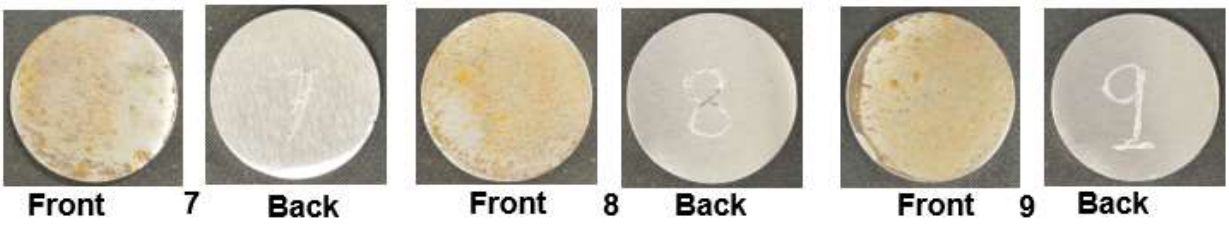


### Vessel 3: Level 2
4 months

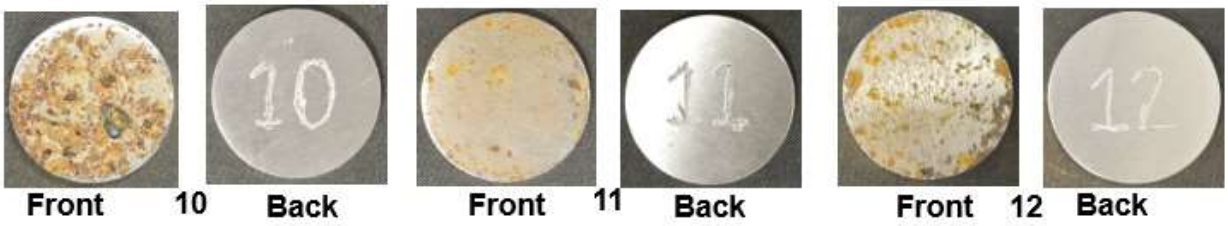

**Vessel 3: Level 1**
**2 months**

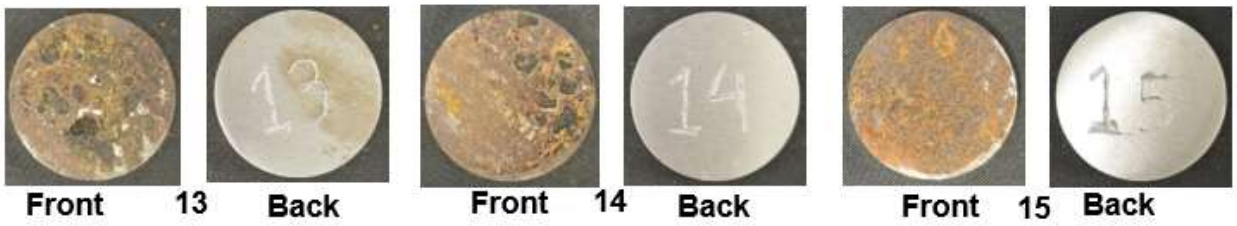


**Vessel 3: Level 1**
**4 months**


**Vessel 3: Immersed**
**2 months**

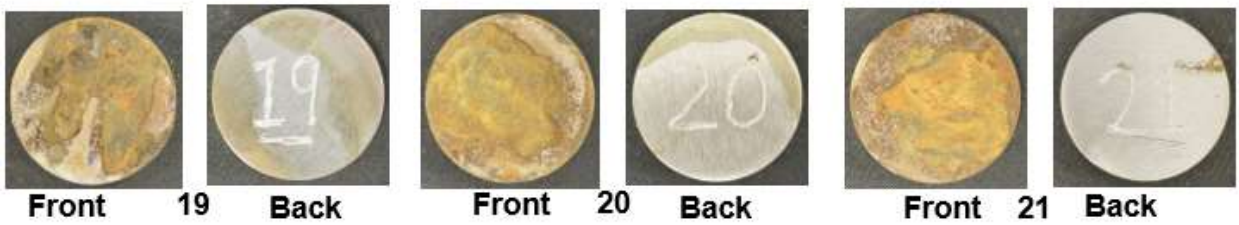


**Vessel 3: Immersed**
**4 months**

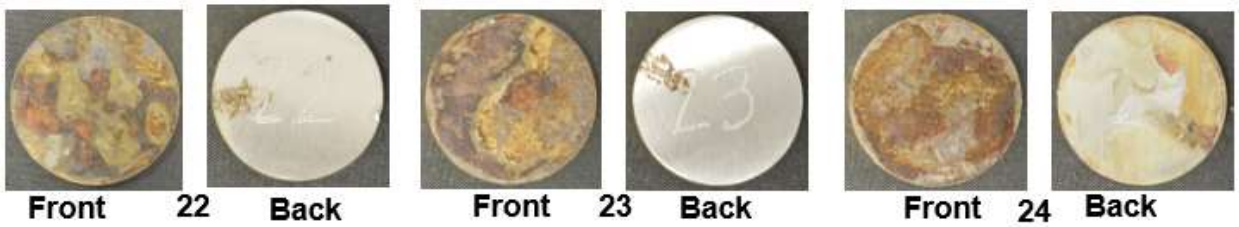

## After cleaning with Clarke's solution

### Vessel 3: Level 3


### Vessel 3: Level 2


### Vessel 3: Level 1


### Vessel 3: Immersed

## Appendix F: Additional Open Circuit Potential Graphs

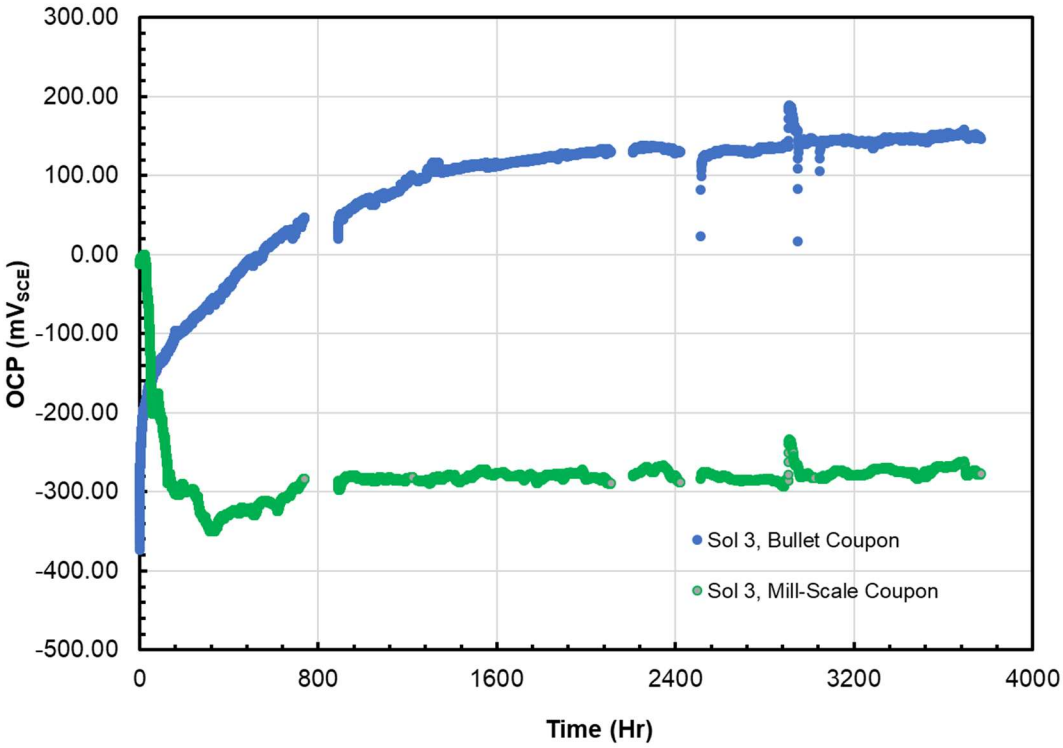


**Figure F-1. Solution 3 Bullet and Mill-Scale Coupons' OCP Evolutions**

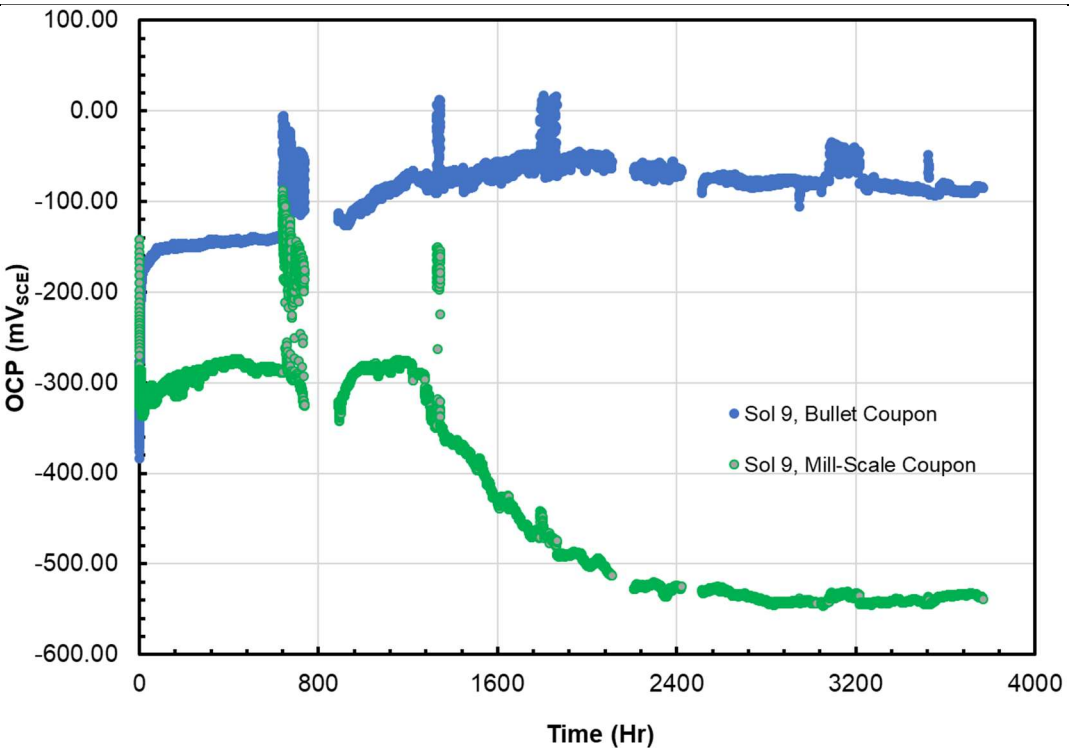


**Figure F-2. Solution 9 Bullet and Mill-Scale Coupons' OCP Evolutions**

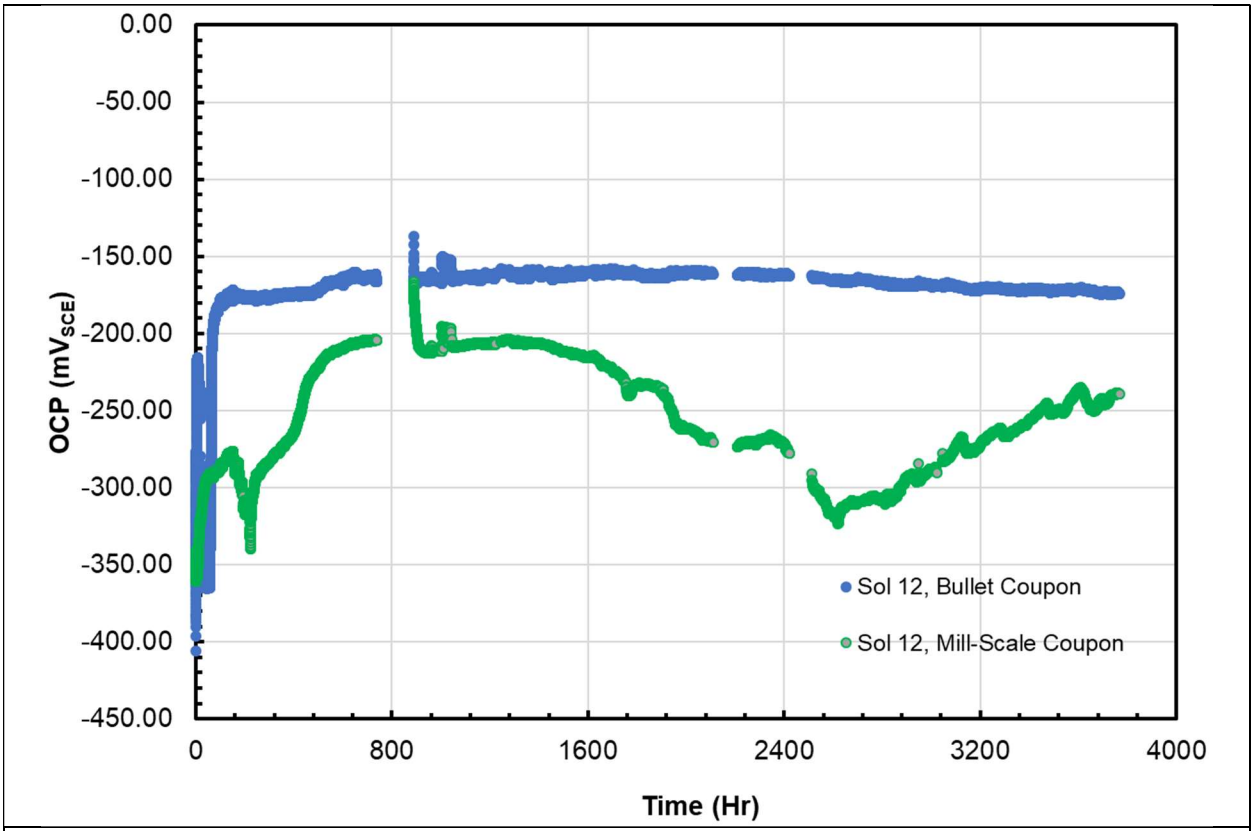


**Figure F-3. Solution 12 Bullet and Mill-Scale Coupons' OCP Evolutions**

**Distribution**

a.fellinger@srnl.doe.gov
alex.cozzi@srnl.doe.gov
Amy.Ramsey@srnl.doe.gov
Anthony.Howe@srnl.doe.gov
Boyd.Wiedenman@srnl.doe.gov
Brenda.Garcia-Diaz@srnl.doe.gov
Bruce.Wiersma@srnl.doe.gov
Christine.langton@srnl.doe.gov
cj.bannochie@srnl.doe.gov
connie.herman@srnl.doe.gov
crystal_l_girardot@rl.gov
daniel.mccabe@srnl.doe.gov
david.crowley@srnl.doe.gov
dennis.jackson@srnl.doe.goveric.skidmore@srnl.doe.goverich.hansen@srnl.doe.gov
frank.pennebaker@srnl.doe.gov
Gregg.Morgan@srnl.doe.gov
jason_s_page@rl.gov
jim_l_castleberry@rl.govJoseph.Manna@srnl.doe.gov
Joshua.boerstler@srnl.doe.gov
Kevin.Fox@srnl.doe.gov
michael.stone@srnl.doe.gov
Records Administration (EDWS)
Richard.wyrwas@srnl.doe.gov
samuel.fink@srnl.doe.gov
shawn_t_campbell@rl.gov
William.Ramsey@srnl.doe.gov